State Estimation and Servo-control of Distributed Parameter Systems

by

Xiaodong Xu

A thesis submitted in partial fulfillment of the requirements for the degree of

Doctor of Philosophy

in

Process Control

Department of Chemical and Material Engineering

University of Alberta

© Xiaodong Xu, 2017

Abstract

The dynamics of many chemical and mechanical processes are influenced by both temporal and spatial factors and these processes are called distributed parameter systems (DPS). Moreover, their mathematical models are given by partial differential equations (PDE) and they belong to infinite-dimensional systems. Due to the existence of the spatial variable in the mathematic model, the state estimation and control of the distributed parameter systems are interesting and challenging. The focus of this thesis is to develop the optimal state estimation method and servo-control (output regulation) methods in the optimal and internal-model framework.

To address the control problems for finite and infinite dimensional systems, the full state information is usually necessary. In this thesis, an optimal state estimation method is developed for spectral distributed parameter systems to account for full state estimation problems with state constraints due to physical limitations. In particular, a modal decomposition technique is applied to reduce the order of the considered dissipative systems that are assumed to satisfy the decomposition assumption.

With the full state information of the control systems, the proposed servo-control approaches in this thesis are able to implement. In this thesis, two types of servo-control (output regulation) are considered: Internal Model Control (IMC) and Optimal control. In fact, the servo-control includes two aspects: stabilization and reference signal tracking. In the aspect of the stabilization, an operator Riccati equation approach and a weak variational optimal method are developed for the first order hyperbolic PDE systems in this

thesis. For the aspect of the reference trajectory tracking, novel output feedback and error feedback regulators are developed to deal with the distributed and/or boundary tracking control problems for general distributed parameter systems.

Finally, the servo-control problems for the countercurrent heat exchanger, the plug flow reactor and the solar-thermal district heating system are addressed in the application part of this thesis. In particular, for the countercurrent heat exchanger, the proposed output regulation approach is applied; for the plug flow reactor, the proposed weak variational optimal stabilization and the output regulation method are combined and applied; and for the solar-thermal district heating system, the receding horizon optimal control and the output regulation approach are implemented to solve the energy maximization and the reference tracking problems.

Preface

Chapter 2 of this thesis has been published as X. Xu, B. Huang and S. Dubljevic, "Optimal continuous-time state estimation for linear finite and infinite-dimensional chemical process systems with state constraints", **Journal of Process Control**, vol. 35, 127-142, 2015. I was responsible for the formulation, simulation and analysis as well as the manuscript composition. B. Huang and S. Dubljevic were the supervisory author and were involved with concept formation and manuscript composition.

Chapter 3 of this thesis is consisting of three works. Section 3.2 has been published as X. Xu and S. Dubljevic, "Output regulation problem for a class of regular hyperbolic systems", **International Journal of Control**, vol. 89, Issue 1, 113-127, 2016. Section 3.3 has been accepted for publication as X. Xu and S. Dubljevic, "Finite-dimensional regulators for a class of regular hyperbolic PDE systems", **International Journal of Control**, 2017. Section 3.4 has been accepted for publication as X. Xu, S. Dubljevic, "Output regulation for a class of linear boundary controlled first-order hyperbolic PIDE systems", **Automatica**, 2017. I was responsible for the formulation, simulation and analysis as well as the manuscript composition. S. Dubljevic was the supervisory author and was involved with concept formation and manuscript composition.

Chapter 4 of this thesis has been published as X. Xu and S. Dubljevic, "Output and error feedback regulator designs for linear infinite-dimensional systems", **Automatica**, vol. 83, 170-178, 2017. I was responsible for the formulation, simulation and analysis as well as the manuscript composition. S. Dubljevic was the supervisory author and was involved with concept formation and manuscript composition.

Chapter 5 of this thesis has been published as X. Xu and S. Dubljevic, "The state feedback servo-regulator for countercurrent heat-exchanger system modelled by system of hyperbolic PDEs", **European Journal of Control**, vol. 29, 51-61, 2016. I was responsible for the formulation, simulation and analysis as well as the manuscript composition. S. Dubljevic was the supervisory author and was involved with concept formation and manuscript composition.

Chapter 6 of this thesis has been submitted for publication as X. Xu and S. Dubljevic, "Optimal tracking control for a class of boundary controlled linear coupled hyperbolic PDE systems: Application to plug flow reactor with temperature output feedback", **European Journal of Control**, 2017. I was responsible for the formulation, simulation and analysis as well as the manuscript composition. S. Dubljevic was the supervisory author and was involved with concept formation and manuscript composition.

Chapter 7 of this thesis has been submitted for publication as X. Xu, Y. Yuan and S. Dubljevic, "Receding horizon optimal operation and control of a solar-thermal district heating system", **AIChE Journal**, 2017. I was responsible for the formulation, simulation and analysis as well as the manuscript composition. Y. Yuan was responsible for formulation and analysis. S. Dubljevic was the supervisory author and was involved with concept formation and manuscript composition.

To my family, for their support and encouragement.

Acknowledgements

I would like to express my sincere gratitude to my supervisors Dr. Biao Huang and Dr. Stevan Dubljevic for their appreciable inspiration, support and patience throughout my research and acting as a mentor to my overall professional development. I would like to thank Dr. Huang for important comments on my research works. I would like to thank Dr. Dubljevic for providing me excellent opportunities for attending international technical conference and interacting with external research group members. Moreover, I appreciate the infinite patience and freedom that Dr. Dubljevic gave to me so that I can explore and enjoy my research. The critical reviews and recommendations that they provided for the improvement of my papers and presentations were very valuable. They were great supervisors and friends and it was a great pleasure to have the opportunity to work under their supervision. Also, I acknowledge for the financial support that Dr. Huang and Dr. Dubljevic provided me throughout my graduate studies. In addition, I appreciate the help from Jukka Pekka and Dr. Paunonen on the corrections of my thesis.

To my family, words cannot fully express how deeply grateful I am for all of your love and support. For my mother Chunzhi, father Bangheng, sister Wenyan and brother Wenqiang, thank you for believing in me and for encouraging me to pursue this path. Without all of your patience and empathy, I would not have been able to see this through. I hope to have made you proud.

To my friends, I cannot imagine a more amazing group of people who's diverse interests and talents have been a profound source of inspiration throughout the many years which we have enjoyed together. I am truly fortunate to be in the company of such compassionate individuals, and I wish the very best in life for each and every one of you.

At the end I would like to express appreciation to my beloved companion Yuan Yuan for her unconditional understanding, love and faith. Her sacrifice, support and compassion was indeed what made this dissertation possible.

Contents

List of Tables

List of Figures

List of Common Notation

$\mathbb{C}$	Set of complex numbers.
$\mathbb{R}$	Set of real numbers.
z, ζ	Spatial variable.
R	Real number set.
$\mathcal{A}, A$	State linear operator.
$\mathcal{B}, B$	PDE input operator.
$\mathcal{C}, C$	PDE output operator.
$\mathcal{C}_\Lambda$	$\Lambda-$extension of the operator $\mathcal{C}$.
$R(\lambda; A)$	Resolvent operator of A for $\lambda \in \rho(A)$.
$D(A)$	Domain of the operator A.
$\sigma(A)$	Spectrum of the operator A.
$\rho(A)$	Resolvent set of the operator A.
$\mathcal{L}(X, Y)$	Space of all linear, bounded operators from X to Y.
$L^2(0,1)^m$	Hilbert space of an m-dimensional vector over $[0, 1]$.
$H^k(0,1)$	Hilbert space defined as the Sobolev space of order k.
$T_A(t)$	C_0-semigroup generated by the operator A.
t	Time variable.
$\lVert\cdot\rVert$	Norm.
$\langle\cdot,\cdot\rangle$	Inner product.

Chapter 1

Introduction

In chemical and mechanical engineering sciences, Partial Differential Equations (PDEs) are widely used as models of transport (transport-reaction) phenomena in formation and separation processes. There continues to be a rich and active research interest in this field which draws upon the well established classical tools of mathematical analysis, and also employ the recent advancements in computer technology for process simulation and numerical studies of complex problems. Many applications include examples in petroleum industry such as heavy oil recovery, and tubular and plug-flow reactor systems which are used for the production and the refinement of large volume chemicals. In manufacturing industries, phase transitions and thermal treatment are critical factors in the fabrication and processing of materials, such as in semiconductor production by crystal growth methods. In mechanical engineering, the modelling of turbulence and meandering wake is crucial to the control of the wind farm and the mathematical description of the fluid transportation plays an important role in the solar-thermal energy systems.

1.1 PDE models and control systems

From the mathematical aspect, a PDE includes one or more partial derivatives of the dependent variables. Suppose that there is a dependent variable $x(z,t)$ which is a function of the independent variables $\boldsymbol{z} = \{z_1, \cdots, z_m\}$ in an m-dimensional domain $\Omega \subset \mathbb{R}^m$, and also the independent variable of time $t \in \mathbb{R}^+$. In particular, the general expression for a second order PDE for the function $x(\boldsymbol{z}, t)$ is:

$$F\left(z_1, \cdots, z_m, t, x, \frac{\partial x}{\partial t}, \frac{\partial x}{\partial z_1}, \cdots, \frac{\partial x}{\partial z_m}, \frac{\partial^2 x}{\partial z_1^2}, \cdots, \frac{\partial^2 x}{\partial z_m^2}, \frac{\partial^2 x}{\partial z_1 \partial z_2}, \cdots\right) = 0 \tag{1.1}$$

The highest order of the derivatives is the order of the equation. All PDEs can be classified into three types of equations: hyperbolic, parabolic and elliptic. Moreover, spurred by the outer space applications, there is another important class of PDE systems – beam equations. For example, the well-known Euler-Bernoulli beam equations is a fourth order PDE system:

$$\begin{aligned}
&\tfrac{\partial^2 x(z,t)}{\partial t^2} + \tfrac{\partial^4 x(z,t)}{\partial z^4} = 0, z \in [0,1], t > 0, \\
&x(0,t) = \tfrac{\partial x(0,t)}{\partial z} = 0, t \geq 0, \\
&\tfrac{\partial^2 x(0,t)}{\partial z^2} = 0, t \geq 0, \\
&\tfrac{\partial^3 x(0,t)}{\partial z^3} = U(t), t \geq 0
\end{aligned} \tag{1.2}$$

The function $x(z,t)$ provides the state of the system at the time t along the entire space, and denotes a process variable of interest, for example temperature or density. The distributed nature of the state is a distinguishing feature of process variables modelled by PDEs in contrast to those modelled by ODEs for which the process variables are represented by functions of only a single independent variable, for example $x(t)$ which is spatially invariant. Many transport-reaction processes in chemical and materials engineering can be described by the linear parabolic PDE:

$$\frac{\partial x}{\partial t}(z,t) = A(z,t)x(z,t) + B(z,t)u(t) + f(z,t) \tag{1.3}$$

The operator $A(z,t)$ is referred to as the spatial operator and is given by:

$$A(z,t) := \sum_{i,j=1}^{N} \frac{\partial}{\partial z_i}\left(D_{ij}(z)\frac{\partial}{\partial z_j}\right) + \sum_{k=1}^{n} v_k(t)\frac{\partial}{\partial z_k} + g(z,t) \tag{1.4}$$

Two important transport mechanisms included in the PDE process model in above equations are diffusion and convection. In particular, consider (1.3)–(1.4) as a chemical reaction system, $x(z,t)$ represents the concentration of a chemical species, $D_{ij}(z)$ are the diffusion coefficients, $v_k(t)$ are the velocity in the z_k direction, $g(z,t)$ is the state related linearized generation/consumption term, and $f(z,t)$ is nonhomogeneous generation/consumption term. The function $B(z,t)u(t)$ in (1.3) can be seen as a heat source or sink within the domain Ω, which can be manipulated by a controller input $u(t)$ to affect the temperature distribution of the system. In fact, this type of system is representative of the class of *distributed control* problems for PDEs. On the other hand, in order for the problem to be properly stated, one must impose additional restrictions on the system in the form of initial conditions, given by the initial temperature distribution $x(z,0)$, and also the boundary conditions, which describe the what happens on the boundary of the domain. Boundary conditions referred to as mixed or Robin boundary conditions for heat transport systems are given by:

$$K_0 \frac{\partial x}{\partial z}(z,t) + hx(z,t)\bigg|_{z=0} = u(t) \tag{1.5}$$

The parameters specified for the boundary conditions in this are are the thermal conductivity of the material K_0, and the convective heat transfer coefficient h. In the absence of convective heat transfer ($hx(0,t) = 0$) the boundary conditions are referred to as zero-flux (Neumann) boundary conditions. In the context of PDE control problems with $B(z,t) = 0$, the (1.3) and (1.5) is representative of the class of boundary control problems for PDEs.

1.2 Thesis scope

The focus of this thesis is the servo-control of different types of distributed parameter systems. In particular, to assist in realizing the control, the state estimation and observer design techniques are investigated as well in this thesis. According to different considered systems, the state estimation and servo-control problems are addressed within the infinite-dimensional systems theoretic framework, and together with the development, formulation, and numerical realization, are explored within the following chapters.

Chapter 2 addresses optimal constrained state estimation problem for finite and infinite-dimensional chemical process systems. The cases are considered when the prior information, in addition to the model parameters and the measurements, is available in the form of an inequality constraint with respect to the systems state. In the latest developments of the optimal state estimation theory, considerations of the state constraints have been often neglected since constraints do not fit easily in the structure of the optimal state estimator. Therefore, the issue of the state constraints being present needs to be addressed adequately, in particular, nonnegativity of concentration. Motivated by this, a sequential, algorithmic optimal constrained state estimator is developed for both finite and infinite-dimensional process systems commonly found in chemical process engineering (CSTR, tubular reactor). Moreover, an optimal constrained state estimator is designed for a large class of dissipative infinite-dimensional systems which involve boundary actuation and point observation. Finally, illustrative examples of chemical process systems and proposed optimal state constrained estimation are presented.

Chapter 3 deals with the distributed and/or boundary output regulation problems for different hyperbolic PDE systems. In particular, state, output and error feedback regulators are designed respectively to drive the controlled output to track a desired reference trajectory which can be modelled by an exogenous signal process. Consequently, various regulator equations (Sylvester equations) are obtained and sufficient conditions ensuring the solvabilities of regulator equations are given to guarantee the feasibility of proposed regulators. Finally, different computer simulations are presented to show the performances of proposed regulators.

Chapter 4 addresses the output regulation problem for linear distributed parameter systems (DPSs) with bounded input and unbounded output operators. In particular, novel methods for the design of the output feedback and error feedback regulators are introduced. In the output feedback regulator design, the measurements available for the regulator do not belong to the set of controlled outputs. The proposed output feedback regulator with the injection of the measurement $y_m(t)$ and reference $y_r(t)$ can realize both the plant and the exosystem states estimation, disturbance rejection and reference signal tracking, simultaneously. Moreover, new design approach provides an alternative choice for seeking the output injection gain in a traditional error feedback regulator design. The regulator parameters are easily configured to solve the output regulation problems, and to ensure the stability of the closed-loop systems. The results are demonstrated via computer simulation in two types of representative systems: the parabolic partial differential equation (PDE) system and the first order hyperbolic PDE system.

Chapter 5 considers the state feedback regulator problem for a network of countercurrent heat exchangers. The system is described by two sets of hyperbolic partial differential equations (PDEs) and the model is nonlinear with respect to the control input. To deal with the nonlinearity, the equilibrium temperature profile is calculated and utilized in the linearization of the original nonlinear system. Then, based on infinite-dimensional representation, the state feedback regulator problem (in particular the tracking problem) is considered, where the target is to design a controller that, while guaranteeing the stability of the closed-loop system, drives the controlled output to track a reference signal generated by an exosystem with its spectrum on the imaginary axis. Given the explicit expression of the transfer function, we provide sufficient conditions such that the resulting linearized system is causal and stable. Given that the controlled system is stable, we propose a simple and novel method to provide the stabilization feedback gain K, such that the controlled system tracks the reference signal. Finally, a numerical simulation illustrating the results is presented.

Chapter 6 addresses the optimal linear quadratic (LQ) boundary output regulator design problem for the plug flow reactor described by the hyperbolic partial differential equations (PDE), with actuation applied only at the inlet of the reactor. By applying the weak variational approach, the necessary optimality conditions are provided and then an optimal state feedback controller is presented. In particular, the time-varying state feedback gain is determined by solving Riccati-type PDEs and this chapter extends the linear quadratic regulator design to the class of boundary controlled hyperbolic PDE systems. Along the line of LQ design, an optimal boundary tracking regulator is designed such that the output of the considered reaction process tracks the desired reference signal generated by an exosystem. A simulation example is included to show performance of the proposed approach.

Chapter 7 investigated optimal operation strategy and optimal control for a solar-thermal district heating system. Optimal operation strategies on the fluid flow rate inside the solar collector tube are studied such that the outlet temperature can be maintained in a desired reference value and moreover the heat (energy) gained by the solar collector is maximized within a certain time period. In particular, this target is formulated as a single-objective optimization problem and a multi-objective optimization problem, respectively, and corresponding operation strategies are studied and compared. For the energy storage system, the heat exchanger plays an important role in the heat transfer process and the maximization of the energy stored. Therefore, two freedoms-fluid flow rates in the heat exchanger are included. In the district heating loop system, a gas heater system collaborate with the solar thermal system to meet the heating demand. For this coupled system, a receding horizon optimal controller and a state-space based internal model controller are developed to address the desired temperature tracking problem. Finally, the proposed optimal operation strategies and controllers are tested through simulation results.

Chapter 2

Optimal continuous-time state estimation for linear chemical process systems with state constraints

2.1 Introduction

Chemical process systems contain a wide range of models spanning from lump parameter systems (e.g. continuous stirred tank reactors (CSTR)) to distributed parameter systems (e.g. axial dispersion reactor, flow systems, tubular reactors and heat exchanger). The chemical process lumped parameter systems (LPSs) are mathematically expressed by ordinary differential equations (ODEs), while distributed parameter systems (DPSs) are given by partial differential equations (PDEs). Such a large variety in modelling representations is complemented with the stringent process products specifications and performance characteristics. In addition to the stringent requirements on product quality, the process contains naturally present limits and constraints on allowed actuation. In many chemical processes, the limitation from devices and production requirement result in certain specification in the form of inequality constraint on states or inputs. In order to include these system characteristics in the state estimation framework, many previous research efforts and significant contributions have been made on optimal state estimation in a linear lumped parameter system, where constrained Kalman filter and moving horizon estimation method were widely utilized (see [5], [6] and [7]). In [8], various ways incorporating state constraints in the Kalman filer are provided. Nevertheless, it is not easy to embed the inequality or equality constraints in the Kalman filter. Moreover, Yang and Blasch [9] developed a method that allows for the use of second-order nonlinear equality state constraints. On the other hand, moving horizon estimation (MHE) can provide 'best' state estimation with help of Kalman filter and MHE is attractive in the generality of its formulation. The problem of MHE is essentially that of solving a quadratic programming (QP) problem which indicates that MHE is slow. In some cases, the MHE quadratic programming problems are not convex and thus optimization may not yield the global optimum (see [10]).

Motivated by the inclusion of constraints in optimal constrained state estimation above, we consider a large range of chemical process systems - starting from state-constrained finite-dimensional lumped parameter models (e.g., [11]) commonly found in chemical engineering practice to the broad class of dissipative distributed parameter systems (DPSs) (see [12], [13], [3], [14], [15] and [16]). Compared with lumped parameter systems, the state estimation work for a class of dissipative DPS systems is more complex. Moreover, the important question of incorporation of state constraints in the optimal state constrained estimation of dissipative DPS has not been explored (for example, transport-reaction processes require that the reactor temperature is maintained within certain bounds to ensure desired and safe operating performance). In particular, this chapter explores the way of utilizing constraints to improve the accuracy of the state estimation for the dissipative DPS systems model by dissipative partial differential equations (PDEs). Thomas et al. [17] investigated the optimal state estimation problem for distributed parameter systems and time delay systems by utilizing the framework of the optimal control theory. More recently, Zavala and Biegler [18] presented the application of MHE for multi-zone low-density polyethylene tubular reactors. In 1981 year, Ray [3] summarized and applied works of [17] in both lumped parameter and distributed parameter systems (see [19]; [20]). The optimal state estimation technique developed by Thomas and Ray was formulated by utilizing the variational method for continuous systems and the resulting estimation formulations have analytical expression. Motivated by the above content, in this chapter, we extended the framework of a continuous optimal state estimation technique to deal with the state estimation problem when the state constraints for continuous chemical process systems are explicitly included. In this chapter, the analytical form of the proposed state estimator is obtained and the estimator is a sequential one step estimator that can be applied directly online without solving the quadratic programming (QP) problem. Moreover, most constrained state estimation work is done in discrete-time, while the work in this chapter is elaborated in continuous-time.

Most of dissipative PDE systems contain the spatial differential operators the spectrum of which satisfies the spectrum decomposition assumption. Therefore, when designing filters or estimators for these PDE systems, modal analysis can be utilized to convert the dissipative PDE system into a finite-dimensional subsystem with its infinite-dimensional subsystem complement (e.g., [21], [3] and [22]). Since the finite-dimensional subsystem can capture the dominant system dynamics, the infinite-dimensional complement subsystem is often neglected. Along the line of approximation of PDE systems within the filter design, in [23], by minimizing the quadratic error least squares, the early lumped optimal filter and late lumped optimal filter are designed and compared. Hence, in [23] it has been shown that approximation which induces a loss of infinite-dimensional complement subsystem yields that the early lumped filter has a slower convergence rate relative to the late lumped filter when starting from a poor prior initial estimate. Moreover, the early lumped filter does not track system dynamics as well as the late lumped filter. Therefore, in this chapter, to eliminate impact of loss of a complement subsystem, we include the complete dynamics of the infinite-dimensional subsystem within the state estimator design. Moreover, in this chapter, we consider a large class of infinite-dimensional systems: Pritchard-Salamon class of linear infinite-dimensional systems which involve many examples of PDE systems with boundary control and observation, which result in the technique difficulties for the analysis of such systems and design of the state estimators as well (see [24], [25]).

2.2 State Estimation for Finite Dimensional Process Systems

2.2.1 Model Description

Let us consider the following linear time-invariant system:

$$\dot{x}(t) = Ax(t) + Bu(t) + G\xi(t),\ x(0) = x_0 \tag{2.1a}$$

$$y(t) = Cx(t) + \eta(t) \tag{2.1b}$$

where $x(t) \in \mathbb{R}^n$, $u(t) \in \mathbb{R}$, $y(t) \in \mathbb{R}$ are the state, input and output, respectively and $A \in \mathbb{R}^{n\times n}$, $B \in \mathbb{R}^{n\times 1}$, $G \in \mathbb{R}^{n\times 1}$, and $C \in \mathbb{R}^{1\times n}$ are the state, input, disturbance and output matrices, respectively. $\xi(t)$ and $\eta(t)$ are the zero-mean random processes with the following stochastic properties:

$$\begin{aligned}
&E(\xi(t)) = 0, E(\xi(t)\xi(\tau)^T) = R^{-1}(t)\delta(t-\tau)\\
&E(\eta(t)) = 0, E(\eta(t)\eta(\tau)^T) = Q^{-1}(t)\delta(t-\tau)\\
&E(\xi(t)\eta(\tau)^T) = 0
\end{aligned} \tag{2.2}$$

where $E(\xi(t))$ and $E(\eta(t))$ are the mean of $\xi(t)$ and $\eta(t)$.

The state $x(t)$ in system (2.1) is subjected to the following constraint:

$$\mathcal{X}^{\min} \le \Gamma x(t) \le \mathcal{X}^{\max} \tag{2.3}$$

where $\Gamma \in \mathbb{R}^{1\times n}$ is a vector.

2.2.2 State Estimation Formulation

In this section, based on system (2.1), we formulate the constrained optimal state estimation problem as the solution to the following quadratic optimization problem:

$$\min_{\hat{x}(t)} \; J(\hat{x}(t)) \tag{2.4}$$

where the objective function is defined by:

$$\begin{aligned}
&J(\hat{x}(t)) = \tfrac{1}{2}[\hat{x}(0) - x_0]^T P_0^{-1}[\hat{x}(0) - x_0] + \\
&\tfrac{1}{2}\int_0^{t_f} \left\{ \left(\dot{\hat{x}}(t) - A\hat{x}(t) - Bu(t)\right)^T G^T R(t) G \left(\dot{\hat{x}}(t) - A\hat{x}(t) - Bu(t)\right) \right\} dt + \\
&\tfrac{1}{2}\int_0^{t_f} \left\{ (y(t) - C\hat{x}(t))^T Q(t) \, (y(t) - C\hat{x}(t)) \right\} dt
\end{aligned}$$

subject to constraint:

$$\mathcal{X}^{\min} \leq \Gamma \hat{x}(t) \leq \mathcal{X}^{\max} \tag{2.5}$$

where t_f is terminal time, $\hat{x}(t)$ is the state estimate of $x(t)$, and $R(t)$, $Q(t)$ are chosen by means in (2.2) and P_0 is defined by:

$$E([\hat{x}(0) - x_0] \, [\hat{x}(0) - x_0]^T) = P_0 \tag{2.6}$$

We shall now define $U(t) = \dot{\hat{x}}(t) - A\hat{x}(t) - Bu(t)$ to convert the optimal state estimation problem to an optimal control problem:

$$\min_{U(t)} \; J(\hat{x}(t)) \tag{2.7}$$

where the objective function is defined by:

$$
\begin{aligned}
&J(\hat{x}(t)) = \tfrac{1}{2}[\hat{x}(0) - x_0]^T P_0^{-1}[\hat{x}(0) - x_0] + \\
&\tfrac{1}{2}\int_0^{t_f} \left\{ U(t)^T G^T R(t) G U(t) \right\} dt + \\
&\tfrac{1}{2}\int_0^{t_f} \left\{ (y(t) - C\hat{x}(t))^T Q(t) \left(y(t) - C\hat{x}(t)\right) \right\} dt
\end{aligned}
$$

subject to constraints:

$$\dot{\hat{x}}(t) = A\hat{x}(t) + Bu(t) + U(t),\ \hat{x}(0) \text{ unspecified} \tag{2.8}$$

$$\mathcal{X}^{\min} \leq \Gamma\hat{x}(t) \leq \mathcal{X}^{\max} \tag{2.9}$$

The essential problem of the optimal state constrained optimization given by (2.7), (2.8) and (2.9) can be reduced to two sub-optimization problems. The first problem is unconstrained optimization which is reflected in the condition that constraints given by equation (2.9) are not active, while the second problem has an equality constraints active and the optimal value is at the constrained boundary ($\Gamma\hat{x}(t) = X^{\max}$ or $\Gamma\hat{x}(t) = X^{\min}$). In other words, one performs the following two algorithmic steps:

(P.1) One solves the optimization problem (2.7) and (2.8) without the constraint (2.9). Then, one inspects if the results satisfy the constraint (2.9). If the results satisfy the constraint, then the estimation is completed at the current estimation time instant. Otherwise, we proceed to step (P.2). In other words, the constraints are not active.

(P.2) In this step, one inspects which side of the constraint (2.9) is not satisfied. In the case that the results do not satisfy the lower side of (2.9), one needs to resolve the inequality constrained optimization problem (2.7) and (2.8) subject to the lower side of (2.9): $\mathcal{X}^{\min} \leq \Gamma\hat{x}(t)$. According to Section 11.2.2 of [26], in this step, the inequality constrained optimization problem can be converted into an equality constrained optimization problem:

$$\min J(\hat{x}(t)) \ \text{ s.t. } \ (2.8) \ \text{ and } \ S_{\min}(\hat{x}, t) = -\Gamma\hat{x}(t) + \mathcal{X}^{\min} = 0 \tag{2.10}$$

Similarly, if the estimation results do not satisfy the upper side of (2.9), one needs to resolve the inequality constrained optimization problem (2.7) and (2.8) subject to the upper side of (2.9): $\Gamma\hat{x}(t) \leq \mathcal{X}^{\max}$, which can be converted into an equality constrained optimization problem:

$$\min J(\hat{x}(t)) \ \text{ s.t. } \ (2.8) \ \text{ and } \ S_{\max}(\hat{x}, t) = -\Gamma\hat{x}(t) + \mathcal{X}^{\max} = 0 \tag{2.11}$$

1). In step (P.1), we directly formulate the unconstrained state estimator according to [3] and the formulations will be given at the end of this section.

2). In step (P.2), we embed the equality constraints within the Ray's optimal state estimation framework. Essentially, the problems (2.10) and (2.11) are the same. In this chapter, we use the problem (2.10) as a representative to illustrate the derivation of the formulation and finally we directly give the formulation for the case (2.11).

Remark 1. *From (P.1) and (P.2), the activation of the constraints is based on the results of the unconstrained solution. Once the unconstrained solution locates at out of the feasible set, the constraints are activated, i.e., (2.10) or (2.11) needs to be resolved. The equality constraint in (2.10) or (2.11) indicates that the solution at the boundary of feasible set is selected. This may result in sub-optimal solution. However, because of the specific form of objective function (2.4), in most cases, this selection is still able to provide a good solution. Therefore, the proposed method in this chapter can provide a better estimation results than the unconstrained state estimation method.*

According to [27], it is easier to deal with the equality constrained optimal control problems through the variational method when the constraint function contains explicit expression of the control variable, i.e. $U(t)$ which is the case in this chapter.

Consider the constraint:

$$S_{\min}(\hat{x}, t) = -\Gamma \hat{x}(t) + \mathcal{X}^{\min} = 0 \tag{2.12}$$

Since the constraint function $S_{\min}(\hat{x}, t)$ in (2.12) does not contain the explicit expression of $U(t)$, an additional formulation needs to be developed. If this constraint (2.12) is applied for all $0 \leq t \leq t_f$, its time derivative along the path must vanish, i.e.,

$$\frac{dS_{\min}(\hat{x}, t)}{dt} = \frac{\partial S_{\min}}{\partial t} + \frac{\partial S_{\min}}{\partial \hat{x}} \dot{\hat{x}} = 0 \tag{2.13}$$

Substituting (2.8) into (2.13), one obtains

$$\Gamma A \hat{x}(t) + \Gamma B u(t) + \Gamma U(t) = 0 \tag{2.14}$$

Apparently, the (2.14) has explicit dependence on $U(t)$ and thus plays the role of a control variable constraint similar to the type (3.3.1) shown in [27]. In this case, we formulate the minimization problem as:

$$\min J(\hat{x}(t)) \;\text{ s.t. }\; (2.8) \;\text{ and }\; \Gamma A \hat{x}(t) + \Gamma B u(t) + \Gamma U(t) = 0 \tag{2.15}$$

We first formulate the augmented Hamiltonian:

$$\begin{aligned} H = {} & \tfrac{1}{2} U^T(t) R_G U(t) + \tfrac{1}{2} (y(t) - C\hat{x}(t))^T Q \, (y(t) - C\hat{x}(t)) \\ & + \lambda^T(t) \left[A\hat{x}(t) + Bu(t) + U(t) \right] \\ & - \mu(t) \left[\Gamma A \hat{x}(t) + \Gamma B u(t) + \Gamma U(t) \right] \end{aligned}$$

where $R_G(t) = G^T R(t) G$, λ is a Lagrange multiplier vector and μ is a Lagrange multiplier scalar. The last term of Hamiltonian originates from the (2.14). Meanwhile, it is necessary to let $\hat{x}(t)$ satisfy (2.12).

In order to ensure the solvability of a constrained minimization problem, the following three conditions have to be satisfied:

$$
\begin{aligned}
&(\text{c.1}) \;\; \frac{\partial H}{\partial U} = U^T(t)R_G + \lambda^T(t) - \mu(t)\Gamma = 0 \\
&(\text{c.2}) \;\; \dot{\lambda}(t) = C^T Q\left(y(t) - C\hat{x}(t)\right) - A^T\lambda(t) + (\Gamma A)^T \mu(t) \\
&(\text{c.3}) \;\; \lambda(t_f) = 0
\end{aligned}
$$

Remark 2. *The most challenging part in the section associated with estimation of constrained linear systems is how to embed the equality constraint (2.12) into the framework. According to Section 3.4 of [27], one can easily solve the problem (2.10) by setting the initial conditions of $\hat{x}(t)$ to satisfy (2.12) and solving the problem (2.15). In the realization of the state estimation process, one can regard the state estimation results at the last estimation time instant as the initial conditions of $\hat{x}(t)$ at the current estimation time instant. Particularly, when the state estimation results are around the constraint, i.e. (2.12) at the last estimation time instant, one can formulate solutions for (2.15) such that the state estimation results satisfy (2.12), since the initial conditions at the current estimation time instant satisfy constraint (2.12) approximately.*

In order to drive $\hat{x}(t)$ to satisfy constraint (2.12) exactly, we take constraint (2.12) into the conditions (c.1-c.2-c.3) and obtain the following extended conditions:

$$
\begin{aligned}
&(c_e.1) \;\; \frac{\partial H}{\partial U} = U^T(t)R_G + \lambda^T(t) - \mu(t)\Gamma = 0 \\
&(c_e.2) \;\; \dot{\lambda}(t) = C^T Q\left(y(t) - C\hat{x}(t) + \Gamma\hat{x}(t) - \mathcal{X}^{\min}\right) - A^T\lambda(t) + (\Gamma A)^T \mu(t) \\
&(c_e.3) \;\; \lambda(t_f) = 0
\end{aligned}
$$

From $(c_e.1)$ and (2.14), we can calculate:

$$\mu(t) = \left(\Gamma R_G^{-1}\Gamma^T\right)^{-1}\left[\Gamma R_G^{-1}\lambda(t) - A\hat{x}(t) - \Gamma Bu(t)\right] \tag{2.16}$$

Based on (2.8), (c_e.2) and (2.16), it is easy to formulate the following coupled ordinary differential equations:

$$
\begin{aligned}
&\dot{\hat{x}}(t) = A\hat{x}(t) + Bu(t) - R_G^{-1}\lambda(t) \\
&+R_G^{-1}\Gamma^T\big(\Gamma R_G^{-1}\Gamma^T\big)^{-1}\big(\Gamma R_G^{-1}\lambda(t) - \Gamma A\hat{x}(t) - \Gamma Bu(t)\big)
\end{aligned}
\tag{2.17}
$$

$$
\begin{aligned}
&\dot{\lambda}(t) = C^T Q\left(y(t) - C\hat{x}(t) + \Gamma\hat{x}(t) - \mathcal{X}^{\min}\right) - A^T\lambda(t) \\
&+(\Gamma A)^T\big(\Gamma R_G^{-1}\Gamma^T\big)^{-1}\big(\Gamma R_G^{-1}\lambda(t) - \Gamma A\hat{x}(t) - \Gamma Bu(t)\big)
\end{aligned}
\tag{2.18}
$$

To produce the filter equations, we need to utilize the more explicit notations $\hat{x}(t|t_f), \lambda(t|t_f)$ denoting the optimal estimates and adjoint variables at time t, which is conditional on data $y(t)$ up to time t_f. According to [3], we have:

$$
\frac{d\hat{x}(t_f|t_f)}{dt_f} = \hat{x}_t(t_f|t_f) + \hat{x}_{t_f}(t_f|t_f) \tag{2.19}
$$

where $\hat{x}_t(t_f|t_f) = \frac{\partial\hat{x}(t|t_f)}{\partial t}\Big|_{t=t_f}$, $\hat{x}_{t_f}(t_f|t_f) = \frac{\partial\hat{x}(t_f|T)}{\partial T}\Big|_{T=t_f}$, where $\frac{\partial\hat{x}(t|t_f)}{\partial t}$ denotes the rate of change of the estimate at time t with fixed data base and $\frac{\partial\hat{x}(t_f|T)}{\partial T}$ denotes the rate of change of the estimate at time t_f with increasing data at time T.

According to the form of equation (2.17), we note that $\hat{x}(t|t_f)$ is a function of $\lambda(t|t_f)$, i.e.:

$$
\hat{x}(t|t_f) = \hat{x}(\lambda(t|t_f)) \tag{2.20}
$$

If we apply the chain rule in (2.20), we obtain derivative of optimal state estimation conditional on data t_f and with respect to t_f:

$$
\frac{\partial\hat{x}(t|t_f)}{\partial t_f} = \frac{\partial\hat{x}(t|t_f)}{\partial\lambda(t|t_f)}\frac{\partial\lambda(t|t_f)}{\partial t_f} = -P(t|t_f)\frac{\partial\lambda(t|t_f)}{\partial t_f} \tag{2.21}
$$

Applying the same decomposition property to $\lambda(t|t_f)$, we have:

$$\frac{d\lambda(t_f|t_f)}{dt_f} = \lambda_t(t_f|t_f) + \lambda_{t_f}(t_f|t_f) = \left.\frac{\partial\lambda(t|t_f)}{\partial t}\right|_{t=t_f} + \left.\frac{\partial\lambda(t_f|T)}{\partial T}\right|_{T=t_f} \tag{2.22}$$

Combining (2.17)-(2.22) and (c_e.3), we finally obtain:

$$\begin{aligned}\dot{\hat{x}}(t_f|t_f) &= A\hat{x}(t_f|t_f) + Bu(t_f) - R_G^{-1}\Gamma^T\left(\Gamma R_G^{-1}\Gamma^T\right)^{-1}\left(\Gamma A\hat{x}(t_f|t_f) + \Gamma Bu(t_f)\right)\\ &+P(t_f|t_f)C^TQ\left(y(t_f) - C\hat{x}(t_f|t_f) + \Gamma\hat{x}(t_f|t_f) - \mathcal{X}^{\min}\right)\\ &-P(t_f|t_f)(\Gamma A)^T\left(\Gamma R_G^{-1}\Gamma^T\right)^{-1}\left(\Gamma A\hat{x}(t_f|t_f) + \Gamma Bu(t_f)\right)\end{aligned} \tag{2.23}$$

Then, the state estimation equation has the form:

$$\begin{aligned}\dot{\hat{x}}(t) &= A\hat{x}(t) + Bu(t) - R_G^{-1}\Gamma^T\left(\Gamma R_G^{-1}\Gamma^T\right)^{-1}\left(\Gamma A\hat{x}(t) + \Gamma Bu(t)\right)\\ &+P(t)C^TQ\left(y(t) - C\hat{x}(t) + \Gamma\hat{x}(t) - \mathcal{X}^{\min}\right)\\ &-P(t)(\Gamma A)^T\left(\Gamma R_G^{-1}\Gamma^T\right)^{-1}\left(\Gamma A\hat{x}(t) + \Gamma Bu(t)\right)\end{aligned} \tag{2.24}$$

Now we proceed with the differential sensitivities $P(t_f|t_f)$. It can be noted that

$$\frac{\partial}{\partial t}\left[\frac{\partial\hat{x}(t|t_f)}{\partial t_f}\right] = \frac{\partial}{\partial t_f}\left[\frac{\partial\hat{x}(t|t_f)}{\partial t}\right] \tag{2.25}$$

$$\frac{\partial}{\partial t}\left[\frac{\partial\lambda(t|t_f)}{\partial t_f}\right] = \frac{\partial}{\partial t_f}\left[\frac{\partial\lambda(t|t_f)}{\partial t}\right] \tag{2.26}$$

With the help of (2.21), (2.25) and (2.18), the left side of (2.25) can be derived as:

$$\begin{aligned}\tfrac{\partial}{\partial t}\left[\hat{x}_{t_f}(t|t_f)\right] &= -\tfrac{\partial}{\partial t}\left[P(t|t_f)\lambda_{t_f}(t_f|t_f)\right]\\ &= -\big[P_t(t|t_f) + P(t|t_f)C^TQ\left(C-\Gamma\right)P(t|t_f) - P(t|t_f)A^T\\ &+P(t|t_f)(\Gamma A)^T\left(\Gamma R_G^{-1}\Gamma^T\right)^{-1}\left(\Gamma R_G^{-1} + \Gamma AP(t|t_f)\right)\big]\lambda_{t_f}(t|t_f)\end{aligned} \tag{2.27}$$

The right side of (2.25) can be calculated through (2.17) as:

$$\frac{\partial}{\partial t_f}\left[\hat{x}_t(t|t_f)\right] = \left[R_G^{-1}\Gamma^T\left(\Gamma R_G^{-1}\Gamma^T\right)^{-1}\left(\Gamma R_G^{-1} + \Gamma AP(t|t_f)\right) - AP(t|t_f) - R_G^{-1}\right]\lambda_{t_f}(t|t_f) \tag{2.28}$$

From (2.25), (2.27) and (2.28), we see that for (2.25) to hold for all $\lambda_{t_f}(t|t_f)$ the coefficient of $\lambda_{t_f}(t|t_f)$ must vanish and then the formulation of $P_t(t|t_f)$ can be obtained. Usually, we use $P_t(t|t_f)$ to represent $P_t(t_f|t_f)$ and as a result the differential sensitivities have the approximate solution:

$$\begin{aligned}\dot{P}(t) &= AP(t) + P(t)A^T + R_G^{-1} - R_G^{-1}\Gamma^T\left(\Gamma R_G^{-1}\Gamma^T\right)^{-1}\left(\Gamma R_G^{-1} + \Gamma AP(t)\right)\\ &\quad -P(t)C^TQ\left(C-\Gamma\right)P(t) - P(t)(\Gamma A)^T\left(\Gamma R_G^{-1}\Gamma^T\right)^{-1}\left(\Gamma R_G^{-1} + \Gamma AP(t)\right)\end{aligned} \tag{2.29}$$

Using the same formulation as in [3], the initial conditions are:

$$\hat{x}(0) = x_0,\ P(0) = P_0 \tag{2.30}$$

Hereto, we completed derivation of the solution to problem (2.10) in step (P.2). Similarly, one can easily provide the solution for the problem (2.11). To sum up, at every estimation time instant, we may need to perform two steps (P.1)-(P.2). At every estimation time instant, one can first perform step (P.1). In step (P.1), one can directly apply the method presented by Ray and the state estimation equation, and the approximate differential sensitivities are given as (for further details, see [3]):

$$\begin{aligned}&\dot{\hat{x}}(t) = A\hat{x}(t) + Bu(t) + P(t)C^TQ(y(t) - C\hat{x}(t))\\ &\dot{P}(t) = P(t)A^T + AP(t) + R_G^{-1}(t) - P(t)C^TQCP(t),\ \ P(0) = P_0\end{aligned} \tag{2.31}$$

After step (P.1), one inspects if or not the unconstrained state estimation results satisfy the constraint $\mathcal{X}^{\min} \leq \Gamma\hat{x}(t) \leq \mathcal{X}^{\max}$. In the case that the estimation results do not satisfy the constraint, one proceeds to perform step (P.2). In step (P.2), when the results do not satisfy

$\mathcal{X}^{\min} \leq \Gamma\hat{x}(t)$, one performs the formulation (2.24) and (2.29) to guarantee the estimation within the constraint. Similarly, when the estimation results do not satisfy the constraint $\Gamma\hat{x}(t) \leq \mathcal{X}^{\max}$, one performs the following formulations, which are solutions to the problem (2.11):

$$\begin{aligned}\dot{\hat{x}}(t) = A\hat{x}(t) + Bu(t) - R_G^{-1}\Gamma^T\left(\Gamma R_G^{-1}\Gamma^T\right)^{-1}\left(\Gamma A\hat{x}(t) + \Gamma Bu(t)\right)\\ +P(t)C^TQ\left(y(t) - C\hat{x}(t) + \Gamma\hat{x}(t) - \mathcal{X}^{\max}\right)\\ -P(t)(\Gamma A)^T\left(\Gamma R_G^{-1}\Gamma^T\right)^{-1}\left(\Gamma A\hat{x}(t) + \Gamma Bu(t)\right),\ \hat{x}(0) = x_0\end{aligned} \tag{2.32}$$

$$\begin{aligned}\dot{P}(t) = AP(t) + P(t)A^T + R_G^{-1} - R_G^{-1}\Gamma^T\left(\Gamma R_G^{-1}\Gamma^T\right)^{-1}\left(\Gamma R_G^{-1} + \Gamma AP(t)\right)\\ -P(t)C^TQ\left(C - \Gamma\right)P(t) - P(t)(\Gamma A)^T\left(\Gamma R_G^{-1}\Gamma^T\right)^{-1}\left(\Gamma R_G^{-1} + \Gamma AP(t)\right),\ P(0) = P_0\end{aligned} \tag{2.33}$$

2.3 State Estimation for Dissipative Infinite-Dimensional Systems

In many dissipative PDE processes, there exist constraints with respect to the state in the form of inequalities which arise from the safety, performance or product quality requirements. Moreover, within dissipative PDE systems, the Pritchard-Salamon class of linear infinite-dimensional systems involve boundary actuation and point observation, which brings mathematic difficulties for the analysis of such systems and design of the state estimators. Motivated by this, we extend the finite dimensional constrained optimal state estimation framework to the Pritchard-Salamon class of PDE systems. In this section, we utilize the modal analysis technique to represent the original dissipative PDE system dynamics as the combination of a computable finite-dimensional subsystem and its infinite-dimensional complement. With the aid of state bound of stable infinite-dimensional complement (see equation (2.49)), we include the state evolution of infinite-dimensional complement subsystem. Then, we formulate the constrained optimal state estimation problem for finite-dimensional subsystem which is augmented by the information from the infinite-dimensional complement.

2.3.1 Model Description

Let us consider the following Pritchard-Salamon infinite-dimensional system which is given by boundary controlled dissipative PDE systems:

$$\dot{x}(t) = \mathcal{A}x(t) + \mathcal{G}\xi(t),\ x(0) = x_0 \in D(\mathcal{A}) \tag{2.34a}$$

$$\mathcal{B}x(t) = u_b(t) \tag{2.34b}$$

$$y(t) = \mathcal{C}x(t) + \eta(t) \qquad t > 0 \tag{2.34c}$$

where $x(t) \in X$ is the state and the state space X is a separable Hilbert space $L^2(0,1)$, $u_b(t)$ is the input in the real Hilbert space U_b, and $y(t)$ is the output in the real Hilbert space Y. The operator $\mathcal{A} : D(\mathcal{A}) \subset X \to X$ is an unbounded linear self-adjoint operator and satisfies the spectrum decomposition assumption, and $\mathcal{B}$ and $\mathcal{C}$ are unbounded linear operators on X taking values in Hilbert spaces U_b and Y, respectively. The distributed disturbance operator $\mathcal{G} \in \mathcal{L}(\Psi, X)$ is bounded on X. The process disturbance: $\xi(t) \in \Psi$ in the real Hilbert space Ψ is bounded, i.e. $\|\xi(t)\| \leq u_n$ and has the same stochastic property as in (2.2), where u_n is a positive constant. The measurement noise is $\eta(t) \in \Omega$ and has the same stochastic property as in (2.2). The measurement noise space Ω is a real Hilbert space, i.e. $\Omega \subset R$.

Definition 1. *[28]. If the set $\sigma_u(A)$ is bounded and is separated from the set $\sigma_s(A)$ in such a way that a rectifiable, simple, closed curve can be drawn so as to enclose an open set containing $\sigma_u(A)$ in its interior and $\sigma_s(A)$ in its exterior, then A is said to satisfy the spectrum decomposition assumption. where $\sigma_u(A) = \sigma(A), \{\lambda : \mathrm{Re}(\lambda) \geq -\delta\}$ and $\sigma_s(A) = \sigma(A), \{\lambda : \mathrm{Re}(\lambda) < -\delta\}$. $\sigma(A)$ denotes the spectrum of A and $\delta > 0$.*

Remark 3. *The systems with boundary control and point observation are very common. Without loss of generality, we consider these systems in the form of (2.34) in this chapter. However, in system (2.34), the unboundedness of operators $\mathcal{B}$ and $\mathcal{C}$ brings the mathematic difficulties. Therefore, we first convert (2.34) into a new system involving no unbounded* *operators except for the dynamic generator. According to [14], if we apply the change of variables $x(t) = p(t) + B_b u_b(t)$, for all $u_b \in U_b, \mathcal{B}B_b u_b = u_b$ and $\dot{u}_b(t) \in U_b$, then (2.34a) can be converted into the following form:*

$$\dot{p}(t) = Ap(t) + \mathcal{A}B_b u_b(t) - B_b \dot{u}_b(t) + \mathcal{G}\xi(t), p(0) = p_0 \tag{2.35}$$

$$\mathcal{B}p(t) = 0 \tag{2.36}$$

where $p(t) \in X$ is the replacement state and the operator $A : D(A) \to X$ is defined by $Ax = \mathcal{A}x$ for all $x \in D(A) = D(\mathcal{A}) \cap Ker\mathcal{B}$. A is an infinitesimal generator of a strongly continuous semigroup $T_A(t)$ on X. $B_b \in L(U_b, X)$ and for all $u_b \in U_b, B_b u_b \in D(\mathcal{A})$, the operator $\mathcal{A}B_b \in \mathcal{L}(U_b, X)$.

$\mathcal{C}$ is the point observation operator, i.e. $\mathcal{C} \in \mathcal{L}(X_1, Y)$, where $X_1 \in D(A)$ is equipped with the norm $\|x\|_1 = \|(\gamma I - A)\|$ for $\gamma \in \rho(A)$, where $\rho(A)$ is the resolvent of the operator A and we can define the operator $C_\beta x = \beta\mathcal{C}(\beta I - A)^{-1}x$. For any parameter β in $\rho(A)$, the resolvent operator $(\beta I - A)^{-1} \in \mathcal{L}(X, X_1)$ and $\mathcal{C} \in \mathcal{L}(X_1, Y)$. Therefore, $\beta\mathcal{C}(\beta I - A)^{-1} \in \mathcal{L}(X, Y)$, which implies that C_β is a bounded linear operator on X. In this chapter, we assume that the original system is an abstract regular system. Then, based on Theorem 5.8. and Remark 6.2. of [29], we can see that

$$\lim_{\beta \to +\infty} y_\beta(t) = \lim_{\beta \to +\infty} C_\beta x(t) = \mathcal{C}x(t) \tag{2.37}$$

Therefore, the output $y(t)$ in (2.34c) can be approximated by

$$y_\beta(t) = C_\beta p(t) + C_\beta B_b u_b(t) + \eta(t) \tag{2.38}$$

For the system (2.34), the state is subjected to the following constraint:

$$\mathcal{X}^{\min} \leq \Upsilon x(t) \leq \mathcal{X}^{\max} \tag{2.39}$$

where $\Upsilon \in \mathcal{L}(X, R)$ is an operator in Hilbert space X, where R is a real number space.

2.3.2 Model Decomposition

Since the operator A also satisfies the spectrum decomposition assumption, then according to [14] for any $p \in X$ there exists the projector

$$P_s p = \frac{1}{2\pi j} \int_{\Gamma} (\lambda I - A)^{-1} p d\lambda$$

where Γ is a rectifiable, closed, simple curve. If we define $P_f = I - P_s$, then $p_s(t) = P_s p(t)$, $p_f(t) = P_f p(t)$ and the system (2.35) and (2.38) can be rewritten in the following equivalent form

$$\dot{p}_s(t) = A_s p_s(t) + \mathcal{K}_s u_b(t) - B_{bs}\dot{u}_b(t) + \mathcal{G}_s \xi(t), \;\; p_s(0) = P_s p_0 \tag{2.40a}$$

$$\dot{p}_f(t) = A_f p_f(t) + \mathcal{K}_f u_b(t) - B_{bf}\dot{u}_b(t) + \mathcal{G}_f \xi(t), \;\; p_f(0) = P_f p_0 \tag{2.40b}$$

$$y_\beta(t) = C_{\beta s} p_s(t) + C_{\beta f} p_f(t) + C_\beta B_b u_b(t) + \eta(t) \tag{2.41}$$

where $A_s = P_s A$, $A_f = P_f A$, $\mathcal{K}_s = P_s \mathcal{A} B_b$, $\mathcal{K}_f = P_f \mathcal{A} B_b$, $B_{bs} = P_s B_b$, $B_{bf} = P_f B_b$, $\mathcal{G}_s = P_s \mathcal{G}$, $\mathcal{G}_f = P_f \mathcal{G}$, $C_{\beta s} = P_s C_\beta$, $C_{\beta f} = P_f C_\beta$. Here, (2.40a) is an $(N+1)$-dimensional subsystem which can capture the dynamics of the system (2.35) and (2.40b) is an infinite-dimensional subsystem. We denote by T_{A_s} and T_{A_f} the strongly continuous semigroup of the generator A_s and A_f, respectively. If we denote the orthonormal eigenfunctions of the operator A and corresponding eigenvalues by $\{\phi_0, \phi_1, \phi_2, \cdots\}$ and $\sigma(A) = \{\lambda_0, \lambda_1, \lambda_2, \cdots\}$, respectively, then

$$\sigma(A_s) = \{\lambda_0, \lambda_1, \cdots, \lambda_N\}, \;\; \sigma(A_f) = \{\lambda_{N+1}, \cdots\} \tag{2.42}$$

The states $p_s(t)$ and $p_f(t)$ have the unique representation

$$p_s(t) = \sum_{n=0}^{N} a_n(t)\phi_n, p_f(t) = \sum_{n=N+1}^{\infty} a_n(t)\phi_n, a_n(t) = \langle p(t), \phi_n \rangle_X \tag{2.43}$$

For $\mathcal{K}_s B_b u_b(t)$, $\mathcal{K}_f B_b u_b(t)$, $B_{bs}\dot{u}_b(t)$, $B_{bf}\dot{u}_b(t)$ and $\mathcal{G}_s\xi(t)$, and $\mathcal{G}_f\xi(t)$ in X, the unique representations are given as

$$\mathcal{K}_s u_b(t) = u_b(t)\sum_{n=0}^{N} k_n\phi_n, \;\; \mathcal{K}_f u_b(t) = u_b(t)\sum_{n=N+1}^{\infty} k_n\phi_n, \;\; k_n = \langle \mathcal{A}B_b, \phi_n \rangle_X \tag{2.44}$$

$$B_{bs}\dot{u}_b(t) = \dot{u}_b(t)\sum_{n=0}^{N} b_n\phi_n, \;\; B_{bf}\dot{u}_b(t) = \dot{u}_b(t)\sum_{n=N+1}^{\infty} b_n\phi_n, \;\; b_n = \langle B_b, \phi_n \rangle_X \tag{2.45}$$

$$\mathcal{G}_s\xi(t) = \xi(t)\sum_{n=0}^{N} c_n\phi_n, \;\; \mathcal{G}_f\xi(t) = \xi(t)\sum_{n=N+1}^{\infty} c_n\phi_n, \;\; c_n = \langle \mathcal{G}, \phi_n \rangle_X \tag{2.46}$$

Since for all $p \in X$ and for all $\beta \in \rho(A)$,

$$(\beta I - A)^{-1}p(t) = \sum_{n=0}^{+\infty} \frac{1}{\beta - \lambda_n} < p(t), \phi_n > \phi_n$$

Then, the output terms $C_\beta p(t)$ and $C_\beta B_b u_b(t)$ in (2.41) can be expressed:

$$C_{\beta s}p(t) = \sum_{n=0}^{N} a_n(t)d_n, \;\; C_{\beta f}p(t) = \sum_{n=N+1}^{\infty} a_n(t)d_n, \;\; d_n = \frac{\beta}{\beta - \lambda_n}\mathcal{C}\phi_n \tag{2.47a}$$

$$C_\beta B_b u_b(t) = u_b(t)\sum_{n=0}^{\infty} b_n d_n \tag{2.47b}$$

We regard the state $p_s(t)$ governed by the $(N+1)$-dimensional system (2.40a) as the estimated modes of the system (2.35) and the state $p_f(t)$ governed by the infinite dimensional system (2.40b) as the unestimated or residual modes of the system (2.35). One can demonstrate that the semigroup T_{A_f} satisfies the spectrum determined growth assumption and according to [28] we have

$$\left\|T_{A_f}(t)\right\| \leq Me^{-\sigma t},\ \sigma \leq -\lambda_n,\ n \geq N \tag{2.48}$$

Taking advantage of inequality (2.48), the following theorem holds.

Theorem 1. *For the infinite dimensional states $p_f(t)$, $\exists M > 0$, $\|\xi(t)\| \leq u_n$ and $\sigma \leq -\lambda_n$, we have the following inequality*

$$\|p_f(t)\| \leq Me^{-\sigma t}\,|p_f(0)| + \tfrac{M}{\sigma}\,\|\mathcal{K}_f u_b(t)\| + \tfrac{M}{\sigma}\,\|B_{bf}\dot{u}_b(t)\| + \tfrac{M}{\sigma}\,\|\mathcal{G}_f\|\,u_n \tag{2.49}$$

Proof. From (2.40b), it is easy to obtain

$$p_f(t) = T_{A_f}(t)p_f(0) + \textstyle\int_0^t T_{A_f}(t-\tau)\left(\mathcal{K}_f u_b(\tau) - B_{bf}\dot{u}_b(\tau) + \mathcal{G}_f\xi(\tau)\right)d\tau$$

According to the lemma 1 of [30], we get

$$\begin{aligned}
&\textstyle\int_0^\infty \left\|T_{A_f}(t)p_f(0)\right\|^2 dt \leq M^2 \int_0^\infty e^{-2\sigma t}\|p_f(0)\|^2 dt \\
&\textstyle\int_0^\infty \left\|\int_0^t T_{A_f}(t-\tau)\left(\mathcal{K}_f u_b(\tau) - B_{bf}\dot{u}_b(\tau) + \mathcal{G}_f\xi(\tau)\right)d\tau\right\|^2 dt \\
&\qquad \leq \tfrac{M^2}{\sigma^2}\textstyle\int_0^\infty \|\mathcal{K}_f u_b(t) - B_{bf}\dot{u}_b(t) + \mathcal{G}_f\xi(t)\|^2 dt
\end{aligned}$$

Therefore, from the inequalities and $\|\xi(t)\| \leq u_n$ for $t \in [0, \infty)$, the following relationship holds

$$\begin{aligned}
\|p_f(t)\| &\leq \left\|T_{A_f}(t)p_f(0)\right\| + \left\|\textstyle\int_0^t T_{A_f}(t-\tau)\left(\mathcal{K}_f u_b(\tau) - B_{bf}\dot{u}_b(\tau) + \mathcal{G}_f\xi(\tau)\right)d\tau\right\| \\
&\leq Me^{-\sigma t}\,|p_f(0)| + \tfrac{M}{\sigma}\,\|\mathcal{K}_f u_b(t) - B_{bf}\dot{u}_b(t) + \mathcal{G}_f\xi(t)\| \\
&\leq Me^{-\sigma t}\,|p_f(0)| + \tfrac{M}{\sigma}\,\|\mathcal{K}_f u_b(t)\| + \tfrac{M}{\sigma}\,\|B_{bf}\dot{u}_b(t)\| + \tfrac{M}{\sigma}\,\|\mathcal{G}_f\|\,u_n
\end{aligned}$$

Thus, the theorem is proved. □

Remark 4. *The equation $x(t) = p(t) + B_b u_b(t)$ implies that the state estimation problem for $x(t)$ is equivalent to the state estimation problem for $p(t)$. In this work, we proceed with the* *state estimation for infinite dimensional systems based on the decomposed extended system (2.40). In order to estimate the state $p(t)$ in the system (2.35), we need first to evaluate $p_s(t)$ and $p_f(t)$. However, $p_f(t)$ is unestimated. As the residual modes of the system (2.36), $p_f(t)$ is very small. Therefore, in this work, the $p_f(t)$ modes evolution is expressed by its upper bound: $Me^{-\sigma t}|p_f(0)| + \frac{M}{\sigma}\|\mathcal{K}_f u_b(t)\| + \frac{M}{\sigma}\|B_{bf}\dot{u}_b(t)\| + \frac{M}{\sigma}\|\mathcal{G}_f\| u_n$ in (2.49) and thus $p_f(t) \approx Me^{-\sigma t}|p_f(0)| + \frac{M}{\sigma}\|\mathcal{K}_f u_b(t)\| + \frac{M}{\sigma}\|B_{bf}\dot{u}_b(t)\| + \frac{M}{\sigma}\|\mathcal{G}_f\| u_n$.*

Applying (2.43)-(2.47) in (2.40)-(2.41) and according to Theorem 1 and Remark 3, the abstract state equation (2.40)-(2.41) can be written as following matrix representation

$$\dot{a}_s(t) = \Lambda_s a_s(t) + K_s u_b(t) + B_s \dot{u}_b(t) + G_s \xi(t) \tag{2.50a}$$

$$\begin{aligned} a_f(t) &\approx Me^{-\sigma t}|a_f(0)| + \tfrac{M}{\sigma}|K_f u_b(t)| \\ &\quad + \tfrac{M}{\sigma}|B_f \dot{u}_b(t)| + \tfrac{M}{\sigma}|G_f| u_n \end{aligned} \tag{2.50b}$$

$$a_s(0) = a_{s0},\ a_f(0) = a_{f0} \tag{2.50c}$$

$$y_\beta(t) = C_s a_s(t) + u_p(t) + \eta(t) \tag{2.50d}$$

where $a_s(t) = [a_0(t), a_1(t), a_2(t), \cdots, a_N(t)]^T$ comes from $p_s(t)$ in (2.40a) and $a_f(t) = [a_{N+1}(t), \cdots]^T$ correspond to $p_f(t)$ in (2.40b), a_{s0} and a_{f0} are from $p_s(0)$ and $p_f(0)$, respectively. $\Lambda_s = diag\{\lambda_0, \lambda_1, \cdots, \lambda_N\}$, $B_s = [-b_0, \cdots, -b_N]^T$, $K_s = [k_0, \cdots, k_N]^T$, $G_s = [c_0, \cdots, c_N]^T$, $C_s = [d_0, d_1, \cdots, d_N]^T$, $\Lambda_f = diag\{\lambda_{N+1}, \cdots\}$, $B_f = [b_{N+1}, \cdots]^T$, $K_f = [k_{N+1}, \cdots]^T$, $G_f = [c_{N+1}, \cdots]^T$, $C_f = [d_{N+1}, \cdots]^T$, $u_p(t) = Me^{-\sigma t}|C_f a_{f0}| + \frac{M}{\sigma}|C_f B_f \dot{u}_b(t)| + \frac{M}{\sigma}|C_f K_f u_b(t)| + \frac{M}{\sigma}|C_f G_f| u_n + C_\beta B_b u_b(t)$.

Applying the decomposition technique, the operator Υ in (2.39) can be expressed as the following:

$$\begin{aligned} \Upsilon x(t) &= \sum_{n=0}^{\infty} (\Upsilon\phi_n) a_n(t) + \Upsilon B_b u_b(t) \\ &= S_s a_s(t) + u_{sp}(t) \end{aligned} \tag{2.51}$$

where $S_s = \begin{bmatrix} \Upsilon\phi_0 & \Upsilon\phi_1 & \cdots & \Upsilon\phi_N \end{bmatrix}$, $S_f = \begin{bmatrix} \Upsilon\phi_{N+1} & \cdots \end{bmatrix}$ and $u_{sp}(t) = Me^{-\sigma t}|S_f a_{f0}| +$

$\frac{M}{\sigma}|S_f B_f \dot{u}_b(t)| + \frac{M}{\sigma}|S_f K_f u_b(t)| + \frac{M}{\sigma}|S_f G_f| u_n + \Upsilon B_b u_b(t)$.

Then the constraint (2.39) has the following form

$$\mathcal{X}^{\min} \leq S_s a_s(t) + u_{sp}(t) \leq \mathcal{X}^{\max} \tag{2.52}$$

2.3.3 State Estimation Formulation

In this section, based on the representation (2.50), we formulate the optimal state estimation problem for the dissipative PDE systems. We have shown that the state $a_f(t)$ can be approximated by its upper bound $\tilde{a}_f(t)$. Therefore, in this section, our target is to estimate $a_s(t)$ in the subsystem (2.50a) which is a finite-dimensional system. Naturally, we can extend the constrained optimal state estimation theory in previous section to this section.

After the estimation of $a_s(t)$, $\hat{a}_s(t)$, is obtained, we are able to utilize $\hat{a}_s(t)$, $\tilde{a}_f(t)$, equation (2.43) and $x(t) = p(t) + B_b u_b(t)$ to obtain the estimation of $x(t)$: $\hat{x}(t)$.

$$\begin{aligned} \hat{x}(t) &= \hat{p}(t) + B_b u_b(t) \\ &= \Phi_s \hat{a}_s + \Phi_f \tilde{a}_f + B_b u_b(t) \end{aligned} \tag{2.53}$$

where $\Phi_s = \begin{bmatrix} \phi_0 & \phi_1 & \cdots & \phi_N \end{bmatrix}$, $\Phi_f = \begin{bmatrix} \phi_{N+1} & \cdots \end{bmatrix}$ and $\tilde{a}_f = Me^{-\sigma t}|a_f(0)| + \frac{M}{\sigma}|K_f u_b(t)| + \frac{M}{\sigma}|B_f \dot{u}_b(t)| + \frac{M}{\sigma}|G_f| u_n$.

Then, we formulate the state estimation problem as the solution to the following quadratic optimization problem:

$$\min_{\hat{a}_s(t)} \; J(\hat{a}_s) \tag{2.54}$$

where the objective function J is defined by:

$$\begin{aligned}
&J(\hat{a}_s) = \tfrac{1}{2}[\hat{a}_s(0) - a_{s0}]^T P_0^{-1} [\hat{a}_s(0) - a_{s0}] \\
&+\tfrac{1}{2}\int_0^{t_f} \left\{ \left(\dot{\hat{a}}_s(t) - \Lambda_s \hat{a}_s(t) - K_s u_b(t) - B_s \dot{u}_b(t) \right)^T \right. \\
&\left. \times G_s^T R G_s \left(\dot{\hat{a}}_s(t) - \Lambda_s \hat{a}_s(t) - K_s u_b(t) - B_s \dot{u}_b(t) \right) \right\} dt \\
&+\tfrac{1}{2}\int_0^{t_f} \left\{ (y_\beta(t) - u_p(t) - C_s \hat{a}_s(t))^T Q \, (y_\beta(t) - u_p(t) - C_s \hat{a}_s(t)) \right\} dt
\end{aligned}$$

subject to the constraint:

$$\mathcal{X}^{\min} \leq S_s \hat{a}_s(t) + u_{sp}(t) \leq \mathcal{X}^{\max} \tag{2.55}$$

Let us now discuss the objective function. The weighted least squares objective to be considered along with the finite dimensional approximation is:

$$\begin{aligned}
&J(\hat{a}_s) = \tfrac{1}{2}[\hat{a}_s(0) - a_{s0}]^T P_0^{-1} [\hat{a}_s(0) - a_{s0}] \\
&+\tfrac{1}{2}\int_0^{t_f} \left\{ \left(\dot{\hat{a}}_s(t) - \Lambda_s \hat{a}_s(t) - K_s u_b(t) - B_s \dot{u}_b(t) \right)^T \right. \\
&\left. \times G_s^T R G_s \left(\dot{\hat{a}}_s(t) - \Lambda_s \hat{a}_s(t) - K_s u_b(t) - B_s \dot{u}_b(t) \right) \right\} dt \\
&+\tfrac{1}{2}\int_0^{t_f} \left\{ (y_\beta(t) - u_p(t) - C_s \hat{a}_s(t))^T Q \, (y_\beta(t) - u_p(t) - C_s \hat{a}_s(t)) \right\} dt
\end{aligned} \tag{2.56}$$

where $R(t), Q(t)$ are chosen the same as (2.2) and P_0 is defined as:

$$E([\hat{a}_s(0) - a_{s0}] \, [\hat{a}_s(0) - a_{s0}]^T) = P_0 \tag{2.57}$$

In this case, if we define $V(t) = \dot{\hat{a}}_s(t) - \Lambda_s \hat{a}_s(t) - K_s u_b(t) - B_s \dot{u}_b(t)$ and rewrite the objective function:

$$\begin{aligned}
J(\hat{a}_s) = {} & \tfrac{1}{2}[\hat{a}_s(0) - a_{s0}]^T P_0^{-1} [\hat{a}_s(0) - a_{s0}] \\
&+\tfrac{1}{2}\int_0^{t_f} \left\{ V^T(t) \; G_s^T R G_s V(t) \right\} dt \\
&+\tfrac{1}{2}\int_0^{t_f} \left\{ (y_\beta(t) - u_p(t) - C_s \hat{a}_s(t))^T Q \, (y_\beta(t) - u_p(t) - C_s \hat{a}_s(t)) \right\} dt
\end{aligned} \tag{2.58}$$

then, the optimal state estimation problem is converted to an optimal control problem, namely selecting the control $V(t)$ such that the objective function $J(\hat{a}_s)$ in (2.58) is minimized subject to:

$$\dot{\hat{a}}_s(t) = \Lambda_s \hat{a}_s(t) + K_s u_b(t) + B_s \dot{u}_b(t) + V(t),\ \hat{a}_s(0) \text{ unspecified} \tag{2.59}$$

$$\mathcal{X}^{\min} \leq S_s \hat{a}_s(t) + u_{sp}(t) \leq \mathcal{X}^{\max} \tag{2.60}$$

where the constraint (2.60) comes from (2.39)-(2.51).

By solving the optimization problem (2.58), (2.59) and (2.60), we can obtain the results of the optimal state estimation for the original infinite-dimensional system. Since the derivation in this section is similar to the derivation of the state estimation formulation in previous section, we directly give the state estimation solution in this section:

First, one solves the unconstrained optimization problem (2.58)-(2.59) without the constraint (2.60) and obtains the state estimation equation and the approximate differential sensitivities:

$$\begin{aligned} \dot{\hat{a}}_s(t) &= \Lambda_s \hat{a}_s(t) + K_s u_b(t) + B_s \dot{u}_b(t) \\ &\quad + P(t) {C_s}^T Q \left(y(t) - u_p(t) - C_s \hat{a}_s(t)\right),\ \hat{a}_s(0) = a_{s0} \end{aligned} \tag{2.61}$$

$$\dot{P}(t) = \Lambda_s P(t) + P(t) {\Lambda_s}^T + R_G^{-1} - P(t) {C_s}^T Q C_s P(t),\ P(0) = P_0 \tag{2.62}$$

Once the unconstrained result is obtained, one needs to inspect if the results satisfy the constraint (2.60). If the results do not satisfy the lower side of the constraint (2.60), one needs to reformulate the constrained optimization problem and obtains a new state estimation equation and the differential sensitivities:

$$\begin{aligned} \dot{\hat{a}}_s &= \Lambda_s \hat{a}_s(t) + K_s u_b(t) + B_s \dot{u}_b(t) \\ &\quad - R_G^{-1} S_s^T \left(S_s R_G^{-1} S_s^T\right)^{-1} \left[S_s \Lambda_s \hat{a}_s(t) + S_s K_s u_b(t) + S_s B_s \dot{u}_b(t) + \dot{u}_{sp}(t)\right] \\ &\quad + P(t) C_s^T Q \left(y(t) - C \hat{a}_s(t) + S_s \hat{a}_s(t) - u_p(t_f) + u_{sp}(t) - \mathcal{X}^{\min}\right) \\ &\quad - P(t) (S_s \Lambda_s)^T \left(S_s R_G^{-1} S_s^T\right)^{-1} \left(S_s \Lambda_s \hat{a}_s(t) + S_s K_s u_b(t) + S_s B_s \dot{u}_b(t) + \dot{u}_{sp}(t)\right) \\ \hat{a}_s(0) &= a_{s0} \end{aligned} \tag{2.63}$$

$$
\begin{aligned}
\dot{P}(t) &= \Lambda_s P(t) + P(t)\Lambda_s^T + R_G^{-1} - R_G^{-1}S_s^T\left(S_s R_G^{-1} S_s^T\right)^{-1}\left[S_s R_G^{-1} + S_s\Lambda_s P(t)\right] \\
&\quad - P(t)C_s^T Q\left(C - S_s\right)P(t) - P(t)(S_s\Lambda_s)^T\left(S_s R_G^{-1} S_s^T\right)^{-1}\left[S_s R_G^{-1} + S_s\Lambda_s P(t)\right] \\
P(0) &= P_0
\end{aligned} \tag{2.64}
$$

If the results do not satisfy the upper side of the constraint (2.60), one needs to reformulate the constrained optimization problem and obtains a new state estimation equation and the differential sensitivities:

$$
\begin{aligned}
\dot{\hat{a}}_s &= \Lambda_s \hat{a}_s(t) + K_s u_b(t) + B_s \dot{u}_b(t) \\
&\quad - R_G^{-1}S_s^T\left(S_s R_G^{-1} S_s^T\right)^{-1}\left[S_s\Lambda_s\hat{a}_s(t) + S_s K_s u_b(t) + S_s B_s \dot{u}_b(t) + \dot{u}_{sp}(t)\right] \\
&\quad + P(t)C_s^T Q\left(y(t) - C\hat{a}_s(t) + S_s\hat{a}_s(t) - u_p(t_f) + u_{sp}(t) - \mathcal{X}^{\max}\right) \\
&\quad - P(t)(S_s\Lambda_s)^T\left(S_s R_G^{-1} S_s^T\right)^{-1}\left(S_s\Lambda_s\hat{a}_s(t) + S_s K_s u_b(t) + S_s B_s \dot{u}_b(t) + \dot{u}_{sp}(t)\right) \\
\hat{a}_s(0) &= a_{s0}
\end{aligned} \tag{2.65}
$$

$$
\begin{aligned}
\dot{P}(t) &= \Lambda_s P(t) + P(t)\Lambda_s^T + R_G^{-1} - R_G^{-1}S_s^T\left(S_s R_G^{-1} S_s^T\right)^{-1}\left[S_s R_G^{-1} + S_s\Lambda_s P(t)\right] \\
&- P(t)C_s^T Q\left(C - S_s\right)P(t) - P(t)(S_s\Lambda_s)^T\left(S_s R_G^{-1} S_s^T\right)^{-1}\left[S_s R_G^{-1} + S_s\Lambda_s P(t)\right] \\
P(0) &= P_0
\end{aligned} \tag{2.66}
$$

where $R_G = G_s^T R G_s$.

At every time instant of the estimation realization, we utilize the unconstrained formulation (2.61)-(2.62) to obtain the estimation result. Then, we inspect if the result satisfies the constraint (2.60). If the result satisfies the constraint, the estimation is completed at the current estimation time instant. Otherwise, if the result does not satisfy the lower side of the constraint (2.60): $\mathcal{X}^{\min} \leq S_s a_s(t) + u_{sp}(t)$, we need to utilize formulation (2.63)-(2.64) to resolve estimation problem. In other words, if the result does not satisfy the upper side of the constraint (2.60): $S_s a_s(t) + u_{sp}(t) \leq \mathcal{X}^{\max}$, we need to utilize formulation (2.65)-(2.66) to resolve estimation problem. Once we obtain the estimation result satisfying the constraint (2.60), we start to proceed with the next time instant state estimation and use the formulation (2.61)-(2.66) again.

2.4 Simulation Study

In this section, two numerical examples illustrating the implementation of the constrained optimal state estimation framework are presented.

Example 1- Consider the coupled ODE systems:

$$\begin{aligned} \tfrac{dx_1(t)}{dt} &= -(1+Da_1)x_1(t) + Da_2 x_2(t) + \xi(t) \\ \tfrac{dx_2(t)}{dt} &= Da_1 x_1(t) - (1 + Da_2 + Da_3)\, x_2(t) + u(t) + \xi(t) \end{aligned} \tag{2.67}$$

$$x_1(0) = x_{10}, \;\; x_2(0) = x_{20} \tag{2.68}$$

$$y(t) = x_2(t) + \eta(t) \tag{2.69}$$

where $Da_1 = 40$, $Da_2 = 0.5$, $Da_3 = 1$ $x_{10} = 1.0$ and $x_{20} = 0$. $\xi(t)$ and $\eta(t)$ are zero mean random processes and have the following stochastic property:

$$\begin{aligned} &E(\xi(t)) = 0, R^{-1}(t) = E(\xi(t)\xi(t)^T) = 2.2615 \\ &E(\eta(t)) = 0, Q^{-1}(t) = E(\eta(t)\eta(\tau)^T) = 0.2457 \\ &E(\xi(t)\eta(\tau)^T) = 0 \end{aligned}$$

We shall now use the state space form of (2.1) to express the example system as,

$$x(t) = \begin{bmatrix} x_1(t) & x_2(t) \end{bmatrix}^T$$

$$\begin{aligned} A &= \begin{bmatrix} -(1+Da_1) & Da_2 \\ Da_1 & -(1+Da_2+Da_3) \end{bmatrix} \\ B &= \begin{bmatrix} 0 \\ 1 \end{bmatrix}, \;\; G = \begin{bmatrix} 1 \\ 1 \end{bmatrix}, \;\; C = \begin{bmatrix} 0 & 1 \end{bmatrix} \end{aligned}$$

Essentially, we can regard the system (2.67) as a finite-dimensional model for the continuous-stirred tank reactor in which the following isothermal multi-component chemical reaction is carried out:

$$A \rightleftarrows B \rightarrow C$$

The states $x(t)$ of the system (2.67) denote the concentrations. Consequently, it is reasonable that we assume that the state constraint is $0 < \Gamma x(t) \leq 0.75$, where $\Gamma = \begin{bmatrix} 0 & 1 \end{bmatrix}$, i.e. $0 < x_2(t) \leq 0.75$. In order to make the system (2.67) satisfy the constraint: $0 < x_2(t) \leq 0.75$, we apply the constrained MPC technique to guarantee the state $x_2(t)$ to stay within $(0, 0.75]$, see Fig.(2.1).

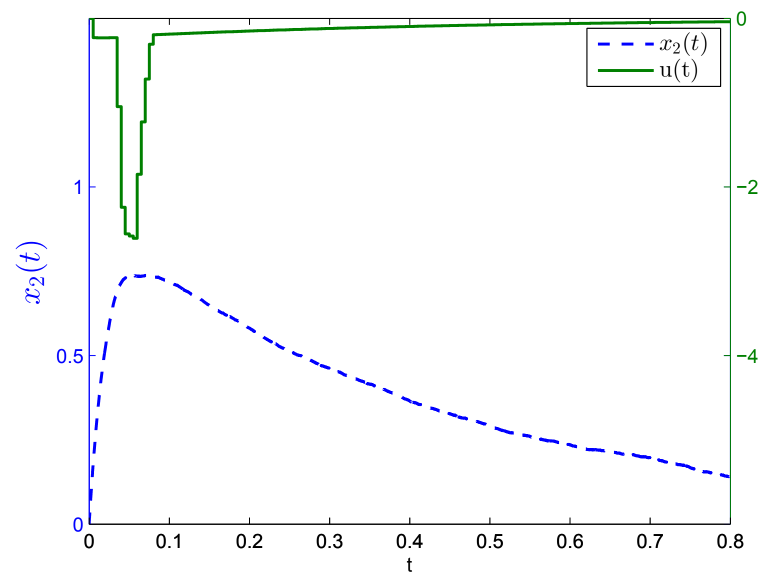

Figure 2.1: Manipulated input $u(t)$ (solid line) and state $x_2(t)$ (dashed line) under the formulation of constrained MPC calculated in [1].

We set the initial value of the estimation state as $\hat{x}(0) = \begin{bmatrix} 1.2 & 0.1 \end{bmatrix}^T$ and the initial value of the sensitivities matrix as $P_0 = E([\hat{x}(0) - x_0] [\hat{x}(0) - x_0]^T)$.

To compare with the unconstrained optimal state estimation method, we apply the constrained optimal state estimation method to the system.

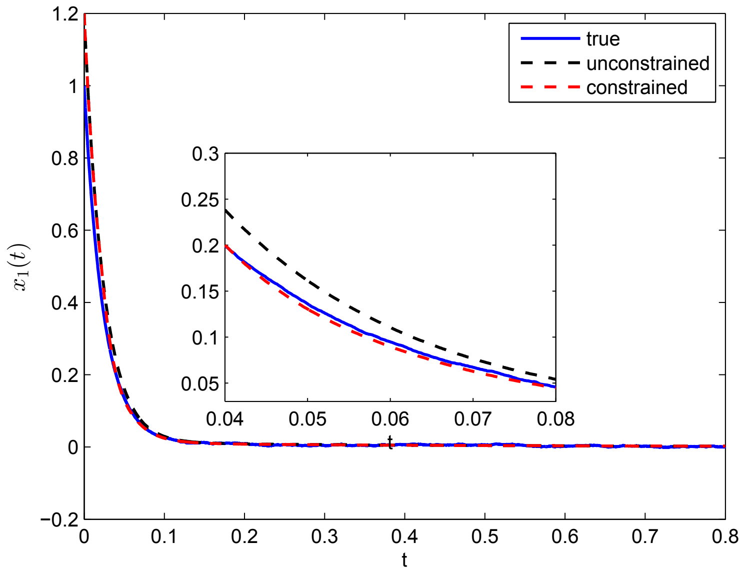

Figure 2.2: State $x_1(t)$, the unconstrained estimation of $x_1(t)$ under the formulation (2.31) and constrained state estimation under the formulation (2.31), (2.24), (2.29), and (2.32)-(2.33).

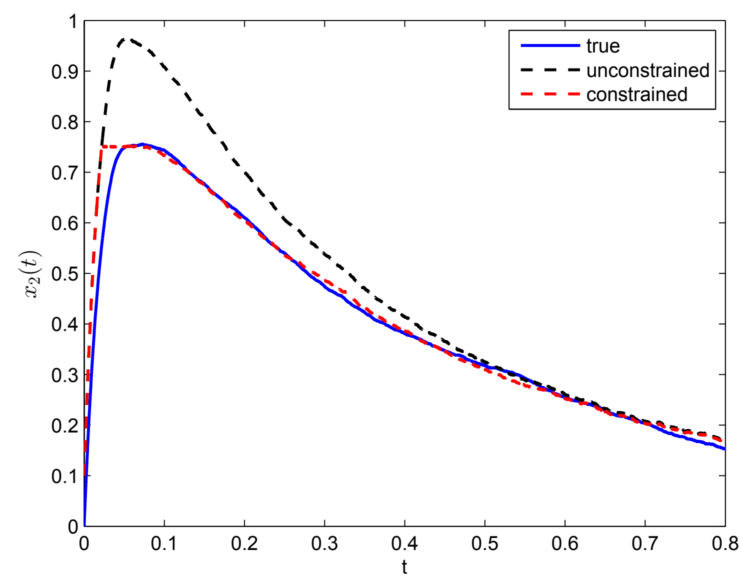

Figure 2.3: State $x_2(t)$, the unconstrained estimation of $x_2(t)$ under the formulation (2.31) and constrained state estimation under the formulation (2.31), (2.24), (2.29), and (2.32)-(2.33).

In Fig.(2.3), we can see that under the framework of constrained state estimation the estimation of state $x_2(t)$ is much closer to the actual state of the example system. Moreover, in Fig.(2.2), the estimation of state $x_1(t)$ is closer to the actual state of the system under the constrained state estimation formulation.

Example 2- In this section we consider a representative example of a heat conduction system described by following dimensionless parabolic PDE system which belongs to the class of Pritchard-Salamon systems (see [25]), e.g., systems with boundary actuation and point observation:

$$\frac{\partial x(z,t)}{\partial t} = \frac{\partial^2 x(z,t)}{\partial z^2} + \xi(t),\ x(z,0) = sin(2\pi z) \tag{2.70a}$$

$$\frac{\partial x(0,t)}{\partial z} = 0,\ \ \frac{\partial x(1,t)}{\partial z} = u_b(t) \tag{2.70b}$$

$$y(t) = x(1,t) + \eta(t) \tag{2.70c}$$

$$\mathcal{X}^{\min} \leq \Upsilon x(z,t) \leq \mathcal{X}^{\max} \tag{2.70d}$$

where $t \geq 0$ and $z \in [0,1]$ are the temporal and spatial variable, respectively. The state of system $x(z,t) \in X$ denotes the temperature profiles, where $X = L^2(0,1)$ is the separable Hilbert space. The operator Υ is defined as $\Upsilon x(z,t) = x(1,t)$, $x(z,t) \in L^2(0,1)$ and $\mathcal{X}^{\min} = -0.4$, $\mathcal{X}^{\max} = 1.5$. $u_b(t)$ is the heat flux entering the system at the boundary point $z = 1$ and $y(t)$ is the measurement of temperature at the boundary point $z = 1$. In this example, for simplification, we assume that the process disturbance $\xi(t)$ is uniform in the spatial space $z \in [0,1]$. $\xi(t)$ and $\eta(t)$ are zero mean random processes and have following stochastic property:

$$\begin{aligned}
&E(\xi(t)) = 0, R^{-1}(t) = E(\xi(t)\xi(t)^T) = 24.7166\\
&E(\eta(t)) = 0, Q^{-1}(t) = E(\eta(t)\eta(\tau)^T) = 0.0035\\
&E(\xi(t)\eta(\tau)^T) = 0
\end{aligned}$$

The dynamic system (2.70) can be interpreted under the general state differential equation described by (2.34). There operator $\mathcal{A} : D(\mathcal{A}) \subset L^2(0,1) \to L^2(0,1)$ is given by $\mathcal{A}x = \frac{\partial^2 x}{\partial z^2}$ on its domain:

$$D(\mathcal{A}) = \left\{ x \in L^2(0,1), x, \frac{dx}{dz} \text{ are a.c}, \frac{dx}{dz}(0) = 0,\ \frac{d^2x}{dz^2} \in L^2(0,1) \right\}$$

The operator $\mathcal{B} : D(\mathcal{B}) \to U_b = R$ is given by $\mathcal{B}x = \frac{\partial x(1,t)}{\partial z}$, the operator $\mathcal{G} = I$ is the identity operator and the operator $\mathcal{C} : D(\mathcal{C}) \to Y = R$ is given by $\mathcal{C}x = x(1,t)$. Hence $\mathcal{C}x = x(1,t) = \Upsilon x$.

The boundary control system (2.70) is a nonhomogeneous system. The change of the variable $x(t) = p(t) + B_b u_b(t)$ can help to transform it into a homogenous system. In that case, the operator A is given by $Ax = \mathcal{A}x$ for all $x \in D(A) = D(\mathcal{A}) \cap Ker\mathcal{B}$, where

$$D(A) = \left\{ x, \frac{d^2x}{dz^2} \in L^2(0,1), x, \frac{dx}{dz} \text{ are a.c, } \frac{dx}{dz}(0) = 0 = \frac{dx}{dz}(1) \right\}$$

Moreover, the multiplication operator $B_b(z)$ is the solution of $\mathcal{A}B_b = 1$ and $\mathcal{B}B_b = 1$.

By applying the change of $x(t) = p(t) + B_b u_b(t)$, it is easy to calculate that $B_b = 0.5z^2, \mathcal{A}B_b = 1$ and then the homogenous system is described by:

$$\dot{p}(t) = Ap(t) + u_b(t) - 0.5z^2 \dot{u}_b(t) + \xi(t), p(0) = p_0 \tag{2.71a}$$

$$\frac{\partial p(1,t)}{\partial z} = 0 = \frac{\partial p(0,t)}{\partial z} \tag{2.71b}$$

$$y(t) = \mathcal{C}p(t) + \mathcal{C}(0.5z^2)u_b(t) + \eta(t) \tag{2.71c}$$

Based on the domain $D(A)$, the eigenfunctions and eigenvalues of the operator A can be easily obtained:

$$\lambda_n = -(n\pi)^2, n = 1, 2, 3, \cdots \tag{2.72a}$$

$$\phi_n(z) = \begin{cases} 1, n = 0 \\ \sqrt{2}\cos(n\pi z), n = 1, 2, 3, \cdots \end{cases} \tag{2.72b}$$

The observation operator $\mathcal{C}$ is given by:

$$\begin{aligned} \mathcal{C}x = x(1) &= \sum_{n=0}^{\infty} < \phi_n, x > \phi_n(1) \\ &= < \sum_{n=0}^{\infty} \tfrac{1}{\alpha - \lambda_n} \phi_n(1)\phi_n, (\alpha I - A)x > \end{aligned} \tag{2.73}$$

where $\alpha \in \rho(A)$. ϕ_n and λ_n, where $n = 0, 1, 2, \cdots$, are the orthonormal eigenfunctions and the corresponding eigenvalues of the operator A. Since $\sum_{n=0}^{\infty} \frac{1}{\alpha - \lambda_n} \phi_n(1)\phi_n \in L^2(0,1)$, it can be shown that the operator $\mathcal{C}$ is A-bounded and therefore $\mathcal{C} \in \mathcal{L}(X_1, Y)$. From [31], the system (2.70) is a regular system. To guarantee the wellposedness of (2.71), the operator C_β is defined by:

$$C_\beta p(t) = \sum_{n=0}^{+\infty} \frac{\beta}{\beta - \lambda_n} \phi_n(1) a_n(t)$$

Then, (2.71c) is approximated by:

$$y_\beta(t) = C_\beta p(t) + C_\beta(0.5z^2)u_b(t) + \eta(t) \tag{2.74}$$

where the parameter $\beta = 800$.

In this example, since $\Upsilon x = \mathcal{C}x$, we also use C_β to approximate Υ. Then, the constraint is as the following:

$$\mathcal{X}^{\min} \leq C_\beta x(z,t) \leq \mathcal{X}^{\max}$$

We shall now proceed with the decomposition of system (2.71). If we assume the dimension of the finite-dimensional subsystem is 4, i.e. $N = 3$, then, the matrix parameters in (2.50) are:

$$\Lambda_s = diag\{\begin{array}{cccc} \lambda_0 & \lambda_1 & \lambda_2 & \lambda_3 \end{array}\}, K_s = \begin{bmatrix} 1 & 0 & 0 & 0 \end{bmatrix}^T$$

$$B_s = \begin{bmatrix} -\frac{1}{6} & \frac{\sqrt{2}}{2\pi} & -\frac{\sqrt{2}}{4\pi^2} & \frac{\sqrt{2}}{9\pi^2} \end{bmatrix}^T, G_s = \begin{bmatrix} 1 & 0 & 0 & 0 \end{bmatrix}^T$$

$$C_s = \begin{bmatrix} \frac{\beta}{\beta - \lambda_0} & -\frac{\beta\sqrt{2}}{\beta - \lambda_1} & \frac{\beta\sqrt{2}}{\beta - \lambda_2} & -\frac{\beta\sqrt{2}}{\beta - \lambda_3} \end{bmatrix}$$

$$\sigma = -10\pi^2, M = 0.25$$

$$\Lambda_f = diag\{\lambda_4, \cdots, \lambda_m\}, B_f = [b_4, \cdots, b_m]^T$$

$$K_f = [k_4, \cdots k_m]^T, G_f = [c_4, \cdots c_m]^T, C_f = [d_4, \cdots, d_m]^T$$

$$u_p(t) = Me^{-\sigma t} |C_f a_{f0}| + \frac{M}{\sigma} |C_f B_f \dot{u}_b(t)| + \frac{M}{\sigma} |C_f K_f u_b(t)| + \frac{M}{\sigma} |C_f G_f| u_n + C_\beta B_b u_b(t)$$

In this example, we set $m = 30$ which means that we use 30 modes to approximate the original PDE system. Based on the matrix parameters above, we can formulate the optimal state estimation equation (2.61)-(2.66).

With the help of the constrained MPC technique in [2], we obtain a boundary manipulated input $u_b(t)$ to make the plant satisfy the constraint (2.70d), as shown in Fig.(2.4).

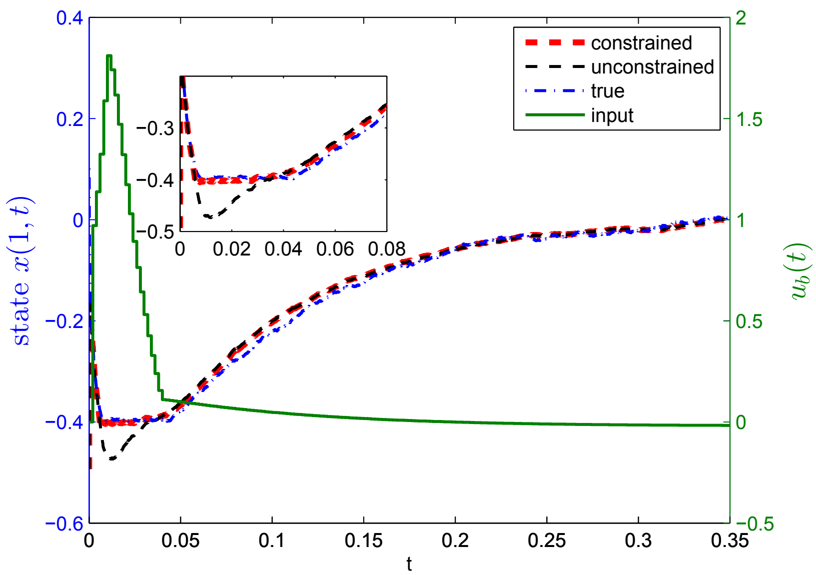

Figure 2.4: The boundary manipulated input profile $u_b(t)$ applied under MPC formulation in [2] and state at point $z = 1$.

In Fig.(2.4), because the effect of the manipulated input $u_b(t)$ (solid line), the state $x(1,t)$ satisfies the constraint $[\mathcal{X}^{\min}, \mathcal{X}^{\max}]$ in the whole simulation period. Assuming that the approximate initial value of the estimation state is known, e.g, $\hat{x}(z,0) = 1.5sin(2\pi z)$, then $p(z,0) = 1.5sin(2\pi z) - 0.5z^2u_b(0)$. By applying the unconstrained and the proposed constrained optimal state estimation methods to the example system, we can obtain first the estimated $\hat{p}(z,t)$ state and then $\hat{x}(z,t)$ through the relationship $\hat{x}(t) = \hat{p}(t) + B_bu_b(t)$. In Fig.(2.4), we can distinctly see that the constrained state estimation (bold dash line) satisfies the constraint. However, the unconstrained state estimation (dash line) violates the lower bound of the constraint. In Fig.(2.2), we can see the proposed constrained optimal state estimation method also improves the state estimation accuracy at different spatial points.

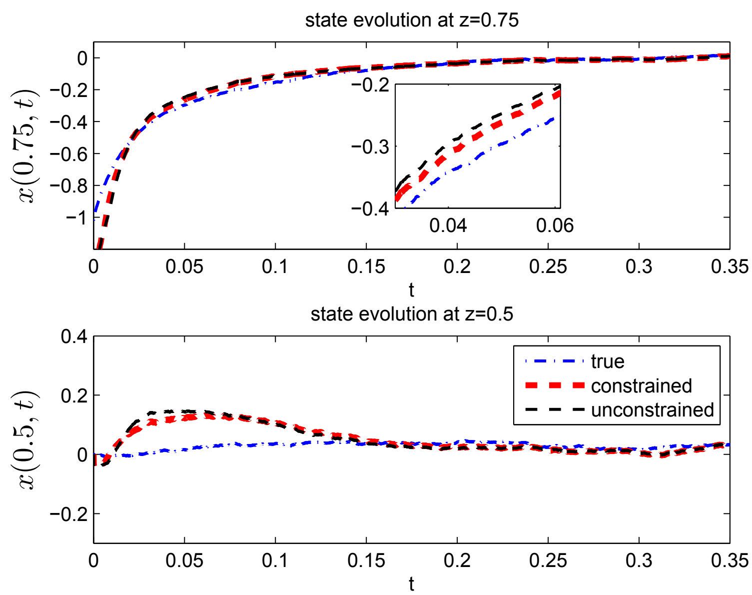

Figure 2.5: State evolution at point $z = 0.75$ and $z = 0.5$.

Fig.(2.6)-Fig.(2.8) show the plant state profile, constrained and unconstrained estimation state profile, respectively. Compared with the state profile by an unconstrained method in Fig.(2.8), the state profile by the constrained method in Fig.(2.7) has a better approximation to the plant state profile in Fig.(2.6), especially around the boundary point where the state constraint is imposed.

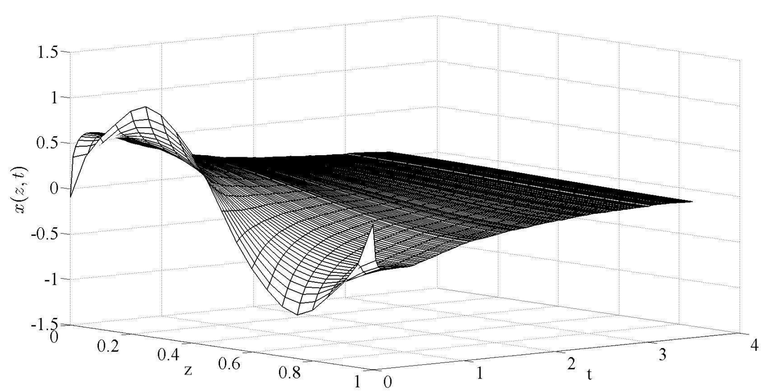

Figure 2.6: State profile in noiseless plant under the MPC formulation in [2].

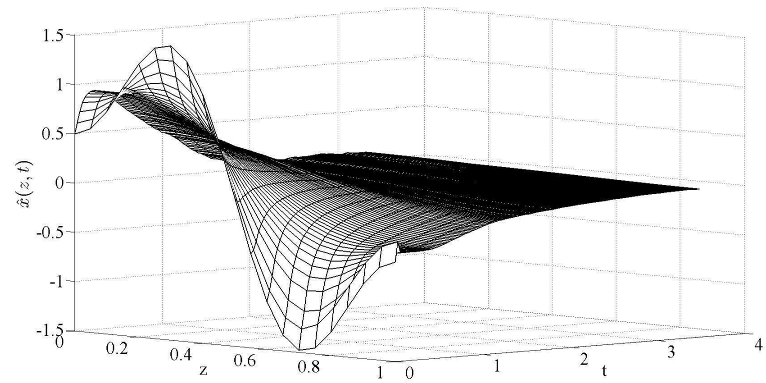

Figure 2.7: State profile under optimal constrained state estimation formulation (2.61)-(2.66).

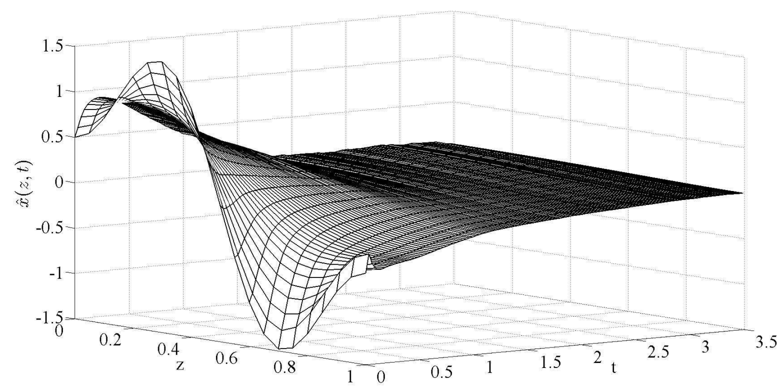

Figure 2.8: State profile given by unconstrained estimator given by [3].

2.5 Conclusion

In this chapter, we have explored the importance of the constraints as prior information in the optimal state estimation framework for both finite and infinite-dimensional systems commonly found in chemical process systems. First, the optimal constrained state estimation problem is formulated for the finite-dimensional systems. Then, we extend the optimal constrained state estimation technique for the dissipative PDE systems that satisfy the spectrum decomposition assumption. In order to eliminate the effect of loss of dynamic of infinite-dimensional complement subsystem, in this chapter we also incorporate the dynamic of the complement subsystem when designing the state estimator. Finally, the numerical examples demonstrate that the proposed state estimation method improves the state estimation performance.

From a implementation point of view, the proposed method in this chapter provides an ad-hoc procedure to deal with the inequality state constraint optimization problem. More precise mathematical optimization methodology still needs to be explored to improve the proposed method. Moreover, the systems considered in this chapter are spectral systems (finite-dimensional systems and parabolic PDE systems). As for non-spectral systems, e.g., first order hyperbolic PDE systems, much work needs to be done to deal with the constrained state estimation problems.

Chapter 3

Internal Model Servo-control for Distributed Parameter Systems

3.1 Introduction

The control of hyperbolic systems is an essential problem that has received significant attention in recent years (see [2], [32], [33], [34]). In particular, spatially varying hyperbolic partial differential equations(PDEs) systems have received a special attention since they are widely employed in modeling of traffic flow, heat exchangers, open channel and tubular chemical reactors (see [35], [36], [37]).

In control theory, the output regulation problem (or, as usually referred as a regulator problem) plays a central role. Research in this direction of control for linear systems has been attractive for over 30 years. The target in output regulation is to construct a controller so that the controlled output $y(t)$ of the plant:

$$\dot{x}(t) = Ax(t) + Bu(t) + B_d d(t), t > 0, x(0) \in X \tag{3.1a}$$

$$y(t) = Cx(t), t \geq 0 \tag{3.1b}$$

tracks a desired reference signal $y_r(t)$ despite of the existence of disturbances $d(t)$. The reference and disturbances are assumed to be generated by an exosystem:

$$\dot{w}(t) = Sw(t),\ t > 0,\ w(0) \in \mathbb{C}^n \tag{3.2a}$$

$$d(t) = Fw(t),\ t \geq 0 \tag{3.2b}$$

$$y_r(t) = Qw(t),\ t \geq 0 \tag{3.2c}$$

By choosing an appropriate finite-dimensional space and a matrix S provided its eigenvalues on imaginary axis, the generated signal by the exosystem includes harmonic signals, polynomials of t, and their linear combinations.

The need for the servo compensator design is abundant in the process industry. For example, the dynamics of the distributed solar collector field is described by a first order hyperbolic PDE, see [38], and it is required that the outlet tube oil temperature tracks the desired specified steplike setpoint. In addition to this novel applications, the control of the mono-tubular heat exchanger process is still an active research topic, see, [39], [40] and [41]. In the last three decades, regulation of irrigation channels has received an increasing interest in the process control community. In particular, water losses in open channels are very large due to inefficient management and control. The dynamics of irrigation channels can be described by hyperbolic partial differential equations of de Saint-Venant, see [42]. It is of interest that the downstream water level tracks a desired steplike setpoint. Finally, a continuum production (manufacturing) model described by a hyperbolic PDE has been introduced to simulate average behavior of production systems which produce a large number of items in many steps, see [43]. Control of the production rate makes a vital goal of any factory or a production system. In order to maximize profitability, a production system must be able to match its projected demand as closely as possible. In this case, the demand tracking (usually steplike) of the production system is one of important applied control problems, see [44]. Therefore, motivated by the above mentioned examples, the output regulation for hyperbolic PDEs needs to be accurately and comprehensively addressed.

The output regulation problem for linear finite-dimensional systems has been investigated extensively in [45], [46] and [47]. In particular, the internal model principle developed by [48] and [47] is of paramount importance for the design of the robust error feedback regulator. Recently, the *p-copy internal model principle* was extended for infinite-dimensional linear system by [49]. More precisely, one of the most important characteristics of internal model principle is that the output regulation problem can be divided into two parts: 1). embedding an internal model of the exosystem into the controller, and 2). stabilizing the closed-loop system.

In recent years, based on semigroup theory, the optimal control approaches and corresponding Operator Raccati equations were developed and provided for general infinite-dimensional systems in [50] and for hyperbolic PDE systems in [32]. Motivated by these contributions and based on the Lyapunov equations theory in [14], this thesis develops adjustable Operator Riccati equations to address the stabilization problem for hyperbolic PDE systems in Section 3.2.

For infinite dimensional systems with discrete spectrum and bounded input and output operators, a direct finite-dimensional compensator achieving output regulation was designed in [51], where an existence result for the finite-dimensional regulator was established. Recently, a dual observer based finite-dimensional regulator was developed by [52] for *Resizs-spectral* systems. To complement their works, this thesis provides a new finite-dimensional regulator for scalar first-order hyperbolic PDE systems in Section 3.3.

In this chapter, the output regulation problem is also considered for boundary controlled hyperbolic PDE systems with boundary observation on one-dimensional spatial domains. In particular, the outputs to be controlled, distributed, pointwise or boundary quantities are allowed. In general, this leads to an output regulation problem with unbounded control and observation. To solve stabilization of boundary controlled PDE systems, the backstepping approach is a powerful technique for the systematic late-lumping design of infinite-dimensional controllers [53, 54].

In this thesis, this chapter focuses on the stabilization and the output regulation for the first-order hyperbolic systems. In particular, Section 3.2 introduces the geometric theory of output regulation to the regular hyperbolic systems, Section 3.3 developed novel finite-dimensional output and error feedback regulators for the first-order hyperbolic systems, and Section 3.4 addressed the output regulation problems for the boundary controlled hyperbolic systems.

3.2 Output Regulation Problem for a Class of Regular Hyperbolic Systems

3.2.1 Problem statement

Consider the following one spatial dimensional linear hyperbolic partial differential equation system:

$$\begin{aligned}
&\tfrac{\partial x(z,t)}{\partial t} = v\tfrac{\partial x(z,t)}{\partial z} + f(z)x(z,t) + b(z)u(t),\ z \in [0,1] \\
&x(0,t) = 0,\ x(z,0) = x_0 \in X \\
&\quad y(t) = x(z_1,t)
\end{aligned} \tag{3.3}$$

where $x(z,t) \in X$ denotes the state variable and X is the separable Hilbert space $L^2(0,1)$, the variables $z \in [0,1]$ and $t \geq 0$ denote the position and time, respectively, $u(t) \in L^2_{loc}([0,\infty),U)$ denotes the input and U is a real Hilbert space, $y(t) \in L^2_{loc}([0,\infty),Y)$ denotes the output and Y is a real Hilbert space, z_1 is the observation point in spatial range $[0,1]$. The parameter v is a negative number, i.e. $v < 0$, $f : [0,1] \mapsto R : z \mapsto f(z)$ is an essentially bounded measurable function where R is the real number space, i.e. $f(z) \in L^\infty(0,1)$, and $b(z) \in L^\infty(0,1)$ is a real continuous space-varying function.

The equivalent abstract differential equation description on Hilbert space X is given by (3.1a)-(3.1b), where A is the linear operator defined on the domain:

$$D(A) = \{h \in X : h(z) \text{ is a.c. } \frac{dh}{dz} \in X \text{ and } h(0) = 0\}$$

where a.c. means 'absolutely continuous', by

$$A = v\frac{d}{dz} + f(z) \cdot I \tag{3.4}$$

, the input operator is given by $B = b(z) \cdot I$, where I is the identity operator and the output operator is given by $Cx(z) = \int_{z_1-r}^{z_1} x(z)dz$ with a small value $r > 0$.

From [55] and [37], based on the fact that $v < 0$ and $x(0, t) = 0$, the operator A given by (3.4) generates an exponentially stable strongly continuous semigroup T_A on X and for any $x \in L^2(0, 1)$, T_A has the representation:

$$(T_A(t)x)(z) = P_\tau \left(\exp\left(\frac{1}{v} \int_{z-vt}^{z} f(\sigma)d\sigma \right) x(z - vt) \right) \tag{3.5}$$

where $\tau = \frac{z}{v}$ and P_τ denotes the projection of $L^2([0, \infty), X)$ onto $L^2([0, \tau), X)$ (by truncation), (see [29]). Since T_A is exponentially stable, then there exists $M_w > 0$ such that $\|T_A(t)\| < M_w e^{w_0 t}$, where $w_0 < 0$ is the growth bound of T_A.

From the definition of the input and output operators B and C above, we know that $B \in \mathcal{L}(U, X)$ and $C \in \mathcal{L}(X, Y)$, i.e. B and C are bounded on X. $x(t)$, $u(t)$, $y(t)$ are state, input and output, respectively and $d(t)$ is disturbance. We have $x(t) \in X$, where X is a Hilbert space $L^2(0, 1)$, $u(t) \in L^2_{loc}([0, \infty), U)$, $y(t) \in L^2_{loc}([0, \infty), Y)$ and $d(t) \in U_d$, where U, Y and U_d are real Hilbert spaces. The operator A is the generator of the exponentially stable operator semigroup T_A on X. The operators $B \in \mathcal{L}(U, X)$ and $B_d \in \mathcal{L}(U_d, X)$ are bounded on X.

Moreover, in the exosystem, the matrix $S : D(S) : \mathbb{C}^n \to \mathbb{C}^n$ is a skew-Hermitian matrix having all its eigenvalues on the imaginary axis, i.e iw_k where $i = \sqrt{-1}$. Then, we have

$$Sw = \sum_{k=1}^{n} iw_k < w, \phi_k > \phi_k \tag{3.6}$$

where $(\phi_k)_{k \in N}$ is an orthonormal basis of C^n. Then, $w(t)$ is given by

$$w(t) = e^{St}w(0) = \sum_{k=1}^{n} e^{iw_k t} < w(0), \phi_k > \phi_k \tag{3.7}$$

In this work, the matrices F, Q, S in (3.2a)-(3.2c) and the disturbance input operator B_d in (3.1a)-(3.1b) are assumed to be known for the state feedback regulator design. We also assume that disturbance $d(t)$ in (3.2b) is not known, whereas the reference signal $y_r(t)$ in (3.2c) is available for the controller to be designed.

We shall now consider the combined system Σ consisting of the plant (3.1a)-(3.1b) and the exosystem (3.2a)-(3.2c)

$$\dot{x}_e(t) = A_e x_e(t) + B_e u(t),\ t > 0,\ x_e(0) \in X_e \tag{3.8}$$

$$y_e(t) = C_e x_e(t),\ t \geq 0 \tag{3.9}$$

on the space $X_e = X \oplus \mathbb{C}^n$ equipped with inner product $\langle p, q \rangle_{X_e} = \langle p_1, q_1 \rangle_X + \langle p_2, q_2 \rangle_{\mathbb{C}^n}$ where $p_i \in X,\ q_i \in C^n$, $p = \begin{bmatrix} p_1 & p_2^T \end{bmatrix}^T$ and $q = \begin{bmatrix} q_1 & q_2^T \end{bmatrix}^T$.

The operators are given by

$$A_e = \begin{bmatrix} A & P \\ 0 & S \end{bmatrix},\ D(A_e) = D(A) \oplus \mathbb{C}^n \subset X_e$$

$$B_e = \begin{bmatrix} B \\ 0 \end{bmatrix} \text{ and } C_e = \begin{bmatrix} C & 0 \\ 0 & Q \end{bmatrix}$$

where $P = B_d F$ and from the definitions above, it is easy to obtain

$$x_e(t) = \begin{bmatrix} x(t) \\ w(t) \end{bmatrix} \text{ and } y_e(t) = \begin{bmatrix} y(t) \\ y_r(t) \end{bmatrix}$$

According to lemma III.2 of [31] and by small modification, it is easy to prove that A_e

generates a C_0-semigroup T_{A_e} on X_e and T_{A_e} has the following form

$$T_{A_e}\begin{bmatrix} x \\ w \end{bmatrix} = \begin{bmatrix} T_A(t)x + \int_0^t T_A(\upsilon)Pe^{S(t-\upsilon)}wd\upsilon \\ e^{St}w \end{bmatrix} \tag{3.10}$$

In this chapter, the output regulation problem is solved by designing a regulator such that the closed-loop system is stable and the tracking error

$$\lim_{t\to+\infty} e(t) = 0,\ \forall x(0) \in X,\ w(0) \in \mathbb{C}^n \tag{3.11}$$

for all regulator initial values, where $e(t) = (y(t) - y_r(t))$.

3.2.2 The output regulation problem

As the problem in finite dimensional systems, the output regulation problem for the regular hyperbolic PDE system (3.1a)-(3.1b) is to design regulators such that the following conditions hold:

[C1.] The closed-loop system operator generates an exponentially stable C_0- semigroup;

[C2.] For the closed-loop system, the tracking error $e(t) \to 0$ as $t \to \infty$, for any initial conditions $x_0 \in X$ and $w_0 \in \mathbb{C}^n$.

Two types of regulator synthesis are provided for the system (3.1a)-(3.1b) in this chapter.
Problem 1-State feedback regulator problem: Find a regulator of the form

$$u(t) = Kx(t) + Lw(t) \tag{3.12}$$

where $K \in \mathcal{L}(X, U)$, $L \in \mathcal{L}(\mathbb{C}^n, U)$, and the information of plant and exosystem state evolution are provided, such that: **(a.1)** $A + BK$ generates an exponentially stable C_0-semigroup. **(a.2)** The error $e(t) \to 0, t \to \infty$ for any $x_0 \in X$ and $w_0 \in \mathbb{C}^n$.

Problem 2-Error feedback regulator problem: Find a regulator of the form

$$\dot{r}(t) = \mathcal{G}_1 r(t) + \mathcal{G}_2 e(t) \tag{3.13a}$$

$$u(t) = Hr(t) \tag{3.13b}$$

where $r \in \Omega = X \oplus \mathbb{C}^n$ for $t > 0$, Ω is a Hilbert space, $\mathcal{G}_1 \in \mathcal{L}(\Omega)$, $\mathcal{G}_2 \in \mathcal{L}(Y, \Omega)$ and $H \in \mathcal{L}(\Omega, U)$, and only error signal is provided, such that

(c.1) The system

$$\dot{x}(t) = Ax(t) + BHr(t)$$

$$\dot{r}(t) = \mathcal{G}_1 r(t) + \mathcal{G}_2 Cx(t)$$

is exponentially stable when $w \equiv 0$, i.e.

$$\begin{bmatrix} A & BH \\ \mathcal{G}_2 C & \mathcal{G}_1 \end{bmatrix}$$

is the infinitesimal generator of an exponentially stable C_0-semigroup.

(c.2) The error $e(t) \to 0, t \to \infty$ for any $x_0 \in X$, $r(0) \in \Omega$ and $w_0 \in \mathbb{C}^n$.

3.2.2.1 The state feedback regulator problem

(1). The stabilization feedback gain

In section 3.2.1, we already know that the operator A generates an exponentially stable semigroup on X. Then, it follows that the pair (A, B) is exponentially stabilizable. Consequently, we have the following essential theorem providing a general method to obtain the stabilizing feedback gain:

Theorem 2. *Based on the fact that (A, B) is exponentially stabilizable, if there exists a nonnegative self-adjoint operator Q_0 that solves the operator Riccati algebraic equation:*

$$A^*Q_0 + Q_0A + M - 2Q_0BB^*Q_0 = 0, \text{ on } D(A) \tag{3.14}$$

where M is a positive definite design parameter operator, such that $Q_0(D(A)) \subset D(A^*)$, and feedback gain is $K = -B^*Q_0 \in \mathcal{L}(X, U)$, then the stability of the closed-loop system is provided, i.e. $(A + BK)$ generates an exponentially stable C_0-semigroup.

Before we start to prove the Theorem 2, a Lemma about the exponentially stability is studied.

Lemma 1. *Let $\mathcal{A}_c$ be the infinitesimal generator of the C_0-semigroup $T_{\mathcal{A}_c}$ on the Hilbert space X. $T_{\mathcal{A}_c}$ is exponentially stable if and only if there exists a nonnegative self-adjoint operator Q_0 such that*

$$< \mathcal{A}_c x, Q_0 x > + < Q_0 x, \mathcal{A}_c x > = - < Mx, x >, \ x \in D(\mathcal{A}_c) \tag{3.15}$$

Proof. The proof is similar to the proof of Theorem 5.1.3 in [14]. According to the Lemma 4.1.24 in [14], if we let observability grammian L_C be Q_0 and $C^*C = M$, then (3.15) is equivalent to the following Lyapunov equation

$$\mathcal{A}_c^*Q_0 + Q_0\mathcal{A}_c + M = 0, \ Q_0D(\mathcal{A}_c) \subset D(\mathcal{A}_c^*) \tag{3.16}$$

Proof of Theorem 2: By arranging some terms in equation (3.14), we obtain the following form:

$$(A - BB^*Q_0)^* Q_0 + Q_0 (A - BB^*Q_0) + M = 0 \tag{3.17}$$

If using K to replace $-B^*Q_0$ in the equation (5.55) and setting $\mathcal{A}_c = A + BK$, we can obtain

$$Q_0\mathcal{A}_c + \mathcal{A}_c^*Q_0 + M = 0 \tag{3.18}$$

Because the feedback control term represents a bounded perturbation of A, we have $D(\mathcal{A}_c) = D(A)$ and $D(A^*) = D(\mathcal{A}_c^*)$ (see [56], p.194). Then, it is easy to see that $Q_0(D(\mathcal{A}_c)) \subset D(\mathcal{A}_c^*)$, since $Q_0(D(A)) \subset D(A^*)$. □

Remark 5. *One can notice that the different selection of M in (3.14) results in the different state feedback gain K. Therefore, we shall now discuss the performance of K according to different M. First, we set two state feedback gains $K_1 = -B^*Q_1$ and $K_2 = -B^*Q_2$, where Q_1 and Q_2 are two nonnegative self-adjoint operators such that:*

$$Q_1\mathcal{A}_c + \mathcal{A}_c^*Q_1 + M_1 = 0,\ Q_1D(\mathcal{A}_c) \subset D(\mathcal{A}_c^*) \tag{3.19a}$$

$$Q_2\mathcal{A}_c + \mathcal{A}_c^*Q_2 + M_2 = 0,\ Q_2D(\mathcal{A}_c) \subset D(\mathcal{A}_c^*) \tag{3.19b}$$

where M_1 and M_2 are positive definite design parameter operators and $M_1 - M_2 = \Delta M$ is positive definite. Then, subtracting (3.19b) from (3.19a), the following equation holds:

$$\Delta Q\mathcal{A}_c + \mathcal{A}_c^*\Delta Q + \Delta M = 0,\ \Delta QD(\mathcal{A}_c) \subset D(\mathcal{A}_c^*) \tag{3.20}$$

It is easy to see that $\Delta Q = Q_1 - Q_2$ is also nonnegative self-adjoint. Then, $\Delta K = K_1 - K_2 = -B^*\Delta Q$. Essentially, ΔQ, Q_1 and Q_2 are the function of spatial variable $z \in [0,1]$. Since B is also the continuous spatial varying function, K_1, K_2 and ΔK are multiplier operators. Then, for any $x \in D(\mathcal{A}_c)$, it follows that

$$\begin{aligned}
&\|K_1x\| = (< K_1x, K_1x >)^{1/2}\\
&= (< K_2x, K_2x > + < \Delta Kx, \Delta Kx > + < K_2x, \Delta Kx > + < \Delta Kx, K_2x >)^{1/2}\\
&= \left(\|K_2x\|^2 + \|\Delta Kx\|^2 + < \Delta K^*K_2x, x > + < K_2^*\Delta Kx, x >\right)^{1/2}\\
&= \left(\|K_2x\|^2 + \|\Delta Kx\|^2 + \Delta K^*K_2\|x\|^2 + K_2^*\Delta K\|x\|^2\right)^{1/2}\\
&= \left(\|K_2x\|^2 + \|\Delta Kx\|^2 + \Delta QBB^*Q_2\|x\|^2 + Q_2BB^*\Delta Q\|x\|^2\right)^{1/2}
\end{aligned}$$

Consequently, the following inequality holds:

$$\begin{aligned}
\|K_1\| &= \sup_{x\neq 0} \tfrac{\|K_1x\|}{\|x\|}\\
&= \sup_{x\neq 0} \tfrac{\left(\|K_2x\|^2+\|\Delta Kx\|^2+\Delta QBB^*Q_2\|x\|^2+Q_2BB^*\Delta Q\|x\|^2\right)^{1/2}}{\|x\|}\\
&> \|K_2\|
\end{aligned} \tag{3.21}$$

The formula (3.21) implies that when selecting M_1 and M_2 such that ΔM is positive definite, *then we can obtain* $\|K_1\| > \|K_2\|$. *We can see that the norm of stabilizing feedback gain* $\|K\|$ *is roughly proportional to* M *in equation (3.14). This is essential, since it implies that by adjusting* M *proportionally in (3.14), we can design a desired feedback gain to stabilize the closed-loop system at a desired rate.* ■

In particular, in order to calculate the operator Riccati equation (3.14) and to construct a state feedback gain for the system (3.1a)-(3.1b) or more specifically for (3.3), the following lemma is provided.

Lemma 2. *Consider the linear plant (3.3) and (3.1a)-(3.1b). For any* $v < 0$, Ψ *is the solution of the matrix Riccati differential equation:*

$$v\frac{d\Psi}{dz} = f^*\Psi + \Psi f + M - 2\Psi BB^*\Psi, \ \Psi(1) = 0 \tag{3.22}$$

and $Q_0 := \Psi(z) \cdot I$ *is the unique self-adjoint nonnegative solution of the operator Riccati algebraic equation (3.14). Hence the operator*

$$K = -B^*(z)\Psi(z) \cdot I \tag{3.23}$$

is the stabilizing state feedback.

Proof. If we substitute $Q_0 := \Psi(z) \cdot I$ into the equation (3.14), then for any $x \in D(A)$:

$$\left(-v\frac{d}{dz}\Psi \cdot I + f^*\Psi \cdot I + v\Psi\frac{d}{dz} + \Psi f \cdot I + M - 2\Psi BB^*\Psi \cdot I\right) x = 0$$

$$\Leftrightarrow v\left(-\frac{d}{dz}(\Psi x) + \Psi\frac{dx}{dz}\right) + (f^*\Psi + \Psi f + M - 2\Psi BB^*\Psi)\, x = 0$$

and from [37], the following equation holds

$$-\frac{d}{dz}(\Psi x) + \Psi\frac{dx}{dz} = -\frac{d\Psi}{dz}x$$

then the operator Riccati algebraic equation (3.14) can be written as follows:

$$v\frac{d\Psi}{dz} = f^*\Psi + \Psi f + M - 2\Psi BB^*\Psi$$

The condition $\Psi(1) = 0$ guarantees that for any $x \in D(A)$ $\Psi(1)x(1) = 0$, which implies that $Q_0\left(D(A)\right) \subset D(A^*)$. Therefore, if Ψ is the unique nonnegative solution on $[0,1]$ of equation (3.22), then $Q_0 := \Psi(z) \cdot I$ is a unique solution of the operator Riccati equation (3.14). □

In this section, the important theorem (see Theorem 2) is investigated to help providing the stabilization feedback gain K, such that the closed-loop stability is guaranteed, i.e. $A + BK$ is exponentially stable. Moreover, the influence of design parameter M on the performance of stabilizing feedback gain in (3.14) is studied (see Remark 5). The results in Theorem 2 and Remark 5 are not only suitable for the regular hyperbolic PDE systems in this chapter but can also be extended to other regular systems.

(2). The state feedback regulator

In this section, we extend the key results about the state feedback regulator to the regular first order hyperbolic PDE systems from [57].

Although the spectrum of operator A is difficultly determined, it is still easy to conclude that the following corollary holds since A is exponentially stable.

Corollary 1. *For any real number $\alpha \in R$, $i\alpha$ is contained in the resolvent set of A, i.e. $i\alpha \in \rho(A)$, where $i = \sqrt{-1}$.*

From the Corollary 1, it is easy to see that $\sigma(S) \subset \rho(A)$ and $\sigma(S) \cap \sigma(A) = \emptyset$, where $\sigma(S)$ and $\sigma(A)$ are the spectrum of S and A, respectively. This corollary is given to ensure the solvability of Sylvester equations in the following theorem.

Theorem 3. *Under the Corollary 1 and since (A, B) is exponentially stabilizable, the state feedback regulator problem is solvable if there exist operators $\Pi \in \mathcal{L}(\mathbb{C}^n, X)$ with $\Pi D(S) \subset D(A)$ and $\Gamma \in \mathcal{L}(\mathbb{C}^n, U)$ which satisfy the constrained Sylvester equations (regulator equations):*

$$\Pi S = A\Pi + B\Gamma + P \tag{3.24}$$

$$C\Pi - Q = 0 \tag{3.25}$$

The state feedback law is given by

$$u(t) = Kx(t) + Lw(t) \tag{3.26}$$

where K stabilizes the pair (A, B) and $L = \Gamma - K\Pi$.

Proof. First we prove the sufficiency. By substituting (3.26) into the system model (3.1a)-(3.1b), the closed loop system is constructed

$$\dot{x}(t) = (A + BK)\,x(t) + (B(\Gamma - K\Pi) + P)\,w(t) \tag{3.27}$$

As mentioned above, the operator $A + BK$ generates the exponentially stable C_0-semigroup T_{abk}.

The mild solution of (3.27) is of the form:

$$x(t) = T_{abk}(t)x(0) + \int_0^t T_{abk}(t-\tau)\,(B(\Gamma - K\Pi) + P)\,w(\tau)d\tau \tag{3.28}$$

Plugging (3.24) in (3.28), the following holds

$$\begin{aligned}
&x(t) = T_{abk}(t)x(0) + \textstyle\int_0^t T_{abk}(t-\tau)\,(B\Gamma + P - BK\Pi)\,w(\tau)d\tau \\
&= T_{abk}(t)x(0) + \textstyle\int_0^t T_{abk}(t-\tau)\,(\Pi S - (A + BK)\,\Pi)\,w(\tau)d\tau \\
&= T_{abk}(t)x(0) + \textstyle\int_0^t T_{abk}(t-\tau)\,(\Pi\dot{w}(\tau) - (A + BK)\,\Pi w(\tau))\,d\tau \\
&= T_{abk}(t)x(0) + \textstyle\int_0^t \frac{d}{d\tau}\,(T_{abk}(t-\tau)\Pi w(\tau))d\tau \\
&= T_{abk}(t)\,(x(0) - \Pi w(0)) + \Pi w(t)
\end{aligned} \tag{3.29}$$

Then, the tracking error in (3.11) can be rewritten as

$$\begin{aligned}
e(t) &= Cx(t) - Qw(t) \\
&= CT_{abk}(t)\,(x(0) - \Pi w(0)) + (C\Pi - Q)\,w(t)
\end{aligned} \tag{3.30}$$

T_{abk} is exponentially stable and C is bounded on X, thus the equation (3.25) implies that in equation (3.30) the tracking error $e(t) \to 0$ as $t \to \infty$. □

From the formula (3.30), we can conclude the following corollary which shows that the tracking error decays exponentially, and provides upper bounds for the decay rate of $\|e(t)\|_Y$.

Corollary 2. *Based on the formula (3.30), the tracking error $e(t)$ satisfies the following inequality:*

$$\|e(t)\|_Y \leq \kappa e^{-\gamma t} \tag{3.31}$$

where κ is a positive constant and $\|T_{abk}(t)\|_Y \leq Me^{-\gamma t}$ with $M > 0$, $0 < \gamma < -\omega_1$ and $w_1 < 0$ is the growth bound of $T_{abk}(t)$, since $T_{abk}(t)$ is exponentially stable.

Proof. From (3.30),

$$\begin{aligned}\|e(t)\|_Y &= \|CT_{abk}(t)\,(x(0) - \Pi w(0))\|_Y \\ &\leq \|(Cx(0) - Qw(0))\|_Y \, \|T_{abk}(t)\| \\ &\leq (\|C\| \, \|x_0\|_X + \|Q\| \, \|w(0)\|_{C^n}) \, \|T_{abk}(t)\| \\ &\leq (\|C\| \, \|x_0\|_X + \|Q\| \, \|w(0)\|_{C^n}) \, Me^{-\gamma t}\end{aligned}$$

If we denote $(\|C\| \, \|x_0\|_X + \|Q\| \, \|w(0)\|_{C^n})$ by κ, then the formula above reduces to $\|e(t)\|_Y \leq \kappa e^{-\gamma t}$. □

By studying the Lemma 6 of [58], the following theorem is given to show that the Sylvester equations (3.24)-(3.25) in Theorem 3 have a unique bounded solution. The same conclusion is also shown in [59].

Theorem 4. *Under Corollary 1 and the fact that (A, B) is exponentially stabilizable, if the state feedback control law (3.26) solves the output regulation problem, then there exists a unique operator Π given by*

$$\Pi w = \sum_{k=1}^{n} \langle w, \phi_k \rangle (iw_k I - A)^{-1} \left(B\Gamma + P \right) \phi_k, w \in \mathbb{C}^n \tag{3.32}$$

that satisfies the constrained Sylvester equations (3.24)-(3.25), where $\{\phi_k\}$ are orthonormal eigenvectors of S.

Proof. First, we define an identity (see [58])

$$\|x\| = \sup_{\|\varepsilon\| \leq 1} |\langle x, \varepsilon \rangle|, \forall x \in X \tag{3.33}$$

Since the operator $(iw_k I - A)^{-1}(B\Gamma + P)$ is bounded, it is natural that

$$M_a = \left(\sum_{k=1}^{n} \left| \left\langle (iw_k I - A)^{-1} (B\Gamma + P) \phi_k, \varepsilon \right\rangle \right|^2 \right)^{1/2} < \infty$$

For every $w \in \mathbb{C}^n$, we get (through Cauchy-Schwarz Inequality)

$$\begin{aligned}
&\|\Pi w\| = \sup_{\|\varepsilon\| \leq 1} |\langle \Pi w, \varepsilon \rangle| = \sup_{\|\varepsilon\| \leq 1} \left| \sum_{k=1}^{n} \langle w, \phi_k \rangle \left\langle (iw_k I - A)^{-1} (B\Gamma + P), \varepsilon \right\rangle \right| \\
&\leq \sup_{\|\varepsilon\| \leq 1} \left(\sum_{k=1}^{n} |\langle w, \phi_k \rangle|^2 \right)^{1/2} \left(\sum_{k=1}^{n} \left| \left\langle (iw_k I - A)^{-1} (B\Gamma + P) w_k, \varepsilon \right\rangle \right|^2 \right)^{1/2} = M_a \|w\|
\end{aligned}$$

that implies that Π is bounded. Now, let $s \in \rho(A)$, utilizing the resolvent identity we have $\forall w \in D(S)$

$$\begin{aligned}
(sI - A)^{-1}\Pi(S - sI)w &= \sum_{k=1}^{n} < Sw - sw, \phi_k > (sI - A)^{-1}(iw_k I - A)^{-1} (B\Gamma + P) \phi_k \\
&= \sum_{k=1}^{n} < w, \phi_k > (iw_k - s)(sI - A)^{-1}(iw_k I - A)^{-1} (B\Gamma + P) \phi_k \\
&= \sum_{k=1}^{n} < w, \phi_k > \left((sI - A)^{-1} - (iw_k I - A)^{-1} \right) (B\Gamma + P) \phi_k \\
&= (sI - A)^{-1} (B\Gamma + P) w - \Pi w
\end{aligned}$$

Then, we have

$$\Pi = (sI - A)^{-1} (B\Gamma + P) - (sI - A)^{-1}\Pi(S - sI)$$

which indicates that $\Pi\mathbb{C}^n \in D(A)$ and (3.24) holds.

Then, we assume that the operator $\tilde{\Pi}$ satisfies (3.24) and for every ϕ_k, $k \in N$

$$\tilde{\Pi} S \phi_k = A\tilde{\Pi}\phi_k + (B\Gamma + P) \phi_k \Leftrightarrow \tilde{\Pi}\phi_k = (iw_k - A)^{-1} (B\Gamma + P) \phi_k$$

Because $\tilde{\Pi}$ is bounded, we have

$$\tilde{\Pi}w = \sum_{k=1}^{n} < w, \phi_k > \tilde{\Pi}\phi_k = \sum_{k=1}^{n} < w, \phi_k > (iw_k I - A)^{-1} (B\Gamma + P) \phi_k = \Pi w, \quad \forall w \in \mathbb{C}^n$$

Thus (3.32) is the unique solution of (3.24).

For $x(0) \in X$ and $w(0) \in \mathbb{C}^n$, from the equation (3.30), we have

$$\begin{aligned} e(t) &= Cx(t) - Qw(t) \\ &= CT_{abk}(t)(x(0) - \Pi w(0)) + (C\Pi - Q) w(t) \end{aligned} \tag{3.34}$$

Since, T_{abk} is exponentially stable and the controller (3.26) solves the output regulation problem, we have

$$\lim_{t\to+\infty} e(t) = \lim_{t\to+\infty} (C\Pi - Q)w(t) = 0 \tag{3.35}$$

Since for every $w(t) \in \mathbb{C}^n$ we have $C\Pi - Q = 0$, the operator Π also satisfies (3.25). $\square$

In this chapter, let us briefly study the robust problem of the state feedback regulator. For simplicity, we assume that A_p is perturbed parameter A, i.e., $A_p = A + \Delta \cdot I$, where $\Delta \cdot I$ is perturbation and I is identity. Then, we replace A with A_p in Sylvester equation to obtain the following:

$$\Pi S - (A + \Delta \cdot I)\Pi + B\Gamma + P = 0$$

$$\Pi S - A\Pi + B\Gamma + P = \Delta \cdot \Pi$$

From above equation, we know that the state feedback regulator (3.26) is not robust, unless we can find some conditions to guarantee that the perturbation $\Delta \cdot I$ decays to zero. In the same way, we can claim that the error feedback regulator in the following section is not robust either.

3.2.2.2 The error feedback regulator problem

In this section, we proceed with the more realistic regulator problem-error feedback regulator problem. The controller is only provided with the tracking error $e(t)$ and incorporates with the models of the plant and the exosystem.

(1). The error feedback regulator

Assumption 1. *The pair*

$$\left(\begin{bmatrix} A & P \\ 0 & S \end{bmatrix}, \begin{bmatrix} C & -Q \end{bmatrix}\right)$$

is exponentially detectable and there exists $\mathcal{G}_2 \in \mathcal{L}(Y, \Omega)$ in the equation (3.13a) such that

$$\begin{bmatrix} A & P \\ 0 & S \end{bmatrix} - \mathcal{G}_2 \begin{bmatrix} C & -Q \end{bmatrix} = \begin{bmatrix} A - G_1C & P + G_1Q \\ -G_2C & S + G_2Q \end{bmatrix}$$

generates an exponentially stable C_0-semigroup.

Theorem 5. *Under Corollary 1 and Assumption 1, if and only if there exist mappings $\Pi \in \mathcal{L}(\mathbb{C}^n, X)$ satisfying $\mathcal{R}(\Pi) \subset D(A)$ and $\Gamma \in \mathcal{L}(\mathbb{C}^n, U)$, such that the following constrained Sylvester equation holds*

$$\Pi S = A\Pi + B\Gamma + P \tag{3.36}$$

$$C\Pi - Q = 0 \tag{3.37}$$

then, the output regulation problem is solved by the error regulator of the form

$$\dot{r}(t) = \mathcal{G}_1 r(t) + \mathcal{G}_2 e(t) \tag{3.38a}$$

$$u(t) = Hr(t) \tag{3.38b}$$

with $r(t) \in \Omega = X \oplus \mathbb{C}^n$

$$\begin{aligned} \mathcal{G}_2 &= \begin{bmatrix} G_1 \\ G_2 \end{bmatrix}, H = \begin{bmatrix} K & \Gamma - K\Pi \end{bmatrix} \\ \mathcal{G}_1 &= \begin{bmatrix} (A + BK - G_1C) & (P + B(\Gamma - K\Pi) + G_1Q) \\ -G_2C & S + G_2Q \end{bmatrix} \end{aligned} \tag{3.39}$$

where $K \in L(X,U)$, $G_1 \in L(Y,X)$ *and* $G_2 \in L(Y,\mathbb{C}_n)$, *such that* K *is an exponentially stabilizing feedback gain for the pair* (A,B) *and* $\mathcal{G}_2 = \begin{bmatrix} G_1 \\ G_2 \end{bmatrix}$ *is an exponentially stabilizing output injection gain for the pair* $\left(\begin{bmatrix} A & P \\ 0 & S \end{bmatrix}, \begin{bmatrix} C & -Q \end{bmatrix} \right)$.

Proof. We first prove the sufficiency. In the regulator (3.38), $r(t)$ can be regarded as the estimation of $\begin{bmatrix} x(t) \\ w(t) \end{bmatrix}$ and the error feedback regulator is actually the "observer-based" controller. Let $r(t) = \begin{bmatrix} \hat{x}(t) & \hat{w}(t)^T \end{bmatrix}^T \in X \oplus \mathbb{C}^n$. We can rewrite the regulator in (3.38) as the following form

$$\begin{bmatrix} \dot{\hat{x}}(t) \\ \dot{\hat{w}}(t) \end{bmatrix} = \begin{bmatrix} G_{11} & G_{12} \\ G_{13} & G_{14} \end{bmatrix} \begin{bmatrix} \hat{x}(t) \\ \hat{w}(t) \end{bmatrix} + \begin{bmatrix} G_1C & -G_1Q \\ G_2C & -G_2Q \end{bmatrix} \begin{bmatrix} x(t) \\ w(t) \end{bmatrix} \tag{3.40a}$$

$$u(t) = \begin{bmatrix} K & \Gamma - K\Pi \end{bmatrix} \begin{bmatrix} \hat{x}(t) \\ \hat{w}(t) \end{bmatrix} \tag{3.40b}$$

where $\mathcal{G}_1 = \begin{bmatrix} G_{11} & G_{12} \\ G_{13} & G_{14} \end{bmatrix}$, $\mathcal{G}_2 \times \begin{bmatrix} C & -Q \end{bmatrix} = \begin{bmatrix} G_1C & -G_1Q \\ G_2C & -G_2Q \end{bmatrix}$. In particular, the operator $\mathcal{G}_1 : D(\mathcal{G}_1) \subset \Omega \to \Omega$ generates a strongly continuous semigroup $T_{\mathcal{G}_1}(t)$ on Ω.

If we substitute $u(t)$ denoted by (3.40b) into the combined system (3.8), we obtain

$$\begin{bmatrix} \dot{x}(t) \\ \dot{w}(t) \end{bmatrix} = \begin{bmatrix} A & P \\ 0 & S \end{bmatrix} \begin{bmatrix} x(t) \\ w(t) \end{bmatrix} + \begin{bmatrix} BK & B\,(\Gamma - K\Pi) \\ 0 & 0 \end{bmatrix} \begin{bmatrix} \hat{x}(t) \\ \hat{w}(t) \end{bmatrix} \tag{3.41}$$

We assume the estimation error to be of the form $e_x(t) = x(t) - \hat{x}(t)$, $e_w(t) = w(t) - \hat{w}(t)$, then, it is easy to obtain the following equation from (3.40a) and (3.41)

$$\begin{bmatrix} \dot{e}_x(t) \\ \dot{e}_w(t) \end{bmatrix} = \begin{bmatrix} A - G_1C & P + G_1Q \\ -G_2C & S + G_2Q \end{bmatrix} \begin{bmatrix} x(t) \\ w(t) \end{bmatrix} + \begin{bmatrix} BK - G_{11} & B\left(\Gamma - K\Pi\right) - G_{12} \\ -G_{13} & -G_{14} \end{bmatrix} \begin{bmatrix} \hat{x}(t) \\ \hat{w}(t) \end{bmatrix} \tag{3.42}$$

A direct calculation implies that the dynamics of $\begin{bmatrix} e_x(t) & e_w(t)^T \end{bmatrix}^T$ can be given by the homogeneous differential equation

$$\begin{bmatrix} \dot{e}_x(t) \\ \dot{e}_w(t) \end{bmatrix} = \begin{bmatrix} A - G_1C & P + G_1Q \\ -G_2C & S + G_2Q \end{bmatrix} \begin{bmatrix} e_x(t) \\ e_w(t) \end{bmatrix} \tag{3.43}$$

From Assumption 1, we can easily conclude that $\begin{bmatrix} e_x(t) & e_w(t)^T \end{bmatrix}^T \to 0$ as $t \to +\infty$. By comparing (3.42) and (3.43), it is natural to obtain

$$\mathcal{G}_1 = \begin{bmatrix} G_{11} & G_{12} \\ G_{13} & G_{14} \end{bmatrix} = \begin{bmatrix} (A + BK - G_1C) & (P + B(\Gamma - K\Pi) + G_1Q) \\ -G_2C & S + G_2Q \end{bmatrix}$$

$\hat{x}(t) \to x(t)$ and $\hat{w}(t) \to w(t)$, as $t \to +\infty$ imply that in (3.40b) $u(t) \to Kx(t) + (\Gamma - K\Pi)w(t)$ as $t \to +\infty$. From the proof of Theorem 3, if the constrained Sylvester equation (3.36)-(3.37) holds, the tracking error $e(t) \to 0$ as $t \to +\infty$ and the output regulation problem is solved.

Now we turn to the necessity. Same with the sufficiency part, let $r(t) = \begin{bmatrix} \hat{x}(t) & \hat{w}(t)^T \end{bmatrix}^T \in X \oplus \mathbb{C}^n$, $e_x(t) = x(t) - \hat{x}(t)$ and $e_w(t) = w(t) - \hat{w}(t)$. Then, by combining the composite system model (3.8), (3.38) and (3.39) together, it follows that

$$\begin{bmatrix} \dot{e}_x(t) \\ \dot{e}_w(t) \end{bmatrix} = \begin{bmatrix} A - G_1C & P + G_1Q \\ -G_2C & S + G_2Q \end{bmatrix} \begin{bmatrix} e_x(t) \\ e_w(t) \end{bmatrix}$$

If we substitute $u(t)$ in (3.38b) into the plant model (3.1a)-(3.1b), we obtain

$$\dot{x}(t) = (A + BK)\, x(t) - BKe_x(t) - B\,(\Gamma - K\Pi)\, e_w(t) + (B\,(\Gamma - K\Pi) + P)\, w(t) \tag{3.44}$$

Then, we consider the system

$$\begin{aligned} \dot{\Phi}(t) &= \mathcal{A}\Phi(t) + \mathcal{P}w(t) + \mathcal{B}u(t) \\ \dot{w}(t) &= Sw(t) \\ e(t) &= \mathcal{C}\Phi(t) - Qw(t) \end{aligned} \tag{3.45}$$

with $\Phi(t) = \begin{bmatrix} x(t) & e_x(t) & e_w(t)^T \end{bmatrix}^T \in X \oplus Y \oplus \mathbb{C}^n$, $\mathcal{C} = \begin{bmatrix} C_\Lambda & 0 & 0 \end{bmatrix}$

$$\mathcal{A} = \begin{bmatrix} A + BK & -BK & -B\,(\Gamma - K\Pi) \\ 0 & A - G_1 C & P + G_1 Q \\ 0 & -G_2 C & S + G_2 Q \end{bmatrix}$$

$$\mathcal{B} = \begin{bmatrix} 0 \\ 0 \\ 0 \end{bmatrix}, \quad \mathcal{P} = \begin{bmatrix} B\,(\Gamma - K\Pi) + P \\ 0 \\ 0 \end{bmatrix}$$

Now, if we claim that the operator $\tilde{\Pi} = \begin{bmatrix} \Pi & 0 & 0^T \end{bmatrix}^T : \mathbb{C}^n \mapsto X \oplus Y \oplus \mathbb{C}^n$ and apply Theorem 3 to design the state feedback regulator for the system (3.45): $u(t) = \mathcal{K}\Phi(t) + (\tilde{\Gamma} - \mathcal{K}\tilde{\Pi})w(t)$ with $\mathcal{K} = \begin{bmatrix} K & 0 & 0 \end{bmatrix}$. The operators $\tilde{\Pi}$ and $\tilde{\Gamma} \in \mathcal{L}(C^n, Y)$ satisfy the following constrained Sylvester equations

$$\tilde{\Pi} S = \mathcal{A}\tilde{\Pi} + \mathcal{B}\tilde{\Gamma} + \mathcal{P} \tag{3.46a}$$

$$\mathcal{C}\tilde{\Pi} - Q = 0 \tag{3.46b}$$

Under Corollary 1 and Assumption 1, it follows that $\mathcal{A}$ is exponentially stable. Since $\mathcal{B}$

is zero, then $\mathcal{A}+\mathcal{B}\mathcal{K}$ is exponentially stable and we can also set $\tilde{\Gamma}=0$. From the first component of equation (3.46a) and equation (3.46b), it is straightforward to obtain

$$
\begin{aligned}
&(A+BK)\Pi + B(\Gamma - K\Pi) + P = \Pi S \\
&C\Pi - Q = 0
\end{aligned}
$$

The second and third components of equation (3.46a) are zero, therefore (3.36)-(3.37) are enough to ensure the validity of the equation (3.46). □

(2). The stabilizing output injection gain

In section 3.2.2.2, one can notice that Assumption 1 is essential to the solvability of the error feedback regulator problem. In this section, we explore how to obtain the output injection gain $\mathcal{G}_2 \in \mathcal{L}(Y,\Omega)$ in the equation (3.13a). First, we recall an important lemma which is a dual statement of Lemma 1:

Lemma 3. *Let $\mathcal{A}_o$ be the infinitesimal generator of the C_0-semigroup $T_{\mathcal{A}_o}(t)$ on the Hilbert space X. Then, $T_{\mathcal{A}_o}(t)$ is exponentially stable if and only if there exists a nonnegative self-adjoint operator $Q_e \in \mathcal{L}(X)$ such that*

$$
< Q_e x, \mathcal{A}_o^* x > + < \mathcal{A}_o^* x, Q_e x > = - < Nx, x >, \text{ for all } x \in D(\mathcal{A}_o^*) \tag{3.47}
$$

The equation (3.47) can be transformed in the following form:

$$
(\mathcal{A}_o Q_e + Q_e \mathcal{A}_o^* + N)x = 0 \text{ for } x \in \mathrm{D}(\mathcal{A}_o^*) \tag{3.48}
$$

with $Q_e(D(\mathcal{A}_o^*)) \subset D(\mathcal{A}_o)$, where N is a positive definite operator and (3.48) is a standard operator Lyapunov equation. Based on Lemma 3, in this section, the following theorem describes a general approach finding the stabilizing output injection gain $\mathcal{G}_2 \in \mathcal{L}(Y,\Omega)$ in (3.13a).

Theorem 6. *Under the assumption that the pair* $\left(\begin{bmatrix} A & P \\ 0 & S \end{bmatrix}, \begin{bmatrix} C & -Q \end{bmatrix}\right)$ *is exponen-*

tially detectable. If there exist the nonnegative self-adjoint operators Θ_1 and Θ_2 that solve the following constrained operator Riccati equations:

$$A\Theta_1 + \Theta_1 A^* - 2\Theta_1 C^* C\Theta_1 + N_1 = 0 \text{ on } D(A) \tag{3.49a}$$

$$S\Theta_2 + \Theta_2 S^* - 2\Theta_2 Q^* Q\Theta_2 + N_2 = 0 \text{ on } \mathbb{C}^n \tag{3.49b}$$

$$P\Theta_2 + 2\Theta_1 C^* Q\Theta_2 = N_3 \tag{3.49c}$$

where N_1 and N_2 are positive definite operator and matrix, respectively, N_3 is decided by the solutions Θ_1 and Θ_2 in equation (3.49c) such that $\begin{bmatrix} N_1 & N_3 \\ N_3^* & N_2 \end{bmatrix}$ is positive definite and $\Theta_1(D(A^*)) \subset D(A)$, then $\mathcal{G}_2 = \begin{bmatrix} G_1 \\ G_2 \end{bmatrix} = \begin{bmatrix} \Theta_1 C^* \\ -\Theta_2 Q^* \end{bmatrix}$ is an exponentially stabilizing output injection gain.

Proof. Utilizing the equation (3.49) to construct a matrix equation

$$\begin{bmatrix} A\Theta_1 + \Theta_1 A^* - 2\Theta_1 C^* C\Theta_1 + N_1 & P\Theta_2 + 2\Theta_1 C^* Q\Theta_2 + N_3 \\ \Theta_2 P^* + 2\Theta_2 Q^* C\Theta_1 + N_3^* & S\Theta_2 + \Theta_2 S^* - 2\Theta_2 Q^* Q\Theta_2 + N_2 \end{bmatrix} = 0 \tag{3.50}$$

The equation above can be written as

$$\begin{bmatrix} A & P \\ 0 & S \end{bmatrix} \begin{bmatrix} \Theta_1 & 0 \\ 0 & \Theta_2 \end{bmatrix} + \begin{bmatrix} \Theta_1 & 0 \\ 0 & \Theta_2 \end{bmatrix} \begin{bmatrix} A & P \\ 0 & S \end{bmatrix}$$
$$-2 \begin{bmatrix} \Theta_1 & 0 \\ 0 & \Theta_2 \end{bmatrix} \begin{bmatrix} C^* \\ -Q^* \end{bmatrix} \begin{bmatrix} C & -Q \end{bmatrix} \begin{bmatrix} \Theta_1 & 0 \\ 0 & \Theta_2 \end{bmatrix} + \begin{bmatrix} N_1 & N_3 \\ N_3^* & N_2 \end{bmatrix} = 0$$

If rearranging the equation above, we obtain

$$\left(\begin{bmatrix} A & P \\ 0 & S \end{bmatrix} - \begin{bmatrix} \Theta_1 C^* \\ -\Theta_2 Q^* \end{bmatrix} \begin{bmatrix} C & -Q \end{bmatrix}\right) \begin{bmatrix} \Theta_1 & 0 \\ 0 & \Theta_2 \end{bmatrix} + \begin{bmatrix} \Theta_1 & 0 \\ 0 & \Theta_2 \end{bmatrix} \times \left(\begin{bmatrix} A & P \\ 0 & S \end{bmatrix} - \begin{bmatrix} \Theta_1 C^* \\ -\Theta_2 Q^* \end{bmatrix} \begin{bmatrix} C & -Q \end{bmatrix}\right)^* + \begin{bmatrix} N_1 & N_3 \\ N_3^* & N_2 \end{bmatrix} = 0 \tag{3.51}$$

Let $\mathcal{G}_2 = \begin{bmatrix} G_1 \\ G_2 \end{bmatrix} = \begin{bmatrix} \Theta_1 C^* \\ -\Theta_2 Q^* \end{bmatrix}$ and according to Lemma 3, we know that $\mathcal{G}_2$ can stabilize the pair $\left(\begin{bmatrix} A & P \\ 0 & S \end{bmatrix}, \begin{bmatrix} C & -Q \end{bmatrix}\right)$ and $G_1 = \Theta_1 C^*$, $G_2 = -\Theta_2 Q^*$. □

In Theorem 6, S, Q and N_2 are matrices, thus (3.49b) is a matrix Riccati equation and it is very easy to calculate Θ_2. The equation (3.49a) is an operator Riccati equation and we can solve it through the similar method in Lemma 2. Once the results of equations (3.49a)-(3.49b) are obtained, we also need to guarantee that the results satisfy the constraint equation (3.49c), i.e. $\begin{bmatrix} N_1 & N_3 \\ N_3^* & N_2 \end{bmatrix}$ is positive definite.

3.2.3 Study of Simulation

In this section, a representative example is presented to illustrate the application of the developed theory in Section 3.2.2. The process plant is the infinite-dimensional system given as a regular first order hyperbolic PDEs with the boundary observation operator and is utilized to present the state feedback and error feedback regulator designs.

Let us consider a homogenous one-dimensional hyperbolic PDE system with boundary observation:

$$\frac{\partial x(z,t)}{\partial t} = v\frac{\partial x(z,t)}{\partial z} + tan(z)x(z,t) + b(z)u(t), z \in [0,1] \tag{3.52a}$$

$$x(0,t) = 0, \quad x(z,0) = x_0(z) \tag{3.52b}$$

$$y(t) = \int_{z_1-r}^{z_1} x(z,t)dz \tag{3.52c}$$

where v is a negative constant, i.e. $v < 0$, the distributed control function $b(z) = 1$, $x_0 \in L^2(0,1)$, $x(z,t)$ is the state of the plant, $u(t)$ is the control signal and the output $y(t)$ is the evolution of state in the domain $[z_1 - r, z_1]$ with $z_1 = 1$ and $r = 0.001$. $t > 0$ and $z \in [0,1]$ are time variable and spatial variable, respectively.

$x(t)$ denotes the state in Hilbert space $X = L^2(0,1)$, $u(t)$ is the control signal in a real Hilbert space $L^2_{loc}([0,\infty), U)$, $y(t)$ is the output of the system in the real Hilbert space $L^2_{loc}([0,\infty), Y)$ where $U \subset R$ and $Y \subset R$, and $x_0 \in X$ is the initial value of the state. The system operator A is defined as:

$$Ah = v\frac{dh}{dz} + tan(z)h \tag{3.53}$$

with the domain $D(A) = \left\{h(z) \in X : h(z) \text{ is a.c.}, \frac{dh(z)}{dz} \in X, \text{ and } h(0) = 0\right\}$. The distributed control operator $B = b(z) = 1$ is an identity operator. The operator C is defined as $C(\cdot) = \int_{z_1-r}^{z_1}(\cdot)dz \in \mathcal{L}(X,Y)$.

Our objective is to construct the regulator that will drive the output $y(t)$ to track a periodic reference signal of the form $y_r(t) = \Upsilon sin(\alpha t)$ generated by the exosystem in the form of (3.2a)

$$\begin{bmatrix} \dot{w}_1(t) \\ \dot{w}_2(t) \end{bmatrix} = \begin{bmatrix} 0 & \alpha \\ -\alpha & 0 \end{bmatrix} \begin{bmatrix} w_1(t) \\ w_2(t) \end{bmatrix}, \quad \begin{bmatrix} w_1(0) \\ w_2(0) \end{bmatrix} = \begin{bmatrix} 0 \\ \Upsilon \end{bmatrix} \tag{3.54}$$

In this example, we set $\alpha = 2$ and $\Upsilon = 5$. In terms of notation defined in (3.2b) and (3.2c), we set $Q = \begin{bmatrix} 1 & 0 \end{bmatrix}$ and $F = \begin{bmatrix} 0 & 0 \end{bmatrix}$ for simplicity. Then, the reference signal $y_r(t) = 5sin(2t)$ and disturbance $d(t) = 0$. Apparently, $w(t) = \begin{bmatrix} w_1(t) \\ w_2(t) \end{bmatrix} \in \mathbb{R}^2$, and $S = \begin{bmatrix} 0 & \alpha \\ -\alpha & 0 \end{bmatrix}$. It is very easy to obtain the eigenvalues and orthonormal eigenvectors of

S:

$$iw_1 = \alpha i = 2i, \;\; iw_2 = -\alpha i = -2i \tag{3.55}$$

$$\phi_1 = \begin{bmatrix} -0.7071i \\ 0.7071 \end{bmatrix}, \;\; \phi_2 = \begin{bmatrix} 0.7071i \\ 0.7071 \end{bmatrix} \tag{3.56}$$

3.2.3.1 The stabilizing feedback gain

If we let $v = -0.15$ in the plant (3.52), we study the performance of the open-loop system (3.52) and apply Theorem 2 to stabilize the closed-loop system, i.e. $u(t) = Kx(t)$ in (3.52). Since $v < 0$, we know the operator A is exponentially stable but the open-loop system cannot achieve the stable state at a desired rate. In this section, we will show that with the help of Theorem 2, we can choose the stabilizing feedback gain K such that the closed-loop system achieves the steady state at a desired rate.

According to Theorem 2 and Lemma 2, we can construct the matrix Riccati differential equation with $M = 1$:

$$-0.15\frac{d\Psi(z)}{dz} = tan(z)\Psi(z) + \Psi(z)tan(z) + 1 - 2\Psi(z)^2, \; \Psi(1) = 0 \tag{3.57}$$

Then, we obtain the feedback control law $u(t) = Kx(t) = -\Psi(z)x(t)$. If we substitute $u(t)$ back into the system (3.52), we can see the result shown in Figure 3.1.

In Figure 3.1, although both the open-loop system (3.52) and the closed-loop system with $u(t) = Kx(t)$ achieve the steady state, the performance of the two cases differs significantly. Under the effect of stabilizing feedback control law $u(t) = -\Psi(z)x(t)$, the closed-loop system rejects the effect of the initial condition about two times faster (according to the residence time) than the open-loop system and converges to the desired steady state. Moreover, under the effect of the initial condition, the response of the open-loop system $y_o(t)$ is extremely large (the maximum value is about 9.8×10^5, see the solid line in Figure 3.1) and apparently exceeds the realistic limitation of the physical systems. However, the response of the closed-loop system $y_c(t)$ is guaranteed within a normal range (the maximum value is less than 21,

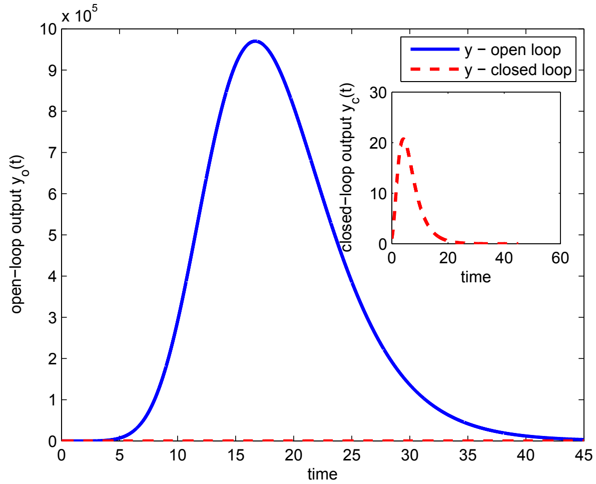

Figure 3.1: open-loop output and closed-loop output given by (3.52) with feedback control law $u(t) = -\Psi(z)x(t)$.

see the dashed line in Figure 3.1) and preforms very well, see Figure 3.1.

3.2.3.2 The state feedback regulator

Let $v = -1$ in the plant (3.52), in this section, we design the state feedback control law $u(t) = K_1 x(t) + Lw(t)$ to force the output of the plant (3.52) tracking the reference trajectory $y_r(t) = Qw(t) = 5sin(2t)$ generated by the exosystem (3.54). Similar to the principle in Section 3.2.3.1, we can easily apply Theorem 2 and Lemma 2 to obtain the stabilizing feedback gain $K_1 = -\Psi(z) \cdot I$, where I is identity operator. Therefore, K_1 can provide the state (including the output) of the system which converges to zero. Then, we need to add the term $Lw(t)$ in the control law to drive the output of the system to have proper amplitude and phase.

A direct calculation indicates that for all $s \in \mathbb{C} \backslash \sigma(A)$ the transfer function of the system (3.52) is

$$G(s) = C(sI - A)^{-1}B \approx \frac{\left(e^{(s-1)}\sin(1) + (s-1)e^{(s-1)}\cos(1) - (s-1)\right)}{e^{(s-1)}\cos(1)\left(1 + (s-1)^2\right)} \tag{3.58}$$

It is easy to see that $G(s)$ is regular.

Apparently, from Theorem 3, we know $L = \Gamma - K_1 \Pi$. According to the expression of

S, we can construct the operators $\Gamma = \begin{bmatrix} \gamma_1 & \gamma_2 \end{bmatrix} \in L(\mathbb{C}^2, U)$, and $\Pi \in L(\mathbb{C}^2, X)$ such that $\left(\Pi w(t)\right)(z) = \begin{bmatrix} \Pi_1(z) & \Pi_2(z) \end{bmatrix} \begin{bmatrix} w_1(t) \\ w_2(t) \end{bmatrix}$ for any $w(t) \in \mathbb{C}^2$. Then, from the expression (3.32) in Theorem 4, the solution of constrained Sylvester equations (3.24)-(3.25) is given by

$$\Pi\phi_1 = (\alpha i I - A)^{-1}(B\Gamma) = (2iI - A)^{-1}(B\Gamma)\,\phi_1$$

A straightforward calculation shows that

$$\begin{bmatrix} \Pi_1(z), & \Pi_2(z) \end{bmatrix} \phi_1 = \begin{bmatrix} \gamma_1(2iI - A)^{-1}b(z), & \gamma_2(2iI - A)^{-1}b(z) \end{bmatrix} \phi_1$$

Then, we obtain the identity

$$\Pi_1(z) = \gamma_1(2iI - A)^{-1}b(z), \;\; \Pi_2(z) = \gamma_2(2iI - A)^{-1}b(z) \tag{3.59}$$

In this example, the equation (3.25) reduces to

$$C\Pi_1(z) = 1, \;\; C\Pi_2(z) = 0 \tag{3.60}$$

From (3.59)-(3.60), we can easily obtain

$$\gamma_1 = \frac{\mathrm{Re}(G(i\alpha))}{|G(i\alpha)|^2} \approx 0.1278, \;\; \gamma_2 = -\frac{\mathrm{Im}(G(i\alpha))}{|G(i\alpha)|^2} \approx 0.3936$$

The equation (3.24) can be written as

$$-\Pi'_1(z) + tan(z)\Pi_1(z) + 2\Pi_2(z) = -\gamma_1 \tag{3.61a}$$

$$-\Pi'_2(z) + tan(z)\Pi_2(z) - 2\Pi_1(z) = -\gamma_2 \tag{3.61b}$$

$$\Pi_1(0) = 0, \quad \Pi_2(0) = 0 \tag{3.61c}$$

where the boundary conditions in (3.61c) come from the definition of domain of the system generator A in (3.53).

Once γ_1 and γ_2 are known, we can calculate Π_1 and Π_2 numerically from equation (3.61). The common numerical method is finite difference. For our example, we set the initial condition $x_0(z) = 10z^2(3/2 - z)$. The results are shown in Figure 3.2 and Figure 3.3

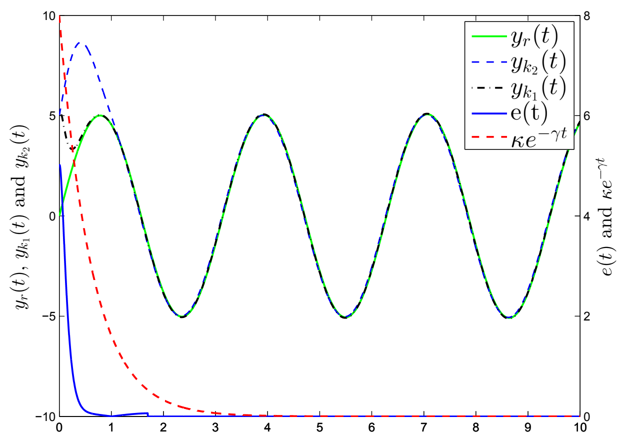

Figure 3.2: The reference trajectory $y_r(t) = 5sin(2t)$, the plant outputs $y_{k_1}(t)$ and $y_{k_2}(t)$ under the state feedback control law $u(t) = Kx(t) + (\Gamma - K\Pi)w(t)$ with different stabilizing feedback gains $K = K_1$ and $K = K_2$, and the tracking error $|e(t)|$.

In Figure 3.2, $y_{k_1}(t)$ and y_{k_2} present outputs of the plant under the state feedback control law with different stabilizing feedback gains K_1 and K_2. K_1 is the solution of (3.19a) with a large design parameter $M_1 = 200$ and K_2 is the solution of (3.19b) with a small design parameter $M_2 = 10$, i.e. $\|K_1\| > \|K_2\|$. We can easily find that under the same effect of the initial condition $x_0(z)$, by comparing with $y_{k_2}(t)$, $y_{k_1}(t)$ tracks the reference signal $y_r(t)$ very quickly. This phenomenon is clearly consistent with the conclusion in Remark 5 and also is a strong support to the feasibility of Theorem 2 and Lemma 2 in the meantime. Moreover, in Figure 3.2, the blue solid line presents the evolution of the absolute value of tracking error $|e(t)|$ and the red dashed line denotes $\kappa e^{-\gamma t}$ with $\kappa > 0$ and $\gamma > 0$. We conclude that the tracking error decays to zero exponentially, which is consistent with the conclusion of Corollary 2.

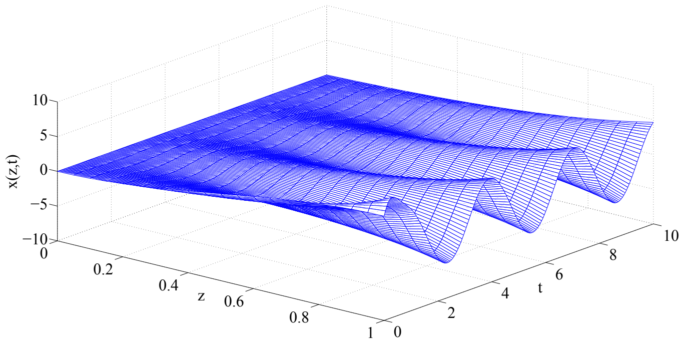

Figure 3.3: State profile $x(z,t)$ under the state feedback control law $u(t) = Kx(t) + (\Gamma - K\Pi)w(t)$.

3.2.3.3 The error feedback regulator

Consider the same plant and the same exosystem in Section 3.2.3.2, i.e. $v = -1$ in the plant (3.52), we construct the error feedback regulator of the form

$$\dot{r}(t) = \mathcal{G}_1 r(t) + \mathcal{G}_2 e(t) \tag{3.62a}$$

$$u(t) = Hr(t) \tag{3.62b}$$

where $r(t) \in \Omega = L^2(0,1) \oplus R^2$ denotes the state of the regulator, i.e. the estimation of $\begin{bmatrix} x(t) & w^T(t) \end{bmatrix}^T$, $\mathcal{G}_1 \in \mathcal{L}(\Omega)$, $\mathcal{G}_2 = \begin{bmatrix} G_1 \\ G_2 \end{bmatrix} : R \mapsto L^2(0,1) \oplus R^2$ exponentially stabilize the pair $\left(\begin{bmatrix} A & P \\ 0 & S \end{bmatrix}, \begin{bmatrix} C & -Q \end{bmatrix} \right)$ and $H \in \mathcal{L}(\Omega, R)$. In this section, our objective is to design the regulator in the form of (3.62) such that the output of plant (3.52) is forced to track the periodic reference trajectory $y_r(t) = 5sin(2t)$ generated by the exosystem (3.54).

By setting $N_1 = 1$ and $N_2 = \begin{bmatrix} 1 & 0 \\ 0 & 1 \end{bmatrix}$, we apply Theorem 6 and obtain the following equations:

$$\frac{d\Psi_o(z)}{dz} = \tan(z)\Psi_o(z) + \Psi_o(z)\tan(z) + 1 - 2\Psi_o(1)^2, \;\; \Psi_o(0) = 0 \tag{3.63}$$

$$\begin{bmatrix} 0 & 2 \\ -2 & 0 \end{bmatrix} X + X \begin{bmatrix} 0 & -2 \\ 2 & 0 \end{bmatrix} - 2X \begin{bmatrix} 1 & 0 \\ 0 & 0 \end{bmatrix} X + \begin{bmatrix} 1 & 0 \\ 0 & 1 \end{bmatrix} = 0 \tag{3.64}$$

Then, $\Theta_1 = \Psi_o \cdot I$, $\Theta_2 = X$ in equation (3.49) and in particular $\Psi_o(0) = 0$ implies that $\Theta_1(D(A^*)) \subset D(A)$. It is easy to obtain

$$\mathcal{G}_2 = \begin{bmatrix} G_1 \\ G_2 \end{bmatrix} = \begin{bmatrix} \Psi_o^*(1) \cdot I \\ X \end{bmatrix}$$

with $\Psi_o^*(1) = \Psi_o(1)$.

The controller system operator is of the form

$$\mathcal{G}_1 = \begin{bmatrix} A + BK - G_1 C & B(\Gamma - K\Pi) + G_1 Q \\ -G_2 C & S + G_2 Q \end{bmatrix}$$

In this section, we take the operators K, Π and Γ to be same as K_1, $\Pi = \begin{bmatrix} \Pi_1 & \Pi_2 \end{bmatrix}$ and $\Gamma = \begin{bmatrix} \gamma_1 & \gamma_2 \end{bmatrix}$ in Section 3.2.3.2. The results are depicted in Figure 3.4 and Figure 3.5.

Remark 6. *In this example, the error feedback regulator (3.62) is infinite-dimensional because of the existence of the operator A defined in (3.53). But it is not hard to see that when substituting the explicit expression of $\mathcal{G}_1$ and $\mathcal{G}_2$ into (3.62), one can utilize a standard numerical method, e.g., finite difference to solve (3.62a) to obtain $r(t)$. Then, one generates $u(t)$ by utilizing $r(t)$ based on (3.62b).*

In Figure 3.4, the reference signal $y_r(t)$ and the output of closed-loop system $y(t)$ are plotted. In Figure (3.5), we plot closed-loop system state profile $x(z,t)$.

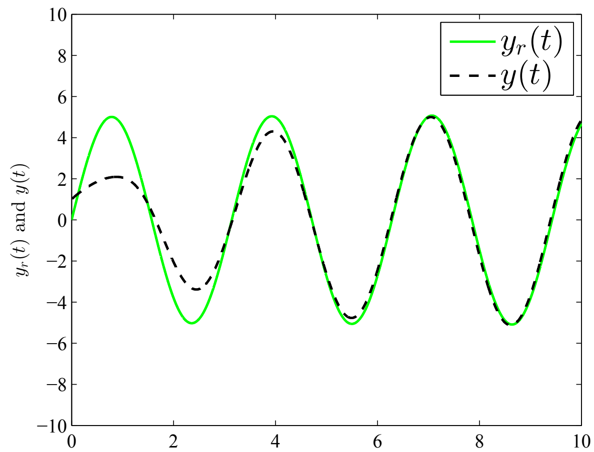

Figure 3.4: The reference trajectory $y_r(t) = 5sin(2t)$ and the plant output $y(t)$ under the error feedback regulator (3.62).

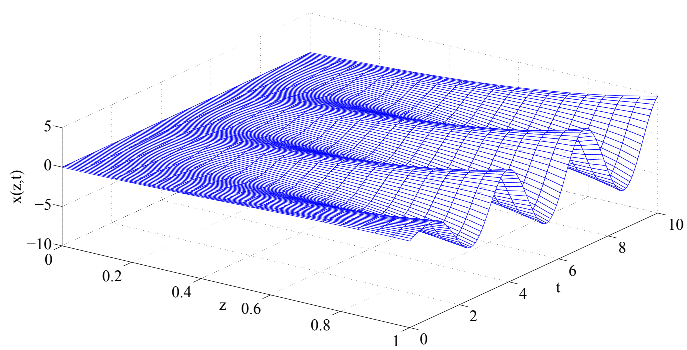

Figure 3.5: State profile $x(z, t)$ under the error feedback regulator (3.62)

3.3 Finite-dimensional regulators for a class of hyperbolic PDE systems

3.3.1 System description

We consider the following 1-D linear hyperbolic partial differential equation single scalar system on the domain $\{t \in \mathbb{R}_+, z \in [0, 1]\}$, which models large class of process control systems, see [32] and [13]:

$$\frac{\partial x(z,t)}{\partial t} = v(z)\frac{\partial x(z,t)}{\partial z} + g(z)x(z,t) + b(z)\mathcal{U}(z,t) \tag{3.65a}$$

$$x(0,t) = 0,\ x(z,0) = x_0 \in X \tag{3.65b}$$

$$y(t) = \int_{z_1-r}^{z_1} x(z,t)dz,\ y_m(t) = \int_{z_0-r}^{z_0} x(z,t)dz, r > 0 \tag{3.65c}$$

In particular, here $\mathcal{U}$ can be a spatially distributed input $\mathcal{U}(z,t) \in L^2(0,1)$ in (3.65) and non-spatially distributed input $\mathcal{U}(t) \in L^2_{loc}([0,\infty),\mathbb{R})$. In particular, in order to consider both spatially and non-spatially distributed inputs, we assume the input space to be $\bar{U} = L^2(0,1) \cap L^2_{loc}([0,\infty),\mathbb{R})$. $x(\cdot,t) \in X = L^2(0,1)$, $\forall t \geq 0$ denotes the state variable and then $x(\cdot,t)$ at the point z is $x(z,t)$. The space $X = L^2(0,1)$ is the state space with the norm $\|\cdot\|_H$ (or $\|\cdot\|$), i.e., $\|x(t)\|^2 = \int_0^1 x^2(z,t)dz$. The output $y(t) \in L^2_{loc}([0,\infty),\mathbb{R})$ is to be controlled and the output $y_m(t) \in L^2_{loc}([0,\infty),\mathbb{R})$ is the measurement. In particular, it is not necessary that the controlled output $y(t)$ can be measured. z_1 and z_0 are specified points in spatial range $[0,1]$. The transport velocity $v(z) \in C^1([0,1])$ is negative and the spatially varying function, i.e. $v(z) < 0$. $g(z) : [0,1] \mapsto \mathbb{R} : z \mapsto g(z)$ is a measurable function, i.e. $g(z) \in L^\infty(0,1)$ and $b(z) \in L^\infty(0,1)$ is a real continuous spatial varying function.

Remark 7. *We consider the hyperbolic PDE systems with distributed control operator instead of boundary control. Actually, for most of hyperbolic PDE systems, the systems with boundary control input can be transformed into the ones with distributed control input, for more detail please refer to [31] and the Chapter 3 in [14].*

3.3.1.1 Stability analysis of the system

We are now concerned with the following system in the form

$$\frac{\partial x(z,t)}{\partial t} = v(z)\frac{\partial x(z,t)}{\partial z} + g(z)x(z,t) \tag{3.66}$$

under the boundary condition:

$$x(0,t) = 0 \tag{3.67}$$

To analyse the stability of the system (3.66), we first provide the essential preliminary results that will help us to account in the stability analysis for the spatially varying nature of the above system given by Eq.(3.66)-(3.67). For $p(z) \in C^0([0,1])$, we are interested in the existence of $f(z) \in C^1([0,1])$ such that

$$f(z) > 0 \text{ in } [0,1] \tag{3.68}$$

$$\frac{df(z)}{dz} < 0 \text{ a. e. in } [0,1] \tag{3.69}$$

$$-\frac{df(z)}{dz} > |p(z)f(z)| \text{ a. e. in } [0,1] \tag{3.70}$$

where a.e. means "almost everywhere".

Proposition 1. *There exits $f(z) \in C^1([0,1])$ such that (3.68)-(3.70) hold if there exists a unique solution $\eta(z)$ of the initial value Cauchy problem*

$$\frac{d\eta(z)}{dz} = |p(z)\eta(z)|\,,\ \eta(0) = \mu,\ \mu > 0 \tag{3.71}$$

defined on $[0,1]$.

Proof. Since there exists a unique solution of (3.71) defined in $[0,1]$, then if we set $\varepsilon > \mu$, the solution $\eta_\varepsilon(z)$ of the initial value Cauchy problem

$$\frac{d\eta_\varepsilon(z)}{dz} = |p(z)\eta_\varepsilon(z)|\,(1+\varepsilon), \qquad \eta_\varepsilon(0) = \varepsilon \tag{3.72}$$

is defined on $[0,1]$. Note that

$$\eta_\varepsilon(z) > \eta(z) > 0 \text{ in } [0,1] \tag{3.73}$$

Then, we can define $f(z) \in C^1([0,1])$ as

$$f(z) := \frac{1}{\eta_\varepsilon(z)}, \qquad \forall z \in [0,1] \tag{3.74}$$

We know that from (3.73), $f(z)$ is well-defined. Obviously, (3.68) and (3.69) hold. Moreover, from (3.74) and (3.72), we have

$$-\frac{df(z)}{dz} = \frac{1}{\left(\eta_\varepsilon(z)\right)^2}\frac{d\eta_\varepsilon(z)}{dz} = \frac{|p(z)\eta_\varepsilon(z)|}{\left(\eta_\varepsilon(z)\right)^2} + \frac{|p(z)\eta_\varepsilon(z)|\,\varepsilon}{\left(\eta_\varepsilon(z)\right)^2} > |p(z)f(z)|$$

i.e. (3.70) holds. ■

Remark 8. *The function*

$$(z, \eta(z)) \in [0,1] \times \mathbb{R} \mapsto |p(z)\eta(z)| \in \mathbb{R}$$

is continuous in $[0,1] \times \mathbb{R}$ *and globally Lipschitz with respect to* $\eta(z)$*. Hence the initial value Cauchy problem (3.71) always has a unique solution.* ■

Based on the Proposition 1, we carry on the stability analysis of the system (3.66)-(3.67). We introduce the following Lyapunov function candidate:

$$\mathcal{V}(x) := \langle q(z)x, x\rangle_{L^2(0,1)} = \int_0^1 q(z)x^2(z,t)dz > 0 \tag{3.75}$$

with $q(z) = -1/(\eta_\varepsilon(z)v(z)) \in C^1([0,1];[0,+\infty])$, where $\eta_\varepsilon(z)$ is the solution of the following Cauchy problem

$$\frac{d\eta_\varepsilon(z)}{dz} = (1+\varepsilon)\left|\frac{2g(z)}{v(z)}\eta_\varepsilon(z)\right|, \quad \eta_\varepsilon(0) = \varepsilon > \mu \tag{3.76}$$

Note that $\eta_\varepsilon(z) > 0$. Therefore, from $v(z) < 0$, $q(z) > 0$ and $\mathcal{V}(x) > 0$. Note that the Cauchy problem (3.76) is actually the Cauchy problem (3.72) with $p(z) = \frac{2g(z)}{v(z)}$.

Then, the time derivative $\dot{\mathcal{V}}(x)$ of $\mathcal{V}$ in terms of the trajectories of (3.66)-(3.67) is

$$\begin{aligned}
\dot{\mathcal{V}}(x) &= \textstyle\int_0^1 2q(z)x(z,t)\frac{\partial x(z,t)}{\partial t}dz \\
&= \textstyle\int_0^1 2q(z)x(z,t)\left(v(z)\frac{\partial x(z,t)}{\partial z} + g(z)x(z,t)\right)dz \\
&\qquad \text{(integration by parts)} \\
&= G - \textstyle\int_0^1 M dz
\end{aligned} \tag{3.77}$$

with

$$G := q(1)v(1)x^2(1,t) - q(0)v(0)x^2(0,t) \tag{3.78}$$

$$M := \left(\frac{d\left(q(z)v(z)\right)}{dz} - 2q(z)g(z)\right)x^2(z,t) \tag{3.79}$$

Since $v(z) < 0$, $q(z) > 0$ and the boundary condition $x(0,t) = 0$, it is easy to show that in (3.78) $G = q(1)v(1)x^2(1,t) < 0$ with $v(1) < 0$ and $q(1) > 0$. The stability of the system (3.66)-(3.67) is explored in the following theorem.

Theorem 7. *Suppose that the lower bound of the function $|g(z)|$ is nonzero, then the system (3.66)-(3.67) is exponentially stable if there exists the unique solution $\eta(z)$ of the initial value Cauchy problem*

$$\frac{d\eta(z)}{dz} = \left|\frac{2g(z)}{v(z)}\eta(z)\right|, \ \eta(0) = \mu, \ \mu > 0 \tag{3.80}$$

defined on $[0,1]$.

Proof. According to afore stated content, we define $q(z)$ and $f(z)$ as:

$$q(z) = \frac{-1}{\eta_\varepsilon(z)v(z)}, \ \ f(z) = \frac{1}{\eta_\varepsilon(z)} = -q(z)v(z) \tag{3.81}$$

where $\eta_\varepsilon(z)$ is the solution of (3.76). Because of the existence of the unique solution $\eta(z)$ of (3.80) and according to Proposition 1, it is easy to show that:

$$f(z) = -q(z)v(z) > 0$$

$$\frac{df(z)}{dz} = \frac{d\left(-q(z)v(z)\right)}{dz} < 0$$

$$-\frac{df(z)}{dz} = \frac{d\left(q(z)v(z)\right)}{dz} > \left|\frac{2g(z)}{v(z)}q(z)v(z)\right| = |2g(z)q(z)| \tag{3.82}$$

The above inequalities imply that M in (3.79) is positive, and thus $\dot{\mathcal{V}}(x) < 0$. In the following section, we demonstrate the exponential stability of the system (3.66)-(3.67). Now, we claim that there exists a constant $\alpha > 0$ such that

$$\frac{d(q(z)v(z))}{dz} - 2q(z)g(z) > \alpha q(z) \tag{3.83}$$

To prove the above claim (3.83), we utilize the expression of $q(z) = \frac{-1}{\eta_\varepsilon(z)v(z)}$. Assume that

$M_g \neq 0$ is lower bound of $|g(z)|$, i.e., $|g(z)| \geq M_g$, then we have

$$
\begin{aligned}
&\tfrac{d(q(z)v(z))}{dz} - 2q(z)g(z) - \alpha q(z) = \tfrac{d}{dz}\left(\tfrac{-1}{\eta_\varepsilon(z)v(z)}v(z)\right) + \tfrac{2g(z)}{\eta_\varepsilon(z)v(z)} + \tfrac{\alpha}{\eta_\varepsilon(z)v(z)} \\
&= \tfrac{\eta'_\varepsilon(z)}{(\eta_\varepsilon(z))^2} + \tfrac{2g(z)}{\eta_\varepsilon(z)v(z)} + \tfrac{\alpha}{\eta_\varepsilon(z)v(z)} = \tfrac{(1+\varepsilon)\left|\frac{2g(z)}{v(z)}\eta_\varepsilon(z)\right|}{(\eta_\varepsilon(z))^2} - \tfrac{2g(z)}{|\eta_\varepsilon(z)v(z)|} - \tfrac{\alpha}{|\eta_\varepsilon(z)v(z)|} \\
&\geq \tfrac{|2g(z)|\varepsilon-\alpha}{|\eta_\varepsilon(z)v(z)|} \geq \tfrac{2M_g\varepsilon-\alpha}{|\eta_\varepsilon(z)v(z)|}
\end{aligned} \tag{3.84}
$$

Based on the boundedness of $g(z)$, we can find $\alpha > 0$ such that $\alpha < 2M_g\varepsilon$, where M_g is upper bound of $|g(z)|$. Therefore, there exists a constant: $0 < \alpha < 2M_g\varepsilon$ such that (3.83) holds. Furthermore, in (3.79), $M > \alpha q(z)x^2(z,t)$. Then, from (3.77), we have

$$
\begin{aligned}
\dot{\mathcal{V}}(x) &< -\int_0^1 M dz \\
&< -\alpha \int_0^1 q(z)x^2(z,t)dz = -\alpha\mathcal{V}(x)
\end{aligned}
$$

which indicates the exponential stability of the system in the L_2-norm. □

Theorem 7 essentially provides a sufficient condition such that the system (3.66)-(3.67) is exponentially stable when the lower bound of $|g(z)|$ is nonzero. However, for the case $g(z) = 0$, it is easy the prove the exponential stability of the system (3.66)-(3.67) by choosing the Lyapunov candidate: $\mathcal{V}(x) = \int_0^1 e^{-\varpi z}\frac{x^2(z,t)}{-v(z)}dz$ with $\varpi > 0$.

Remark 9. *Motivated by Remark 1 and Proposition 1, it is easy to see that if the condition* $\frac{2g(z)}{v(z)} \in C^0([0,1])$ *is satisfied, then the function* $(z,\eta(z)) \in [0,1]\times\mathbb{R} \mapsto \left|\frac{2g(z)}{v(z)}\eta(z)\right| \in \mathbb{R}$ *is continuous in* $[0,1]\times\mathbb{R}$ *and globally Lipschitz with respect to* $\eta(z)$. *As a result, the initial value Cauchy problem (3.80) always has a unique solution and the system (3.66)–(3.67) is exponentially stable. Since the function* $v(z)$ *is assumed to be* $v(z) \in C^1([0,1])$, *then the condition* $g(z) \in C^0([0,1])$ *ensures that the function* $\frac{2g(z)}{v(z)}$ *satisfies* $\frac{2g(z)}{v(z)} \in C^0([0,1])$ *and to guarantee that the system (3.66)–(3.67) is exponentially stable.*

3.3.1.2 Problem formulation

The equivalent linear infinite-dimensional representation of the system (3.65) on the state space X is given by (3.1a)-(3.1b) by replacing $u(t)$ with $\mathcal{U}(z,t)$. And the linear system operator A defined on the domain:

$$D(A) = \left\{ x \in X : x(z) \text{ is a.c.} \frac{dx}{dz} \in X \text{ and } x(0) = 0 \right\} \tag{3.85}$$

where a.c. means 'absolutely continuous', as:

$$A = v(z)\frac{d}{dz} + g(z) \cdot I \tag{3.86}$$

The input operator is given by $B = b(z) \cdot I$, where I is the identity operator and the function $b(z)$ is assumed to be continuous on $[0,1]$, i.e, $b(z) \in C^0([0,1])$. The controlled output operator is given by $Cx(\cdot,t) = \int_{z_1-r}^{z_1} x(z,t)dz$ and the measured output operator is expressed by $C_m x(\cdot,t) = \int_{z_0-r}^{z_0} x(z,t)dz$ with $z_1, z_0 \in [0,1]$ and $r > 0$. In particular, r can be chosen infinitesimal.

The disturbance $d(t)$ and the reference trajectory $y_r(t)$ are generated by a known autonomous finite-dimensional signal process (exogenous system) defined in (3.2a)-(3.2c).

Let $X_c = X \oplus \mathbb{C}^n$ be the composite state-space, consisting of the states of plant and the exosystem, and we obtain the composite system

$$\dot{x}_c(t) = A_c x_c(t) + B_c U(t), \ \ t > 0, \ \ x_c(0) \in D(A_c) \tag{3.87}$$

$$e(t) = C_c x_c(t) \tag{3.88}$$

$$y_r(t) = C_Q x_c(t) \tag{3.89}$$

$$y_m(t) = C_y x_c(t) \tag{3.90}$$

with the composite state $x_c(t) = \begin{bmatrix} x(t)^T & w(t)^T \end{bmatrix}^T$, where the composite system operator is given by

$$A_c = \begin{bmatrix} A & P \\ 0 & S \end{bmatrix} \text{ with } P = B_d F$$

where $D(A_c) = D(A) \oplus \mathbb{C}^n \subset X_c$, the operators $C_c \in \mathcal{L}(X_c, \mathbb{R})$, $C_Q \in \mathcal{L}(X_c, \mathbb{R})$, $C_y \in \mathcal{L}(X_c, \mathbb{R})$ and $B_c \in \mathcal{L}(\bar{U}, X_c)$ are given by

$$C_c = \begin{bmatrix} C & -Q \end{bmatrix},\ C_Q = [\ 0 \quad Q\ ],\ C_y = \begin{bmatrix} C_m & 0 \end{bmatrix},\ B_c = \begin{bmatrix} B \\ 0 \end{bmatrix}$$

It is evident that the system generator A_c generates a C_0-semigroup on X_c. In this chapter, we propose to design finite-dimensional output and error feedback regulator such that

$$\lim_{t\to\infty} (y(t) - y_r(t)) = 0,\ \forall x(0) \in X,\ w(0) \in \mathbb{C}^n \tag{3.91}$$

in the sense of exponential tracking error $(e(t) = y(t) - y_r(t))$ decay.

3.3.2 The output regulation problem

The essential mission of the output regulation problem for the hyperbolic PDE system is to design regulators to guarantee the following conditions:

[c1.] The closed-loop system operator generates an exponentially stable C_0-semigroup;

[c2.] In the closed-loop system, for any initial conditions $x(0) \in X$ and $w(0) \in \mathbb{C}^n$, the tracking error $e(t)$ decays to zero w.r.t time variable t exponentially.

In this chapter, two types of regulators are designed to solve the output regulation problem of the system.

Problem 3.1 - Output feedback regulator problem: under the assumption that the measured output $y_m(t)$ (different from $y(t)$) and the reference signal $y_r(t)$ are available, and we design the following output feedback regulators with the spatially distributed input and the lumped input, respectively:

- Output feedback regulation with the spatially distributed input that is the function of both space variable z and time variable t:

$$\begin{aligned} \dot{r}_w(t) &= Sr_w(t) + \begin{bmatrix} L_r & 0 \\ 0 & L_m \end{bmatrix} \begin{bmatrix} y_r(t) - C_Q\tilde{\Pi}r_w(t) \\ y_m(t) - C_y\tilde{\Pi}r_w(t) \end{bmatrix} \\ \mathcal{U}(z,t) &= \Gamma r_w(t) + \begin{bmatrix} k_r(z) & k_m(z) \end{bmatrix} \begin{bmatrix} y_r(t) - C_Q\tilde{\Pi}r_w(t) \\ y_m(t) - C_y\tilde{\Pi}r_w(t) \end{bmatrix} \end{aligned} \tag{3.92}$$

- Output feedback regulation with the lumped input that is only the function of time variable t:

$$\begin{aligned} \dot{r}_w(t) &= Sr_w(t) + \begin{bmatrix} L_r & 0 \\ 0 & L_m \end{bmatrix} \begin{bmatrix} y_r(t) - C_Q\tilde{\Pi}r_w(t) \\ y_m(t) - C_y\tilde{\Pi}r_w(t) \end{bmatrix} \\ u(t) &= \Gamma r_w(t) + \begin{bmatrix} K_r & K_m \end{bmatrix} \begin{bmatrix} y_r(t) - C_Q\tilde{\Pi}r_w(t) \\ y_m(t) - C_y\tilde{\Pi}r_w(t) \end{bmatrix} \end{aligned} \tag{3.93}$$

with $\tilde{\Pi}$ to be defined in following sections, $\mathcal{U}(\cdot,t) \in L^2(0,1)$, $L_r \in \mathcal{L}(\mathbb{R},\mathbb{C}^{n_r})$, $L_m \in \mathcal{L}(\mathbb{R},\mathbb{C}^{n_d})$, $\Gamma \in \mathcal{L}(\mathbb{C}^n,\mathbb{R})$, $k_r(z), k_m(z) \in C^0(0,1)$ and $K_r, K_m \in \mathbb{R}$, such that: (a.1) the closed-loop system is exponentially stable; (a.2) the tracking error $e(t) \to 0$ as $t \to +\infty$. Here $n_r + n_d = n$.

Problem 3.2 - Error feedback regulator problem: In this case, we assume that only the tracking error $e(t)$ can be measured, and we design the following error feedback regulators with the spatially distributed input and the lumped input, respectively:

- Error feedback regulation with the spatially distributed input that is function of both space variable z and time variable t:

$$\begin{aligned} \dot{r}_w(t) &= Sr_w(t) + L(e(t) - C_c\tilde{\Pi}r_w(t)) \\ \mathcal{U}(z,t) &= \Gamma r_w(t) + k_e(z)(e(t) - C_c\tilde{\Pi}r_w(t)) \end{aligned} \tag{3.94}$$

- Error feedback regulation with the lumped input that is only the function of time variable t:

$$\begin{aligned} \dot{r}_w(t) &= Sr_w(t) + L(e(t) - C_c\tilde{\Pi}r_w(t)) \\ u(t) &= \Gamma r_w(t) + K_e(e(t) - C_c\tilde{\Pi}r_w(t)) \end{aligned} \tag{3.95}$$

with $\mathcal{U}(\cdot,t) \in L^2(0,1)$, $L \in \mathcal{L}(\mathbb{R},\mathbb{C}^n)$, $\Gamma \in \mathcal{L}(\mathbb{C}^n,\mathbb{R})$, $k_e(z) \in C^0(0,1)$ and $K_e \in \mathbb{R}$, such that: (a.1) the closed-loop system is exponentially stable; (a.2) the tracking error $e(t) \to 0$ as $t \to +\infty$.

We now demonstrate first the design of the finite-dimensional feedforward regulator on the space W:

$$\begin{aligned} \dot{r}_w(t) &= Sr_w(t) \\ U(t) &= \Gamma r_w(t) \end{aligned} \tag{3.96}$$

with the initial condition $r_w(0) = r_{w0} \in \mathbb{C}^n$ and $\Gamma \in \mathcal{L}(\mathbb{C}^n,\mathbb{R})$. By applying the feedforward regulator, the composite system (3.87) tracks the linear function

$$x_c(t) = \tilde{\Pi} r_w(t) \tag{3.97}$$

where $\tilde{\Pi} = \begin{bmatrix} \Pi \\ I \end{bmatrix}$ with the bounded operator $\Pi \in \mathcal{L}(\mathbb{C}^n, X)$ with $\Pi\mathbb{C}^n \in D(A)$, if the initial condition is given by

$$x_c(0) = \tilde{\Pi} r_w(0) \tag{3.98}$$

The following theorem provides conditions such that (3.96) solves the output regulation problem.

Theorem 8. *For the system (3.65), the feedforward regulator (3.96) achieves exponentially stable tracking in the sense of (3.91) for initial values (3.98), if there exist operators* $\Pi \in \mathcal{L}(\mathbb{C}^n, X)$ *defined in (3.97) and* $\Gamma \in \mathcal{L}(\mathbb{C}^n, \bar{U})$ *satisfying the Sylvester equations:*

$$\Pi S - A\Pi = B\Gamma + P \tag{3.99}$$

$$C_\Lambda \Pi - Q = 0 \tag{3.100}$$

where the eigenvalues of S *do not coincide with an invariant zero of the plant (3.1a)-(3.1b). In this case, the feedforward regulator (3.96) has the form:*

$$\begin{aligned} \dot{r}_w(t) &= Sr_w(t) \\ U(t) &= \Gamma r_w(t) \end{aligned} \tag{3.101}$$

Proof. The dynamics of $x_c(t) - \tilde{\Pi} r_w(t)$ are described by the autonomous abstract differential equation $\dot{x}_c(t) - \tilde{\Pi}\dot{r}_w(t) = A_c[x_c(t) - \tilde{\Pi} r_w(t)]$ with the initial value $x_c(0) - \tilde{\Pi} r_w(0) \in X_c$ if there exists a bounded linear operator $\tilde{\Pi}$ such that the following Sylvester operator equation holds:

$$\begin{bmatrix} A & P \\ 0 & S \end{bmatrix} \tilde{\Pi} - \tilde{\Pi} S = - \begin{bmatrix} B \\ 0 \end{bmatrix} \Gamma \tag{3.102}$$

Since A_c is the generator of an infinitesimal C_0-semigroup, the initial value problem has a unique solution. If (3.98) holds, the solution of $\dot{x}_c(t) - \tilde{\Pi}\dot{r}_w(t) = A_c[x_c(t) - \tilde{\Pi} r_w(t)]$ is $x_c(t) - \tilde{\Pi} r_w(t) = 0$. Then, the plant state $x(t)$ and the state of exosystem $w(t)$ can be expressed by $x(t) = \Pi r_w(t)$ and $w(t) = r_w(t)$, so that the tracking error in (3.91) takes the form $y(t) - y_r(t) = C\Pi r_w(t) - Q r_w(t)$. Therefore, in order to achieve output regulation (3.91), the operator Π has in addition to satisfy $C\Pi - Q = 0$ since S is an anti-Hurwitz matrix. A direct calculation shows that the equation (3.99) is equivalent to the equation (3.102). In [57], it is shown that there exists a solution (Π, Γ) of the Sylvester equation (3.99)-(3.100), if the eigenvalues of S do not coincide with an invariant zero of the plant (3.1a)-(3.1b). It should be mentioned that the operator Π is a spatially varying operator, i.e. $\Pi = \Pi(z)$, because $\Pi \in \mathcal{L}(\mathbb{C}^n, X)$. □

Due to the fact that in the general case the state of exosystem cannot be measured, the initial values $r_w(0)$ of the feedforward controller (3.96) cannot be chosen such that (3.98) holds. Therefore, in general, the initial error $x_c(0) - \Pi r_w(0) \neq 0$ may result so that the output regulation is not achieved. However, the exponentially decaying tracking error in (3.91) can be obtained by stabilizing the dynamics of $x_c(t) - \tilde{\Pi} r_w(t)$. Therefore, in this section, we proposed two regulator versions to solve the output regulation problem. The first one is the output feedback regulator when only the measurable output $y_m(t)$ shown in (3.65c) is available, whereas the second realistic one is error feedback regulator, where only the tracking error $e(t)$ can be measured instead of the output.

3.3.2.1 Output feedback regulator problem

For the output feedback regulator design, throughout this subsection, the configuration of the exosystem (3.2a)–(3.2c) is given as follows:

$$\dot{w}_d(t) = S_d w_d(t),\ w_d(0) = w_{d0} \in \mathbb{C}^{n_d} \tag{3.103}$$

$$\dot{w}_r(t) = S_r w_r(t),\ w_r(0) = w_{r0} \in \mathbb{C}^{n_r} \tag{3.104}$$

$$d(t) = Fw(t) = f_d w_d(t),\ t \geq 0 \tag{3.105}$$

$$y_r(t) = Qw(t) = q_r w_r(t),\ t \geq 0 \tag{3.106}$$

where the matrix S in (3.2a) is a block diagonal diagonalizable skew-Hermitian matrix: $S = \mathrm{bdiag}(S_d, S_r)$ and the exosystem state is constructed by $w = \mathrm{col}(w_d, w_r)$ with $n = n_d + n_r$. (3.103) and (3.105) is the disturbance model and (3.104) and (3.106) is the reference model. Obviously, eigenvalues of S_d and S_r are given by $\sigma(S_d) = \{\lambda_k\}_{k=1,\cdots,n_d}$ and $\sigma(S_r) = \{\lambda_k\}_{k=n_d+1,\cdots,n}$ and one has $F = \begin{bmatrix} f_d & 0 \end{bmatrix}$ and $Q = \begin{bmatrix} 0 & q_r \end{bmatrix}$. In this section, for the above configuration of exosystem, the following assumption is made.

Assumption 2. *It is assumed that (q_r, S_r) is observable and that the matrix S_d is a skew-Hermitian matrix.*

It is easy to calculate:

$$S_d v_d(t) = \sum_{k=1}^{n_d} \lambda_k \langle v_d(t), \phi_{dk} \rangle \phi_{dk} \tag{3.107}$$

$$v_d(t) = e^{S_d t} v_d(0) = \sum_{k=1}^{n_d} e^{\lambda_k t} \langle v_d(0), \phi_{dk} \rangle \phi_{dk} \tag{3.108}$$

where $\{\phi_{dk}\}$ with $k = 1, \cdots, n_d$ are orthonormal eigenvectors of S_d corresponding to eigenvalues of S_d.

In this section, we assume that the measurement $y_m(t)$ and the reference signal $y_r(t)$ are available for the regulator design. Using the output injection, we design the following output feedback regulators:

(I). Regulator with spatially distributed input: $\mathcal{U}(z,t)$

$$\dot{r}_w(t) = Sr_w(t) + \begin{bmatrix} L_m & 0 \\ 0 & L_r \end{bmatrix} \begin{bmatrix} y_m(t) - C_y\tilde{\Pi}r_w(t) \\ y_r(t) - C_Q\tilde{\Pi}r_w(t) \end{bmatrix} \tag{3.109}$$

$$\mathcal{U}(z,t) = \Gamma r_w(t) + \begin{bmatrix} k_m(z) & k_r(z) \end{bmatrix} \begin{bmatrix} y_m(t) - C_y\tilde{\Pi}r_w(t) \\ y_r(t) - C_Q\tilde{\Pi}r_w(t) \end{bmatrix} \tag{3.110}$$

(II). Regulator with non-spatially distributed input: $\mathcal{U}(t)$

$$\dot{r}_w(t) = Sr_w(t) + \begin{bmatrix} L_m & 0 \\ 0 & L_r \end{bmatrix} \begin{bmatrix} y_m(t) - C_y\tilde{\Pi}r_w(t) \\ y_r(t) - C_Q\tilde{\Pi}r_w(t) \end{bmatrix} \tag{3.111}$$

$$\mathcal{U}(t) = \Gamma r_w(t) + \begin{bmatrix} K_m & K_r \end{bmatrix} \begin{bmatrix} y_m(t) - C_y\tilde{\Pi}r_w(t) \\ y_r(t) - C_Q\tilde{\Pi}r_w(t) \end{bmatrix} \tag{3.112}$$

Furthermore, (3.109)–(3.110) and (3.111)–(3.112) can be rewritten as:

$$\dot{r}_w(t) = Sr_w(t) + \tilde{L}_M\tilde{C}_M\left(x_c(t) - \tilde{\Pi}r_w(t)\right) \tag{3.113}$$

$$\mathcal{U} = \Gamma r_w(t) + \tilde{K}_M\tilde{C}_M\left(x_c(t) - \tilde{\Pi}r_w(t)\right) \tag{3.114}$$

with $\tilde{L}_M = \begin{bmatrix} L_m & 0 \\ 0 & L_r \end{bmatrix}$ and $\tilde{C}_M = \begin{bmatrix} C_y \\ C_Q \end{bmatrix}$. In particular, for (3.110), $\tilde{K}_M = \begin{bmatrix} \tilde{k}_m & \tilde{k}_r \end{bmatrix} = \begin{bmatrix} k_m(z) & k_r(z) \end{bmatrix}$ and for (3.112), $\tilde{K}_M = \begin{bmatrix} \tilde{k}_m & \tilde{k}_r \end{bmatrix} = \begin{bmatrix} K_m & K_r \end{bmatrix}$.

The output feedback regulator (3.109)-(3.110) and (3.111)–(3.112) are extensions of the feedforward regulator (3.96). First of all, we investigate the dynamics of $x_c(t) - \tilde{\Pi}r_w(t)$ when applying (3.113)-(3.114):

$$\begin{aligned} \dot{x}_c(t) - \tilde{\Pi}\dot{r}_w(t) &= A_c x_c(t) - \left(\tilde{\Pi}S - B_c\Gamma\right) r_w(t) + \left(B_c\tilde{K}_M\tilde{C}_M - \tilde{\Pi}\tilde{L}\tilde{C}_M\right)\left(x_c(t) - \tilde{\Pi}r_w(t)\right) \\ &= \left(A_c + B_c\tilde{K}_M\tilde{C}_M - \tilde{\Pi}\tilde{L}\tilde{C}_M\right)\left(x_c(t) - \tilde{\Pi}r_w(t)\right) \\ &= \hat{A}_c\left(x_c(t) - \tilde{\Pi}r_w(t)\right) \end{aligned}$$

with $x_c \in D(A_c)$.

From Theorem 8 and the above equation, it is easy to conclude the following lemma.

Lemma 4. *For the plant (3.1a)-(3.1b) and the exosystem (3.103)-(3.106), the finite dimensional regulator (3.113)-(3.114) solves the output regulation problem (3.91) if the operators* $\Pi \in \mathcal{L}(\mathbb{C}^n, X)$ *with* $\Pi\mathbb{C}^n \in D(A)$ *and* $\Gamma \in \mathcal{L}(\mathbb{C}^n, \mathbb{R})$ *satisfy the Sylvester equations (3.99)-(3.100) and if there exist controller parameters* $\tilde{L}_M$ *and* $\tilde{K}_M$ *such that the operator* $\hat{A}_c$ *in the above equation is the infinitesimal generator of an exponentially stable* C_0-*semigroup.*

Consequently, we investigate the choice of the regulator parameters $\tilde{L}_M$ and $\tilde{K}_M$ such that the operator $\hat{A}_c$ generates an exponentially stable C_0-semigroup and thus the output regulation problem is solved.

Theorem 9. *The controller (3.113)-(3.114) stabilizes the operator* $\hat{A}_c$*, provided that parameters in* $\tilde{L}_M$ *and* $\tilde{K}_M$ *are chosen as follows:*

(a). $\tilde{k}_r$ *can be chosen as a free constant, e.g.,* $\tilde{k}_r = 0$*. As a consequence, we have* $k_r(z) = 0$ *in (3.110) and* $K_r = 0$ *in (3.112).*

(b). Given that the pair (q_r, S_r) *in Assumption 2 is observable,* L_r *is chosen such that* $S_r + L_r q_r$ *is Hurwitz matrix.*

(c). L_m *can be chosen such that* $S_d + L_m C_m \Pi_0$ *is exponentially stable, where* $\Pi_0 \in \mathcal{L}(\mathbb{C}^{n_d}, X)$ *is the following solution of the Sylvester equation*

$$\Pi_0 S_d - (A + k_1 B C_m)\Pi_0 = -p_d \tag{3.115}$$

with $p_d = B_d f_d$ *and* $\Pi_0 \mathbb{C}^{n_d} \in D(A)$.

(d). Assume that $\tilde{k}_m = k_1 + k_2$ *and* $\Pi = \begin{bmatrix} \Pi_d & \Pi_r \end{bmatrix}$ *with* $\Pi_d \in \mathcal{L}(\mathbb{C}^{n_d}, X)$*. Choose* k_1 *such that the operator* $A + k_1 B C_m$ *generates an exponentially stable* C_0-*semigroup.* k_2 *can be chosen as:* $k_2(z) = \frac{(\Pi_d(z)+\Pi_0(z))L_m}{b(z)}$ *or* $k_2 = \mu_o \int_0^1 \frac{(\Pi_d(z)+\Pi_0(z))L_m}{b(z)} dz$*. Therefore, in (3.110) the parameter* $k_m(z)$ *is given by* $k_m(z) = k_1 + \frac{(\Pi_d(z)+\Pi_0(z))L_m}{b(z)}$ *and in (3.112) the parameter* K_m *is* $K_m = k_1 + \mu_o \int_0^1 \frac{(\Pi_d(z)+\Pi_0(z))L_y}{b(z)} dz$*. Here* μ_o *is a tuning parameter.*

Proof. According to the structure of the exosystem (3.103)–(3.106), the operators A_c, B_c, $\tilde{C}_M$ and $\tilde{\Pi}$ are rewritten as:

$$A_c = \begin{bmatrix} A & p_d & 0 \\ 0 & S_d & 0 \\ 0 & 0 & S_r \end{bmatrix}, B_c = \begin{bmatrix} B \\ 0 \\ 0 \end{bmatrix}, \tilde{C}_M = \begin{bmatrix} C_m & 0 & 0 \\ 0 & 0 & q_r \end{bmatrix}, \tilde{\Pi} = \begin{bmatrix} \Pi_d & \Pi_r \\ I_d & 0 \\ 0 & I_r \end{bmatrix}$$

with $p_d = B_d f_d$, and $\Pi = \begin{bmatrix} \Pi_d & \Pi_r \end{bmatrix}$. I_d and I_r are identity matrices. As a result, the operator $\hat{A}_c$ is calculated:

$$\begin{aligned} \hat{A}_c &= A_c + B_c \tilde{K}_M \tilde{C}_M - \tilde{\Pi}\tilde{L}\tilde{C}_M \\ &= \begin{bmatrix} A + B\tilde{k}_m C_m + \Pi_d L_m C_m & p_d & \Pi_r L_r q_r + B\tilde{k}_r q_r \\ L_m C_{\Lambda m} & S_d & 0 \\ 0 & 0 & S_r + L_r q_r \end{bmatrix} \end{aligned}$$

Apparently, the stability of $\hat{A}_c$ can be determined by the block operators $\tilde{A}_{mc}$ and $S_r + L_r q_r$, where $\tilde{A}_{mc} = \begin{bmatrix} A + B\tilde{k}_m C_m + \Pi_d L_m C_m & p_d \\ L_m C_m & S_d \end{bmatrix}$.

Obviously, $\tilde{k}_r$ will not influent the stability of $\hat{A}_c$. Due to Assumption 2, it is possible to find L_r such that the matrix $S_r + L_r q_r$ is Hurwitz. With the bounded similarity transformations, the operator $\tilde{A}_{mc}$ is transformed into block lower triangular form, where diagonal blocks can be stabilized by choosing appropriate regulator parameters. By assuming $\tilde{k}_m = k_1 + k_2$, we rewrite $\tilde{A}_{mc}$ as:

$$
\begin{aligned}
\tilde{A}_{mc} &= \begin{bmatrix} A & p_d \\ 0 & S_d \end{bmatrix} + \begin{bmatrix} \tilde{k}_m B - \Pi_d L_m \\ -L_m \end{bmatrix} \begin{bmatrix} C_m & 0 \end{bmatrix} \\
&= \begin{bmatrix} A & p_d \\ 0 & S_d \end{bmatrix} + \begin{bmatrix} k_1 B \\ 0 \end{bmatrix} \begin{bmatrix} C_m & 0 \end{bmatrix} + \begin{bmatrix} k_2 B \\ 0 \end{bmatrix} \begin{bmatrix} C_m & 0 \end{bmatrix} + \begin{bmatrix} -\Pi_d L_m \\ -L_m \end{bmatrix} \begin{bmatrix} C_m & 0 \end{bmatrix} \\
&= \begin{bmatrix} A + k_1 B C_m & p_d \\ 0 & S_d \end{bmatrix} + \begin{bmatrix} k_2 B - \Pi_d L_m \\ -L_m \end{bmatrix} \begin{bmatrix} C_m & 0 \end{bmatrix}
\end{aligned}
$$

By applying the following similarity transformation: $T = \begin{bmatrix} I & \Pi_0 \\ 0 & I \end{bmatrix}$ and $T^{-1} = \begin{bmatrix} I & -\Pi_0 \\ 0 & I \end{bmatrix}$, we transform $\tilde{A}_{mc}$ into the form:

$$
\begin{aligned}
T\tilde{A}_{mc}T^{-1} &= \begin{bmatrix} I & \Pi_0 \\ 0 & I \end{bmatrix} \begin{bmatrix} A + k_1 B C_m & p_d \\ 0 & S_d \end{bmatrix} \begin{bmatrix} I & -\Pi_0 \\ 0 & I \end{bmatrix} \\
&\quad + \begin{bmatrix} I & \Pi_0 \\ 0 & I \end{bmatrix} \begin{bmatrix} k_2 B - \Pi_d L_m \\ -L_m \end{bmatrix} \begin{bmatrix} C_m & 0 \end{bmatrix} \begin{bmatrix} I & -\Pi_0 \\ 0 & I \end{bmatrix} \\
&= \begin{bmatrix} A + k_1 B C_m & p_d + \Pi_0 S_d \\ 0 & S_d \end{bmatrix} \begin{bmatrix} I & -\Pi_0 \\ 0 & I \end{bmatrix} \\
&\quad + \begin{bmatrix} k_2 B - \Pi_d L_m - \Pi_0 L_m \\ -L_m \end{bmatrix} \begin{bmatrix} C_m & -C_m \Pi_0 \end{bmatrix}
\end{aligned}
\tag{3.116}
$$

Let $k_2 B - \Pi_d L_m - \Pi_0 L_m = 0$, then from (3.116) we have

$$
T\tilde{A}_{mc}T^{-1} = \begin{bmatrix} A + k_1 B C_m & p_d + \Pi_0 S_d - A\Pi_0 - k_1 B C_m \Pi_0 \\ -L_m C_m & S_d + L_m C_m \Pi_0 \end{bmatrix}
$$

For specified k_1, if we let Π_0 satisfy the following Sylvester equation:

$$
\Pi_0 S_d - A\Pi_0 - k_1 B C_{\Lambda m} \Pi_0 + p_d = 0
$$

with $\Pi_0\mathbb{C}^{n_d} \in D(A)$, then, $\tilde{A}_{mc}$ can be written as block lower triangular form: $T\tilde{A}_{mc}T^{-1} = \begin{bmatrix} A + k_1BC_m & 0 \\ -L_mC_m & S_d + L_mC_m\Pi_0 \end{bmatrix}$.

Then, we choose k_1 and L_m such that $A + k_1BC_m$ generates an exponentially stable C_0-semigroup, $S + L_mC_m\Pi_0$ is Hurwitz and thus $\tilde{A}_{mc}$ generates an exponentially stable C_0-semigroup. Furthermore, $\hat{A}_c$ generates an exponentially stable C_0-semigroup. Observe (3.116), in order to guarantee $k_2B-\Pi_dL_m-\Pi_0L_m = 0$, one can choose $k_2(z) = \frac{(\Pi_d(z)+\Pi_0(z))L_m}{b(z)}$.

Moreover, k_2 can also chosen as a constant $k_2 = \mu_o \int_0^1 \frac{(\Pi_d(z)+\Pi_0(z))L_m}{b(z)}dz$ to ensure $k_2B - \Pi_dL_m - \Pi_0L_m \approx 0$. Here the tunning parameter μ_o in k_2 is used to adjust the value of $k_2B - \Pi_dL_m - \Pi_0L_m$ so that its value can approach to zero sufficiently. $\square$

From the above proof, it is shown that the solvability of the Sylvester equation (3.115) is essential. In the following lemma, we show the solvability condition for the Sylvester equation (3.115).

Lemma 5. *(**Solvability of Sylvester equation (3.115)**) The transfer function $F_m(s)$ of (3.65a)–(3.65c) from $u(t)$ to $y_m(t)$ is $F_m(s) = -\int_0^{z_0}\left(\exp\left(\int_\eta^{z_0}\frac{(s-g(\zeta))}{v(\zeta)}d\zeta\right)\frac{b(\eta)}{v(\eta)}\right)d\eta$. There exists a unique classical solution of the Sylvester equation (3.115) if and only if the solvability condition: $1 - k_1F_m(\lambda) \neq 0$, $\forall\lambda \in \sigma(S_d)$ holds, where $\sigma(S_d)$ is the spectrum of S_d. In particular, the solution of (3.115) can be given by:*

$$\Pi_0 = \sum_{k=1}^{n_d} \langle \cdot, \phi_{dk}\rangle R\left(\lambda_k; A + k_1BC_m\right)(-p_d)\phi_{dk} \tag{3.117}$$

Proof. Since S_d is a diagonalizable matrix (even including one zero eigenvalue, e.g $w_1 = 0$ and thus $\lambda_1 = 0$), there exists a similarity transformation $V_d^{-1}S_dV_d = diag(\lambda_1, ..., \lambda_{n_d})$ with $V_d = \begin{bmatrix} \phi_{d1} & \cdots & \phi_{dn_d} \end{bmatrix}$ with $\lambda_k = iw_k, k = 1, ..., n_d$, where iw_k and ϕ_k are eigenvalues and eigenvectors of S_d (see (3.107)), respectively. Postmultiplying (3.115) by V_d yields to the decoupled set of ODEs:

$$\frac{d\pi^*_{0,k}(z)}{dz} = \frac{(\lambda_k - g(z))}{v(z)}\pi^*_{0,k}(z) - \frac{k_1 b(z)}{v(z)}\pi^*_{0,k}(z_0) + \frac{p^*_{dk}}{v(z)} \tag{3.118}$$

$$\pi^*_{0,k}(0) = 0 \tag{3.119}$$

with $\pi^*_{0k}(z) = \Pi_0(z)\phi_k$ and $p^*_{dk} = p_d\phi_k$, where the boundary condition (3.119) comes from the definition of $D(A)$, see (3.85) and the term $\frac{k_1 b(z)}{v(z)}\pi^*_{0,k}(z_0)$ is from $k_1 B C_m \Pi_0(z)\psi_k$ with (3.65a), (3.65c). Then, it is easy to calculate the corresponding general solution:

$$\begin{aligned}\pi^*_{0,k}(z) &= -\int_0^z \left(\exp\left(\int_\eta^z \frac{(\lambda_k - g(\zeta))}{v(\zeta)}d\zeta\right)\frac{k_1 b(\eta)}{v(\eta)}\right)d\eta\,\pi^*_{0,k}(z_0) \\ &+ \int_0^z \left(\exp\left(\int_\eta^z \frac{(\lambda_k - g(\zeta))}{v(\zeta)}d\zeta\right)\frac{p^*_{dk}}{v(\eta)}\right)d\eta\end{aligned} \tag{3.120}$$

By evaluating $\pi^*_{0,k}(z)$ at the point $z = z_0$, one obtains:

$$a_{\pi_0}(\lambda_k)\pi^*_{0,k}(z_0) = \int_0^{z_0} \left(\exp\left(\int_\eta^{z_0} \frac{(\lambda_k - g(\zeta))}{v(\zeta)}d\zeta\right)\frac{p^*_{dk}}{v(\eta)}\right)d\eta$$

with $a_{\pi_0}(\lambda_k) = \left(1 + k_1\int_0^{z_0}\left(\exp\left(\int_\eta^{z_0}\frac{(\lambda_k - g(\zeta))}{v(\zeta)}d\zeta\right)\frac{b(\eta)}{v(\eta)}\right)d\eta\right)$. Obviously, the above equation can be uniquely solved for $\pi^*_{0,k}(z_0)$ if and only if the solvability condition $a_{\pi_0}(\lambda) \neq 0$ for $\lambda \in \sigma(S_d)$ holds. By applying the method in [60], one obtains the transfer function from $u(t)$ to $y_m(t)$ is $F_m(s) = \frac{\hat{y}_m(s)}{\hat{u}(s)} = -\int_0^{z_0}\left(\exp\left(\int_\eta^{z_0}\frac{(s-g(\zeta))}{v(\zeta)}d\zeta\right)\frac{b(\eta)}{v(\eta)}\right)d\eta$ with $\hat{u}(s)$ and $\hat{y}_m(s)$ as the Laplace transform of $u(t)$ and $y_m(t)$. Therefore, once the solvability condition in the lemma holds, the equation (3.118)-(3.119) can be uniquely solved and the solution of the Sylvester equation (3.115) can be uniquely calculated by $\Pi_0(z) = \left[\pi^*_{0,1}(z), \cdots, \pi^*_{0,n_d}(z)\right] V_d^{-1}$. Moreover, the solvability condition is easily guaranteed, since the parameter k_1 can be freely chosen in a certain range, e.g. $k_1 = 0$, see Lemma 10. Furthermore, the expression in (3.117) can be easily obtained using the approach in Section 3.2. □

From Theorem 9, in order to guarantee the feasibility of the proposed regulator, the detectability of the pair $(C_m\Pi_0, S_d)$ is crucial. In the following lemma, the sufficient and necessary conditions related to the transfer function from the disturbance $d(t)$ to the measurement $y_m(t)$ are given to ensure the detectability.

Lemma 6. (Detectability) *The pair* $(C_m\Pi_0, S_d)$ *is detectable, if and only if the transfer function* $G_{md}(s) = C_m(sI - A)^{-1}B_d, s \in \rho(A)$ *in the plant from* $d(t)$ *to* $y_m(t)$ *satisfies:*

$$G_{md}\left(\lambda_k\right) f_d \phi_{dk} \neq 0, k = 1, 2, \cdots, n_d \tag{3.121}$$

in which ϕ_{dk} *are the eigenvectors of* S_d *with respect to the eigenvalues* λ_k *of* S_d*. As a consequence, there exists* L_m *such that* $S_d + L_m C_m \Pi_0$ *is Hurwitz.*

Proof. According to Th.6.2-5 of [61], the detectability of the pair $(C_m\Pi_0, S_d)$ can be verified by showing $C_m\Pi_0\phi_{dk} \neq 0$ for $k = 1, 2, \cdots, n_d$. Using the solution (3.117) yields:

$$\begin{aligned}
&C_m\Pi_0\phi_{dk} = C_m R\left(\lambda_k; A + k_1 B C_m\right)(-p_d)\phi_{dk} \\
&= -C_m R\left(\lambda_k; A + k_1 B C_m\right) B_d f_d \phi_{dk} \\
&= G_K(\lambda_k) f_d \phi_{dk}
\end{aligned}$$

where $G_K(\lambda) = C_m R\left(\lambda; A + k_1 B C_m\right) B_d$ with $\lambda \in \overline{\mathbb{C}^+}$. By applying the Woolbury formula and the following formula:

$$R\left(\lambda; A + k_1 B C_m\right) = R\left(\lambda; A\right)\left(I - k_1 B C_m R\left(\lambda; A\right)\right)^{-1}$$

for every $\lambda \in \rho(A) \cap \rho(A + k_1 B C_m)$, we have

$$G_K(\lambda) = \left(I - k_1 C_m R\left(\lambda; A\right) B\right)^{-1} G_{md}\left(\lambda\right)$$

Due to Assumption 2 that the eigenvalues of S_d are distinct, it is possible to guarantee that conditions in (3.121) hold for all eigenvectors of S_d. Furthermore, the solvability in Lemma 5 guarantees the existence of $\left(I - k_1 C_m R\left(\lambda; A\right) B\right)^{-1}$ and thus the conditions in (3.121) ensure that the pair $(C_m\Pi_0, S_d)$ is detectable. $\square$

3.3.3 Error feedback regulator

In this section, we proceed with another realistic realization: the error feedback regulator where only the tracking error $e(t)$ is available to the regulator design. Different from previous section, throughout this section, the configuration in (3.103)–(3.106) and Assumption 2 are not applied. In this subsection, the exosystem (3.2a)–(3.2c) is still employed. Moreover, the following assumption is made within this subsection:

Assumption 3. *The matrix S is diagonizable. The pair in the following equation is exponential detectable:*

$$\left(\begin{bmatrix} \mathcal{A} & P \\ 0 & S \end{bmatrix}, \begin{bmatrix} C & -Q \end{bmatrix} \right) \tag{3.122}$$

The feedforward regulator (3.96) is extended by the injection of the tracking error $e(t) - C_c\tilde{\Pi}r_w(t)$, where the tracking error $e(t)$ is available for measurement. This leads to the following finite-dimensional regulator:

(I). Regulator with spatially distributed input: $\mathcal{U}(z,t)$

$$\dot{r}_w(t) = Sr_w(t) + L(e(t) - C_c\tilde{\Pi}r_w(t)) \tag{3.123}$$

$$\mathcal{U}(z,t) = \Gamma r_w(t) + k_e(z)(e(t) - C_c\tilde{\Pi}r_w(t)) \tag{3.124}$$

(II). Regulator with non-spatially distributed input: $\mathcal{U}(t)$

$$\dot{r}_w(t) = Sr_w(t) + L(e(t) - C_c\tilde{\Pi}r_w(t)) \tag{3.125}$$

$$\mathcal{U}(t) = \Gamma r_w(t) + K_e(e(t) - C_c\tilde{\Pi}r_w(t)) \tag{3.126}$$

with the initial condition $r_w(0) = r_{w0} \in \mathbb{C}^n$.

Then, write (3.123)–(3.124) and (3.125)–(3.126) in the following general form:

$$\dot{r}_w(t) = Sr_w(t) + LC_c(x_c(t) - \tilde{\Pi}r_w(t)) \tag{3.127}$$

$$\mathcal{U} = \Gamma r_w(t) + \tilde{K}_E C_c(x_c(t) - \tilde{\Pi} r_w(t)) \tag{3.128}$$

Here, $\tilde{K}_E = k_e(z)$ for (3.124) and $\tilde{K}_E = K_e$ for (3.126). Then, by applying the regulator (3.127)–(3.128), the dynamics of $x_c(t) - \tilde{\Pi} r_w(t)$ is given by

$$\begin{aligned}
\dot{x}_c(t) - \tilde{\Pi}\dot{r}_w(t) &= A_c x_c(t) + \left(B_c \Gamma - \tilde{\Pi} S\right) r_w(t) \\
&\quad + \left(B_c \tilde{K}_E C_c - \tilde{\Pi} L C_c\right)\left(x_c(t) - \tilde{\Pi} r_w(t)\right) \\
&= \left(A_c + B_c \tilde{K}_E C_c - \tilde{\Pi} L C_c\right)\left(x_c(t) - \tilde{\Pi} r_w(t)\right) \\
&= \tilde{A}_c \left(x_c(t) - \tilde{\Pi} r_w(t)\right)
\end{aligned}$$

with $x_c(0) - \tilde{\Pi} r_w(0) \in D(A_c)$ and $x_c \in D(A_c)$. Then, the following theorem shows that the output regulation problem is solvable if there exist controller parameters L and $\tilde{K}_E$.

Lemma 7. *For the plant (3.65) and the exosystem (3.2a)-(3.2c), the following finite dimensional regulator*

$$\begin{aligned}
\dot{r}_w(t) &= S r_w(t) + L e(t) \\
\mathcal{U} &= \Gamma r_w(t) + \tilde{K}_E e(t)
\end{aligned} \tag{3.129}$$

solves the output regulation problem (3.91) if the operators $\Pi \in \mathcal{L}(W, X)$ with $\Pi \mathbb{C}^n \in D(A)$ and $\Gamma \in \mathcal{L}(W, \bar{U})$ satisfy Sylvester equations (3.99)-(3.100) and if there exist controller parameters L and $\tilde{K}_E$ such that the operator $\tilde{A}_c$ in the above equation is the infinitesimal generator of an exponentially stable C_0-semigroup.

Proof. From the definition of C_c and $\tilde{\Pi}$, we can easily calculate $C_c \tilde{\Pi} = C\Pi - Q = 0$. Therefore, it is natural that the regulators in (3.123)-(3.124) and (3.125)–(3.126) can be rewritten as (3.129). If L and $\tilde{K}_E$ can be chosen such that $\tilde{A}_c$ is an infinitesimal generator of an exponentially stable C_0-semigroup, then under control of the regulator (3.129) the composite state $x_c(t) \to \tilde{\Pi} r_w(t)$ as $t \to +\infty$. From the proof of Theorem 8, it is easy to see that the output regulation problem can be solved. □

The next theorem provides a choice of the controller parameters L and $\tilde{K}_E$ such that the operator $\tilde{A}_c$ is the infinitesimal generator of an exponentially stable C_0-semigroup.

Theorem 10. *The controller (3.129) stabilizes the operator $\tilde{A}_c$, provided that L and $\tilde{K}_E$ are chosen as follows: Assume $\tilde{K}_E = k_3 + k_4$. Choose k_3 so that $A + k_3BC$ is exponentially stable. Choose L such that $S + L(C\Pi_e + Q)$ is exponentially stable, where Π_e is the solution of the Sylvester equation*

$$\Pi_e S - (A + k_3BC)\Pi_e = -P - k_3BQ \tag{3.130}$$

The parameter k_4 can be chosen as a spatially varying function $k_4(z) = \frac{(\Pi_e(z)+\Pi(z))L}{b(z)}$ and also k_4 can be chosen as a constant value given by $k_4 = \mu_e \int_0^1 [\frac{(\Pi_e(z)+\Pi(z))L}{b(z)}]dz$. Finally, we choose $k_e(z) = k_3 + \frac{(\Pi_e(z)+\Pi(z))L}{b(z)}$ for (3.124) and $K_e = k_3 + \mu_e \int_0^1 [\frac{(\Pi_e(z)+\Pi(z))L}{b(z)}]dz$ for (3.126). Here μ_e is a tunning parameter.

Proof. With the bounded similarity transformations, the operator $\tilde{A}_c$ is transformed into the block lower triangular form, where the diagonal blocks generate exponentially stable C_0-semigroups.

The operator $\tilde{A}_c$ can be written as:

$$\tilde{A}_c = \begin{bmatrix} A & P \\ 0 & S \end{bmatrix} + \begin{bmatrix} \tilde{K}_E B - \Pi L \\ -L \end{bmatrix} \begin{bmatrix} C & -Q \end{bmatrix}$$

Now let $\tilde{K}_E = k_3 + k_4$,$k_r B - \Pi L = k_3 B + h_2$. Then

$$\begin{aligned} \tilde{A}_c &= \begin{bmatrix} A & P \\ 0 & S \end{bmatrix} + \begin{bmatrix} k_3 B \\ 0 \end{bmatrix} \begin{bmatrix} C & -Q \end{bmatrix} + \begin{bmatrix} k_4 B - \Pi L \\ -L \end{bmatrix} \begin{bmatrix} C & -Q \end{bmatrix} \\ &= \begin{bmatrix} A + k_3BC & P - k_3BQ \\ 0 & S \end{bmatrix} + \begin{bmatrix} k_4 B - \Pi L \\ -L \end{bmatrix} \begin{bmatrix} C & -Q \end{bmatrix} \end{aligned}$$

Since A generates an exponentially stable C_0-semigroup, it implies that A is exponentially stabilizable. In the following section, we will show that small gain k_3 can be chosen such that $A_k = A + k_3BC$ with $D(A_k) = D(A)$ is exponentially stable. Now the following similarity transformation is applied to $\tilde{A}_c$: $T_1 = \begin{bmatrix} I & \Pi_e \\ 0 & I \end{bmatrix}$, $T_1^{-1} = \begin{bmatrix} I & -\Pi_e \\ 0 & I \end{bmatrix}$, where $\Pi_e \in \mathcal{L}(W, X)$ has to be determined. Then, applying the similar derivation in Theorem 9 yields the equation (3.130) and the following result

$$T_1 \tilde{A}_c T_1^{-1} = \begin{bmatrix} A_k & 0 \\ -LC & S + L\left(C\Pi_e + Q\right) \end{bmatrix} \tag{3.131}$$

In equation (3.131), A_k is exponentially stable. Then, $\tilde{A}_c$ is exponentially stable if we choose L such that $S + L(C\Pi_e + Q)$ is exponentially stable. Finally, the choices of $k_e(z)$ in (3.124) and K_e in (3.126) here are similar to the proof of Theorem 9. $\square$

Since the solvability of the Sylvester equation (3.130) directly determines the feasibility of the regulator (3.126), the following lemma provides solvability conditions ensuring the solvability of the Sylvester equation (3.130).

Lemma 8. ***(Solvability of the Sylvester equation (3.130))*** *The transfer function $G(s)$ of (3.65a)–(3.65c) from $u(t)$ to $y(t)$ is $G(s) = \frac{\hat{y}(s)}{\hat{u}(s)} = -\int_0^{z_1} \left(\exp\left(\int_\eta^{z_1} \frac{(s-g(\zeta))}{v(\zeta)} d\zeta\right) \frac{b(\eta)}{v(\eta)}\right) d\eta$ with $\hat{u}(s)$ and $\hat{y}(s)$. There exists a unique classical solution of the Syvester equation (3.130) if and only if the solvability condition $1 - k_3 G(\lambda) \neq 0$ holds, $\forall \lambda \in \sigma(S)$ with $\sigma(S)$ as the spectrum of S. Moreover, the solution of (3.130) is given by:*

$$\Pi_e = \sum_{k=1}^{n} \langle \cdot, \psi_k \rangle R\left(\lambda_k; A + k_3 BC\right)(-P - k_3 BQ)\psi_k \tag{3.132}$$

Proof. The proof is similar to lemma 5. $\square$

Similar to the previous section, we turn to the analysis of the conditions on the detectability of the pair $(C\Pi_e + Q, S)$ in the following lemma.

Lemma 9. (Detectability) *The pair $(C\Pi_e + Q, S)$ is detectable, if and only if the transfer function $G_e(s) = C(sI - A)^{-1} B_d$, $s \in \rho(A)$ from the disturbance $d(t)$ to the controlled output*

$y(t)$ satisfies the following conditions:

$$\left(G_e(\lambda_k)F + Q\right)\psi_k \neq 0, k = 1, 2, \cdots, n \tag{3.133}$$

where ψ_k are the eigenvectors of S with respect to the eigenvalues λ_k, $k = 1, 2, \cdots, n$. Consequently, there exists L such that the matrix $S + L(C\Pi_e + Q)$ is Hurwitz.

Proof. The conditions $\left(C\Pi_e + Q\right)\psi_k \neq 0, k = 1, 2, \cdots, n$ indicates the detectability property of $(C\Pi_e + Q, S)$ directly. Then using the formula (3.132) and Woodbury formula show for $k = 1, 2, \cdots, n$:

$$\begin{aligned}
&\left(C\Pi_e + Q\right)\psi_k \\
&= R\left(\lambda_k; A + k_3BC\right)\left(-P - k_3BQ\right)\psi_k + Q\psi_k \\
&= -R\left(\lambda_k; A + k_3BC\right)\left(k_3B + I\right)Q\psi_k \\
&-R\left(\lambda_k; A + k_3BC\right)B_dF\psi_k \\
&= \left(I - k_3CR\left(\lambda_k; A\right)B\right)^{-1}\left(G_e(\lambda_k)F + Q\right)\psi_k
\end{aligned}$$

Due to Assumption 3, the eigenvalues of the matrix S are distinct and it is possible to ensure that conditions in (3.133) hold. Moreover, the solvability conditions in Lemma 8 ensures the existence of $\left(I - k_3CR\left(\lambda_k; A\right)B\right)^{-1}$ and the conditions in (3.133) guarantees that the pair $(C\Pi_e + Q, S)$ is detectable. □

In Theorem 9 and Theorem 10, it is necessary to choose k_1 (or k_3) such that $[A + k_1BC_m]$ (or $[A + k_3BC]$) is exponentially stable. In this chapter, we provide the choice of k_1 (or k_3) in the following lemma which was proposed in Chapter 5.

Lemma 10. *Under assumption that the operator A generates an exponentially stable C_0-semigroup e^{At} on H and the operator C is $A-$admissible, then there exists $k_p^* > 0$ such that $\forall k \in [-k_p^*, k_p^*]$ so that the extended operator $A + kBC$ still generates an exponentially stable C_0-semigroup on X.*

Proof. For the proof of lemma, please refer to the proof part of Theorem 4.3.7 in [62]. Moreover, it should be noted that $k \in [-k_p^*, k_p^*]$ is a sufficient condition ensuing $\left\|(1 - kBCR(\lambda; A))^{-1}\right\| <$

$+\infty$. In practice, alternatively k can also be chosen outside of the range $[-k_p^*, k_p^*]$ as long as $\sup\left\{\|R(\lambda; A + kBC)\|\,; \mathrm{Re}(\lambda) \geq -\frac{\varepsilon}{2}\right\} < +\infty$ for some $\varepsilon > 0, -\varepsilon < w_0$, where $-w_0$ is the stability margin of the C_0-semigroup generated by the operator A. $\square$

3.3.4 Numerical Simulations

In this section, we apply the proposed results to two examples including: a numerical example and a nonlinear advection dominated axial dispersion reactor, see [3].

3.3.4.1 Numerical Example with spatially distributed input $\mathcal{U}(z,t)$

We consider a homogenous one-dimensional first-order hyperbolic PDE system on $[0,1]$ with boundary observation and point output:

$$\frac{\partial x(z,t)}{\partial t} = v(z)\frac{\partial x(z,t)}{\partial z} + g(z)x(z,t) + b(z)\mathcal{U}(z,t), z \in (0,1] \tag{3.134a}$$

$$x(0,t) = 0, \quad x(z,0) = x_0(z) \tag{3.134b}$$

$$y(t) = x(z_1,t), \quad y_m(t) = x(z_0,t) \tag{3.134c}$$

with $v(z) = -2(z+1)$, $g(z) = e^{-z}$ and $b(z) = z^2 + 1$. $x(z,t)$ is the state of the plant and $\mathcal{U}(z,t)$ is the control signal. The controlled output $y(t)$ is the evolution of the state at point $z_1 = 0.5$ and the measured output $y_m(t)$ is the evolution of the state at boundary point $z_0 = 1$. Obviously, the controlled output and the measured output are different.

From the proof part of Theorem 1, one can see that in order to guarantee the exponential stability of the system, it is sufficient that there exists the unique solution $\eta(z)$ defined over the interval $[0,1]$. Given the coefficients $g(z)$, $v(z)$ and initial value $\eta(0) : \mu = 0.00001$, we can compute the solution the initial value Cauchy problem (3.80). The unique solution of $\eta(z)$ is defined in $[0,1]$ and thus the system (3.134) without input, i.e. $\mathcal{U}(z,t) = 0$ is exponentially stable as shown in Figure 3.6.

In this section, our objective is to design output and error feedback regulators, respectively such that the controlled output $y(t)$ (3.134c) tracks a given harmonic trajectory reference signal: $y_r(t) = 5\sin(2t)$ and rejects the constant disturbance $d(t) = 1$ as well. The

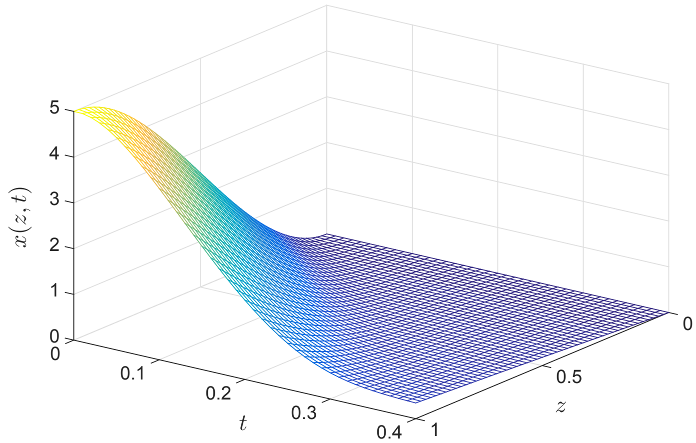

Figure 3.6: The evolution of the state $x(z,t)$ decays exponentially.

disturbance $d(t)$ and the reference signal $y_r(t)$ can be modelled by (3.103)–(3.106) with $S_d = 0,\ f_d = 1,\ S_r = \begin{bmatrix} 0 & 2 \\ -2 & 0 \end{bmatrix}$, $q_r = [1, 0]$.

According to the content in previous section, we know the plant (3.134) is regular and the infinite-dimensional representation on the Hilbert space $X = L^2(0,1)$ is in the form of (3.1a)–(3.1b) and the system operator A is defined as $A = v(z)\frac{\partial}{\partial z} + g(z) \cdot I$ with its domain given by $D(A) = \left\{x \in L^2(0,1) : x \text{ is a.c }, \frac{dx}{dx} \in L^2(0,1), x(0) = 0\right\}$. The input operator $B \in \mathcal{L}(\bar{U}, L^2(0,1))$ and the disturbance location operator $B_d \in \mathcal{L}(U_d, L^2(0,1))$, where $\bar{U}, U_d \subset \mathbb{R}$, are defined by $B = 1$ and $B_d = 0.2$.

Given the defined operators A, B and C and according to Lemma 9, the performance of the operator $A + kBC$ is investigated in Figure 3.7. Obviously, as shown in Figure 3.7, changing the value of k would change the stability margin of the operator $A + kBC$. In particular, in this chapter, we choose $k \in [-1, 1]$ to ensure good stability which stays in the region χ shown in Figure 3.7.

We now carry on solving the constrained Sylvester equation (3.99)-(3.100). Given the expression $\Pi = \begin{bmatrix} \Pi_d & \Pi_r \end{bmatrix}$, (3.99)-(3.100) can be rewritten as:

$$\Pi_d S_d - A\Pi_d = B\Gamma_d + p_d \tag{3.135}$$

$$C\Pi_d = 0$$

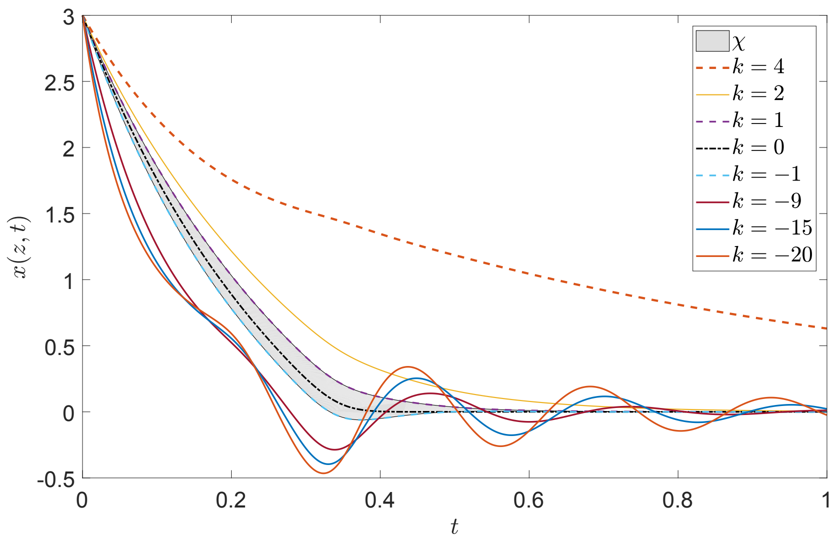

Figure 3.7: The performance of the operator $A+kBC$ with different values of k. The region χ denotes that the operator $A+kBC$ has similar stability margin with the operator A with $k \in [-1,1]$.

$$\begin{aligned} &\Pi_r S_r - A\Pi_r = B\Gamma_r \\ &C\Pi_r = q_r \end{aligned} \tag{3.136}$$

with $p_d = B_d f_d = 0.2$. It is easy to solve (3.135) for Π_d and Γ_d: $\Pi_d = 0$ and $\Gamma_d = -p_d$. Then, we turn to solving (3.136) for Γ_r. According to the structure of S_r, it is straightforward to write $\Gamma_r = \begin{bmatrix} \gamma_1 & \gamma_2 \end{bmatrix} \in \mathcal{L}(\mathbb{C}^2, U)$. By applying the methods in Section 3.2, one can get the explicit expression of γ_1 and γ_2:

$$\gamma_1 = \frac{\mathrm{Re}\,(G(2i)) - \mathrm{Im}\,(G(2i))}{|G(2i)|^2}$$

$$\gamma_2 = -\frac{\mathrm{Re}\,(G(2i)) + \mathrm{Im}\,(G(2i))}{|G(2i)|^2}$$

with $G(s) = C(sI-A)^{-1}b(z), s \in \rho(A)$. It is apparent that the specified value of the transfer function is essential to the calculation of γ_1 and γ_2.

Applying the technique in [63] leads to $G(2i) = -\int_0^{0.5} \left(\exp\left(-\int_\eta^{0.5} \frac{g(\zeta)-2i}{v(\zeta)} d\zeta\right) \frac{b(\eta)}{v(\eta)}\right) d\eta$. It is easy to get $G(2i) = x(0.5, 2i) = 0.2286 - 0.0457i$. With the value of $G(2i)$, one can calculate: $\gamma_1 = 4.2051$, $\gamma_2 = 0.6539$.

Output feedback regulator — Now, we carry on the construction of the output feedback regulator of (3.109)-(3.110) form. Under the control of the regulator (3.109)-(3.110), we show that the controlled output $y(t)$ tracks the reference signal $y_r(t) = 5\sin(2t)$ despite of the existence of the constant disturbance $d(t) = 1$. We assume that the measurement of the plant $y_m(t)$ and the reference signal $y_r(t)$ are available to the regulator and the controlled output $y(t)$. Obviously, the measured output $y_m(t)$ are different, i.e., $y(t) = x(0.5,t)$ and $y_m(t) = x(1,t)$.

In this part, from Theorem 9, $k_r(z)$ is free and therefore it can be set as $k_r(z) = 0$. Then, it is essential to calculate $k_m(z)$, L_m and L_r. According to Theorem 9 and Lemma 10, one can first set $k_1 = 0$ since A is exponentially stable. Then, one can rewrite (3.115) as:

$$\begin{aligned}&\tfrac{d\Pi_0(z)}{dz} = -\tfrac{g(z)}{v(z)}\Pi_0(z) - \tfrac{p_d}{v(z)}\\ &\Pi_0(0) = 0\end{aligned}$$

To solve the above equation, we get the closed form solution $\Pi_0(z)$ as:

$$\Pi_0(z) = -\int_0^z \left(\exp\left(\int_\eta^z \left(-\frac{g(\zeta)}{v(\zeta)}\right) d\zeta\right) \frac{p_d}{v(\eta)}\right) d\eta$$

It is easy to calculate $C_m\Pi_0(z) = \begin{bmatrix} \Pi_{01}(1) & \Pi_{02}(1) \end{bmatrix} = -0.0706$. Then, one can easily find L_m, e.g. $L_m = 20$ such that $S_d + L_m C_m \Pi_0$ is exponentially stable. Consequently, the parameter of the regulator k can be computed through the explicit expression: $k_m(z) = k_2(z) = \frac{(\Pi_d(z)+\Pi_0(z))L_m}{b(z)} = \frac{(\Pi_0(z))L_m}{z^2+1}$. Finally, with the initial condition: $r_w(0) = [0, 0.1, 4.6]^T$, the output feedback regulator (3.109)-(3.110) is established. The results are shown in Figure 3.8 and Figure 3.9.

In Figure 3.8, we can see that despite of the existence of disturbance $d(t) = 1$, the controlled output $y(t)$ tracks the reference signal $y_r(t)$ well under the control of the proposed output feedback regulator (3.109)-(3.110). In Figure 3.9, the evolution of the state $x(z,t)$ is plotted. Moreover, the locations of $y(t)$ and $y_m(t)$ are pointed out. Therefore, we conclude that in this part, an output feedback regulator is constructed with the measurement $y_m(t)$

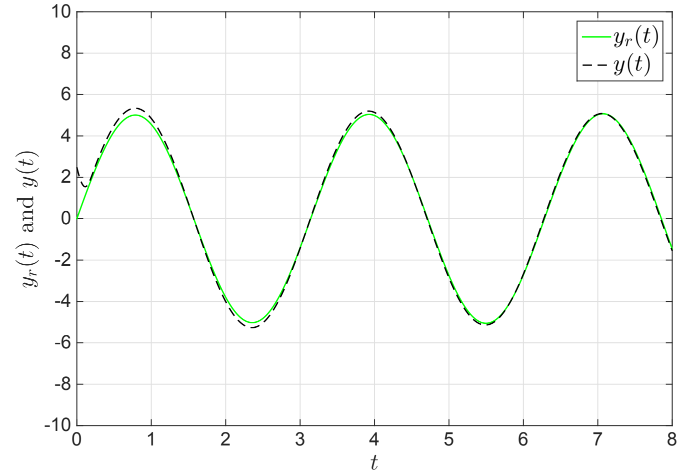

Figure 3.8: The controlled output $y(t)$ tracks the reference signal $y_r(t) = 5\sin(2t)$ under the control of regulator (3.109)-(3.110).

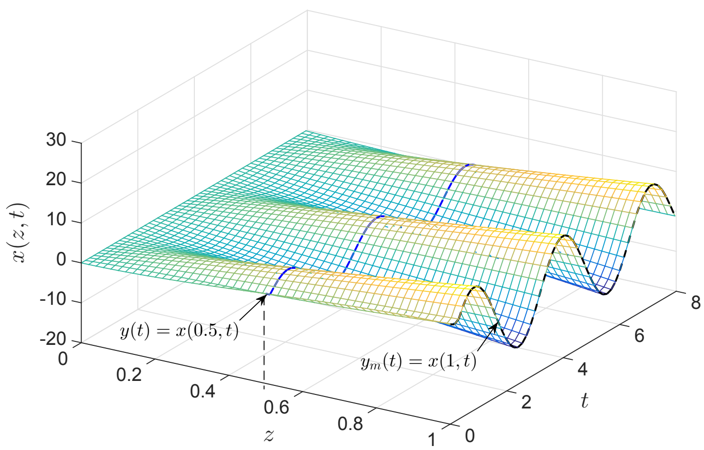

Figure 3.9: The evolution of the state $x(z,t)$ under the control of the output feedback regulator (3.109)-(3.110).

and the reference signal $y_r(t)$ as its inputs, such that the controlled output $y(t)$ of the plant tracks the reference signal $y_r(t)$ despite of the disturbance $d(t)$.

3.3.4.2 Advection dominated axial dispersion reactor application

A mathematical model for an advection dominated axial dispersion reactor is obtained by assuming no dispersion, see [32]:

$$\frac{\partial T}{\partial t} = v(z)\frac{\partial T}{\partial z} - \frac{\Delta H k_0}{\rho C_p}\exp\left(-\frac{E}{RT}\right) - \frac{A_s h}{\rho C_p}\left(T - T_c\right), z \in (0, l] \quad (3.137)$$

$$T(0,t) = T_{in}, t \geq 0 \quad (3.138)$$

$$y(t) = T(l,t), t \geq 0 \quad (3.139)$$

In these equations, $v(z)$, ΔH, ρ, C_p, k_0, E, R, h and T_{in} hold for the superficial fluid velocity, heat of reaction, density, specific heat, kinetic constant, activation energy, ideal gas constant, heat transfer coefficient and the inlet temperature, respectively. $T_c(t)$ denotes the coolant temperature and control input of (3.137)–(3.139). The parameter values used here are depicted in Table 3.1.

process parameters	notations	numerical values
superficial fluid velocity	$v(z)$	$-(0.025 + 0.075z)\ m/s$
length of the reactor	l	1 m
activation energy	E	$11250\ cal/mol$
kinetic constant	k_0	$10^6\ s^{-1}$
reaction coefficient	$\frac{\Delta H}{\rho C_p}$	85
heat transfer coefficient	$\frac{A_s h}{\rho C_p}$	$0.2\ s^{-1}$
ideal gas constant	R	$1.986\ cal/(mol.K)$
inlet temperature	T_{in}	$340\ K$

Table 3.1: Process parameters used in the simulation.

Let us consider the following state transformation: $\theta = \frac{T - T_{in}}{T_{in}}$ and the new output $y_\theta(t) = \frac{y(t) - T_{in}}{T_{in}}$. Then, one obtains the following equivalent representation of the model (3.137)–(3.138):

$$\frac{\partial \theta}{\partial t} = v(z)\frac{\partial \theta}{\partial z} - \kappa \exp\left(\frac{\mu\theta}{1+\theta}\right) + \beta\left(\theta_c - \theta\right) \quad (3.140)$$

$$\theta(0,t) = 0 \quad (3.141)$$

$$y_\theta(t) = \theta(l,t) \quad (3.142)$$

Consequently, for the transformed system (3.140)–(3.142), the input signal is $\theta_c(t)$. The parameters κ, μ and β are related to the original parameters as follows:

$$\mu = \frac{E}{RT_{in}}, \quad \kappa = \frac{\Delta H}{\rho C_p T_{in}} k_0 \exp(-\mu), \quad \beta = \frac{A_s h}{\rho C_p}$$

Let us denote by (θ_e, θ_{ce}) a given equilibrium profile of the model (3.140)–(3.141). Then, we consider the state transformation: $x(t) = \theta(t) - \theta_e(t)$, the new output $y_x(t) = y_\theta(t) - \theta_e(l)$ and the new input $u(t) = \theta_c(t) - \theta_{ce}$. The linearization of the system (3.140)–(3.141) around its equilibrium profile leads to the linear infinite-dimensional system on the Hilbert space $X = L_2(0,1)$. A is the linear operator defined on its domain: $D(A) = \left\{x \in L_2(0,1) : x \text{ is a.c.}, \frac{dx}{dx} \in L_2(0,1) \text{ and } x(0) = 0\right\}$, by $A = v(z)\frac{\partial}{\partial z} + \alpha(z)I$ with the function α given by $\alpha(z) = -\kappa \exp\left(\frac{\mu\theta_e}{1+\theta_e}\right) \frac{\mu}{(1+\theta_e)^2} - \beta$. The input operator $B \in \mathcal{L}(\bar{U}, L_2(0,1))$ is the linear bounded operator defined by: $B = \beta$. The new output is expressed by $y_x(t) = Cx(t) = \int_{l-r}^{l} x(z,t)dz$, $t \geq 0$ with $r = 0.0001$. According to [32], we can assume a uniform(constant) equilibrium profile $\theta_e(z) = 0$ if the equilibrium input signal is set as $\theta_{ce} = \frac{\kappa}{\beta}$. The parameter values of the resulting infinite-dimensional system are shown in Table 3.2.

$v(z)$	α	κ	μ	β	θ_e
$-(0.025 + 0.075z)$	-0.4421	0.0145	16.7	0.2	0

Table 3.2: Parameter values in the linear infinite-dimensional system.

In this example, our objective is the design of the error feedback regulator (3.126) in such a way that the output $y_x(t)$ tracks a step signal $y_r(t) = \Upsilon$, and rejects an unknown constant disturbance $d(t)$. We assume the disturbance spatial distribution to be given by the operator $B_d = e^z \cdot I, z \in [0, l]$. Therefore, the exosystem can be constructed simply as: $\dot{v}(t) = 0, v_0 = \Upsilon \in \mathbb{R}$. Obviously, by adjusting the initial condition v_0, one obtains different step signals y_r, see Figure 3.11.

In terms of previous notation in (3.2a)–(3.2c), $Q = 1$, $F = 0.5$ and then $P = 0.5e^z$. Now, the Sylvester equation (3.99)–(3.100) reduces to:

$$\frac{\partial \Pi(z)}{\partial z} = \frac{\alpha(z)}{-v(z)}\Pi(z) + \frac{(\beta\Gamma + 0.5e^z)}{-v(z)} \tag{3.143}$$

$$\Pi(0) = 0, \ \Pi(l) = 1 \tag{3.144}$$

where $\Pi(0) = 0$ comes from the definition of $D(A)$ and $\Pi(l) = 1$ comes from (3.100). Then, it is straightforward to compute the general solution of (3.143) given by $\Pi(z) = \exp\left(\int_0^z \frac{\alpha(\zeta)}{-v(\zeta)} d\zeta\right) \Pi(0) + \int_0^z \left(\exp\left(\int_\eta^z \frac{\alpha(\zeta)}{-v(\zeta)} d\zeta\right) \frac{\beta}{-v(\eta)}\right) d\eta \Gamma + \int_0^z \left(\exp\left(\int_\eta^z \frac{\alpha(\zeta)}{-v(\zeta)} d\zeta\right) \frac{(0.5e^\eta)}{-v(\eta)}\right) d\eta$. By applying the boundary conditions in (3.144), one obtains: $\Gamma = \frac{1-\int_0^l \left(\exp\left(\int_\eta^l \frac{\alpha(\zeta)}{-v(\zeta)} d\zeta\right) \frac{(0.5e^\eta)}{-v(\eta)}\right) d\eta}{\int_0^l \left(\exp\left(\int_\eta^l \frac{\alpha(\zeta)}{-v(\zeta)} d\zeta\right) \frac{\beta}{-v(\eta)}\right) d\eta} = 5.671$. In order to design the error feedback regulator (3.126), the Sylvester equation given by (3.130) needs to be solved and it reduces to:

$$\frac{\partial \Pi_e(z)}{\partial z} = \frac{-\alpha(z)}{v(z)} \Pi_e(z) + \frac{(0.5e^z + k_3\beta)}{v(z)} - \frac{k_3\beta\Pi_e(l)}{v(z)} \tag{3.145}$$

$$\Pi_e(0) = 0 \tag{3.146}$$

where according to Lemma 10, k_3 is chosen as $k_3 = 0.7$. The general solution of (3.145)–(3.146) can be calculated analytically and $\Pi_e(l)$ can be computed by evaluating $\Pi_e(z)$ at $z = l$ and is given by $\Pi_e(l) = \frac{\int_0^l \left(\exp\left(\int_\eta^l \frac{-\alpha(\zeta)}{v(\zeta)} d\zeta\right) \frac{(0.5e^\eta + k_3\beta)}{v(\eta)}\right) d\eta}{\left(1+\int_0^l \left(\exp\left(\int_\eta^l \frac{-\alpha(\zeta)}{v(\zeta)} d\zeta\right) \frac{k_3\beta}{v(\eta)}\right) d\eta\right)} = -4.1728$. As a consequence, the parameter gain L can be easily configured, e.g $L = 1$ such that $S + L(\Pi_e(l) + Q) = -3.1728$ is negative and since $S = 0$, the spatially varying function gain is given by: $k_e(z) = \frac{k_3\beta + \Pi_e(z)L + \Pi(z)L}{\beta}$.

Consequently, the spatially distributed input $\mathcal{U}(z,t)$ in (3.124) and (3.129) can be constructed as

$$\begin{aligned}\mathcal{U}(z,t) &= \Gamma r_w(t) + k_e(z)e(t) \\ &= \Gamma r_w(t) + k_3 e(t) + \tfrac{\Pi_e(z)L + \Pi(z)L}{\beta} e(t)\end{aligned}$$

and the performance of $\mathcal{U}(z,t)$ is shown in Figure 3.11 (black dashed line $y_x(t)$). However, the control law $\mathcal{U}(z,t)$ in (3.124) may not be practical to implement. According to Theorem 10, the feedforward gain K_e is given by $K_e = k_3 + \mu_e \left(\int_0^1 \frac{\Pi_e(z)L + \Pi(z)L}{\beta} dz\right)$. Therefore, the time varying control law $u(t)$ in (3.126) and (3.129) is given by:

$$\begin{aligned}\mathcal{U}(t) &= \Gamma r_w(t) + K_e e(t) \\ &= \Gamma r_w(t) + k_3 e(t) + \mu_e \left(\int_0^1 \tfrac{\Pi_e(z)L + \Pi(z)L}{\beta} dz\right) e(t)\end{aligned}$$

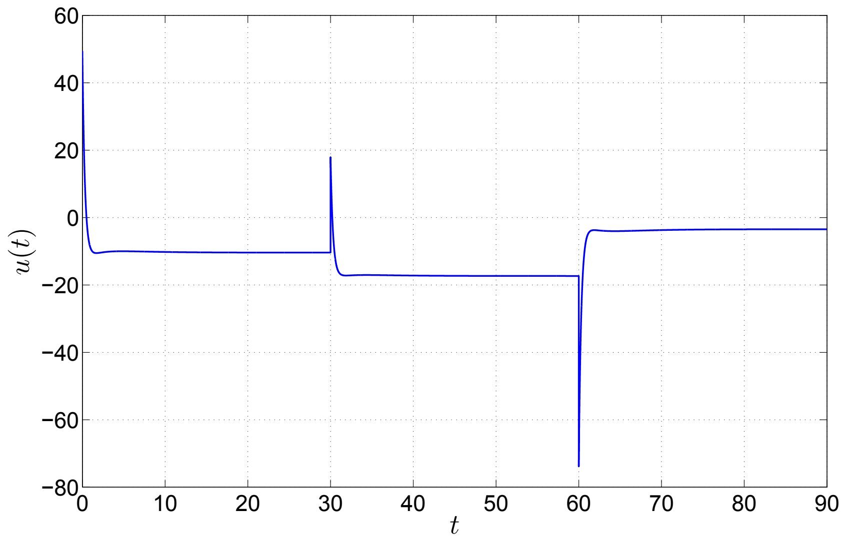

Figure 3.10: Manipulated input $\mathcal{U}(t)$.

with $\mu_e = 1$, which is only the function of time and is shown in Figure 3.10. The corresponding performance of $u(t)$ is also shown in Figure 3.11 (blue dashed line $y_{xin}(t)$). Compared with the performance of $\mathcal{U}(z,t)$, the averaged control law $\mathcal{U}(t)$ still can achieve the tracking target with an overshoot and a longer actuation time. In Figure 3.12, the evolution of state $x(z,t)$ under the control law $\mathcal{U}(t)$ is given.

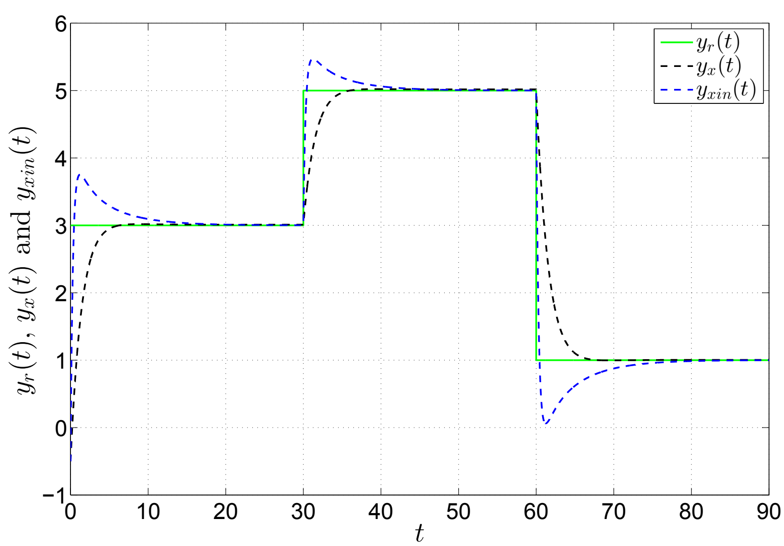

Figure 3.11: The evolution of the controlled outputs $y_x(t)$, $y_{xin}(t)$ and the reference trajectory $y_r(t) = \Upsilon$: $\Upsilon = 3$ when $0 \le t \le 30$; $\Upsilon = 5$ when $30 \le t \le 60$;$\Upsilon = 1$ when $60 \le t \le 90$.

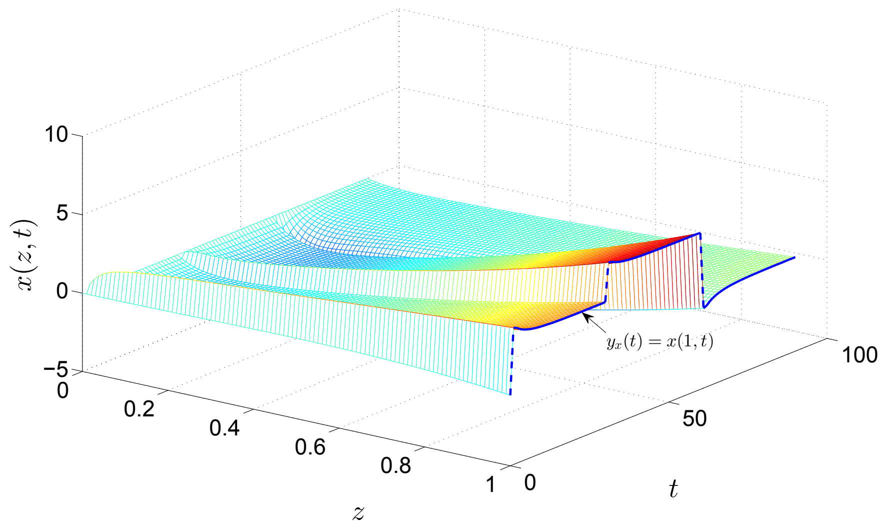

Figure 3.12: The evolution of state $x(z,t)$ under the regulator given by $\mathcal{U}(t) = \Gamma r_w(t) + k_3 e(t) + \mu_e \left(\int_0^1 \frac{(\Pi_e(z)+\Pi(z))L}{\beta} dz \right) e(t)$.

3.4 Output regulation for a class of linear boundary controlled first-order hyperbolic PIDE systems

3.4.1 Problem formulation

We consider the following hyperbolic PIDE systems on the domain $\{t \in \mathbb{R}^+, z \in (0,1)\}$ presented in [64]:

$$\begin{aligned} \partial_t x(z,t) = {} & \partial_z x(z,t) + f(z)x(0,t) \\ & + \int_0^z g(z,\xi)x(\xi,t)d\xi \\ & + \int_z^1 h(z,\xi)x(\xi,t)d\xi + g_1(z)d_1(t) \end{aligned} \tag{3.147}$$

$$x(1,t) = u(t) + g_2 d_2(t) \tag{3.148}$$

$$y(t) = \mathcal{C}x(t) \tag{3.149}$$

$$y_m(t) = x(0,t) \tag{3.150}$$

with the input $u(t) \in \mathbb{R}$. $d_1(t) \in \mathbb{R}$ and $d_2(t) \in \mathbb{R}$ are unmeasurable process and boundary input disturbances, respectively. f, g and h are real-valued continuous functions. $g_1 \in C[0,1]$

and $g_2 \in \mathbb{R}$ in (3.147)–(3.148) are known functions that characterize the distribution of disturbances. $x(\cdot,t) \in X = L_2(0,1)$, $\forall t \in \mathbb{R}^+$ denotes the state variable and then $x(\cdot,t)$ at the point z is $x(z,t)$. The real space $X = L_2(0,1)$ is the state space with the norm $\|\cdot\|_2$, i.e., $\|x(t)\|^2 = \int_0^1 x^2(z,t)dz$. In (3.149), $y(t) \in \mathbb{R}$ is the output to be controlled. The corresponding output operator $\mathcal{C}$ may describe point-wise or distributed in domain outputs, i.e.

$$y(t) = \mathcal{C}x(t) = \int_0^1 c(z)x(z,t)dz \tag{3.151}$$

where $c(z) = \sum_{i=1}^N c_i\delta(z - z_i), z_i \in (0,1)$ and $c_i \in \mathbb{R}$, or $c(z) \in L_2(0,1)$. The measurement $y_m(t) \in \mathbb{R}$ is different from the controlled output $y(t)$. In particular, it is not necessary that the controlled output $y(t)$ can be measured.

The following scalar hyperbolic PIDE system:

$$\begin{aligned}\partial_t x(z,t) = {} & v(z)\partial_z x(z,t) + \alpha(z)x(z,t) \\ & +\bar{f}(z)x(0,t) + \textstyle\int_0^z \bar{g}(z,\xi)x(\xi,t)d\xi \\ & + \textstyle\int_z^1 \bar{h}(z,\xi)x(\xi,t)d\xi + g_1(z)d_1(t)\end{aligned}$$

on the domain $(z,t) \in (0,1) \times (0,T]$ can be transformed into (3.147)–(3.150) by applying an appropriate change of variables, see [64]. Concomitantly, the resulting boundary conditions and outputs remain the same as in (3.148)–(3.150). Hence, the following results of this chapter are also valid for this general system class that describes many transport processes.

Remark 10. *Without considering the integration term in (3.147)–(3.150) and assuming that the function $f(z) \neq 0$, in [4] it has been shown that the system of equations described by (3.147)–(3.148) is a spectral system. However, according to Th.4.1. and Co.4.2 in [39], it is shown that the system (3.147)–(3.148) without the integration term and with $f(z) \neq 0$ is not a Riesz-spectral system. This is in sharp contrast to the results associated with parabolic PDE and second order hyperbolic PDE systems, which usually rely on the Riesz-spectral system properties.*

To ensure that the plant (3.147) is stabilizable in finite time, the following assumption providing sufficient conditions for the coefficients of (3.147) is given [64]:

Assumption 4. *Define the triangles*

$$\mathcal{T}_l = \{(z, \xi) \in [0, 1] \times [0, 1], z \geq \xi\}$$

$$\mathcal{T}_u = \{(z, \xi) \in [0, 1] \times [0, 1], z \leq \xi\}$$

and the spaces $X_l = C(\mathcal{T}_l; \mathbb{R})$ *and* $X_u = C(\mathcal{T}_u; \mathbb{R})$ *equipped with the norms*

$$\|h\|_{X_i} = \sup_{(z,\xi)\in\mathcal{T}_i} |h(z, \xi)|, \forall h \in X_i, i = l, u$$

then the coefficients in (3.147) satisfy: $f \in C([0, 1]; \mathbb{R})$, $g \in X_l$ *and* $h \in X_u$. *Moreover,* f, g *and* h *satisfy:* $\max\left\{\sup_{\zeta\in[0,1]} |f(\zeta)|, \|g\|_{X_l}, \|h\|_{X_u}\right\} < 0.25$. *In particular, if* $f(z) \equiv 0$, *then the coefficients* g *and* h *satisfy:* $\max\{\|g\|_{X_l}, \|h\|_{X_u}\} < 0.5$.

Actually, by introducing Assumption 4, the plant is limited into a certain class of systems with heavily bounded coefficients. However, for some systems, even though the plant coefficients are larger than the sufficient conditions, these systems still can be stabilized, see *Section II-E* in [64]. Moreover, when some coefficients such as f and h are zero functions, this limitation is relaxed. For example, in (3.147), when $h(z, \xi) \equiv 0$, the plant reduces to the system in [54] and is always stabilizable in finite time. Furthermore, for the case that g and h are only functions of z, i.e., $g(z, \xi) = g(z)$ and $h(z, \xi) = h(z)$, sufficient and necessary conditions were studied and provided in [65].

The disturbances $d_1(t)$ and $d_2(t)$ in (3.147), (3.148) and the reference signal $y_r(t) \in \mathbb{R}$ to be asymptotically tracked by the controlled output $y(t)$ can be modelled by the known finite-dimensional exosystem:

$$\dot{v}(t) = Sv(t), v(0) = v_0 \in \mathbb{C}^{n_v} \tag{3.152}$$

$$d_1(t) = p_{d_1}^T v(t) = r_{d_1}^T v_d(t),\ t \in \mathbb{R}^+ \tag{3.153}$$

$$d_2(t) = p_{d_2}^T v(t) = r_{d_2}^T v_d(t),\ t \in \mathbb{R}^+ \tag{3.154}$$

$$y_r(t) = q^T v(t) = q_r^T v_r(t),\ t \in \mathbb{R}^+ \tag{3.155}$$

where S is a block diagonal matrix $S = bdiag(S_d, S_r)$ having all its eigenvalues on the imaginary axis, i.e. iw_k where $i = \sqrt{-1}$, $k = 1, \cdots, n_v$ and w_k can have zero values. Correspondingly, $v = col(v_d, v_r)$ with the signal models $\dot{v}_d(t) = S_d v_d(t), v_d(0) = v_{d0} \in \mathbb{C}^{n_d}$, and $\dot{v}_r(t) = S_r v_r(t), v_r(0) = v_{r0} \in \mathbb{C}^{n_r}$, $n_d + n_r = n_v$.

In particular, we can design the above matrix S to have the form: $S = bdiag(S_d, S_r) = bdiag(S_m, S_n)$ and the block S_n is a nilpotent matrix with dimension n_n, i.e. its spectrum: $\sigma(S_n) = 0$. In this chapter, we assume S_n is a sub-block matrix in the matrix S_r. The matrix S_m is a diagonalizable matrix with dimension n_m. Obviously, we have $n_n + n_m = n_v$. In particular, in this chapter, S_n is given by

$$S_n = \begin{bmatrix} 0 & 0 & \cdots & 0 & 0 \\ 1 & 0 & \cdots & 0 & 0 \\ 0 & 2 & \cdots & 0 & 0 \\ \vdots & \vdots & \ddots & \vdots & \vdots \\ 0 & 0 & \cdots & (n_n - 1) & 0 \end{bmatrix} \tag{3.156}$$

If we write $v = col(v_m, v_n)$ and $q^T = \left[q_m^T, q_n^T\right]$ with $q_n^T = [\alpha_1, \alpha_2, \cdots, \alpha_{n_n}]$ and $v_n(0) = [1, 0, \cdots, 0]^T$, then it is easy to obtain the polynomial signal:

$$q_n^T v_n(t) = \alpha_1 + \alpha_2 t + \cdots + \alpha_{n_n} t^{n_n - 1}$$

According to this assumption, the exosystem can generate sinusoidal, steplike, ramp and polynomial exogenous signals. In particular, since we assume that S_n is a block matrix in the matrix S_r, a polynomial type exogenous signal is only possible for the reference signal $y_r(t)$.

In this chapter, we assume that the disturbances cannot be measured and the reference signal $y_r(t)$ in (3.150) is available for the regulator design. Moreover, throughout this chapter, the disturbance distributions $g_1(z)$ and g_2, and the matrices S, $p_{d_1}^T$, $p_{d_2}^T$ and q^T are assumed to be known for the regulator design.

In this chapter, the output regulation problem is solved, which is equivalent to a regulator design such that, with the state feedback control the output tracking error satisfies:

$$e(t) = y(t) - y_r(t) = 0,\ t \geq T \tag{3.157}$$

for a finite time $T \in \mathbb{R}^+$, and with the output feedback control, the output tracking error satisfies:

$$\lim_{t\to\infty} (e(t)) = \lim_{t\to\infty} (y(t) - y_r(t)) = 0 \tag{3.158}$$

for all initial values of the plant (3.147)–(3.150), of the exosystem (3.152)–(3.155) and of the regulator. Moreover, the resulting closed-loop system has to be exponentially stable.

3.4.2 Output regulation by state feedback

First, the backstepping approach in [64] is applied to transform the plant (3.147)–(3.150) into a target system with a simple structure. Thereby, the new coordinates $\tilde{x}(z,t)$ are introduced in the form of the integral transformation

$$\begin{aligned}\tilde{x}(z,t) &= \mathcal{T}_c\left[x(t)\right](z)\\ &= x(z,t) - \textstyle\int_0^z p(z,\xi)x(\xi,t)d\xi - \int_z^1 o(z,\xi)x(\xi,t)d\xi\end{aligned} \tag{3.159}$$

with $x(t) = \{x(z,t), z \in (0,1)\}$ and integral kernels $p(z,\xi)$ and $o(x,\xi)$. Assume that the kernel $p(z,\xi)$ and $o(z,\xi)$ are the solutions of the kernel boundary value problems (BVP):

$$\begin{aligned}\partial_\xi p(z,\xi) + \partial_z p(z,\xi) &= -g(z,\xi) + o(z,1)p(1,\xi)\\ &+ \textstyle\int_\xi^z g(\eta,\xi)p(z,\eta)d\eta + \int_z^1 g(\eta,\xi)o(z,\eta)d\eta\\ &+ \textstyle\int_0^\xi h(\eta,\xi)p(z,\eta)d\eta, \forall z,\xi \in [0,1] \text{ s.t. } \xi \leq z\end{aligned} \tag{3.160}$$

$$\begin{aligned}\partial_\xi o(z,\xi) + \partial_z o(z,\xi) &= -h(z,\xi) + o(z,1)p(1,\xi)\\ &+ \textstyle\int_\xi^1 o(z,\eta)g(\eta,\xi)d\eta + \int_z^\xi o(z,\eta)h(\eta,\xi)d\eta\\ &+ \textstyle\int_0^z p(z,\eta)h(\eta,\xi)d\eta, \forall z,\xi \in [0,1] \text{ s.t. } z \leq \xi\end{aligned} \tag{3.161}$$

with boundary conditions

$$\begin{aligned}p(z,0) = -f(z) &+ \textstyle\int_0^z p(z,\eta)f(\eta)d\eta\\ &+ \textstyle\int_z^1 o(z,\eta)f(\eta)d\eta, \forall z \in [0,1]\end{aligned} \tag{3.162}$$

$$o(z,1) = 0 \tag{3.163}$$

A straightforward computation leads to

$$
\begin{aligned}
\tilde{g}_1^T(z) &= g_1(z)p_{d_1}^T - \textstyle\int_0^z p(z,\xi)g_1(y\xi)d\xi p_{d_1}^T \\
&\quad - \textstyle\int_z^1 o(z,\xi)g_1(\xi)d\xi p_{d_1}^T \\
&= \mathcal{T}_c\left[g_1\right](z)p_{d_1}^T
\end{aligned}
\tag{3.164}
$$

and the resulting system:

$$\dot{v}(t) = Sv(t) \tag{3.165}$$

$$\partial_t \tilde{x}(z,t) = \partial_z \tilde{x}(z,t) + \tilde{g}_1^T(z)v(t) \tag{3.166}$$

$$\tilde{x}(1,t) = \pi_v^T v(t) + g_2 p_{d_2}^T v(t) \tag{3.167}$$

by implementation of the state feedback regulator, with the state feedback and feedforward gains, of the following form:

$$u(t) = \int_0^1 k(\xi)x(\xi,t)dz + \pi_v^T v(t),\ k(\xi) = p(1,\xi) \tag{3.168}$$

From [64], the Assumption 4 indicates that the kernel BVPs (3.160)–(3.163) has a unique bounded solution $\left[\begin{array}{cc} p & o \end{array}\right]^T$. As a consequence, the feedback gain $k(\xi)$ in (3.168) exists such that the closed-loop system (3.147), (3.148) for $v(t) \equiv 0$ is finite-time stable.

In order to determine the feedforward gain π_v^T in (3.168), we introduce for (3.165)–(3.167) the error state:

$$\tilde{e}(z,t) = \tilde{x}(z,t) - \pi^T(z)v(t) \tag{3.169}$$

where $\pi^T(z)$ has to be found. Therein, $\pi^T(z)v(t)$ describes the behaviour of $\tilde{x}(z,t)$ to achieve output regulation (3.157). By applying (3.152), (3.166), and (3.169) one obtains:

$$\partial_t \tilde{e}(z,t) = \partial_z \tilde{e}(z,t),\ (z,t) \in (0,1) \times \mathbb{R}^+ \tag{3.170}$$

$$\tilde{e}(1,t) = \tilde{x}(1,t) - \pi^T(1)v(t) = 0 \tag{3.171}$$

$$e(t) = \mathcal{C}x(t) - q^T v(t) = \mathcal{C}\mathcal{T}_c^{-1}\left[\tilde{e}(t)\right] \tag{3.172}$$

if $\pi^T(z)$ is the solution of the regulator equations

$$\frac{d\pi^T}{dz}(z) - \pi^T(z)S + \tilde{g}_1^T(z) = 0 \tag{3.173}$$

$$\mathcal{C}\mathcal{T}_c^{-1}\left[\pi^T\right] = q^T \tag{3.174}$$

on the spatial domain $z \in (0,1)$ and π_v^T in (3.168) is chosen as:

$$\pi_v^T = \pi^T(1) - g_2 p_{d_2}^T \tag{3.175}$$

From Lemma 6 of [64], the Assumption 4 implies that the inverse transformation $\mathcal{T}_c^{-1}$ given in (3.172) exists. It has the following integral form:

$$\begin{aligned} x(z,t) &= \mathcal{T}_c^{-1}\left[\tilde{x}(t)\right](z) \\ &= \tilde{x}(z,t) + \textstyle\int_0^z k(z,\xi)\tilde{x}(\xi,t)d\xi \\ &\quad + \textstyle\int_z^1 l(z,\xi)\tilde{x}(\xi,t)d\xi \end{aligned} \tag{3.176}$$

where the kernels $k(z,\xi)$ and $l(z,\xi)$ are bounded functions. The corresponding inverse control kernel BVPs for $k(z,\xi)$ and $l(z,\xi)$ have the following forms:

$$\begin{aligned} \partial_\xi k(z,\xi) + \partial_z k(z,\xi) &= -g(z,\xi) - f(z)l(0,\xi) \\ &- \textstyle\int_\xi^z g(z,\eta)k(\eta,\xi)d\eta - \int_0^\xi g(z,\eta)l(\eta,\xi)d\eta \\ &- \textstyle\int_z^1 h(z,\eta)k(\eta,\xi)d\eta, \forall z,\xi \in [0,1] \text{ s.t. } \xi \leq z \end{aligned} \tag{3.177}$$

$$\begin{aligned} \partial_\xi l(z,\xi) + \partial_z l(z,\xi) &= -h(z,\xi) - f(z)l(0,\xi) \\ &- \textstyle\int_\xi^1 h(z,\eta)k(\eta,\xi)d\eta - \int_0^z g(z,\eta)l(\eta,\xi)d\eta \\ &- \textstyle\int_z^\xi h(z,\eta)l(\eta,\xi)d\eta, \forall z,\xi \in [0,1] \text{ s.t. } z \leq \xi \end{aligned} \tag{3.178}$$

with boundary conditions:

$$k(z,0) = -f(z) \tag{3.179}$$

$$l(0,\xi) = 0 \tag{3.180}$$

Then, the tracking error system (3.170)–(3.172) is finite-time stable. Therefore, the output regulation with the closed-stability is achieved, see the proof part of Theorem 11. Equivalently, we can claim that (3.173)–(3.174) are the *regulator equations*, since they play the same role as the regulator equations (constrained Sylvester equations) derived for the general class of distributed parameter systems with distributed control in [57], and with boundary control in [31]. Since the ODE (3.173) has a very simple form, it admits a general closed-form analytic solution. Consequently, the solvability of the regulator equations (3.173)–(3.174) can be easily demonstrated, and it depends on the behavior of the system (3.147)–(3.149). The transfer function can be obtained on the basis of the representation of the plant in the backstepping coordinates – a simple hyperbolic system. Thus, the transfer function is attainable in a closed-form. In order to utilize the transfer function explicitly, we apply the method in [60]. With the aid of the transfer function and motivated by [53] for parabolic systems, the following lemma demonstrates the solvability condition for the regulator equations (3.173)–(3.174).

Lemma 11. *(Regulator Equations). The transfer function of (3.147)–(3.149) from $u(t)$ to $y(t)$ is $G(s) = \mathcal{C}\mathcal{T}_c^{-1}\left[e^{sz}\right]e^{-s}$. Then, the regulator equations (3.173)–(3.174) have a unique solution if and only if $G(\lambda) \neq 0$, $\forall \lambda \in \sigma(S)$.*

Proof. We assume that $\{\phi_k\}$ with $k = 1, \cdots, n_m$ are eigenvectors of S_m with eigenvalues as $\{\lambda_k\}_{k=1,\cdots,n_m}$. Consequently, equations (3.173)–(3.174) can be decomposed into:

$$\frac{d\pi_m^T}{dz}(z) - \pi_m^T(z)S_m + \tilde{g}_{1m}^T(z) = 0 \tag{3.181}$$

$$\mathcal{C}\mathcal{T}_c^{-1}\left[\pi_m^T\right] = q_m^T \tag{3.182}$$

$$\frac{d\pi_n^T}{dz}(z) - \pi_n^T(z)S_n + \tilde{g}_{1n}^T(z) = 0 \tag{3.183}$$

$$\mathcal{C}\mathcal{T}_c^{-1}\left[\pi_n^T\right] = q_n^T \tag{3.184}$$

with $\pi^T(z) = \left[\pi_m^T(z), \pi_n^T(z)\right]$. First, we focus on solving (3.183)–(3.184). Assume $\pi_n^T(z) = [\pi_{n,1}(z), \pi_{n,2}(z), \cdots, \pi_{n,n_n}(z)]$ and $\tilde{g}_{1n}^T = [g_{1n,1}(z), g_{1n,2}(z), \cdots, g_{1n,n_n}(z)]$, then (3.183) can be written as a set of cascade ODEs:

$$\begin{aligned} &\tfrac{d\pi_{n,k}}{dz}(z) = k\pi_{n,k+1}(z) - g_{1n,k}(z) \\ &\tfrac{d\pi_{n,n_n}}{dz}(z) = -g_{1n,n_n}(z) \end{aligned} \tag{3.185}$$

with $k = 1, 2, \cdots, (n_n - 1)$. Consequently, the general solutions are given by:

$$\begin{aligned}
\pi_{n,k}(z) &= \pi_{n,k}(0) + \int_0^z \left(k\pi_{n,k+1}(\xi) - g_{1n,k}(\xi)\right) d\xi \\
\pi_{n,n_n}(z) &= \pi_{n,n_n}(0) - \int_0^z g_{1n,n_n}(\xi) d\xi
\end{aligned}$$

Obviously, it is easy to see that the existence and uniqueness of $\pi_{n,k+1}(z)$ directly indicates the existence and uniqueness of $\pi_{n,k}(z)$. Let $q_n^T = [q_{n,1}, q_{n,2}, \cdots q_{n,n_n}]$ and applying (3.184) yields:

$$\begin{aligned}
&\mathcal{C}\mathcal{T}_c^{-1}[e^{0z}]\pi_{n,n_n}(0) = q_{n,n_n} + \mathcal{C}\mathcal{T}_c^{-1}\left[\int_0^z g_{1n,n_n}(\xi)d\xi\right] \\
&\mathcal{C}\mathcal{T}_c^{-1}[e^{0z}]\pi_{n,k}(0) = q_{n,k} \\
&\qquad\qquad + \mathcal{C}\mathcal{T}_c^{-1}\left[\int_0^z \left(k\pi_{n,k+1}(\xi) - g_{1n,k}(\xi)\right) d\xi\right]
\end{aligned}$$

Therefore, the condition $\mathcal{C}\mathcal{T}_c^{-1}\left[e^{0z}\right] \neq 0$ ensures the existence and uniqueness of $\pi_{n,n_n}(0)$ and $\pi_{n,k}(0)$, $k = 1, 2, \cdots, (n_n - 1)$ and thus the existence and uniqueness of $\pi_n^T(z)$.

As defined in previous section, the matrix S_m is diagonalizable, there exists a similarity transformation $V^{-1}S_mV = diag\left(\lambda_1, \cdots, \lambda_{n_m}\right)$ with $V = [\phi_1, \cdots, \phi_{n_m}]$. Postmultiplying (3.173) by V gives us a decoupled set of ODEs:

$$\frac{d\pi_m^*}{dz}(z) - \pi_{mk}^*(z)\lambda_k + \tilde{g}_{1mk}^*(z) = 0 \tag{3.186}$$

with $\pi_{mk}^*(z) = \pi_m^T(z)\phi_k$ and $\tilde{g}_{1mk}^*(z) = \tilde{g}_{1m}^T(z)\phi_k$ for $k = 1, \cdots, n_m$. In terms of an unknown boundary condition, the corresponding general solution is

$$\pi_{mk}^*(z) = e^{\lambda_k z}\pi_{mk}^*(0) - \int_0^z e^{\lambda_k(z-s)}\tilde{g}_{1mk}^*(s)ds \tag{3.187}$$

Therefore, the condition (3.174) can be rewritten as $\mathcal{C}\mathcal{T}_c^{-1}\left[\pi_{mk}^*(z)\right] = q_{mk}^*$ with $q_{mk}^* = q_m^T\phi_k$. By inserting the general solution $\pi_i^*(z)$, one obtains:

$$\begin{aligned}
&\mathcal{C}\mathcal{T}_c^{-1}\left[e^{\lambda_k z}\right]\pi_{mk}^*(0) \\
&= \mathcal{C}\mathcal{T}_c^{-1}\left[\int_0^z e^{\lambda_k(z-s)}\tilde{g}_{1mk}^*(s)ds\right] + q_{mk}^*
\end{aligned} \tag{3.188}$$

This equation can be solved directly for $\pi_{mk}^*(0)$ if and only if the solvability condition $\mathcal{C}\mathcal{T}_c^{-1}\left[e^{\lambda z}\right] \neq 0, \forall\lambda \in \sigma(S_m)$ holds. Therefore, the solution of the regulator equations (3.181)–(3.182) can be uniquely obtained as $\pi_m^T(z) = \left[\pi_{m1}^*(z), \cdots, \pi_{mn_m}^*(z)\right]V^{-1}$ if and only if the solvability condition of Lemma 11 holds. From the above, the regulator equation (3.173)–(3.174) has a unique solution as long as the condition $\mathcal{C}\mathcal{T}_c^{-1}\left[e^{\lambda z}\right] \neq 0, \forall\lambda \in \sigma(S)$ holds.

The system (3.147)–(3.149) has the representation $\partial_t \tilde{x}(z,t) = \partial_z \tilde{x}(z,t), (z,t) \in (0,1)\times\mathbb{R}^+$ with the boundary condition $\tilde{x}(1,t) = u(t) - \int_0^1 p(1,\xi)\mathcal{T}_c^{-1}[\tilde{x}(t)](\xi)d\xi, t > 0$ and the output $y(t) = \mathcal{C}\mathcal{T}_c^{-1}[\tilde{x}(t)]$ in the coordinates (3.159). By applying the technique in [60], the transfer function can be easily computed: $G(s) = \mathcal{C}\mathcal{T}_c^{-1}[e^{sz}]\,e^{-s}$. Obviously, $\forall\lambda \in \sigma(S)$, $e^{-\lambda}$ is non-zero and invertible. Then, $\forall\lambda \in \sigma(S)$, $G(\lambda) \neq 0$ means $\mathcal{C}\mathcal{T}_c^{-1}\left[e^{\lambda z}\right] \neq 0$ and this completes the proof of the Lemma 11. □

From Lemma 11 it is implied that the eigenmodes of the exosystem (3.152)–(3.155) can be transferred to the output $y(t)$ to compensate for the process and boundary input disturbances $d_1(t)$ and $d_2(t)$ and to attain the reference signal $y_r(t)$. In the proof of Lemma 11 it is shown that the solution $\pi^T(z)$ of the regulator equations (3.173)–(3.174) can be readily computed in closed-form given that the backstepping transformations (3.159) and (3.176) have been determined (see (3.164) and (3.174)). Consequently, the full state feedback regulator (3.168) achieving output regulation has the form:

$$u(t) = \int_0^1 p(1,\xi)x(\xi,t)d\xi + \left(\pi^T(1) - g_2 p_{d_2}^T\right)v(t) \tag{3.189}$$

For the design of the full state feedback regulator (3.189), these results show that at first the control kernel BVPs (3.160)–(3.163) and the corresponding inverse control kernel BVPs (3.177)–(3.180) have to be solved in order to get $p(1,\xi)$, $\tilde{g}_1^T(z)$ and thus $\pi^T(z)$. In the following theorem it is shown that output regulation in the coordinates (3.159) also ensures the output regulation in the original coordinates. Thereby, the dynamics of the tracking error $e_{tr}(z,t) = x(z,t) - \pi_c^T(z)v(t)$ with $\pi_c^T(z) = \mathcal{T}_c^{-1}\left[\pi^T\right](z)$ is finite-time stable.

Theorem 11. *(State Feedback Regulator). Let $\kappa(z,\xi)$ and $\pi^T(z)$ be the solution of the control-kernel BVP (3.160)–(3.163) and the regulator equations (3.173)–(3.174), respectively. Then, the state feedback (3.189) achieves output regulation (3.157) for the system*

(3.147)–(3.149) and (3.152)–(3.155) with an exponentially stable tracking error dynamics in the L_2−norm, i.e., the tracking error $e_{tr}(t) = \{e_{tr}(z,t), z \in [0,1]\}$ satisfies

$$\|e_{tr}(\cdot,t)\|_2 \leq M_c(p,o,k,l)\|e_{tr}(\cdot,0)\|_2, t \in (0,T] \tag{3.190}$$

for all $e_{tr}(\cdot,0) \in L_2(0,1)$ with $M_c > 0$ and $\alpha_0 > 0$. In particular, the finite-time output regulation by state feedback control (3.189) is achieved.

Proof. The tracking error (3.170)–(3.171) can be solved as

$$\tilde{e}(t) = \begin{cases} \tilde{e}_0(z+t), & z+t \leq 1 \\ 0, & z+t > 1 \end{cases} \tag{3.191}$$

for all $t \geq 0$, $z \in [0,1]$. For the unbounded output operator defined in Section 3.4.1, based on *Cauchy-Schwarz inequality*, the boundedness of the kernels $k(z,\xi)$ and $l(z,\xi)$, it can be shown that there exists a positive constant $M(k,l) > 0$ (i.e. depending on k, l) such that the norms

$$\|\tilde{e}(\cdot,t)\|_2 \leq \|\tilde{e}(0)\|_2$$

$$\begin{aligned} |e(t)| &= |\mathcal{C}\mathcal{T}_c^{-1}(\tilde{e}(t))| \\ &\leq \|\tilde{e}(z_0,t)\|_2 + \left\|\int_0^{z_0} k(z_0,\xi)\,\tilde{e}(\xi,t)d\xi\right\|_2 \\ &\quad + \left\|\int_{z_0}^{1} l(z_0,\xi)\,\tilde{e}(\xi,t)d\xi\right\|_2 \\ &\leq (1 + M(k,l))\,\|\tilde{e}(0)\|_2 \end{aligned}$$

hold for all $t \in \mathbb{R}^+$. Moreover,

$$\|\tilde{e}(\cdot,t)\|_2 = 0, \forall t > 1$$

$$|e(t)| = 0, \forall t > 1$$

This proves the output regulation (3.157) for the considered unbounded operators $\mathcal{C}$ within finite time. For the bounded operator $\mathcal{C}$ the same also holds, since $\mathcal{T}_c^{-1}$ is bounded. To prove (3.190), by applying *Cauchy-Schwarz inequality* we have:

$$\begin{aligned}\|\tilde{e}(\cdot,t)\|_2 &= \|\mathcal{T}_c\left(e_{tr}(\cdot,t)\right)\|_2 \\ &\le \|e_{tr}(\cdot,t)\|_2 + \left\|\int_0^z p(z,\xi)e_{tr}(\xi,t)d\xi\right\|_2 \\ &+ \left\|\int_z^1 o(z,\xi)e_{tr}(\xi,t)d\xi\right\|_2\end{aligned}$$

Due to $\left\|\int_0^z p(z,\xi)e_{tr}(\xi,t)d\xi\right\|_2^2 \le \int_0^1\int_0^1 |p(z,\xi)|^2 d\xi dz\cdot\|e_{tr}(\cdot,t)\|_2^2$ and $\left\|\int_z^1 o(z,\xi)e_{tr}(\xi,t)d\xi\right\|_2^2 \le \|e_{tr}(\cdot,t)\|_2^2\cdot\int_0^1\int_0^1 |o(z,\xi)|^2 d\xi dz$, then the boundedness of the kernels $p(z,\xi)$ and $o(z,\xi)$ implies the existence of a positive constant $c_0(p,q)$ such that the following inequality

$$\left\|\int_0^z p(z,\xi)e_{tr}(\xi,t)d\xi\right\|_2^2 + \left\|\int_z^1 q(z,\xi)e_{tr}(\xi,t)d\xi\right\|_2^2 \le c_0^2(p,o)\,\|e_{tr}(\cdot,t)\|_2^2$$

yields $\|\tilde{e}(\cdot,t)\|_2 \le (1+c_0(p,o))\,\|e_{tr}(\cdot,t)\|_2$ and thus one has

$$\|\tilde{e}(\cdot,0)\|_2 \le (1+c_0(p,o))\,\|e_{tr}(\cdot,0)\|_2$$

Because the kernels $k(z,\xi)$ and $l(z,\xi)$ in the inverse transformation (3.176) are also bounded, there is a positive constant $c_1(k,l)$ such that $\|e_{tr}(\cdot,t)\|_2 \le (1+c_1(k,l))\,\|\tilde{e}(\cdot,t)\|_2$. This leads to (3.190) with $M_c(p,o,k,l) = (1+c_1(k,l))\,(1+c_0(p,o))$. Moreover, $\|e_{tr}(\cdot,t)\|_2 = 0, \forall t > 1$. Therefore, the finite-time stability of error dynamics in the original coordinates is ensured.

□

3.4.3 The design of output feedback regulator

In this section, the output regulator is designed to realize the output regulation of the system (3.147)–(3.150). In this section, we make the following assumptions:

(i) It is assumed that (q_r^T, S_r) is observable.

(ii) Eigenvalues of S_d are distinct.

(iii) The reference signal $y_r(t)$ and the measurement $y_m(t)$ (different from the controlled output $y(t)$) are known for the regulator design.

Since $y_r(t)$ is known, the state $v_r(t)$ of (3.152) can be estimated by applying the finite-dimensional reference observer

$$\dot{\hat{v}}_r(t) = S_r\hat{v}_r(t) + l_r\left(y_r(t) - q_r^T\hat{v}_r(t)\right), t > 0 \tag{3.192}$$

with the initial condition $\hat{v}_r(0) = \hat{v}_{r0} \in \mathbb{C}^{n_r}$. Due to assumption **(i)**, there exists an output injection gain l_r such that the dynamics of the estimation error $e_r(t) = v_r(t) - \hat{v}_r(t)$ decays asymptotically.

To estimate the states $x(z,t)$ and $v_d(t)$ in (3.147) and (3.152) the PDE-ODE coupled observer is constructed as follows:

$$\dot{\hat{v}}_d(t) = S_d\hat{v}_d(t) + l_d\left(y_m(t) - \hat{x}(0,t)\right), t > 0 \tag{3.193}$$

$$\begin{aligned}\partial_t\hat{x}(z,t) = {} & \partial_z\hat{x}(z,t) + f(z)\hat{x}(0,t) \\ & + \textstyle\int_0^z g(z,\xi)\hat{x}(\xi,t)d\xi \\ & + \textstyle\int_z^1 h(z,\xi)\hat{x}(\xi,t)d\xi + g_1(z)r_{d_1}^T\hat{v}_d(t) \\ & + l(z)\left(y_m(t) - \hat{x}(0,t)\right), t > 0\end{aligned} \tag{3.194}$$

$$\hat{x}(1,t) = u(t) + g_2 r_{d_2}^T\hat{v}_d(t), t > 0 \tag{3.195}$$

on the domain $(z,t) \in (0,1) \times \mathbb{R}^+$ with the initial conditions $\hat{v}_d(0) = \hat{v}_{d0} \in \mathbb{C}^{n_d}$ and $\hat{x}(z,0) = \hat{x}_0(z), z \in [0,1]$. Then, in view of (3.147)–(3.148), (3.152) and (3.193)–(3.195), the corresponding observer error system can be constructed as

$$\dot{e}_d(t) = S_d e_d(t) - l_d e_x(0,t) \tag{3.196}$$

$$\begin{aligned}\partial_t e_x(z,t) = {} & \partial_z e_x(z,t) + \gamma(z)e_x(0,t) \\ & + \textstyle\int_0^z g(z,\xi)e_x(\xi,t)d\xi \\ & + \textstyle\int_z^1 h(z,\xi)e_x(\xi,t)d\xi + g_1(z)r_{d_1}^T e_d(t)\end{aligned} \tag{3.197}$$

$$e_x(1,t) = g_2 r_{d_2}^T e_d(t) \tag{3.198}$$

with $\gamma(z) = f(z) - l(z)$, $e_d(t) = v_d(t) - \hat{v}_d(t)$ and $e_x(z,t) = x(z,t) - \hat{x}(z,t)$. In order to ensure the convergence of the observer, the observer error system (3.196)–(3.198) has to be stabilized. This problem can be solved by applying the backstepping forwarding approach. To this end, the coordinates $\tilde{e}_x(z,t)$ are introduced for the infinite-dimensional system (3.197)–(3.198) by the inverse integral transformation

$$\begin{aligned} e_x(z,t) &= \mathcal{T}_o^{-1}\left[\tilde{e}_x(t)\right](z) \\ &= \tilde{e}_x(z,t) + \textstyle\int_0^z k_{obs}(z,\xi)\tilde{e}_x(\xi,t)d\xi \\ &\quad + \textstyle\int_z^1 l_{obs}(z,\xi)\tilde{e}_x(\xi,t)d\xi \end{aligned} \tag{3.199}$$

in order to simplify the design of the output injection gains $l(z)$ and l_d. Assume that the observer kernels $k_{obs}(z,\xi)$ and $l_{obs}(z,\xi)$ are the solutions of the inverse observer-kernel BVPs:

$$\begin{aligned} \partial_\xi k_{obs}(z,\xi) + \partial_z k_{obs}(z,\xi) = &-g(z,\xi) - \gamma(z)l_{obs}(0,\xi) \\ &- \textstyle\int_\xi^z g(z,\eta)k_{obs}(\eta,\xi)\tilde{e}_x(\xi,t)d\eta \\ &- \textstyle\int_0^\xi g(z,\eta)l_{obs}(\eta,\xi)\tilde{e}_x(\xi,t)d\eta \\ &- \textstyle\int_z^1 h(z,\eta)k_{obs}(\eta,\xi)\tilde{e}_x(\xi,t)d\eta \\ &\forall z,\xi \in [0,1] \text{ s.t. } \xi \le z \end{aligned} \tag{3.200}$$

$$\begin{aligned} \partial_\xi l_{obs}(z,\xi) + \partial_z l_{obs}(z,\xi) = &-h(z,\xi) - \gamma(z)l_{obs}(0,\xi) \\ &- \textstyle\int_\xi^1 h(z,\eta)k_{obs}(\eta,\xi)\tilde{e}_x(\xi,t)d\eta \\ &- \textstyle\int_z^\xi h(z,\eta)l_{obs}(\eta,\xi)\tilde{e}_x(\xi,t)d\eta \\ &- \textstyle\int_0^z g(z,\eta)l_{obs}(\eta,\xi)\tilde{e}_x(\xi,t)d\eta \\ &\quad \forall z,\xi \in [0,1] \text{ s.t. } z \le \xi \end{aligned} \tag{3.201}$$

$$k_{obs}(1,\xi) = 0 \tag{3.202}$$

$$l_{obs}(0,\xi) = 0 \tag{3.203}$$

After the straightforward derivation, one obtains the output injection gain:

$$l(z) = f(z) + \mathcal{T}_o^{-1}[\tilde{l}](z) + k_{obs}(z,0) \tag{3.204}$$

and the representation:

$$\dot{e}_d(t) = S_d e_d(t) - l_d \tilde{e}_x(0,t) \tag{3.205}$$

$$\partial_t \tilde{e}_x(z,t) = \partial_z \tilde{e}_x(z,t) - \tilde{l}(z)\tilde{e}_x(0,t) + \tilde{g}_{1o}^T(z) e_d(t) \tag{3.206}$$

$$\tilde{e}_x(1,t) = g_2 r_{d_2}^T e_d(t) \tag{3.207}$$

of (3.196)–(3.198) in new coordinates. Therein, $\tilde{g}_{1o}^T(z) = \mathcal{T}_o[g_1](z) r_{d_1}^T - \mathcal{T}_o[l_{obs}(\cdot,1)](z) g_2 r_{d_2}^T$ holds. The new output injection gain $\tilde{l}(z)$ in (3.204) and (3.206) is needed as an additional degree of freedom for the further design. The transformation $\mathcal{T}_o$ in $\tilde{g}_{1o}^T(z)$ is given by the integral transformation:

$$\begin{aligned} \mathcal{T}_o[e_x(t)](z) &= e_x(z,t) + \textstyle\int_0^z p_{obs}(z,\xi) e_x(\xi,t) d\xi \\ &\quad + \textstyle\int_z^1 q_{obs}(z,\xi) e_x(\xi,t) d\xi \\ &= \tilde{e}_x(z,t) \end{aligned} \tag{3.208}$$

The corresponding observer kernel BVPs for $p_{obs}(z,\xi)$ and $q_{obs}(z,\xi)$ have the form:

$$\begin{aligned} \partial_z p_{obs}(z,\xi) + \partial_\xi p_{obs}(z,\xi) &= g(z,\xi) + \tilde{l}(z) q_{obs}(0,\xi) \\ &\quad + \textstyle\int_\xi^z p_{obs}(z,\eta) g(\eta,\xi) d\eta \\ &\quad + \textstyle\int_0^\xi p_{obs}(z,\eta) h(\eta,\xi) d\eta \\ &\quad + \textstyle\int_z^1 q_{obs}(z,\eta) g(\eta,\xi) d\eta \\ &\quad \forall z,\xi \in [0,1] \text{ s.t. } \xi \le z \end{aligned} \tag{3.209}$$

$$\begin{aligned} \partial_z q_{obs}(z,\xi) + \partial_\xi q_{obs}(z,\xi) &= h(z,\xi) + \tilde{l}(z) q_{obs}(0,\xi) \\ &\quad + \textstyle\int_0^z p_{obs}(z,\eta) h(\eta,\xi) d\eta \\ &\quad + \textstyle\int_\xi^1 q_{obs}(z,\eta) g(\eta,\xi) d\eta \\ &\quad + \textstyle\int_z^\xi q_{obs}(z,\eta) h(\eta,\xi) d\eta \\ &\quad \forall z,\xi \in [0,1] \text{ s.t. } z \le \xi \end{aligned} \tag{3.210}$$

$$p_{obs}(1,\xi) = 0 \tag{3.211}$$

$$q_{obs}(0,\xi) = 0 \tag{3.212}$$

If submitting (3.208) into (3.199), it is not difficult to obtain:

$$\begin{aligned}-p_{obs}(z,\xi) = k_{obs}(z,\xi) &+ \textstyle\int_{\xi}^{z} p_{obs}(z,\eta)k_{obs}(\eta,\xi)d\eta \\ &+ \textstyle\int_{0}^{\xi} p_{obs}(z,\eta)l_{obs}(\eta,\xi)d\eta \\ &+ \textstyle\int_{z}^{1} q_{obs}(z,\eta)k_{obs}(\eta,\xi)d\eta\end{aligned} \tag{3.213}$$

$$\begin{aligned}-q_{obs}(z,\xi) = l_{obs}(z,\xi) &+ \textstyle\int_{0}^{z} p_{obs}(z,\eta)l_{obs}(\eta,\xi)d\eta \\ &+ \textstyle\int_{z}^{\xi} q_{obs}(z,\eta)l_{obs}(\eta,\xi)d\eta \\ &+ \textstyle\int_{\xi}^{1} q_{obs}(z,\eta)k_{obs}(\eta,\xi)d\eta\end{aligned} \tag{3.214}$$

Remark 11. *In (3.200)–(3.203) and (3.209)–(3.212), the boundary conditions* $l_{obs}(0,\xi) = 0$ *and* $q_{obs}(0,\xi) = 0$ *eliminate the effects of coefficients* $\gamma(z)$ *and* $\tilde{l}(z)$ *on the existence of the kernels* k_{obs}*,* l_{obs}*,* p_{obs} *and* q_{obs}*. According to* Lemma 13 and Lemma 15 *of [64], the Assumption 4 directly means that kernel equations (3.200)–(3.203) and (3.209)–(3.212) have bounded and unique solutions.*

In order to decouple the PDE subsystem (3.206)–(3.207) from the ODE system (3.205) and motivated by [66], the following error coordinates are defined:

$$\varepsilon_x(z,t) = \tilde{e}_x(z,t) - \tilde{n}^T(z)e_d(t) \tag{3.215}$$

with $\tilde{n}^T(z) \in \mathbb{R}^{n_d}$. Simple calculation yields the ODE-PDE cascade

$$\dot{e}_d(t) = \left(S_d - l_d\tilde{n}^T(0)\right)e_d(t) - l_d\varepsilon_x(0,t) \tag{3.216}$$

$$\partial_t\varepsilon_x(z,t) = \partial_z\varepsilon_x(z,t), z \in [0,1] \tag{3.217}$$

$$\varepsilon_x(1,t) = 0, t > 0 \tag{3.218}$$

on the domain $(z,t) \in (0,1) \times \mathbb{R}^+$. Therefore, $\tilde{n}^T(z)$ has to satisfy the triangular decoupling BVP:

$$\frac{d\tilde{n}^T}{dz}(z) - \tilde{n}^T(z)S_d + \tilde{g}_{1o}^T(z) = 0 \tag{3.219}$$

$$\tilde{n}^T(1) = g_2 r_{d_2}^T \tag{3.220}$$

and

$$\tilde{l}(z) = \tilde{n}^T(z) l_d \tag{3.221}$$

has to hold.

Lemma 12. *(Triangular Decoupling BVP). The triangular decoupling BVP (3.219)–(3.220) always has a unique classical solution.*

Proof. The BVP (3.219)–(3.220) has the same form with (3.173)–(3.174) when replacing (3.174) by a Dirichlet boundary condition (see (3.220)). Therefore, if we denote the eigenvalues of S_d, $\lambda_{d,i}, i = 1, 2, ..., n_d$, the solvability condition $e^{\lambda_{d,i}} \neq 0, i = 1, 2, ..., n_d$, can be easily obtained from the proof of Lemma 11. Obviously, no matter what values of $\lambda_{d,i}$ are, this condition always holds. This yields the result of Lemma 12. □

The conclusion shows that in order to design the observer gains l_d and $l(z)$ for the exosystem and the plant observers (3.193)–(3.195), first the inverse observer kernel BVPs (3.200)–(3.203) and the corresponding observer kernel BVPs (3.209)–(3.212) have to be solved so that $k_{obs}(z, 0)$ in (3.204) and $\tilde{g}_1^T(z)$ in (3.206) can be computed. Then, the solution $\tilde{n}^T(z)$ of the triangular decoupling BVP (3.219)–(3.220) is attainable. With the resulting vector $\tilde{n}^T(0)$ the exosystem observer gain l_d in (3.193) can be determined such that the matrix $S_d - l_d\tilde{n}^T(0)$ is Hurwitz, see (3.216) given that $(\tilde{n}^T(0), S_d)$ is observable. Consequently, by applying (3.204) and (3.221), the plant observer gain $l(z)$ in (3.194) is

$$l(z) = f(z) + \mathcal{T}_o^{-1}[\tilde{n}^T](z) l_d + k_{obs}(z, 0) \tag{3.222}$$

realizing the plant and the exosystem observer design. The observability of $\left(\tilde{n}^T(0), S_d\right)$ can be guaranteed whenever the conditions in the following lemma are satisfied.

Lemma 13. *(Observability). The numerator of the transfer matrix $F_{dm}^T(s) = \frac{N_d^T(s)}{D_d(s)}$ of*

(3.147)–(3.148) and (3.150) from $col\,(d_1(t), d_2(t))$ *to* $y_m(t)$ *is*

$$N_d(s) = \begin{bmatrix} \int_0^1 e^{-s\zeta}\left(\mathcal{T}_o\left[g_1\right](\zeta)\right)d\zeta \\ e^{-s}g_2 + \int_0^1 e^{-s\xi}q_{obs}(\xi,1)d\xi g_2 \end{bmatrix} \tag{3.223}$$

Then, denoting $v_{d,i}$ *and* $\lambda_{d,i}$ *the eigenvectors and corresponding eigenvalues of* S_d*, respectively, the pair* $(\tilde{n}^T(0), S_d)$ *is observable if and only if*

$$N_d^T(\lambda_{d,i})\begin{bmatrix} r_{d_1}^T v_{d,i} \\ r_{d_2}^T v_{d,i} \end{bmatrix} \neq 0, i = 1,2,\cdots,n_d. \tag{3.224}$$

Proof. From Th. 6.2-5 in [61], the pair $(\tilde{n}^T(0), S_d)$ is observable if and only if $\tilde{n}_i^*(0) = \tilde{n}^T(0)v_{d,i} \neq 0, i = 1,2,...,n_d$, since the eigenvalues of S_d are distinct. By applying the similar method in the proof of Lemma 11 the result $\tilde{n}_i^*(0) = N_d^T(\lambda_{d,i})col\left(r_{d_1}^T v_{d,i}, r_{d_2}^T v_{d,i}\right)$ can be easily obtained for $i = 1,2,...,n_d$. By utilizing the transformation $\tilde{x}(z,t) = \mathcal{T}_o\left[x(t)\right](z)$, (see (3.208), the plant (3.147)–(3.148) and (3.150) becomes

$$\begin{aligned} \partial_t\tilde{x}(z,t) &= \partial_z\tilde{x}(z,t) + \left(\mathcal{T}_o[f](z) - p_{obs}(z,0)\right)\tilde{x}(0,t) \\ &\quad + \mathcal{T}_o[g_1](z)d_1(t) + q_{obs}(z,1)g_2d_2(t) \\ &\quad + q_{obs}(z,1)u(t) \\ \tilde{x}(1,t) &= u(t) + g_2d_2(t) \\ y_m(t) &= \tilde{x}(0,t) \end{aligned} \tag{3.225}$$

where $q_{obs}(z,1) = -\mathcal{T}_o[l_{obs}(\cdot,1)](z)$ according to (3.214). For this representation of the plant the transfer matrix $F_{dm}^T(s) = \frac{N_d^T(s)}{D_d(s)}$ can be derived in a closed-form, where $D_d(s)$ is an irrational denominator. This completes the proof. □

Remark 12. *Lemma 13 indicates that the estimation of the disturbance states* $v_d(t)$ *is only possible if the transmission of the disturbances* $d_1(t)$ *and* $d_2(t)$ *to the measurement* $y_m(t)$ *is not blocked by the corresponding transfer behavior. Therefore, (3.224) requires* $r_{d_1}^T v_{d,i} \neq 0$ *or* $r_{d_2}^T v_{d,i} \neq 0, i = 1,2,...,n_d$*. This implies that each eigenmode of* $\dot{v}_d(t) = S_d v_d(t)$ *is observable in* $d_1(t)$ *or* $d_2(t)$*.* ■

The triangular system (3.216)–(3.218) suggests an exponential stability of the observer error dynamics (3.205)–(3.207) if $S_d - l_d\tilde{n}^T(0)$ in (3.216) is a Huwitz matrix and the PDE subsystem (3.217)–(3.218) is finite time stable. The following theorem demonstrates this result.

Theorem 12. *Let $l(z)$ be given by (3.222). Then, the observer error dynamics (3.205)–(3.207) is for $t > 1$ exponentially stable in the norm $\|\cdot\|_{X_{ce}} = \left(\|\cdot\|^2_{\mathbb{C}^{n_d}} + \|\cdot\|_2^2\right)^{\frac{1}{2}}$, i.e. the observer error $e_{ce}(t) = col(e_d(t), e_x(t))$ with $e_x(t) = \{e_x(z,t), z \in [0,1]\}$ satisfies*

$$\|e_{ce}(t)\|_{X_{ce}} \leq M_{ce}e^{-\alpha_{ce}t}\|e_{ce}(0)\|_{X_{ce}}, t \in (0,T] \tag{3.226}$$

for all $e_{ce}(0) \in X_{ce} = \mathbb{C}^{n_d} \oplus L_2(0,1)$ and positive constants α_{ce} and M_{ce}.

Proof. Consider the Lyapunov function:

$$V(t) = e_d^T(t)Pe_d(t) + c\int_0^1 (1+z)\varepsilon_x^2(z,t)dz \tag{3.227}$$

where $c > 0$ and $P = P^T > 0$ is the solution of the Lyapunov equation

$$\left(S_d - l_d\tilde{n}^T(0)\right)^T P + P\left(S_d - l_d\tilde{n}^T(0)\right) = -Q \tag{3.228}$$

for some $Q = Q^T > 0$. Taking the time derivative of (3.227) along the trajectories of (3.216) and (3.217), we get

$$\begin{aligned}
\dot{V}(t) &= \left(\left(S_d - l_d\tilde{n}^T(0)\right)e_d(t) - l_d\varepsilon_x(0,t)\right)^T Pe_d(t) \\
&\quad + e_d^T(t)p\left(\left(S_d - l_d\tilde{n}^T(0)\right)e_d(t) - l_d\varepsilon_x(0,t)\right) \\
&\quad + 2c\textstyle\int_0^1 (1+z)\varepsilon_x(z,t)\partial_z\varepsilon_x(z,t)dz \\
&= e_d^T(t)\left(\left(S_d - l_d\tilde{n}^T(0)\right)^T P + P\left(S_d - l_d\tilde{n}^T(0)\right)\right) \\
&\quad \times e_d(t) - 2e_d^T Pl_d\varepsilon_x(0,t) \\
&\quad + 2c\textstyle\int_0^1 (1+z)\varepsilon_x(z,t)\partial_z\varepsilon_x(z,t)dz
\end{aligned} \tag{3.229}$$

Integrating the last term in (3.229)

$$\begin{aligned}
&2c\textstyle\int_0^1 (1+z)\varepsilon_x(z,t)\partial_z\varepsilon_x(z,t)dz \\
&\qquad = -c\varepsilon_x^2(0,t) - c\textstyle\int_0^1 \varepsilon_x^2(z,t)dz
\end{aligned} \tag{3.230}$$

and utilizing (3.228), we obtain

$$\begin{aligned}\dot{V}(t) &= -e_d^T(t)Qe_d(t) - 2e_d^T Pl_d\varepsilon_x(0,t) \\ &\quad -c\varepsilon_x^2(0,t) - c\int_0^1 \varepsilon_x^2(z,t)dz\end{aligned} \tag{3.231}$$

Since the parameter c can be chosen arbitrarily, we choose it to be sufficiently large to guarantee that

$$\frac{1}{2}e_d^T(t)Qe_d(t) + 2e_d^T Pl_d\varepsilon_x(0,t) + c\varepsilon_x^2(0,t) \geq 0 \tag{3.232}$$

So that

$$\dot{V}(t) \leq -\tfrac{1}{2}e_d^T(t)Qe_d(t) - c\int_0^1 \varepsilon_x^2(z,t)dz \tag{3.233}$$

It follows from (3.227) and (3.233) that there exists $\mu > 0$ such that

$$\dot{V}(t) \leq \mu V(t) \tag{3.234}$$

This implies that the system (3.205) and (3.207) is exponentially stable in the norm defined in (3.227) which is equivalent to the norm $\|\cdot\|_{X_{ce}}$. Therefore, there exist $\tilde{\alpha}_{ce} > 0$ and $\tilde{M}_{ce} > 0$ such that

$$\begin{aligned}\|\tilde{e}_{ce}(t)\|_{x_{ce}} &= (\|e_d(t)\|_{\mathbb{C}^{n_d}}^2 + \|\tilde{e}_x(\cdot,t)\|_2^2)^{\frac{1}{2}} \\ &\leq \tilde{M}_{ce}e^{-\tilde{\alpha}_{ce}t}(\|e_d(0)\|_{\mathbb{C}^{n_d}}^2 + \|\tilde{e}_x(\cdot,0)\|_2^2)^{\frac{1}{2}}\end{aligned} \tag{3.235}$$

with $\tilde{e}_{ce} = col(e_d, \tilde{e}_x)$. From [64], kernels p_{obs}, q_{obs}, k_{obs} and l_{obs} are bounded. Similar to the proof in Theorem 11, according to the *Cauchy-Schwarz inequality*, there exist positive constants: $c_3(p_{obs}, q_{obs})$ and $c_4(k_{obs}, l_{obs})$ such that $\|\tilde{e}_x(\cdot,t)\|_{L_2} \leq (1 + c_3(p_{obs}, q_{obs}))\|e_x(\cdot,t)\|_{L_2}$ and $\|e_x(\cdot,t)\|_{L_2} \leq (1 + c_4(k_{obs}, l_{obs}))\|\tilde{e}_x(\cdot,t)\|_{L_2}$. As a consequence, we have

$$\begin{aligned}&\|e_{ce}(t)\|_{X_{ce}} \leq (\|e_d(t)\|_{\mathbb{C}^{n_d}}^2 + \|e_x(\cdot,t)\|_2^2)^{\frac{1}{2}} \\ &\leq \left(\|e_d(t)\|_{\mathbb{C}^{n_d}}^2 + (1 + c_4(k_{obs}, l_{obs}))^2\|\tilde{e}_x(\cdot,t)\|_2^2\right)^{\frac{1}{2}} \\ &\leq \tilde{M}_{ce}e^{-\tilde{\alpha}_{ce}t}(1 + c_4(k_{obs}, l_{obs})) \\ &\quad \times (\|e_d(0)\|_{\mathbb{C}^{n_d}}^2 + \|\tilde{e}_x(\cdot,0)\|_2^2)^{\frac{1}{2}} \\ &\leq \tilde{M}_{ce}e^{-\tilde{\alpha}_{ce}t}(1 + c_4(k_{obs}, l_{obs})) \\ &\quad \times (1 + c_3(p_{obs}, q_{obs}))\|e_{ce}(0)\|_{X_{ce}}\end{aligned} \tag{3.236}$$

This leads to (3.226) with $M_{ce} = \tilde{M}_{ce}(1 + c_4(k_{obs}, l_{obs}))$
$\times (1 + c_3(p_{obs}, q_{obs}))e^{-\tilde{\alpha}_{ce}t}$. □

The regulator achieving the output regulation consists of observers (3.192)–(3.195) for the plant and the exosystem combined with the feedback:

$$u(t) = \int_0^1 p(1,z)\hat{x}(z,t)dz + \left(\pi^T(1) - g_2 p_{d_2}^T\right)\hat{v}(t) \tag{3.237}$$

when utilizing the state estimates $\hat{x}(z,t)$ and $\hat{v}(t) = col(\hat{v}_d, \hat{v}_r)$ in (3.168). The following theorem shows that for the resulting observer-based regulator, the separation principle holds implying the output regulation.

Theorem 13. *Consider the output feedback regulator (3.192)–(3.195) with (3.222), and (3.237). Then, the output regulation (3.158) is achieved in the norm*

$$\|\cdot\|_{X_{cl}} = \left(\|\cdot\|_{\mathbb{C}^{n_r}}^2 + \|\cdot\|_{\mathbb{C}^{n_d}}^2 + \|\cdot\|_2^2 + \|\cdot\|_2^2\right)^{\frac{1}{2}}$$

i.e. let $\hat{e} = \hat{x} - \pi_c^T \hat{v}$ *and* $\pi_c^T(z) = \mathcal{T}_c^{-1}[\pi^T](z)$*, then the state* $e_{cl} = col\left(e_r, e_d, e_x, \hat{e}\right)$ *satisfies the following inequality:*

$$\|e_{cl}(t)\|_{X_{cl}} \leq M_{cl} e^{-\alpha_{cl} t} \|e_{cl}(0)\|_{X_{cl}}, t \geq 0 \tag{3.238}$$

for all $e_{cl}(0) \in X_{cl} = \mathbb{C}^{n_r} \oplus \mathbb{C}^{n_d} \oplus L_2(0,1) \oplus L_2(0,1)$ *and positive constants* M_{cl} *and* α_{cl}*.*

Proof. By defining the new coordinate $\hat{\tilde{x}}(z,t) = \mathcal{T}_c[\hat{x}(t)](z)$, the observer (3.193)–(3.195) can be transformed into the following form through the integral transformation $\mathcal{T}_c$ defined in (3.159):

$$\partial_t \hat{\tilde{x}}(z,t) = \partial_z \hat{\tilde{x}}(z,t) + \tilde{g}_1^T(z)\hat{v}(t) + \tilde{l}_c(z) e_x(0,t) \tag{3.239}$$

$$\hat{\tilde{x}}(1,t) = \pi^T(1)\hat{v}(t) \tag{3.240}$$

where $\tilde{g}_1^T(z)$ is defined in (3.164) and $\tilde{l}_c(z) = \mathcal{T}_c[l](z)$. In view of (3.199), one has $e_x(0,t) = \tilde{e}_x(0,t)$. Then, by applying the change of variables $\hat{\varepsilon}_x(z,t) = \hat{\tilde{x}}(z,t) - \pi^T(z)\hat{v}(t)$, i.e., $\hat{\varepsilon}(z,t) = \mathcal{T}_c[\hat{e}(t)](z)$ and expressing $\pi^T(z) = \begin{bmatrix} \pi_1^T(z) & \pi_2^T(z) \end{bmatrix}$ (see (3.173)–(3.174)), one can get:

$$\begin{aligned} \partial_t \hat{\varepsilon}_x(z,t) = {} & \partial_z \hat{\varepsilon}_x(z,t) + a_1^T(z) e_d(t) \\ & + a_2(z)\varepsilon_x(0,t) - \pi_2^T(z) l_r q_r^T e_r(t) \end{aligned}$$

with boundary condition $\hat{\varepsilon}_x(1,t) = 0$, where the parameters $a_1^T(z)$ and $a_2(z)$ are given by $a_1^T(z) = \left(\tilde{l}_c(z) - \pi_1^T(z)l_d\right)\tilde{n}^T(0)$ and $a_2(z) = \tilde{l}_c(z) - \pi_1^T(z)l_d$. In the derivation, $\varepsilon_x(z,t) = \tilde{e}_x(z,t) - \tilde{n}^T(z)e_d(t)$ and $e_x(0,t) = \tilde{e}_x(0,t)$ were utilized. This system, with $\dot{e}_r(t) = \left(S_r - l_r q_r^T\right)e_r(t)$ (see (3.192)) and (3.216)–(3.218), describes the closed-loop system as a cascade of two exponentially stable subsystems. Then, defining the state of the closed-loop system as $\tilde{e}_{cl}(t) = col(e_r(t), e_d(t), \varepsilon_x(t), \hat{\varepsilon}_x(t))$ in the Hilbert space $X_{cl} = \mathbb{C}^{n_r} \oplus \mathbb{C}^{n_d} \oplus L_2(0,1) \oplus L_2(0,1)$ with the standard inner product. Consider Lyapunov function

$$\begin{aligned} V(t) = {} & e_r^T(t)P_r e_r(t) + e_d^T(t)P_d e_d(t) \\ & + c_1 \int_0^1 (1+z)\varepsilon_x^2(z,t)dz \\ & + c_2 \int_0^1 (1+z)\hat{\varepsilon}_x^2(z,t)dz \end{aligned} \tag{3.241}$$

where $c_1 > 0$, $c_2 > 0$, $P_r = P_r^T > 0$ and $P_d = P_d^T > 0$ are solutions of Lyapunov equations:

$$P_r\left(S_r - l_r q_r^T\right) + \left(S_r - l_r q_r^T\right)^T P_r = -Q_r \tag{3.242}$$

$$P_d\left(S_d - l_d\tilde{n}^T(0)\right) + \left(S_d - l_d\tilde{n}^T(0)\right)^T P_d = -Q_d \tag{3.243}$$

for some $Q_r = Q_r^T > 0$ and $Q_d = Q_d^T > 0$, which can be chosen arbitrarily. Following the proof in Theorem 11 and differentiating (3.241) with respect to time, we get

$$
\begin{aligned}
&\dot{V}(t) = e_r^T(t)\left(\left(S_r - l_r q_r^T\right)^T P_r + P_r\left(S_r - l_r q_r^T\right)\right)e_r(t) \\
&+e_d^T(t)\left(\left(S_d - l_d\tilde{n}^T(0)\right)^T P_d + P_d\left(S_d - l_d\tilde{n}^T(0)\right)\right)e_d(t) \\
&-2e_d^T P_d l_d \varepsilon_x(0,t) - c_1\varepsilon_x^2(0,t) - c_1\int_0^1 \varepsilon_x^2(z,t)dz \\
&-c_2\hat{\varepsilon}_x^2(0,t) - c_2\int_0^1 \hat{\varepsilon}_x^2(z,t)dz \\
&+2c_2\int_0^1 (1+z)\hat{\varepsilon}_x(z,t)a^T(z)dz e_d(t) \\
&+2c_2\int_0^1 (1+z)\hat{\varepsilon}_x(z,t)a_2(z)dz\varepsilon_x(0,t) \\
&-2c_2\int_0^1 (1+z)\hat{\varepsilon}_x(z,t)\pi_2^T(z)dz l_r q_r^T e_r(t) \\
&\leq -\tfrac{1}{2}e_r^T(t)Q_r e_r(t) - \tfrac{1}{2}e_d^T(t)Q_q e_d(t) - c_1\int_0^1 \varepsilon_x^2(z,t)dz \\
&-\tfrac{1}{4}c_2\int_0^1 \hat{\varepsilon}_x^2(z,t)dz - c_2\hat{\varepsilon}_x^2(0,t) \\
&-2c_2\int_0^1 (1+z)\hat{\varepsilon}_x(z,t)\pi_2^T(z)dz l_r q_r^T e_r(t) \\
&-\tfrac{1}{4}c_2\int_0^1 \hat{\varepsilon}_x^2(z,t)dz - \tfrac{1}{2}e_r^T(t)Q_r e_r(t) \\
&-\tfrac{1}{4}e_d^T(t)Q_q e_d(t) - 2e_d^T P_d l_d\varepsilon_x(0,t) - \tfrac{1}{2}c_1\varepsilon_x^2(0,t) \\
&-\tfrac{1}{4}e_d^T(t)Q_q e_d(t) - \tfrac{1}{4}c_2\int_0^1 \hat{\varepsilon}_x^2(z,t)dz \\
&+2c_2\int_0^1 (1+z)\hat{\varepsilon}_x(z,t)a^T(z)dz e_d(t) \\
&-\tfrac{1}{2}c_1\varepsilon_x^2(0,t) + 2c_2\int_0^1 (1+z)\hat{\varepsilon}_x(z,t)a_2(z)dz\varepsilon_x(0,t) \\
&-\tfrac{1}{4}c_2\int_0^1 \hat{\varepsilon}_x^2(z,t)dz
\end{aligned} \tag{3.244}
$$

Since c_1 and c_2 can be chosen arbitrarily, we choose c_1 sufficiently large and c_2 sufficiently small to ensure that

$$
\begin{aligned}
\tfrac{1}{2}e_r^T(t)Q_r e_r(t) + 2c_2\int_0^1 (1+z)\hat{\varepsilon}_x(z,t)\pi_2^T(z)dz l_r q_r^T e_r(t)& \\
+\tfrac{1}{4}c_2\int_0^1 \hat{\varepsilon}_x^2(z,t)dz \geq 0&
\end{aligned}
$$

$$
\frac{1}{4}e_d^T(t)Q_q e_d(t) + 2e_d^T P_d l_d\varepsilon_x(0,t) + \frac{1}{2}c_1\varepsilon_x^2(0,t) \geq 0
$$

$$
\begin{aligned}
&\tfrac{1}{4}e_d^T(t)Q_q e_d(t) + \tfrac{1}{4}c_2\int_0^1 \hat{\varepsilon}_x^2(z,t)dz \\
&-2c_2\int_0^1 (1+z)\hat{\varepsilon}_x(z,t)a^T(z)dz e_d(t) \geq 0
\end{aligned}
$$

$$
\begin{aligned}
\tfrac{1}{2}c_1\varepsilon_x^2(0,t) - 2c_2\int_0^1 (1+z)\hat{\varepsilon}_x(z,t)a_2(z)dz\varepsilon_x(0,t)& \\
+\tfrac{1}{4}c_2\int_0^1 \hat{\varepsilon}_x^2(z,t)dz \geq 0&
\end{aligned}
$$

so that

$$\begin{aligned}\dot{V}(t) \leq & -\tfrac{1}{2}e_r^T(t)Q_r e_r(t) - \tfrac{1}{2}e_d^T(t)Q_q e_d(t) \\ & -c_1\int_0^1 \varepsilon_x^2(z,t)dz - \tfrac{1}{4}c_2\int_0^1 \hat{\varepsilon}_x^2(z,t)dz\end{aligned} \tag{3.245}$$

Following from (3.241) and (3.247), there exists $\nu > 0$ such that

$$\dot{V}(t) \leq -\nu V(t) \tag{3.246}$$

This indicates that the systems for $\hat{e}_{cl} = col(e_r, e_d, \tilde{e}_x, \hat{\varepsilon}_x)$ are for $t > 1$ exponentially stable in the norm defined in (3.241), which is equivalent to $\|\cdot\|_{X_{cl}}$, i.e., there exist positive constants $\hat{M}_{cl} > 0$ and $\alpha_{cl} > 0$ such that

$$\begin{aligned}\|\hat{e}_{cl}(t)\|_{X_{cl}} \leq & \hat{M}_{cl}e^{-\alpha_{cl}t}\,(\|e_r(0)\|^2_{\mathbb{C}^{n_r}} + \|e_d(0)\|^2_{\mathbb{C}^{n_d}} \\ & + \|\tilde{e}_x(\cdot,0)\|_2^2 + \|\hat{\varepsilon}_x(\cdot,0)\|_2^2)^{\frac{1}{2}}\end{aligned} \tag{3.247}$$

Due to the boundedness of operators $\mathcal{T}_c$ and $\mathcal{T}_c^{-1}$, there exist positive constants $c_5(p,q)$ and $c_6(k,l)$ such that $\|\hat{\varepsilon}_x(\cdot,t)\|_2 \leq (1 + c_5(p,q))\,\|\hat{e}(\cdot,t)\|_2$ and $\|\hat{e}(\cdot,t)\|_2 \leq (1 + c_6(k,l))\,\|\hat{\varepsilon}_x(\cdot,t)\|_2$. Moreover, from the proof part in Theorem 12, we have $\|e_x(\cdot,t)\|_2 \leq (1 + c_4(k_{obs}, l_{obs}))\,\|\tilde{e}_x(\cdot,t)\|_2$ and

$\|\tilde{e}_x(\cdot,t)\|_2 \leq (1 + c_3(p_{obs}, q_{obs}))\,\|e_x(\cdot,t)\|_2$. This yields the result in (3.238) with $M_{cl} = \hat{M}_{cl}(1 + c_m)(1 + c_n)$, $c_m = \max(c_4, c_6)$ and $c_n = \max(c_3, c_5)$, and completes the proof. □

3.4.4 Examples

3.4.4.1 Example 1. Application to KdV-like equation

We take the example of the Korteweg-de Vries-like equations used in [54]. The system is determined by three coefficients a, γ and ε and the transformation yields the following PIDE ($b = \sqrt{\frac{a}{\varepsilon}}$):

$$\begin{aligned}\partial_t x(z,t) = & \varepsilon\partial_z x(z,t) - \gamma b\sinh(bz)x(0,t) \\ & +\gamma b^2\int_0^z \cosh(b(z-\xi))x(\xi,t)d\xi\end{aligned}$$

Considering $\varepsilon = 1$ and assuming that we want to control PIDE (3.248) by applying the full state feedback regulator (3.168). In this example, the parameters are set as $a = 1$, $\gamma = 4$. The output $y(t)$ to be controlled is in-domain and pointwise with $c(z) = \delta(z - 0.5)$

in (3.151). We assume that there are no disturbances and the reference signal $y_r(t)$ is designed as $y_r(t) = \begin{cases} 1+4t, \ 0 \le t \le 4 \\ -10, \ t > 4 \end{cases}$ and then the corresponding S_r and q_r^T have forms of $S_r = \begin{cases} \begin{bmatrix} 0 & 0 \\ 1 & 0 \end{bmatrix}, \ 0 \le t \le 4 \\ 0, \ t > 4 \end{cases}$ and $q_r^T = \begin{cases} \begin{bmatrix} 1 & 4 \end{bmatrix}, \ 0 \le t \le 4 \\ -10, \ t > 4 \end{cases}$. It is easy to find

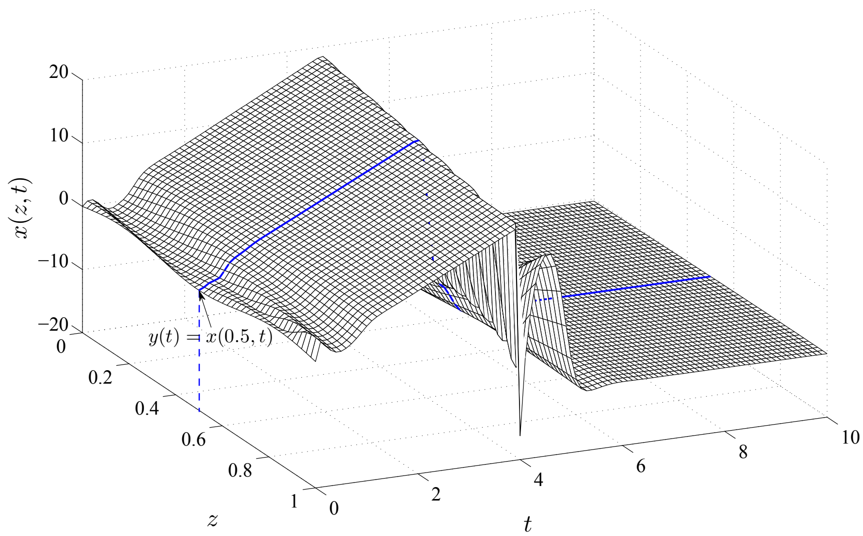

Figure 3.13: The evolution of the state $x(z,t)$ under the state feedback control law (3.168).

that in the designed exosystem (3.152)-(3.155), the matrix $S = S_r = S_n$ is a nilpotent matrix. Given $k(z,\xi)$ and $l(z,\xi)$ and by using the formula for $G(s)$, it is easy to compute $G(0) = -0.2387 \neq 0$, the condition in Lemma 11 holds and the state feedback regulator exists. Applying the technique proposed in Lemma 11 easily yields the feedforward gain $\pi_v^T = \begin{cases} \begin{bmatrix} 3.6 & 4.55 \end{bmatrix}, \ 0 \le t \le 4 \\ -11.348, \ t > 4 \end{cases}$. The results are shown in Figure 3.13 and 3.14. It should be noted that since the stabilized system is finite-time stable, the control output $y(t)$ tracks the reference signal $y_r(t)$ within finite-time $t \in (0,T), T \ge 1$.

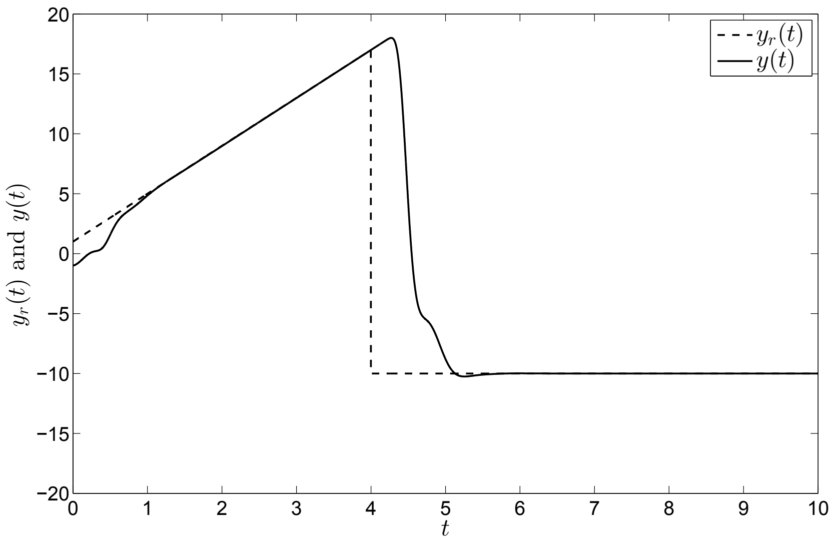

Figure 3.14: The reference trajectory $y_r(t)$and the controlled output $y(t) = x(0.5, t)$ under the state feedback control law (3.168). The output regulations are achieved with $t \in (0, T_1]$ and $t \in (4, T_2]$ with $T_1 \geq 1$ and $T_2 \geq 5$.

3.4.5 Example 2. Application to a PDE-ODE Interconnected system

We consider the system given in [64] with $f(z) = a + \frac{bd\sinh(\sqrt{c}(1-z))}{\sqrt{c}\cosh(\sqrt{c})}$, $g(z,\xi) = -\frac{bd\cosh(\sqrt{c}z)\cosh(\sqrt{c}(1-\xi))}{\cosh(\sqrt{c})} + bd\cosh(\sqrt{c}(z-\xi))$ and $h(z,\xi) = -\frac{bd\cosh(\sqrt{c}z)\cosh(\sqrt{c}(1-\xi))}{\cosh(\sqrt{c})}$ with $a = 1.25$, $b = c = 0.1$ and $d = 10$, and the system can be obtained from a first-order PDE coupled with a second order ODE, see [64].

The output to be controlled is in domain and pointwise with $N = 1$ and $z_1 = 0.5$ in (3.151). We assume that disturbance distributions are give by $g_1(z) = 0.5e^{-z}$ and $g_2 = 1$. The disturbances are constant: $d_1(t) = 1$ and $d_2(t) = 2$, which leads to a first-order disturbance model with $S_d = 0$, $r_{d1} = 1$ and $r_{d2} = 2$. According to (3.223) and (3.224)and given q_{obs} and p_{obs}, it is not hard to compute $N_d^T(0)\begin{bmatrix} v_{d,1} \\ 2v_{d,1} \end{bmatrix} = 4.6398 \neq 0$ with $v_{d,1} = 1$. Therefore, the observability is guaranteed and the output feedback regulator exists. The reference signal $y_r(t)$ is sinusoidal with $y_r(t) = 2sin(2t)$. Therefore, the corresponding model can be given by (3.152) and (3.155) with $S_r = \begin{bmatrix} 0 & 2 \\ -2 & 0 \end{bmatrix}$ and $q_r^T = \begin{bmatrix} 2 & 0 \end{bmatrix}$.

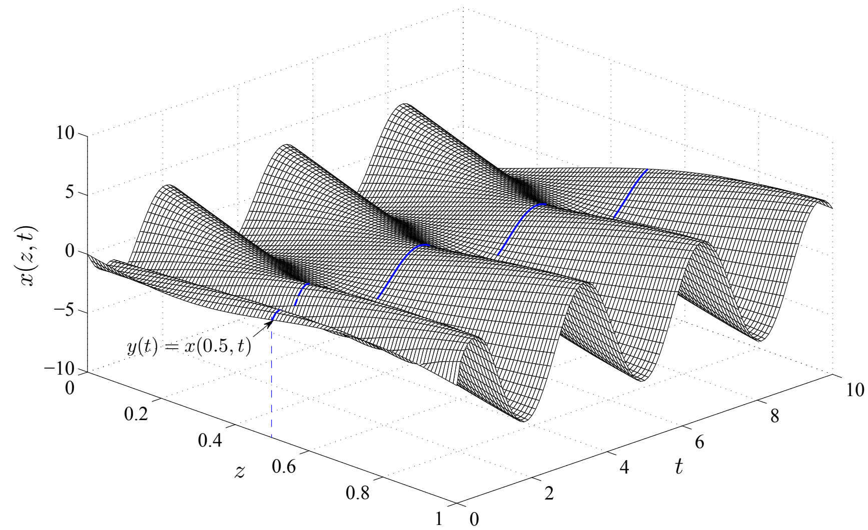

Figure 3.15: The evolution of the state $x(z,t)$ under the control of the output feedback regulator (3.192)–(3.195) and (3.237).

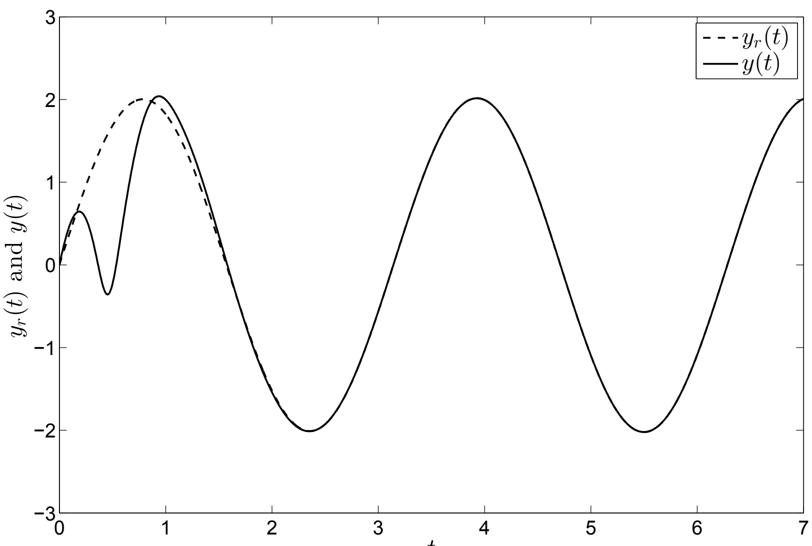

Figure 3.16: The reference trajectory $y_r(t)$and the controlled output $y(t) = x(0.5,t)$ under the control of the proposed output feedback regulator. The output regulation is achieved for $t > 1$.

Therefore, for the estimation of $v_r(t) \in \mathbb{C}^2$, an observer (3.192) can be designed with the spectrum $\sigma(S_r - l_r q_r^T) = \{-18, -10\}$. The regulator equations (3.173)–(3.174) and the triangular decoupling BVP (3.219)–(3.220) can be directly solved in a closed-form. The corresponding control and observer kernel equations are solved through a successive approximation with 30 fixpoint iterations. Moreover, the gain l_d is chosen such that $-l_d\tilde{n}^T(0) = -10$. Figure 3.15 and 3.16 show the performance of the proposed output feedback regulator

(3.192)–(3.195) and (3.237). Since the observer error systems and tracking error systems are exponentially stable for $t > 1$, the output regulation is achieved exponentially for $t > 1$.

3.5 Conclusions

In this chapter, the output regulation problem for the distributed and boundary control first order hyperbolic PDE systems are addressed. In particular, for different types of the hyperbolic systems, different regulator equations (Sylvester equations) are derived. Correspondingly, their solvabilities have been investigated and sufficient conditions are provided. In details, for the designed output and error feedback regulators, the corresponding detectabilities are studied and the sufficient conditions are given. Finally, computer simulations are presented to show the performances of the proposed regulators.

Chapter 4

Output and error feedback regulator designs for linear infinite-dimensional systems

4.1 Introduction

In Chapter 3, the geometric approaches were extended, and finite-dimensional regulators were designed to solve the output regulation problem for the first-order hyperbolic systems with bounded control and output operators. Due to some restrictions on the design of regulators and on the characteristics of considered plant, the proposed regulators may not be constructed successfully. In this chapter, novel output feedback and error feedback regulators are designed to relax those restrictions in Chapter 3 and proposed regulators are easier to design.

In practice, the boundary/pointwise control and observation are frequently encountered, and the relevant control schemes involve mathematic difficulties due to unbounded operators [62]. In [67], *p-copy internal model principle* and $\mathcal{G}-$conditions were introduced to the regular linear systems where both control and observation operators are unbounded. In this thesis, in order to address the output regulation problem for the linear systems with unbounded observation operators and to avoid the mathematic difficulties caused by the unboundedness of operators, Yosida-type approximate boundary observation is used in the design of the output regulators [68].

Recently, in [69], three dynamic error feedback controllers were introduced for regular linear systems. In particular, one observer-based robust controller (Section VI) was designed based on $\mathcal{G}-$condition motivated by [58] where the controller has Internal Model Structure (IMS) and the controller operator $\mathcal{G}_1$ has a triangular form. Moreover, an *auxiliary operator* (not function-type) *Sylvester equation* needs to be solved. In this chapter, a new form of the observer-based error feedback regulator is proposed and the solution of the auxiliary Sylvester equation is the function of the spatial variable, which simplifies and reduces complexity associated with the calculation of the auxiliary Sylvester equation.

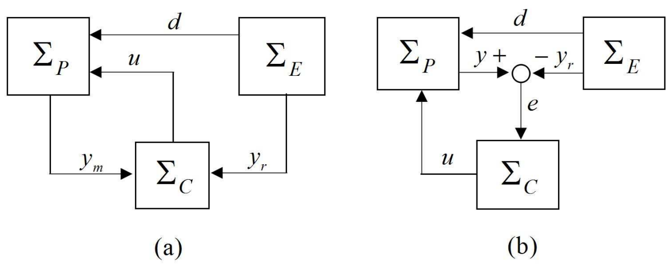

Figure 4.1: Block diagram of systems interconnection (plant Σ_P, exosystem Σ_E and regulators Σ_C) with disturbance d, measurement y_m, reference y_r, output y, input u and tracking error e. (a). configuration of the output feedback regulator; (b). configuration of the error feedback regulator.

In this chapter, two types of regulators are proposed and designed, see Figure 4.1. The main contribution is given as the observers design, i.e. the weighted regulator state $\begin{bmatrix} (\tilde{H}r_m(t))^T & \hat{v}_r^T(t) \end{bmatrix}^T$ (or $\tilde{H}_e r_e(t)$) is used to obtain exponentially accurate estimates for the plant and exosystem states. To achieve the observer convergence, the observer error system is decoupled into the PDE-subsystem and the ODE-subsystem so that the ODE-subsystem and the PDE-subsystem can be stabilized separately by fixing free regulator parameters. This decomposition idea was applied in backstepping designs of the output regulator, see [53] and in internal model regulator designs, see [58], [69]. However, compared with [53]), the proposed regulators in this chapter can address output regulation problems for coupled

PDE systems with distributed or boundary control (with the aid of the approach in [31]) inputs. Compared with, see [58] or [69], a novel output feedback regulator is provided in this chapter and the auxiliary Sylvester equations introduced here are easier to solve (by introducing weights $\tilde{H}$ and $\tilde{H}_e$).

In more detail, the constructed output feedback regulator is driven by the measurement $y_m(t)$ and the reference $y_r(t)$. Therefore, the observability conditions are studied. Here, the measurement $y_m(t)$ does not belong to the set of the controlled output $y(t)$, while in the design of the error feedback regulator, the proposed approach yields an alternative and easy choice for finding the output injection gain for the traditional error feedback regulator design, see [57] and Chapter 3. In contrast, the regulator parameters in this chapter can be easily designed and configured. For infinite-dimensional systems, the proposed two regulator designs are both applicable and valid for Riesz-spectral systems, see [52] and non-spectral systems, see [37]. In particular, the free design parameters of the regulators are configured by applying the separation principle.

Assume that X and Y are Hilbert spaces and $\mathcal{A} : X \mapsto Y$ is a linear operator, then $D(\mathcal{A})$ denotes the domain of $\mathcal{A}$. $\mathcal{L}(X, Y)$ denotes the space of all linear, bounded operators from X to Y (If $X = \mathbb{C}^{n_X}$ and $Y = \mathbb{C}^{n_Y}$, then $\mathcal{L}(X, Y) = \mathbb{C}^{n_X \times n_Y}$). If $X = Y$, then we write $\mathcal{L}(X)$. If $\mathcal{A} : X \to X$, then $\sigma(\mathcal{A})$ is the spectrum of $\mathcal{A}$ (the set of eigenvalues, if $\mathcal{A} \in \mathbb{C}^{n_X \times n_X}$), $\rho(\mathcal{A}) = \mathbb{C} \backslash \sigma(\mathcal{A})$ is the resolvent set and $R(\lambda; \mathcal{A}) = (\lambda I - \mathcal{A})^{-1} \in \mathcal{L}(X)$ denotes the resolvent operator for $\lambda \in \rho(\mathcal{A})$. The inner product is denoted by $\langle \cdot, \cdot \rangle$. $L^2(0,1)^m$ with a non-negative integer m is a Hilbert space of an $m-$dimensional vector of the real functions that are a square integrable over $[0,1]$. $H^k(0,1)$ with a non-negative integer k, denotes a Hilbert space defined as the Sobolev space of order k, i.e. $H^k(0,1)^m = \left\{h(\cdot) \in L^2(0,1)^m : \left(\frac{d^p h}{dz^p}\right) \in L^2(0,1)^m, p = 1, 2, \ldots, k\right\}$. In particular, $H^0(0,1) = L^2(0,1)$. If the plant is a finite-dimensional system, the assumption: $\mathcal{A}$ generates a C_0-semigroup $T_{\mathcal{A}}(t)$ is always satisfied, and the semigroup is the matrix exponential function, i.e., $T_{\mathcal{A}}(t) = e^{\mathcal{A}t}, t \geq 0$ [14]. $e^{\mathcal{A}t}$ is exponentially stable if and only if $\sigma(\mathcal{A}) \subset \mathbb{C}^-$, i.e., the matrix $\mathcal{A}$ is Hurwitz.

4.2 Problem formulation

The plant – We are concerned with the following infinite-dimensional linear system Σ_P:

$$\dot{x}(t) = \mathcal{A}x(t) + \mathcal{B}u(t) + \mathcal{G}d(t), t > 0, x(0) = x_0 \in X \tag{4.1}$$

$$y(t) = \mathcal{C}x(t), t \geq 0 \tag{4.2}$$

$$y_m(t) = \mathcal{C}_m x(t), t \geq 0 \tag{4.3}$$

where

$x \in X$ is the state of the system,

X is a complex Hilbert state space,

$u \in U$ is an input,

$y \in Y$ is the controlled output, and

$y_m \in Y_m$ is the measured output.

U, Y and Y_m are complex Hilbert control and output spaces, respectively. $\mathcal{A} : D(\mathcal{A}) \subset X \to X$ is the infinitesimal generator of a C_0-semigroup $T_{\mathcal{A}}(t)$ on X, $\mathcal{B} \in \mathcal{L}(U, X)$. The output operators $\mathcal{C}, \mathcal{C}_m \in \mathcal{L}(X_1, Y)$ are $\mathcal{A}-$admissible (see [70]), where the space $X_1 = D(\mathcal{A})$ is equipped with the norm $\|x\|_1 = \|(\beta I - \mathcal{A})x\|$ and $\beta \in \rho(\mathcal{A})$. $d(t) \in U_d$ is disturbance and U_d is a complex Hilbert space. $\mathcal{G} \in \mathcal{L}(U_d, X)$ denotes disturbance location operator. According to Proposition 4.9 of [71], the system (4.1)–(4.3) is well-posed and the Yosida-type approximation of operators $\mathcal{C}$ and $\mathcal{C}_m$ in X are defined by $\mathcal{C}_\alpha x = \alpha \mathcal{C} \left(\alpha I - \mathcal{A}\right)^{-1} x$ and $\mathcal{C}_{m\alpha} x = \alpha \mathcal{C}_m \left(\alpha I - \mathcal{A}\right)^{-1} x$, $x \in X$, where $R\left(\alpha; \mathcal{A}\right)$ is the resolvent operator for $\alpha \in \rho(\mathcal{A})$. It is natural that the transfer functions are expressed as follows:

$$G(s) = \mathcal{C}_\alpha R(s; \mathcal{A})\mathcal{B}, s \in \rho(\mathcal{A}) \tag{4.4}$$

$$G_d(s) = \mathcal{C}_\alpha R(s; \mathcal{A})\mathcal{G}, s \in \rho(\mathcal{A}) \tag{4.5}$$

$$G_m(s) = \mathcal{C}_{m\alpha} R(s; \mathcal{A})\mathcal{G}, s \in \rho(\mathcal{A}) \tag{4.6}$$

where $G(s)$, $G_d(s)$ and $G_m(s)$ are transfer functions from $u(t)$ to $y(t)$, from $d(t)$ to $y(t)$ and from $d(t)$ to $y_m(t)$, respectively.

This class of systems can be utilized to model behavior of both non-spectral and spectral systems, and in particular transport processes (described by the first order hyperbolic PDEs), heat and diffusion processes (described by parabolic PDEs) and vibrations (described by the second order hyperbolic PDEs and higher order PDEs describing beam models). Moreover, the class also contains all finite-dimensional systems by choosing the state space $X = \mathbb{C}^{n_X}$, and letting $\mathcal{A}$, $\mathcal{B}$ and $\mathcal{C}$ be matrices of appropriate sizes. The transfer functions are defined by (4.4)–(4.6) provided that $s \in \mathbb{C}$ is not an eigenvalue of $\mathcal{A}$. Actually, the following results in this chapter are also applicable to finite-dimensional systems.

The exosystem – The reference trajectory $y_r(t) \in Y$ to be tracked by $y(t)$ and the process disturbance $d(t)$ in (4.1) are generated by the known n-dimensional exosystem Σ_E:

$$\dot{v}(t) = Sv(t),\ t > 0,\ v(0) = v_0 \in \mathbb{C}^n \tag{4.7}$$

$$d(t) = Fv(t),\ t \geq 0 \tag{4.8}$$

$$y_r(t) = Qv(t) \in Y,\ t \geq 0 \tag{4.9}$$

with F and Q matrices of appropriate dimensions which are assumed to be known for the regulator design.

Assumption 5. *$S : D(S) \subset \mathbb{C}^n \to \mathbb{C}^n$ is a diagonalizable matrix having all its eigenvalues on the imaginary axis, i.e. $\sigma(S) = \{\lambda_k\}_{k=1,\ldots,n}$. Note that the spectrum of S can include zero eigenvalues. This accounts for the modeling of steplike and sinusoidal exogenous signals.*

Remark 13. *In this chapter, two regulators are designed. For different regulators, different and specific configurations of S will be made in the following sections, respectively.*

The output regulation problem – The main control problem in this chapter is defined as follows: Design regulators such that the following conditions are satisfied:

(i). The closed-loop system operator generates an exponentially stable C_0−semigroup;

(ii). Let $e(t) = y(t) - y_r(t)$ denote the tracking error, then for some $\alpha < 0$,

$$e(t) \in L^2_\alpha[0, \infty) \tag{4.10}$$

Here, $L^2_\alpha[0, \infty)$ is defined by [72]:

$$L^2_\alpha[0, \infty) = \left\{ f \in L^2_{loc}[0, \infty) \middle| \int_0^\infty e^{-2\alpha t} |f(t)|^2 dt < \infty \right\}$$

Throughout this chapter, we make the following general assumptions:

Assumption 6. *The pair $(\mathcal{A}, \mathcal{B})$ is exponentially stabilizable.*

Assumption 7. *The pairs $(\mathcal{C}_\alpha, \mathcal{A})$ and $(\mathcal{C}_{m\alpha}, \mathcal{A})$ are exponentially detectable.*

Assumption 8. *The spectrum of S is contained in the resolvent set of $\mathcal{A}$, i.e., $\sigma(S) \subset \rho(\mathcal{A})$.*

Remark 14. *Due to the characteristic of the matrix S in the Assumption 5, for some unstable systems, Assumption 8 may not hold, i.e., $\sigma(S) \not\subset \rho(\mathcal{A})$. In this case, one can first stabilize the system to shift the spectrum of $\mathcal{A}$ away from the spectrum of S such that the condition in Assumption 8 is guaranteed.*

The following lemma presented in Chapter 3 proposed the full state feedback control law solving the output regulation problems.

Lemma 14. *Let Assumptions 6 and 8 hold. The linear state feedback regulator can be designed if and only if there exist mappings $\Pi \in \mathcal{L}(\mathbb{C}^n, X)$ with $\Pi\mathbb{C}^n \in D(\mathcal{A})$ and $\Gamma \in \mathcal{L}(\mathbb{C}^n, U)$ satisfying the regulator equations:*

$$\Pi S = \mathcal{A}\Pi + \mathcal{B}\Gamma + \mathcal{G}F \tag{4.11}$$

$$\mathcal{C}_\alpha \Pi = Q \tag{4.12}$$

The full state feedback regulator is given by:

$$u(t) = Kx(t) + Lv(t) \tag{4.13}$$

where $K \in \mathcal{L}(X, U)$ is any exponentially stabilizing feedback gain for the pair $(\mathcal{A}, \mathcal{B})$ and the operator $L \in \mathcal{L}(\mathbb{C}^n, U)$ is given by $L = \Gamma - K\Pi$.

According to Lemma 14, in the following sections, two regulators are designed to estimate states of the plant and the exosystem such that the control law (4.13) can be applied to address the output regulation problem.

4.3 The output feedback regulator

In this section, provided that the measurement $y_m(t)$ and the reference signal $y_r(t)$ are available, an output feedback regulator will be designed to estimate the states of plant (4.1)–(4.3) and the exosystem (4.7)–(4.9). Consequently, the control law in (4.13) can be applied to achieve the output regulation **(i)–(ii)**. Similar works can be found in [52] and [53]. The contribution in [52] is the development of an finite-dimensional output feedback regulator addressing the control of Riesz-spectral systems. While [53] designed the regulator in the backstepping coordinates. In this chapter, the output feedback regulator is designed to address the control problems for general infinite-dimensional systems including spectral and non-spectral systems.

Similar to the above two elaborate works, the configuration of the exosystem in this section is also given as follows:

$$\dot{v}_d(t) = S_d v_d(t),\ v_d(0) = v_{d0} \in \mathbb{C}^{n_d} \tag{4.14}$$

$$\dot{v}_r(t) = S_r v_r(t),\ v_r(0) = v_{r0} \in \mathbb{C}^{n_r} \tag{4.15}$$

$$d(t) = Fv(t) = f_d v_d(t),\ t \geq 0 \tag{4.16}$$

$$y_r(t) = Qv(t) = q_r v_r(t),\ t \geq 0 \tag{4.17}$$

where the matrix S in (4.7) is a block diagonal diagonalizable matrix: $S = \mathrm{bdiag}(S_d, S_r)$ and the exosystem state is constructed by $v = \mathrm{col}(v_d, v_r)$ with $n = n_d + n_r$. (4.14) and (4.16) is the disturbance model and (4.15) and (4.17) is the reference model. Obviously, eigenvalues of S_d and S_r are given by $\sigma(S_d) = \{\lambda_k\}_{k=1,\cdots,n_d}$ and $\sigma(S_r) = \{\lambda_k\}_{k=n_d+1,\cdots,n}$ and one has $F = \begin{bmatrix} f_d & 0 \end{bmatrix}$ and $Q = \begin{bmatrix} 0 & q_r \end{bmatrix}$.

In this section, for the above configuration of exosystem, the following assumption is made:

Assumption 9. *It is assumed that (q_r, S_r) is observable and that the eigenvalues of S_d are distinct.*

It is easy to calculate:

$$S_d v_d(t) = \sum_{k=1}^{n_d} \lambda_k \langle v_d(t), \phi_{dk} \rangle \phi_{dk} \tag{4.18}$$

$$v_d(t) = e^{S_d t} v_d(0) = \sum_{k=1}^{n_d} e^{\lambda_k t} \langle v_d(0), \phi_{dk} \rangle \phi_{dk} \tag{4.19}$$

where $\{\phi_{dk}\}$ with $k = 1, \cdots, n_d$ are eigenvectors of S_d corresponding to eigenvalues of S_d.

In this section, given the measurement $y_m(t)$ and the reference signal $y_r(t)$, an output feedback regulator will be designed to estimate the states of the plant (4.1)–(4.3) and the exosystem (4.7)–(4.9), and then the control law (4.13) can be applied to achieve the output regulation **(i)–(ii)**.

The abstract form of the regulator is given as follows:

$$\dot{r}_M(t) = \mathcal{R}_M r_M(t) + L_M \begin{bmatrix} y_m(t) \\ y_r(t) \end{bmatrix} \tag{4.20}$$

$$u(t) = K_M r_M(t), t > 0 \tag{4.21}$$

on a space X_{rM}, where $\mathcal{R}_M : D(\mathcal{R}_M) \subset X_{rM} \to X_{rM}$ generates a C_0-semigroup $T_{\mathcal{R}_M}$ on X_{rM}, $L_M \in \mathcal{L}(Y_m \times Y, X_{rM})$ and $K_M \in \mathcal{L}(X_{rM}, U)$.

The plant and the output feedback regulator can be written as a closed-loop system on the composite state space $\mathcal{X}_{cm} = X \times X_{rM}$:

$$\dot{x}_{cm}(t) = \mathcal{A}_{cm} x_{cm}(t) + \mathcal{B}_{cm} v(t), x_{cm}(0) \in \mathcal{X}_{cm} \tag{4.22}$$

with $x_{cm}(t) = \begin{bmatrix} x(t) \\ r_M(t) \end{bmatrix}$, $\mathcal{A}_{cm} = \begin{bmatrix} \mathcal{A} & \mathcal{B}K_M \\ L_{CM} & \mathcal{R}_M \end{bmatrix}$, $\mathcal{B}_{cm} = \begin{bmatrix} \mathcal{G}F \\ L_{QM} \end{bmatrix}$, $L_{CM} = L_M \begin{bmatrix} \mathcal{C}_{m\alpha} \\ 0 \end{bmatrix}$ and $L_{QM} = L_M \begin{bmatrix} 0 \\ Q \end{bmatrix}$. The operator $\mathcal{A}_{cm}$ generates a C_0-semigroup $T_{\mathcal{A}_{cm}}(t)$ on $\mathcal{X}_{cm}$.

We turn to the output feedback regulator design, by writing (4.20)–(4.21) in the following form:

$$\begin{bmatrix} \dot{r}_m(t) \\ \dot{\hat{v}}_r(t) \end{bmatrix} = \begin{bmatrix} \mathcal{R}_m & \mathcal{O}_r \\ 0 & \mathcal{R}_r \end{bmatrix} \begin{bmatrix} r_m(t) \\ \hat{v}_r(t) \end{bmatrix} + \begin{bmatrix} L_m y_m(t) \\ L_r y_r(t) \end{bmatrix} \tag{4.23}$$

$$u(t) = \begin{bmatrix} K_m & K_r \end{bmatrix} \begin{bmatrix} r_m(t) \\ \hat{v}_r(t) \end{bmatrix} \tag{4.24}$$

with $r_M(t) = \begin{bmatrix} r_m^T(t) & \hat{v}_r^T(t) \end{bmatrix}^T \in X_{rM}$. In the equation (4.23), the upper equation is used to estimate plant state $x(t)$ and the disturbance model state $v_d(t)$ given the measurement $y_m(t)$. While the lower equation is employed to estimate the reference model state $v_r(t)$. Therefore, we have $\mathcal{R}_m : D(\mathcal{R}_m) \subset X_{rm} \to X_{rm}$ with $X_{rm} = X \times \mathbb{C}^{n_d}$, $\mathcal{O}_r : \mathbb{C}^{n_r} \to X_{rm}$, $\mathcal{R}_r : \mathbb{C}^{n_r} \to \mathbb{C}^{n_r}$, $L_m \in \mathcal{L}(Y_m, X_{rm})$, $L_r \in \mathcal{L}(Y, \mathbb{C}^{n_r})$, $K_m \in \mathcal{L}(X_{rm}, U)$ and $K_r \in \mathcal{L}(\mathbb{C}^{n_r}, U)$. Correspondingly, the state r_m can be defined by $r_m(t) = \begin{bmatrix} \hat{x}_1^T(t) & \hat{v}_d^T(t) \end{bmatrix}^T \in X_{rm}$.

Let $x_d(t) = \begin{bmatrix} x^T(t) & v_d^T(t) \end{bmatrix}^T \in X \times \mathbb{C}^{n_d}$ and define an operator $\tilde{H} = \begin{bmatrix} I & H \\ 0 & I \end{bmatrix} \in L\left(X_{rm}, X \times \mathbb{C}^{n_d}\right)$ with $H \in \mathcal{L}(\mathbb{C}^{n_d}, X)$ to be determined and identity operator I with appropriate dimensions, the following lemma provides a choice of the regulator design such that the state $\begin{bmatrix} x_d^T(t) & v_r^T(t) \end{bmatrix}^T$ can be estimated by the weighted state $\begin{bmatrix} (\tilde{H}r_m(t))^T & \hat{v}_r^T(t) \end{bmatrix}^T$. In particular, the observation error

$$e_M(t) = \begin{bmatrix} x_d^T(t) & v_r^T(t) \end{bmatrix}^T - \begin{bmatrix} (\tilde{H}r_m(t))^T & \hat{v}_r^T(t) \end{bmatrix}^T$$

decays to zero exponentially.

Lemma 15. *(**Observer Design**) Define operators:* $\mathcal{A}_d = \begin{bmatrix} \mathcal{A} & P_d \\ 0 & S_d \end{bmatrix} : D(\mathcal{A}_d) \subset X \times \mathbb{C}^{n_d} \to X \times \mathbb{C}^{n_d}$ *with* $P_d = \mathcal{G} f_d$, $\tilde{\mathcal{C}}_m = \begin{bmatrix} \mathcal{C}_{m\alpha} & 0 \end{bmatrix} \in \mathcal{L}(X \times \mathbb{C}^{n_d}, Y_m)$ *and* $\tilde{\mathcal{B}} = \begin{bmatrix} \mathcal{B} \\ 0 \end{bmatrix} \in \mathcal{L}(U, X \times \mathbb{C}^{n_d})$*, then the dynamics of the observation error* $e_M(t)$ *is given by:*

$$\dot{e}_M(t) = \mathcal{A}_M e_M(t), t > 0 \tag{4.25}$$

with the initial condition $e_M(0) \in X \times \mathbb{C}^{n_d} \times \mathbb{C}^{n_r}$*, where*

$$\mathcal{A}_M = \begin{bmatrix} \mathcal{A}_d - \tilde{H} L_m \tilde{\mathcal{C}}_m & 0 \\ 0 & S_r - L_r q_r \end{bmatrix}$$

if operators in (4.23): $\mathcal{R}_m$, $\mathcal{O}_r$ *and* $\mathcal{R}_r$ *are chosen as:* $\mathcal{R}_m = \tilde{H}^{-1}\mathcal{A}_d\tilde{H} - L_m\tilde{\mathcal{C}}_m\tilde{H} + \tilde{H}^{-1}\tilde{\mathcal{B}}K_m$, $\mathcal{O}_r = \tilde{H}^{-1}\tilde{\mathcal{B}}K_r$ *and* $\mathcal{R}_r = S_r - L_r q_r$*. Furthermore, let* $\mathcal{R}_m = \begin{bmatrix} R_{m1} & R_{m2} \\ R_{m3} & R_{m4} \end{bmatrix}$, $L_m = \begin{bmatrix} L_{m1} \\ L_{m2} \end{bmatrix}$ *and* $K_m = \begin{bmatrix} K_{m1} & K_{m2} \end{bmatrix}$*. Assume that the operator* H *satisfies the following auxiliary Sylvester equation*

$$HS_d - (\mathcal{A} - L_{m1}\mathcal{C}_{m\Lambda})\, H = P_d \text{ on } D(S_d) \tag{4.26}$$

with $P_d = \mathcal{G} f_d$ *and that observer injection gains* L_{m1}, L_{m2} *and* L_r *are chosen such that the operator* $\mathcal{A} - L_{m1}\mathcal{C}_{m\alpha}$ *generates an exponentially stable semigroup on the space* X*, and* $S_d - L_{m2}\mathcal{C}_{m\alpha}H$ *and* $S_r - L_r q_r$ *are Hurwitz, then the observation error* $e_M(t)$ *decays to zero exponentially.*

Proof. The controller in (4.23) is rewritten as:

$$\begin{bmatrix} \dot{r}_m(t) \\ \dot{\hat{v}}_r(t) \end{bmatrix} = \begin{bmatrix} \mathcal{R}_m & \mathcal{O}_r \\ 0 & \mathcal{R}_r \end{bmatrix} \begin{bmatrix} r_m(t) \\ \hat{v}_r(t) \end{bmatrix} + \begin{bmatrix} L_m\tilde{\mathcal{C}}_m & 0 \\ 0 & L_r q_r \end{bmatrix} \begin{bmatrix} x_d(t) \\ v_r(t) \end{bmatrix}$$

with $\tilde{\mathcal{C}}_m = \begin{bmatrix} \mathcal{C}_{m\alpha} & 0 \end{bmatrix}$. With the substitution of the control law in (4.24), the dynamic system for $\begin{bmatrix} x_d^T(t) & v_r^T(t) \end{bmatrix}^T$ is given by:

$$\begin{bmatrix} \dot{x}_d(t) \\ \dot{v}_r(t) \end{bmatrix} = \begin{bmatrix} \mathcal{A}_d & 0 \\ 0 & S_r \end{bmatrix} \begin{bmatrix} x_d(t) \\ v_r(t) \end{bmatrix} + \begin{bmatrix} \tilde{\mathcal{B}} K_m & \tilde{\mathcal{B}} K_r \\ 0 & 0 \end{bmatrix} \begin{bmatrix} r_m(t) \\ \hat{v}_r(t) \end{bmatrix}$$

with $\mathcal{A}_d = \begin{bmatrix} \mathcal{A} & \mathcal{G} f_d \\ 0 & S_d \end{bmatrix}$ and $\tilde{\mathcal{B}} = \begin{bmatrix} \mathcal{B} \\ 0 \end{bmatrix}$. Then, a direct calculation shows that the dynamics of $e_M(t)$ are given by the homogeneous differential equation:

$$\dot{e}_M(t) = \begin{bmatrix} \mathcal{A}_d - \tilde{H} L_m \tilde{\mathcal{C}}_m & 0 \\ 0 & S_r - L_r q_r \end{bmatrix} e_M(t), t > 0$$

with the initial condition $e_M(0) \in X \times \mathbb{C}^{n_d} \times \mathbb{C}^{n_r}$ if the regulator satisfies: $\mathcal{O}_r = \tilde{H}^{-1} \tilde{\mathcal{B}} K_r$, $\mathcal{R}_r = S_r - L_r q_r$ and $\mathcal{R}_m = \tilde{H}^{-1} \mathcal{A}_d \tilde{H} - L_m \tilde{\mathcal{C}}_m \tilde{H} + \tilde{H}^{-1} \tilde{\mathcal{B}} K_m$.

Let A_{dm} denote the following operator:

$$\begin{aligned} \mathcal{A}_{dm} &= \tilde{H}^{-1} \left(\mathcal{A}_d - \tilde{H} L_m \tilde{\mathcal{C}}_m \right) \tilde{H} \\ &= \begin{bmatrix} \mathcal{A} - L_{m1} \mathcal{C}_{m\alpha} & (\mathcal{A} - L_{m1} \mathcal{C}_{m\alpha}) H - H S_d + P_d \\ -L_{m2} \mathcal{C}_{m\alpha} & S_d - L_{m2} \mathcal{C}_{m\alpha} H \end{bmatrix} \end{aligned}$$

Due to the equation (4.26), the exponential stabilities of $\mathcal{A} - L_{m1} \mathcal{C}_{m\alpha}$ and $S_d - L_{m2} \mathcal{C}_{m\alpha} H$ directly indicate that the semigroup $T_{\tilde{A} L_m}(t)$generated by $\left(\mathcal{A}_d - \tilde{H} L_m \tilde{\mathcal{C}}_m \right)$ is exponentially stable and has the growth property $\left\| T_{\tilde{A} L_m}(t) \right\| \leq M_{\tilde{A} L_m} e^{-\kappa_m t}, t \geq 0$ for positive constants $\tilde{M}_{\mathcal{A} \mathcal{L}_m}$ and κ_m. Moreover, the exponential stabilities of $\left(\mathcal{A}_d - \tilde{H} L_m \tilde{\mathcal{C}}_m \right)$ and $S_r - L_r q_r$ imply that the semigroup $T_{\mathcal{A}_M}(t)$ generated by $\mathcal{A}_M$ in (4.25) is exponentially stable and has the growth property $\| T_{\mathcal{A}_M}(t) \| \leq M_{\mathcal{A}_M} e^{-\alpha_M t}, t \geq 0$, for positive constants $M_{\mathcal{A}_M}$ and $\alpha_M = \min \left(\kappa_M, -\tilde{\lambda}_o \right)$ with $\tilde{\lambda}_o = \max_{k=1,\cdots n_r} R_e \tilde{\lambda}_{rk} < 0$, where $\left\{ \tilde{\lambda}_{rk} \right\}_{k=1,\cdots,n_r}$ are eigenvalues of $S_r - L_r q_r$. Therefore, the observation error $e_M(t)$ decays to zero exponentially. □

From Lemma 15, the exact configuration of operators in (4.23): $\mathcal{R}_m$, $\mathcal{O}_r$ and $\mathcal{R}_r$ is given by:

$$\mathcal{R}_m = \begin{bmatrix} \mathcal{A} - L_{m1}\mathcal{C}_{m\alpha} + \mathcal{B}K_{m1} & \mathcal{B}K_{m2} \\ -L_{m2}\mathcal{C}_{m\alpha} & S_d - L_{m2}\mathcal{C}_{m\alpha}H \end{bmatrix} \tag{4.27}$$

$$\mathcal{O}_r = \begin{bmatrix} \mathcal{B}K_r \\ 0 \end{bmatrix}, \quad \mathcal{R}_r = S_r - L_r q_r \tag{4.28}$$

Compared with existing works in literature such as [52], the observer design in Lemma 15 is novel and the injection gains design is easier.

Moreover, in Lemma 15, all output injection gains: L_{m1}, L_{m2} and L_r are designed to ensure the exponential convergence of the observe in the regulator (4.23)–(4.24). In particular, due to Assumption 7 and 9, it is possible to find L_{m1} and L_r. However, the existence of the operator H and the detectability of the pair $(\mathcal{C}_{m\alpha}H, S_d)$ are essential to the existence of L_{m2}. In the following theorem, the conditions for solvability of (4.26) and detectability of $(\mathcal{C}_{m\alpha}H, S_d)$ are provided. Moreover, feedback and feedforward gains are chosen to address the output regulation problem.

Theorem 14. *The conditions for solvability of (4.26) and observability of $(\mathcal{C}_{m\alpha}, S_d)$ are given in following:*

***a)**. (**Solvability**) $H \in \mathcal{L}(\mathbb{C}^{n_d}, X)$ defined by:*

$$H = \sum_{k=1}^{n_d} \langle \cdot, \phi_{dk} \rangle R\left(\lambda_k; \mathcal{A} - L_{m1}\mathcal{C}_{m\alpha}\right) P_d \phi_{dk} \tag{4.29}$$

is the unique and bounded solution of the auxiliary Sylvester equation (4.26), if and only if the following solvability conditions are satisfied:

$$I + \mathcal{C}_{m\alpha}(\lambda I - \mathcal{A})^{-1} L_{m1} \neq 0, \; \forall \lambda \in \sigma(S_d) \tag{4.30}$$

***b)**. (**Observability**) Finally, the pair $(\mathcal{C}_{m\alpha}H, S_d)$ is observable, if and only if the transfer function $G_m(s)$ in (4.6) from $d(t)$ to $y_m(t)$ satisfies:*

$$G_m(\lambda_k) f_d \phi_{dk} \neq 0, \; k = 1, 2, ..., n_d \tag{4.31}$$

in which ϕ_{dk} are the eigenvectors of S_d with respect to the eigenvalues λ_k of S_d. Consequently, there exists L_{m2} such that $S_d - L_{m2}\mathcal{C}_{m\alpha}H$ is Hurwitz.

In particular, with the configuration of output injection gains L_{m1}, L_{m2} and L_r given in Lemma 15, the regulator (4.23)–(4.24) solves the output regulation problem, given that K_{m1}, K_{m2} and K_r are chosen as: $K_{m1} = K$, $K_{m2} = KH + \Gamma_d - K\Pi_d$ and $K_r = \Gamma_r - K\Pi_r$ where $K \in \mathcal{L}(X, U)$ satisfies that the operator $\mathcal{A} + \mathcal{B}K$ generates an exponentially stable C_0-semigroup, where the operators $\Pi = \begin{bmatrix} \Pi_d & \Pi_r \end{bmatrix} \in \mathcal{L}(\mathbb{C}^{n_d} \times \mathbb{C}^{n_r}, X)$ and $\Gamma = \begin{bmatrix} \Gamma_d & \Gamma_r \end{bmatrix} \in \mathcal{L}(\mathbb{C}^{n_d} \times \mathbb{C}^{n_r}, U)$ are defined in Lemma 14.

Proof. We begin by verifying the properties given in parts **a)–c)** of the theorem.

a). For the expression (4.29), we can easily apply the approach in Chapter 3 or in Re. 3.3 of [59] to obtain it. According to Assumption 5, there exists a similarity transformation $V_d^{-1}S_dV_d = diag\,(\lambda_1, \lambda_2, \cdots, \lambda_{n_d})$ with $V_d = [\phi_{d1}, \phi_{d2}, \cdots, \phi_{n_d}]$. Postmultiplying (4.26) by V_d yields a decoupled set of equations:

$$h_k^* + (\lambda_k I - \mathcal{A})^{-1} L_{m1}\mathcal{C}_{m\alpha}h_k^* = p_k^*$$

with $h_k^* = H\phi_{dk}$, $p_{dk}^* = P_d\phi_{dk}$ for $k = 1, 2, ..., n_d$. Then, the solution h_k^* is uniquely determined by $\mathcal{C}_{m\alpha}h_k^*$ and applying $\mathcal{C}_{m\alpha}$ indicates that $\mathcal{C}_{m\alpha}h_k^*$ can be uniquely solved by $(I + \mathcal{C}_{m\alpha}R\,(\lambda_k; \mathcal{A})L_{m1})\,\mathcal{C}_{m\alpha}h_k^* = \mathcal{C}_{m\alpha}p_{dk}^*$ if and only if the conditions in (4.30) hold. Consequently, we have $H = \left[h_1^*, h_2^*, \cdots, h_{n_d}^*\right] V_d^{-1}$.

b). In Th. 6.2-5 of [61], the observability of the pair $(\mathcal{C}_{m\alpha}H, S)$ can be verified by showing $\mathcal{C}_{m\alpha}H\phi_{dk} \neq 0$ for $k = 1, 2, \cdots, n$. Utilizing the solution (4.29) leads to:

$$\begin{aligned}\mathcal{C}_{m\alpha}H\phi_{dk} &= \mathcal{C}_{m\alpha}R\,(\lambda_k; \mathcal{A} - L_{m1}\mathcal{C}_{m\alpha})\,P\phi_{dk} \\ &= \mathcal{C}_{m\alpha}R\,(\lambda_k; \mathcal{A} - L_{m1}\mathcal{C}_{m\alpha})\,\mathcal{G}f_d\phi_{dk} = G_L(\lambda_k)f_d\phi_{dk}\end{aligned}$$

where $G_L(\lambda) = \mathcal{C}_{m\alpha}R\,(\lambda; \mathcal{A} - L_{m1}\mathcal{C}_{m\alpha})\,\mathcal{G}$ with $\lambda \in \overline{\mathbb{C}^+}$. By applying the Woodbury formula and the following formula:

$$R(\lambda; \mathcal{A} - L_{m1}\mathcal{C}_{m\alpha}) = R(\lambda; \mathcal{A})(I + L_{m1}\mathcal{C}_{m\alpha}R(\lambda; \mathcal{A}))^{-1}$$

for every $\lambda \in \rho(\mathcal{A}) \cap \rho(\mathcal{A} - L_{m1}\mathcal{C}_{m\alpha})$, we have $G_L(\lambda) = \left(I + \mathcal{C}_{m\alpha} R\left(\lambda; \mathcal{A}\right) L_{m1}\right)^{-1} G_m(\lambda)$. As a result, the solvability conditions in (4.30) guarantee the existence of $\left(I + \mathcal{C}_{m\alpha} R\left(\lambda; \mathcal{A}\right) L_{m1}\right)^{-1}$ and thus the condition in (4.31) ensures $\mathcal{C}_{m\alpha} H \phi_{dk} \neq 0$. Due to Assumption 9 that eigenvalues of S_d are distinct, it is possible to guarantee that conditions in (4.31) hold for all eigenvectors of S_d. Once the detectability conditions are satisfied, it is possible to find L_{m2} such that $S_d - L_{m2}\mathcal{C}_{m\alpha} H$ is Hurwitz. If we assume $\tilde{\lambda}_{dk}, k = 1, 2, \cdots, n_d$ to be eigenvalues of $S_d - L_{m2}\mathcal{C}_{m\alpha} H$, then $Re\tilde{\lambda}_{dk} < 0$.

Once conditions in ***a)–b)*** hold, the design of L_{m1}, L_{m2} and L_r in Lemma 15 realizes $\lim\limits_{t\to+\infty} e_M(t) = 0$, i.e., $\lim\limits_{t\to+\infty} \left(x_d(t) - \tilde{H} r_m(t)\right) = 0$ and $\lim\limits_{t\to+\infty} \left(v_r(t) - \hat{v}_r(t)\right) = 0$. Now, we turn to the solving of the following initial value problem (IVP) with $\tilde{r}_m(t) = \begin{bmatrix} \tilde{x}_1(t) \\ \tilde{v}_d(t) \end{bmatrix} \in X \times \mathbb{C}^{n_d}$ and $\tilde{v}_r(t) \in \mathbb{C}^{n_r}$:

$$\begin{aligned} &\dot{\tilde{r}}_m(t) = \mathcal{R}_m \tilde{r}_m(t) + \mathcal{O}_r \tilde{v}_r(t) + L_m \tilde{\mathcal{C}}_m \tilde{H} \tilde{r}_m(t) \\ &\tilde{r}_m(0) = r_m(0), \ \ \tilde{v}_r(0) = \tilde{v}_r(0) \end{aligned} \tag{4.32}$$

Then, a direct calculation yields the solution to $\tilde{x}_1(t)$ (here $\Pi = \begin{bmatrix} \Pi_d & \Pi_r \end{bmatrix}$ and $\Gamma = \begin{bmatrix} \Gamma_d & \Gamma_r \end{bmatrix}$ are applied):

$$\begin{aligned} &\tilde{x}_1(t) = T_K(t)\tilde{x}_1(0) + \textstyle\int_0^t T_K(t-\tau)\left(\Pi - H\right)\dot{\tilde{v}}(\tau) d\tau \\ &+ \textstyle\int_0^t T_K(t-\tau)\left(-\left(\mathcal{A} + \mathcal{B}K\right)\left(\Pi - H\right)\tilde{v}(\tau)\right) d\tau \\ &= T_K(t)\tilde{x}_1(0) + \textstyle\int_0^t \frac{d}{d\tau}\left(T_K(t-\tau)\left(\Pi - H\right)\tilde{v}(\tau)\right) d\tau \\ &= T_K(t)\left(\tilde{x}_1(0) - \left(\Pi - H\right)\tilde{v}(0)\right) + \left(\Pi - H\right)\tilde{v}(t) \end{aligned}$$

where $T_K(t), t \geq 0$ is an exponentially stable strongly continuous semigroup generated by the operator $\mathcal{A} + \mathcal{B}K$ and $\tilde{v}(t) = \left[\tilde{v}_d^T(t), \tilde{v}_r^T(t)\right]^T \in \mathbb{C}^n$. In view of (4.23) and (4.32), $\lim\limits_{t\to+\infty} \left(x_d(t) - \tilde{H} r_m(t)\right) = 0$ indicates that $\lim\limits_{t\to\infty} \left(\hat{x}_1(t) - \tilde{x}_1(t)\right) = 0$ and $\lim\limits_{t\to\infty} \left(\hat{v}(t) - \tilde{v}(t)\right) = 0$. As a consequence, the output regulation is achieved since the following limitation holds:

$$
\begin{aligned}
&(y(t) - y_r(t)) \\
&= (\mathcal{C}_\alpha \tilde{x}_1(t) + \mathcal{C}_\alpha H \tilde{v}(t) - Q\tilde{v}(t)) \\
&= (\mathcal{C}_\alpha T_K(t)\left(\tilde{x}_1(0) - (\Pi - H)\,\tilde{v}(0)\right)) \\
&+ (\mathcal{C}_\alpha\left(\Pi - H\right)\tilde{v}(t) + \mathcal{C}_\alpha H \tilde{v}(t) - Q\tilde{v}(t)) \\
&\qquad (\text{ due to } \mathcal{C}_\alpha \Pi - Q = 0) \\
&= (\mathcal{C}_\alpha T_K(t)\left(\tilde{x}_1(0) - (\Pi - H)\,\tilde{v}(0)\right))
\end{aligned}
$$

Based on the above equation, the tracking error decays exponentially in the sense that $e(t) \in L_\alpha(0, \infty)$ with $\alpha < 0$, given the admissibility of the observation output $\mathcal{C}_\alpha$. The remainning part of the proof is to show the exponential stability of the closed-loop system. By rewriting the operator $\mathcal{A}_{cm}$ in (4.22), one has:

$$
\mathcal{A}_{cm} = \begin{bmatrix} \mathcal{A} & \mathcal{B}K_m & \mathcal{B}K_r \\ L_m \mathcal{C}_{m\alpha} & \mathcal{R}_m & \mathcal{O}_r \\ 0 & 0 & \mathcal{R}_r \end{bmatrix}
$$

with $\mathcal{R}_r = S_r - L_r q_r$, which is Hurwitz. Let $\mathcal{A}_\mathcal{R}$ denote the matrix:

$$
\mathcal{A}_\mathcal{R} = \begin{bmatrix} \mathcal{A} & \mathcal{B}K_m \\ L_m \mathcal{C}_{m\alpha} & \mathcal{R}_m \end{bmatrix}
$$

Then, the exponential stabilities of $\mathcal{A}_\mathcal{R}$ and $\mathcal{R}_r$ directly indicate the exponential stability of $\mathcal{A}_{cm}$.

By plugging $\mathcal{R}_m$, K_m and L_m into $\mathcal{A}_\mathcal{R}$ given in Lemma 15, we have:

$$
\mathcal{A}_\mathcal{R} = \begin{bmatrix} \mathcal{A} & \mathcal{B}K_{m1} & \mathcal{B}K_{m2} \\ L_{m1}\mathcal{C}_{m\alpha} & \mathcal{A} - L_{m1}\mathcal{C}_{m\alpha} + \mathcal{B}K_{m1} & \mathcal{B}K_{m2} \\ L_{m2}\mathcal{C}_{m\alpha} & -L_{m2}\mathcal{C}_{m\alpha} & S_d - L_{m2}\mathcal{C}_{m\alpha} H \end{bmatrix}
$$

If we choose a similarity transformation $T \in \mathcal{L}(X_{\mathcal{A}_\mathcal{R}})$ with the space $X_{\mathcal{A}_\mathcal{R}} = X \times X \times \mathbb{C}^{n_d}$ defined by:

$$T = \begin{bmatrix} I & 0 & 0 \\ 0 & 0 & I \\ -I & I & 0 \end{bmatrix} \text{ and } T^{-1} = \begin{bmatrix} I & 0 & 0 \\ I & 0 & I \\ 0 & I & 0 \end{bmatrix}$$

we can define $\tilde{\mathcal{A}}_{\mathcal{R}}$ on $\mathcal{X}_{\mathcal{R}}$ and compute:

$$\begin{aligned} \tilde{\mathcal{A}}_{\mathcal{R}} &= T\mathcal{A}_{\mathcal{R}}T^{-1} \\ &= \begin{bmatrix} \mathcal{A} + \mathcal{B}K_{m1} & \mathcal{B}K_{m2} & \mathcal{B}K_{m1} \\ 0 & S_d - L_{m2}\mathcal{C}_{m\alpha}H & -L_{m2}\mathcal{C}_{m\alpha} \\ 0 & 0 & \mathcal{A} - L_{m1}\mathcal{C}_{m\alpha} \end{bmatrix} \end{aligned}$$

Given the configuration in this theorem, $T_K(t)$ has the growth property $\|T_K(t)\| \leq M_K e^{-\beta t}, t \geq 0$ with positive constants M_K and β. The operators $\mathcal{B}K_{m1}$, $\mathcal{B}K_{m2}$, $L_{m1}\mathcal{C}_{m\alpha}$ and $L_{m2}\mathcal{C}_{m\alpha}$ are bounded linear operators, and the matrix $\mathcal{R}_r$ is bounded. Thus, the operator $\mathcal{A}_{cm}$ is an infinitesimal generator of the C_0-semigroup $T_{\mathcal{A}_{cm}}(t)$ on $\mathcal{X}_{cm}$. Furthermore, there exists a positive constant $M_{\mathcal{A}_{cm}}$ such that $\|T_{\mathcal{A}_{cm}}\| \leq M_{\mathcal{A}_{cm}} e^{-\alpha_{cm} t}, t \geq 0$ with $\alpha_{cm} = \min(\beta, \alpha_M) > 0$, where α_M is defined in the proof part of Lemma 15. This means that the closed-loop systems (4.22) is exponentially stable for $v(t) \equiv 0$. □

4.4 The error feedback regulator

Different from Section 3, in this section, it is supposed that only the tracking error $e(t)$ is available as input to the regulator and similar cases can be found in [57], [73], [74] and [69]. Throughout this section, the configuration of exosystem in (4.14)–(4.17) and Assumption 9 are not applied. Instead, the configuration in (4.7)–(4.9) is applied and the following assumption on the matrix S for the design of the error feedback regulator is made.

Assumption 10. *The matrix S is diagonalizable. The the following pair is exponentially detectable:*

$$\left(\begin{bmatrix} \mathcal{A} & P \\ 0 & S \end{bmatrix}, \begin{bmatrix} \mathcal{C}_\alpha & -Q \end{bmatrix} \right)$$

Due to Assumption 5 and Assumption 10, the following expressions can be obtained:

$$Sv(t) = \sum_{k=1}^{n} \lambda_k \langle v(t), \phi_k \rangle \phi_k \tag{4.33}$$

$$v(t) = e^{St}v(0) = \sum_{k=1}^{n} e^{\lambda_k t} \langle v(0), \phi_k \rangle \phi_k \tag{4.34}$$

where $\{\phi_k\}$ with $k = 1, \cdots, n$ are eigenvectors corresponding to eigenvalues of S.

It should be noted that Assumption 10 is the standard assumption in [57]. In Chapter-3, constrained operator Riccati equations (OREs) were utilized to construct the injection gains for the pair in Assumption 10 and especially for the first order hyperbolic systems. However, due to the constraint, solutions of OREs may not be able to be calculated and the injection gains will not be obtained. In this chapter, motivated by the proposed approach in Section 3, a novel method is provided to realize the design of the injection gains. The detectability of the pair in Assumption 10 is equivalent to the detectabilities of pairs $(\mathcal{C}_\alpha, \mathcal{A})$ and $(\mathcal{C}_\alpha H_e - Q, S)$ and the solvability for H_e. In particular, this chapter works on the design of error feedback regulator for general infinite-dimensional systems, e.g. parabolic and hyperbolic PDE systems.

Given the tracking error $e(t)$, the error feedback regulator has the following form:

$$\dot{r}_e(t) = \mathcal{R}_e r_e(t) + L_e e(t), r_e(0) \in X_{re} \tag{4.35}$$

$$u(t) = K_e r_e(t), t > 0 \tag{4.36}$$

on a Hilbert space X_{re}. Here, the regulator operator $\mathcal{R}_e : D(\mathcal{R}_e) \subset X_{re} \to X_{re}$ is a generator of C_0-semigroup, $L_e \in \mathcal{L}(Y, X_{re})$ and $K_e \in \mathcal{L}(X_{re}, U)$.

The plant and the error feedback regulator form a closed-loop system on the composite state space $\mathcal{X}_{ce} = X \times X_{re}$:

$$\dot{x}_{ce}(t) = \mathcal{A}_{ce} x_{ce}(t) + \mathcal{B}_{ce} v(t), x_{ce}(0) \in \mathcal{X}_{ce} \tag{4.37}$$

$$e(t) = \mathcal{C}_{ce} x_{ce}(t) + \mathcal{D}_{ce} v(t) \tag{4.38}$$

with $\mathcal{C}_{ce} = \begin{bmatrix} \mathcal{C}_\alpha & 0 \end{bmatrix}$, $\mathcal{D}_{ce} = -Q$, $\mathcal{B}_{ce} = \begin{bmatrix} \mathcal{G}F \\ -L_e Q \end{bmatrix}$ and $\mathcal{A}_{ce} = \begin{bmatrix} \mathcal{A} & \mathcal{B}K_e \\ L_e\mathcal{C}_\alpha & \mathcal{R}_e \end{bmatrix}$, $D(\mathcal{A}_{ce}) = D(\mathcal{A}) \oplus D(\mathcal{R}_e)$.

It is straightforward to show that the operator $\mathcal{A}_{ce}$ is the infinitesimal generator of a C_0-semigroup $T_{\mathcal{A}_{ce}}$ on $\mathcal{X}_{ce}$.

Let $X_{re} = X \times \mathbb{C}^n$, $r_e(t) = \begin{bmatrix} \hat{x}_2^T(t) & \hat{v}^T(t) \end{bmatrix}^T \in X_{re}$ and define an operator $\tilde{H}_e \in \mathcal{L}(X_{re}, X_e)$, following the similar approach in Section 4.3, the following lemma and theorem will provide a parametric choice of the regulator design and conditions such that the extended state $x_e(t) = \begin{bmatrix} x^T(t) & v^T(t) \end{bmatrix}^T$ can be observed by the weighted regulator state $\tilde{H}_e r_e(t)$ with $\tilde{H}_e = \begin{bmatrix} I & H_e \\ 0 & I \end{bmatrix}$, where I are identity operators with appropriate dimensions, and the operator $H_e \in \mathcal{L}(\mathbb{C}^n, X)$ is an unknown operator to be determined. Moreover, the output regulation (4.10) and the exponential stability of the closed-loop system are achieved, simultaneously.

Lemma 16. *(**Observer Design**) Define* $\mathcal{A}_e = \begin{bmatrix} \mathcal{A} & P \\ 0 & S \end{bmatrix} : D(\mathcal{A}_e) \subset X \times \mathbb{C}^n \to X \times \mathbb{C}^n$ *with* $P = \mathcal{G}F$, $\tilde{\mathcal{C}}_e = \begin{bmatrix} \mathcal{C}_\alpha & -Q \end{bmatrix} \in \mathcal{L}(X \times \mathbb{C}, Y)$ *and* $\tilde{\mathcal{B}} = \begin{bmatrix} \mathcal{B} \\ 0 \end{bmatrix} \in \mathcal{L}(U, X \times \mathbb{C})$, *then the dynamics of observation error* $e_e(t) = x_e(t) - \tilde{H}_e r_e(t)$ *is given by:*

$$\dot{e}_e(t) = \tilde{\mathcal{A}}_E e_e(t), t > 0 \tag{4.39}$$

with initial condition $e_e(0) \in X \times \mathbb{C}^n$ *and* $\tilde{\mathcal{A}}_E = \mathcal{A}_e - \tilde{H}_e L_e \tilde{\mathcal{C}}_e$, *if the operator* $\mathcal{R}_e$ *is given by:* $\mathcal{R}_e = \tilde{H}_e^{-1}\mathcal{A}_e\tilde{H}_e - L_e\tilde{\mathcal{C}}_e\tilde{H}_e + \tilde{H}_e^{-1}\tilde{\mathcal{B}}K_e$. *In particular, define* $L_e = \begin{bmatrix} L_{e1} \\ L_{e2} \end{bmatrix} \in \mathcal{L}(Y, X \times \mathbb{C}^n)$, $K_e = \begin{bmatrix} K_{e1} & K_{e2} \end{bmatrix} \in \mathcal{L}(X \times \mathbb{C}^n, U)$. *Assume that the operator* H_e *satisfies the following* *auxiliary Sylvester equation:*

$$H_e S - (\mathcal{A} - L_{e1}\mathcal{C}_\alpha)\, H_e = L_{e1} Q + P \tag{4.40}$$

and that the injection gains L_{e1} *and* L_{e2} *are chosen such that the operator* $\mathcal{A} - L_{e1}\mathcal{C}_\alpha$ *generates an exponentially stable semigroup and the matrix* $S - L_{e2}(\mathcal{C}_\alpha H_e - Q)$ *is Hurwitz, then the observation error* $e_e(t)$ *decays to zero exponentially.*

The proof is similar to the proof part in Lemma 15. Obviously, the pair in Assumption 10 can be rewritten as $\left(\tilde{\mathcal{C}}_e, \mathcal{A}_e\right)$ and therefore the detectability of $\left(\tilde{\mathcal{C}}_e, \mathcal{A}_e\right)$ made in Assumption 10 ensures the possibility of finding injection gains L_{e1} and L_{e2}. As a consequence, the output injection gain $G = \begin{bmatrix} G_1 \\ G_2 \end{bmatrix}$ in [57] can be constructed as: $G = \tilde{H}_e L_e = \begin{bmatrix} L_{e1} + H_e L_{e2} \\ L_{e2} \end{bmatrix}$. Obviously, this chapter provides an alternative and easy way to establish the output injection gain for the pair $\left(\tilde{\mathcal{C}}_e, \mathcal{A}_e\right)$.

A direct calculation gives

$$\mathcal{R}_e = \begin{bmatrix} \mathcal{A} - L_{e1}\mathcal{C}_\alpha + \mathcal{B}K_{e1} & \mathcal{B}K_{e2} \\ -L_{e2}\mathcal{C}_\alpha & S - L_{e2}\left(\mathcal{C}_\alpha H_e - Q\right) \end{bmatrix}$$

Theorem 15. *The conditions for the solvability of (4.40) and the observability of the pair* $(\mathcal{C}_\Lambda H_e - Q, S)$ *are given as follows:*

a) (Solvability) $H_e \in \mathcal{L}(\mathbb{C}^n, X)$ *is defined by:*

$$H_e = \sum_{k=1}^{n} \langle \cdot, \phi_k \rangle R\left(\lambda_k; \mathcal{A} - L_{e1}\mathcal{C}_\alpha\right)\left(L_{e1} Q + P\right)\phi_k \tag{4.41}$$

that is the unique and bounded solution of the auxiliary Sylvester equation (4.40), if and only if the solvability conditions hold:

$$I + \mathcal{C}_\alpha(\lambda I - \mathcal{A})^{-1} L_{e1} \neq 0, \forall \lambda \in \sigma(S) \tag{4.42}$$

b) (Observability) *Consequently, the pair* $(\mathcal{C}_\alpha H_e - Q, S)$ *is observable, if and only if the* *transfer function $G_d(s)$ in (4.5) from $d(t)$ to $y(t)$ satisfies the following observability conditions:*

$$(G_d(\lambda_k)F - Q)\,\phi_k \neq 0,\ k = 1, 2, \cdots, n \tag{4.43}$$

Then, L_{e2} is chosen such that the matrix $S - L_{e2}(\mathcal{C}_\alpha H_e - Q)$ is Hurwitz.

Moreover, provided with the configuration of injection gains L_{e1} and L_{e2} in Lemma 16, the output regulation problem can be solved by the regulator (4.35)–(4.36), if the operators K_{e1} and K_{e2} are chosen as: $K_{e1} = K$ and $K_{e2} = K_{e1}H_e + (\Gamma - K_{e1}\Pi)$ where K satisfies that the operator $\mathcal{A} + \mathcal{B}K$ generates an exponentially stable semigroup $T_K(t)$ on X. The operators $\Pi \in \mathcal{L}(\mathbb{C}^n, X)$ and $\Gamma \in \mathcal{L}(\mathbb{C}^n, U)$ are defined in Lemma 14.

Proof. We first verify the properties in ***a)-b)***.

a). By applying a similar approach, the expression (4.41) can be obtained and the Sylvester equation (4.40) is decoupled into a set of equations:

$$h_{ek}^* = -(\lambda_k I - \mathcal{A})^{-1} L_{e1}\mathcal{C}_\alpha h_{ek}^* + (\lambda_k I - \mathcal{A})^{-1} l p_k^*$$

with $h_{ek}^* = H_e\phi_k$ and $lp_k^* = (L_{e1}Q + P)\,\phi_k$ for $k = 1, 2, \cdots, n$. If applying $\mathcal{C}_\alpha$, the value of $\mathcal{C}_\alpha h_{ek}^*$ can be uniquely determined by solving the equation:

$$\left(I + \mathcal{C}_\alpha(\lambda_k I - \mathcal{A})^{-1} L_{e1}\right)\mathcal{C}_\alpha h_{ek}^* = \mathcal{C}_\alpha(\lambda_k I - \mathcal{A})^{-1} l p_k^*$$

as long as the solvability conditions in (4.42) are satisfied. Finally, H_e is computed through $H_e = [h_{e1}^*, h_{e2}^*, \cdots, h_{en}^*]\,V^{-1}$.

b). The conditions $(\mathcal{C}_\alpha H_e - Q)\,\phi_k \neq 0, \forall k = 1, \cdots n$ indicates the observability property of $(\mathcal{C}_\alpha H_e - Q, S)$ directly. Then, using the formula (4.41) and Woodbury formula show for $k = 1, 2, \cdots, n$:

$$
\begin{aligned}
& \left(\mathcal{C}_\Lambda H_e - Q\right)\phi_k \\
= \quad & \mathcal{C}_\alpha R\left(\lambda_k; \mathcal{A} - L_{e1}\mathcal{C}_\alpha\right)\left(L_{e1}Q + P\right)\phi_k - Q\phi_k \\
= \quad & -\left(\mathcal{C}_\alpha R\left(\lambda_k; \mathcal{A} - L_{e1}\mathcal{C}_\alpha\right)\left(-L_{e1}\right) + I\right)Q\phi_k \\
& + \mathcal{C}_\alpha R\left(\lambda_k; \mathcal{A} - L_{e1}\mathcal{C}_\alpha\right)\mathcal{G}F\phi_k \\
= \quad & \left(I + \mathcal{C}_\alpha R\left(\lambda_k; \mathcal{A}\right)L_{e1}\right)^{-1}\left(G_e(\lambda_k)F - Q\right)\phi_k
\end{aligned}
$$

Due to Assumption 10, the matrix S has distinct eigenvalues and it is possible to ensure that conditions in (4.43) hold. Since the solvability condition in ***a)*** guarantees the existence of $\left(I + \mathcal{C}_\alpha R\left(\lambda_k; \mathcal{A}\right)L_{e1}\right)^{-1}$, then the conditions in (4.43) ensure the observability of $(\mathcal{C}_\alpha H_e - Q, S)$. Therefore, it is possible to find L_{e2} such that $S - L_{e2}(\mathcal{C}_\alpha H_e - Q)$ is Hurwitz.

Similar analysis in Theorem 14 can be applied such that the output regulation (4.10) is achieved by the regulator (4.35)–(4.36) and the closed-loop stability can be ensured, simultaneously. □

Remark 15. *The conditions in (4.43) means that an estimation of the exosystem state $v(t)$ is only possible if the transmission of the disturbance $d(t)$ or the reference signal $y_r(t)$ to the error $e(t)$ is not blocked by the corresponding transfer behaviour. More directly, (4.43) means that each eigenmode of $\dot{v}(t) = Sv(t)$ is observable in $d(t)$ or in $y_r(t)$, and therefore the transmission of disturbance $d(t)$ should not be blocked by the reference signal $y_r(t)$.*

4.5 Numerical Simulation

Example 1. *– Periodic reference Control with Constant Disturbance for a 1–D Heat Equation:* (Output feedback regulator) Consider a controlled heat equation on the interval $[0, 1]$ with Neumann boundary conditions:

$$\partial_t x(z,t) = \partial_z^2 x(z,t) + b(z)u(t) + d(t) \tag{4.44}$$

$$\partial_z x(0,t) = 0, \;\; \partial_z x(1,t) = 0 \tag{4.45}$$

$$x(z,0) = x_0(z), \;\; y(t) = \mathcal{C}x = x(0.45,t) \tag{4.46}$$

$$y_m(t) = \mathcal{C}_m x = x(1,t) \tag{4.47}$$

with the initial condition is $x_0(z) = 4z^2(3/2 - z)$. The temperature input is uniform over a small interval around the fixed point $z_0 \in (0,1)$, i.e., $b(z) = \frac{1}{2\varepsilon}\mathbf{1}_{[z_0-\varepsilon, z_0+\varepsilon]}(z)$, where $\mathbf{1}_{[a,b]}(z)$ denotes the characteristic function of the interval $[a,b]$: $\mathbf{1}_{[a,b]}(z) = \left\{ \begin{array}{l} 1, \;\; z \in [a,b] \\ 0, \;\; \text{otherwise} \end{array} \right\}$. We choose an actuator with $z_0 = 3/4$ and $\varepsilon = 1/4$. Our design objective in this example is to construct an output feedback regulator (4.20)-(4.21) that will drive the controlled output $y(t)$ to track a periodic reference trajectory of the form $y_r(t) = 5\sin(2t)$ and reject a constant disturbance $d(t) = d_0$ as well. The above reference and disturbance can be modelled by (4.14)–(4.17) with $S_d = 0$, $f_d = 1$, $q_r = \begin{bmatrix} 1 & 0 \end{bmatrix}$ and $S_r = \begin{bmatrix} 0 & 2 \\ -2 & 0 \end{bmatrix}$.

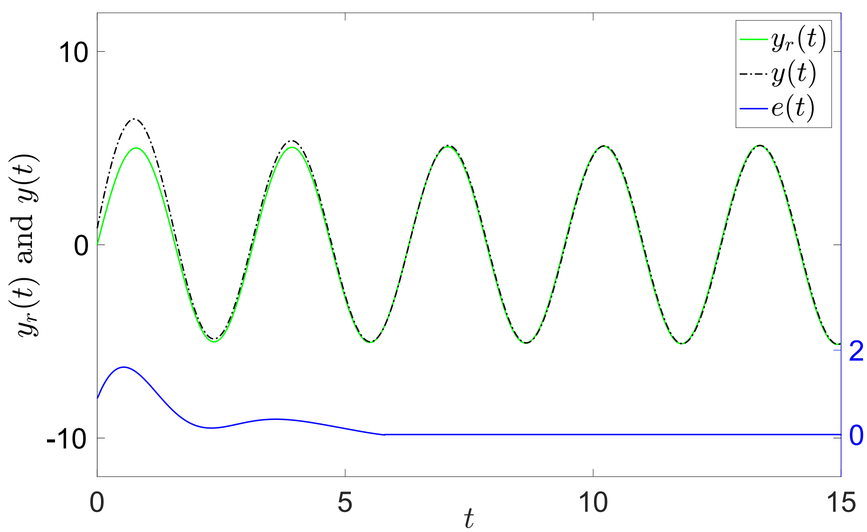

Figure 4.2: The reference trajectory $y_r(t) = 5sin(2t)$ and the controlled output $y(t) = x(0.45,t)$. $e(t)$ presents the tracking error.

It should be noted that the operator $A = \frac{d^2}{dz^2}$ equipped with $D(A) = \{h \in H^2(0,1), \frac{dh}{dz}(0) = 0 = \frac{dh}{dz}(1)\}$, includes zero eigenvalue in its spectrum $\sigma(A)$. Then, the Assumption 8 does not hold. To address this problem, the system needs to be stabilized at first. From Eq.(III.6) in [57], the stabilization gain K can be chosen as $K\Phi = -\beta\langle\Phi, \mathbf{1}(z)\rangle$ with $\beta > 0$, e.g., $\beta = 1$. For the stabilized system, a new operator $\mathcal{A}$ is obtained: $\mathcal{A} = \frac{d^2}{dz^2} + b(z)K$ with

$D(\mathcal{A}) = D(A)$. Obviously, $\sigma(S) \subset \rho(\mathcal{A})$ and Assumption 8 is ensured. To solve the output regulation problem, the output feedback regulator is constructed through the following steps:

Algorithm 1: Construction of the output feedback regulator
step 1: Solve Sylvester equation (4.11)–(4.12) for Γ and Π;
step 2: Find L_{m1} to stabilize the operator $\mathcal{A} - L_{m1}\mathcal{C}_{m\alpha}$ and solve Sylvester equation (4.26) for H;
step 3: Find L_{m2} and L_r to stabilize operators $S_d - L_{m2}\mathcal{C}_{m\alpha}H$ and $S_r - L_r q_r$;
step 4: Find K_{m1} to stabilize operator $\mathcal{A} + \mathcal{B}K_{m1}$ and let $K_{m2} = K_{m1}H + \Gamma_d - K_{m1}\Pi_d$ and $K_r = \Gamma_r - K_{m1}\Pi_r$.
step 5: Construct the output feedback regulator (4.23)–(4.24).

The output injection gain L_r in (4.23) is chosen such that the spectrum $\sigma(S_r - L_r q_r) = \{-6, -4\}$ is assigned. For this example, we may choose the stabilizing output injection L_{m1} as:

$$(L_{m1}\psi)(z) = \mu\psi\mathbf{1}_{[0,1]}(z), \text{ for } z \in [0,1], \psi \in Y = \mathbb{R}$$

where $\mathbf{1}_{[0,1]}(z)$ denotes the characteristic function $\mathbf{1}_{[a,b]}(z)$ with $a = 0$ and $b = 1$, and μ is a positive constant $\mu = 0.5$. Then, the auxiliary Sylvester equation (4.26) can be solved for $H(z)$ and $H(z) = 0.6667$ and the output injection gain $L_{m2} = 2$ can be selected such that $S_d - L_{m2}\mathcal{C}_{m\alpha}H = -1.333 < 0$. Since we have the exponentially stable operator $\mathcal{A}$, bounded input operator $\mathcal{B}$ and admissible operator $\mathcal{C}_{m\alpha}$, K_{m1} can be chosen as $K_{m1} = k_m\mathcal{C}_{m\alpha}$ and $k \in [-k_m^*, k_m^*], \exists k_m^* > 0$ such that $\mathcal{A} + \mathcal{B}K_{m1}$ is still exponentially stable. The results are shown in Figure 4.2–4.3.

By applying the regulator (4.23)–(4.24), the output, which is the temperature at the point $z = 0.45$, converges very rapidly to the desired trajectory $y_r(t) = 5sin(2t)$ despite of the disturbance d_0.

Example 2.– *Set Point Control with Period Disturbance for a coupled hyperbolic PDE systems:* (Error feedback regulator) We shall consider the following equation:

$$\begin{aligned}\frac{\partial x_1(z,t)}{\partial t} &= -\frac{\partial x_1(z,t)}{\partial z} + \alpha_1(z)x_1(z,t) \\ &+\alpha_2(z)x_2(z,t) + \beta u(t)\end{aligned} \tag{4.48a}$$

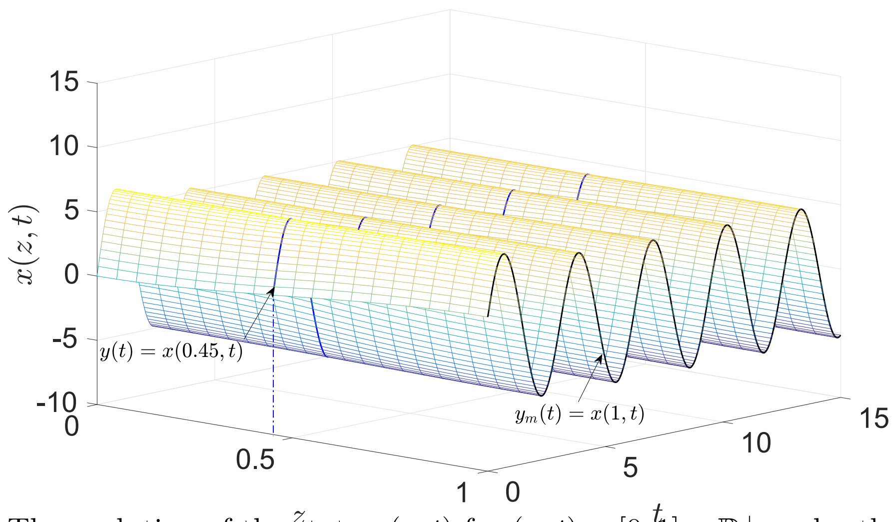

Figure 4.3: The evolution of the state $x(z,t)$ for $(x,t) \in [0,1] \times \mathbb{R}^+$ under the control of the output feedback regulator (4.20)–(4.21).

$$\frac{\partial x_2(z,t)}{\partial t} = -\frac{\partial x_2(z,t)}{\partial z} + \alpha_4(z)x_2(z,t) \\ +\alpha_3(z)x_1(z,t) + 0.8e^z d(t) \tag{4.48b}$$

$$x_1(0,t) = 0,\ x_2(0,t) = 0 \tag{4.48c}$$

$$x_1(z,0) = x_{10}(z),\ x_2(z,0) = x_{20}(z) \tag{4.48d}$$

$$y(t) = x_2(1,t) \tag{4.48e}$$

with $\begin{bmatrix} x_1(t) \\ x_2(t) \end{bmatrix} \in L^2(0,1)^2$, $z \in [0,1]$ and $\beta = 2$. The output $y(t)$ is obtained via boundary point evaluation of the state $x_2(z,t)$, the spatial varying coefficients are: $\alpha_1(z) = 2z^2(z+2)$, $\alpha_2(z) = -5e^z$, $\alpha_3(z) = \frac{3}{4}(1+z)$ and $\alpha_4(z) = -3(1+e^z)$, and the initial values are assumed as: $x_{10}(z) = z^2(\frac{3}{2} - z)$, $x_{20}(z) = -3z(1-z)$. In this example, we assume that only the error $e(t) = y(t) - y_r(t)$ is available and we are interested in designing an error feedback regulator (4.35)–(4.36) such that the output $y(t)$ tracks a constant reference trajectory $y_r(t) = 5$ and the disturbance $d(t) = 3sin(2t)$ is rejected simultaneously. The reference signal and disturbance can be modelled by (4.7)–(4.9) with $F = \begin{bmatrix} 0 & 3 & 0 \end{bmatrix}$, $Q = \begin{bmatrix} 5 & 0 & 0 \end{bmatrix}$ and

$$S = \begin{bmatrix} 0 & 0 & 0 \\ 0 & 0 & 2 \\ 0 & -2 & 0 \end{bmatrix}.$$

We define operators in (4.48) as follows:

$$\mathcal{A} = \begin{bmatrix} -\frac{d}{dz} + \alpha_1(z) & \alpha_2(z) \\ \alpha_3(z) & -\frac{d}{dz} + \alpha_4(z) \end{bmatrix}$$

with $D(\mathcal{A}) = \left\{h \in H^1(0,1)^2 : h(0) = 0\right\}$, $\mathcal{B} = \begin{bmatrix} \beta & 0 \end{bmatrix}^T$ and $\mathcal{C} = \begin{bmatrix} 0 & \tilde{\mathcal{C}} \end{bmatrix}$ with $\tilde{\mathcal{C}}h = \int_0^1 \delta(z-1)h(z)dz$ for $h \in L^2(0,1)$. And $\Lambda-$extension of $\mathcal{C}$ in the on space $L^2(0,1)^2$ is given by $\mathcal{C}_\alpha = \begin{bmatrix} 0 & \tilde{\mathcal{C}}_\alpha \end{bmatrix}$ with $\tilde{\mathcal{C}}_\alpha x = \alpha\tilde{\mathcal{C}}\left(\alpha I - \tilde{\mathcal{A}}\right)^{-1} x$, $x \in L^2(0,1)$ and $\tilde{\mathcal{A}} = -\frac{d}{dz} + \alpha_4(z)$ equipped with $D(\tilde{\mathcal{A}}) = \{x \in H^1(0,1) : x(0) = 0\}$.

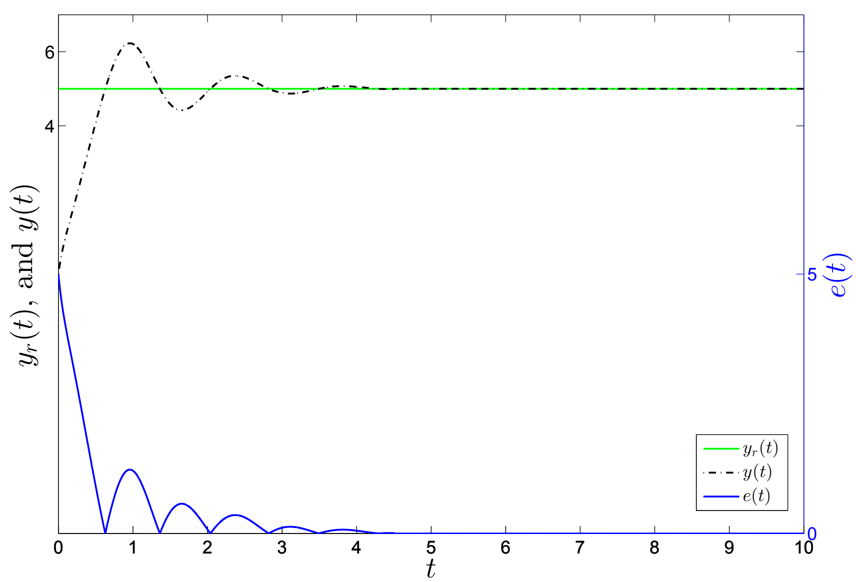

Figure 4.4: The reference trajectory $y_r(t) = 5$ and the controlled output $y(t) = x_2(1,t)$ under the control of the error feedback regulator (4.35)–(4.36). $e(t)$ presents the tracking error.

The construction of the error feedback regulator (4.35)–(4.36) is given as follows:

Algorithm 2: Construction of the error feedback regulator
step 1: Solve Sylvester equation (4.11)–(4.12) for Γ and Π;
step 2: Find L_{e1} to stabilize the operator $\mathcal{A} - L_{e1}\mathcal{C}_\alpha$ and solve Sylvester equation (4.40) for H_e;
step 3: Find L_{e2} to stabilize the operator $S_d - L_{e2}\left(\mathcal{C}_\alpha H_e - Q\right)$;
step 4: Find $K_{e1} = K$ to stabilize operator $\mathcal{A} + \mathcal{B}K_{e1}$ and let $K_{e2} = KH_e + \Gamma_d - K\Pi$.
step 5: Construct the error feedback regulator (4.35)–(4.36).

Since $\mathcal{A}$ generates an exponentially stable C_0-semigroup, $\mathcal{B}$ is bounded and $\mathcal{C}_\alpha$ is admissible, there exists a positive constant k^* such that for each $k \in [-k^*, k^*]$ the perturbed operator $\mathcal{A} + k\mathcal{B}\mathcal{C}_\alpha$ generates an exponentially stable semigroup. Therefore, we can choose $K = k\mathcal{C}_\alpha$ and $L_{e1} = k\mathcal{B}$ in Theorem 15. In particular, it is easy to see that only the output feedback $y(t)$ rather than the plant states $x_1(t)$ and $x_2(t)$ is utilized to achieve the stabilization the closed-loop system. The auxiliary Sylvester equation (4.40) can be solved through the approach in *a)* of Theorem 15 for $H_e(z)$. As a consequence, the proposed error feedback regulator (4.35)–(4.36) can be configured and the resulting tracking behaviour is shown in Figures 4.4.

4.6 Conclusion

This chapter addressed the output regulation problem for linear infinite-dimensional systems with bounded input operators and unbounded output operators. In particular, Yosida-type approximate boundary observation operator is defined to avoid the mathematic difficulties caused by unbounded output operators. Consequently, two types of observer-based regulators are investigated: the output feedback and error feedback regulators. Weighted regulator states are utilized to estimate the plant and exosystem states. In particular, similarity transformation and auxiliary Sylvester equations are applied such that the observation error system can be decoupled into a PDE subsystem and an ODE subsystem. Therefore, parameters in regulators can be designed independently to realize the stabilization of the PDE subsystem and the ODE subsystem and thus the observation error system. Based on designed observers, full state feedback control law can be applied to achieve the output regulation (4.10). In addition, to guarantee the feasibility of proposed regulators, the solvability conditions of auxiliary Sylvester equations and relative observability conditions are studied. Finally, the main results are verified by two types of representative systems: the heat equation described by a parabolic PDE and the first order coupled hyperbolic PDE, via computer simulations.

Chapter 5

The state feedback servo-regulator for countercurrent heat-exchanger system modelled by system of hyperbolic PDEs

5.1 Introduction

With well-developed state feedback regulator in Chapter 3 and based on the good properties of the considered plant, the output feedback stabilization controller equipped with a feed-forward controller to solve the output regulation problem in this chapter. The controlled system in this chapter is a network of countercurrent heat exchangers described by two sets of hyperbolic PDEs. This class of systems covers packed mass exchange columns [75], countercurrent heat exchangers [76] and irrigation canals [77]. The system considered in this chapter consists of two countercurrent heat exchangers connected in cascade and the fluid flow rates are considered as control variables. Hence, the resulting system is quasi-linear. Given an equilibrium state profile, by linearizing the quasi-linear system around the equilibrium state profile, one obtains the linearized system. In particular, the linearized system characteristic is that it is a non-minimum phase system: the transfer function from $u(t)$ to $y(t)$ has zeros in the open right half-plane.

5.2 Problem Formulation

5.2.1 Model description

The countercurrent heat exchanger is an essential equipment broadly utilized as a part of numerous genuine process industry applications. The counter-stream heat exchanger has three critical advantages over the parallel stream design. First and foremost, the more uniform temperature contrast between the two liquids minimizes the thermal stresses throughout the exchanger. Second, the outlet temperature of the cool liquid can approach the most noteworthy temperature of the hot fluid, see Figure 5.1. Third, a more uniform temperature distinction creates a more uniform rate of hotness exchange throughout the heat exchanger. In this chapter, a network of counter flow heat exchangers is considered and modelled by two sets of hyperbolic PDEs by assuming no diffusion phenomena. In order to deal with the nonlinearity of the system, an explicit expression of an equilibrium profile is utilized. Then, a state feedback regulator is designed to control the output of the system to track a reference signal generated by an exosystem. As shown in Figure 5.2, the heat exchanger includes three input fluids denoted by FL_1, FL_2 and FL_3. The process of interest to control is to heat the fluid FL_3 by mixing FL_1 with FL_2.

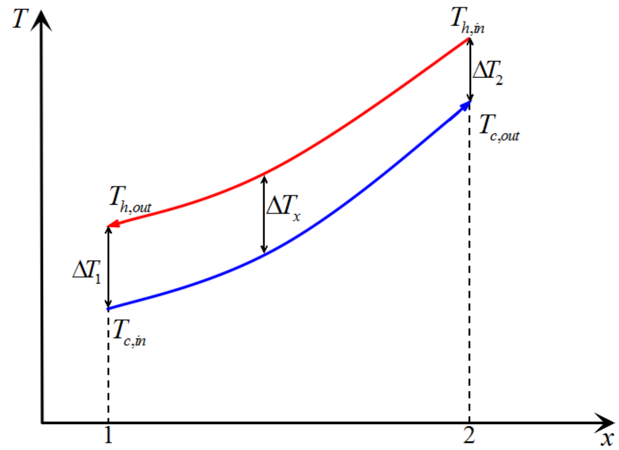

Figure 5.1: Temperature profiles in counter-flow. Note that in a counter-flow heat exchanger the outlet temperature of the cold fluid can exceed the outlet temperature of the hot fluid but this cannot happen in a parallel flow system

The fluid FL_3 that needs to be heated enters the heat exchanger at $x = 0$. The hot fluid FL_1 enters the exchanger at $x = l_1$ and is mixed with the fluid FL_2 coming from the right side. Table 5.1 gives the physical properties of three fluids and the geometric description of the heat exchanger. We assume that the physical properties of the fluids FL_1 and FL_2 are the same and the flow rate of FL_3 is a constant F_2. In Table 5.1, $s_1 = \pi(r_1^2 - r_2^2)$ and $s_2 = \pi r_2^2$ and $l = 2\pi r_2$.

Specification	FL_1	FL_2	FL_3
Specific weight	ρ_1	ρ_1	ρ_2
Specific heat	C_{p1}	C_{p1}	C_{p2}
Cross-section of path	s_1	s_1	s_2
Contact circumference of exchanger	l	l	l
Temperature			
$0 \leq x < l_1$	$T_1^-(x,t)$	$T_1^-(x,t)$	$T_2^-(x,t)$
$l_1 \leq x \leq l_2$		$T_1^+(x,t)$	$T_2^+(x,t)$
Exchanger coefficient	k	k	k
Mass flow rate	$\alpha F_1(t)$	$(1-\alpha)F_1(t)$	F_2
Input temperature	T_{01}	T_{02}	T_{03}

Table 5.1: Model Parameters

According to the energy balance, the following PDEs are obtained to describe the two parts of the heat exchanger shown in Figure 5.2, respectively.

$$\left.\begin{aligned} \frac{\partial T_1^-}{\partial t} &= \frac{F_1(t)}{\rho_1 s_1}\frac{\partial T_1^-}{\partial x} - \frac{kl}{C_{p1}\rho_1 s_1}\left(T_1^- - T_2^-\right) \\ \frac{\partial T_2^-}{\partial t} &= -\frac{F_2}{\rho_2 s_2}\frac{\partial T_2^-}{\partial x} + \frac{kl}{C_{p2}\rho_2 s_2}\left(T_1^- - T_2^-\right) \end{aligned}\right\} 0 < x < l_1, t > 0 \tag{5.1}$$

$$\left.\begin{aligned} \frac{\partial T_1^+}{\partial t} &= \frac{(1-\alpha)F_1(t)}{\rho_1 s_1}\frac{\partial T_1^+}{\partial x} - \frac{kl}{C_{p1}\rho_1 s_1}\left(T_1^+ - T_2^+\right) \\ \frac{\partial T_2^+}{\partial t} &= -\frac{F_2}{\rho_2 s_2}\frac{\partial T_2^+}{\partial x} + \frac{kl}{C_{p2}\rho_2 s_2}\left(T_1^+ - T_2^+\right) \end{aligned}\right\} l_1 < x < l_2, t > 0 \tag{5.2}$$

with boundary conditions:

$$\left.\begin{aligned} T_1^+(l_2,t) &= T_{02} \\ T_2^-(0,t) &= T_{03} \end{aligned}\right\} \tag{5.3}$$

where $T_2^\pm$ denotes temperature distribution of the fluid FL_3, T_1^- denotes the temperature of mixed fluid FL_1 and FL_2 on the left side and T_1^+ denotes the temperature of the fluid FL_2. Here the superscripts $\pm$ in '$T_i^\pm$' just denote the different sides of the system, i.e., '$-$' denotes the left side: $0 < x < l_1$ and '$+$' denotes the right side: $l_1 < x < l_2$.

The additional conditions at the mixing point $x = l_1$ are given as follows:

$$\left.\begin{aligned} T_1^-(l_1,t) &= (1-\alpha)T_1^+(l_1,t) + \alpha T_{01} \\ T_2^-(l_1,t) &= T_2^+(l_1,t) \end{aligned}\right\} \tag{5.4}$$

where T_{01} denotes the temperature of the fluid FL_1 entering the system at $x = l_1$, T_{02} is the temperature of the fluid FL_2 entering the system at $x = l_2$, and T_{03} denotes the temperature of the fluid FL_3 entering the system at $x = 0$. We assume that T_{01}, T_{02} and T_{03} are positive constants and $0 < \alpha < 1$.

The initial conditions are given by:

$$\left.\begin{aligned} T_1^-(x,0) &= f_1^-(x) \\ T_2^-(x,0) &= f_2^-(x) \end{aligned}\right\} 0 < x < l_1 \tag{5.5}$$

$$\left.\begin{aligned} T_1^+(x,0) &= f_1^+(x) \\ T_2^+(x,0) &= f_2^+(x) \end{aligned}\right\} l_1 \leq x \leq l_2 \tag{5.6}$$

Therefore, the system (5.1), (5.2) with boundary conditions (5.3), (5.4) and initial conditions (5.5), (5.6) describes the dynamics of the countercurrent heat exchanger shown in Figure 5.2. In the system (5.1), (5.2) to be controlled, the flow rate $F_1(t)$ is the control input and $T_2^+(l_2,t)$ is the output. In other words, the temperature of the fluid FL_3 at the outlet $x = l_2$ is controlled by the flow rate $F_1(t)$, see Figure 5.2.

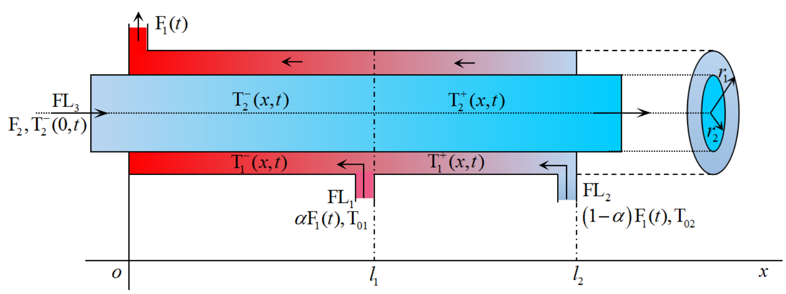

Figure 5.2: Heat exchanger systems geometry.

In order to explore when the system exhibits a non-minimum phenomenon, in this chapter the following conditions are set as:

$$T_{02} < T_{03} < \alpha T_{01}, \;\; 0.5 \ll \alpha < 1 \tag{5.7}$$

According to (5.7), the fluid FL_3 is heated at the left side: $0 < x < l_1$ and heats the fluid FL_2 at the right side: $l_1 < x < l_2$. Here $0.5 \ll \alpha$ means that the parameter α is larger than and is not close to 0.5, e.g., $\alpha > 0.6$. The condition: $0.5 \ll \alpha < 1$ implies that the temperature of the fluid FL_3 at $x = l_2$ will increase.

First, we assume that the system reaches the equilibrium point under the fixed control input $F_1(t) = F_0$. Then, by increasing $F_1(t) = F_0$ by a positive unitary step, the fluid FL_2 will cool more the fluid FL_3 at the right side of the heat exchanger and at the same time, the mixed fluid of FL_1 and FL_2 will heat the fluid FL_3 at the left side of the heat exchanger.

This is shown in Figure 5.3, since the fluid FL_3 moves from the left side to the right side. It can be observed that at $x = l_2$, $T_2^+(l_2, t)$ first decreases before the left side heated fluid reaches. Then, $T_2^+(l_2, t)$ increases due to the arrival of the heated fluid FL_3 from the left end. This is essentially the non-minimum phase behavior, i.e., the conditions (5.7) guarantee a non-minimum phase of the plant system.

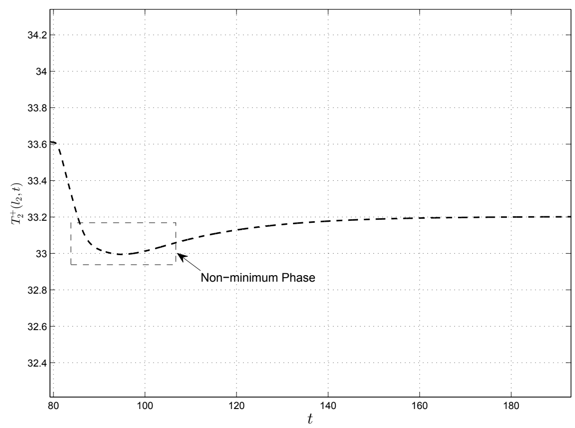

Figure 5.3: The non-minimum phase response of the heat exchanger system to a positive step control.

5.2.2 Temperature equilibrium profiles

In this chapter, we are interested in temperature equilibrium profiles for the model (5.1)–(5.6):

$$T_e = \left[T_{1e}^-(\cdot), T_{2e}^-(\cdot), T_{1e}^+(\cdot), T_{2e}^+(\cdot)\right]^T \tag{5.8}$$

in the state space $L^2(0, l_1)^2 \times L^2(l_1, l_2)^2$, given by a set of parameters T_{01}, T_{02}, T_{03} and α and by fixing the control input as $F_1(t) = F_0$.

Remark 16. *The equilibrium profiles T_e must satisfy the boundary conditions (5.3), (5.4). By selecting different constant control inputs F_0, one can obtain different temperature equilibrium profiles. The temperature equilibrium profiles are given in Figure 5.4.*

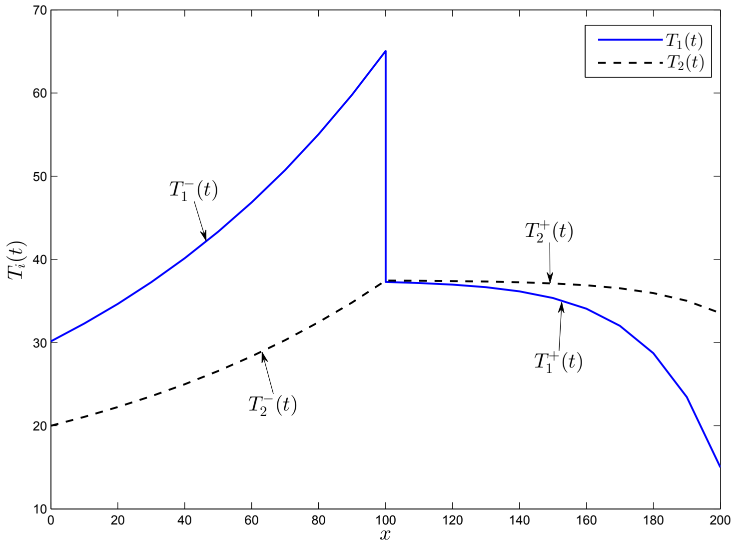

Figure 5.4: Equilibrium temperature profiles.

By integrating the equilibrium ordinary differential equations corresponding to (5.1)–(5.4), one can easily obtain the equilibrium profiles described by:

$$\left.\begin{aligned} T_{1e}^{-}(x) &= \left(\tfrac{\alpha_1}{\alpha_1-\beta_1}\right) C_0 \exp\left((\alpha_1-\beta_1)x\right) + C_1 \\ T_{2e}^{-}(x) &= \left(\tfrac{\beta_1}{\alpha_1-\beta_1}\right) C_0 \exp\left((\alpha_1-\beta_1)x\right) + C_1 \end{aligned}\right\} 0 < x < l_1, \tag{5.9}$$

$$\left.\begin{aligned} T_{1e}^{+}(x) &= \left(\tfrac{\frac{\alpha_1}{1-\alpha}}{\frac{\alpha_1}{1-\alpha}-\beta_1}\right) \tilde{C}_0 \exp\left(\left(\tfrac{\alpha_1}{1-\alpha}-\beta_1\right)x\right) + \tilde{C}_1 \\ T_{2e}^{+}(x) &= \left(\tfrac{\beta_1}{\frac{\alpha_1}{1-\alpha}-\beta_1}\right) \tilde{C}_0 \exp\left(\left(\tfrac{\alpha_1}{1-\alpha}-\beta_1\right)x\right) + \tilde{C}_1 \end{aligned}\right\} l_1 \le x \le l_2 \tag{5.10}$$

where $\alpha_1 = \frac{kl}{F_0 C_{p1}}$, $\beta_1 = \frac{kl}{F_2 C_{p2}}$ *and the boundary conditions (5.3), (5.4) can uniquely determine the constants* C_0, C_1, $\tilde{C}_0$ *and* $\tilde{C}_1$, *i.e.:*

$$\Lambda \times \Xi = \mathrm{T}_\alpha \tag{5.11}$$

where $\Xi = \left[C_0, C_1, \tilde{C}_0, \tilde{C}_1\right]^T$ *and* $\mathrm{T}_\alpha = [\alpha T_{01}, 0, T_{03}, T_{02}]^T$

$$\Lambda = \begin{bmatrix} \left(\frac{\alpha_1}{\alpha_1-\beta_1}\right)\exp\left(\left(\alpha_1-\beta_1\right)l_1\right) & 1 & -\left(\frac{\alpha_1}{\frac{\alpha_1}{1-\alpha}-\beta_1}\right)\exp\left(\left(\frac{\alpha_1}{1-\alpha}-\beta_1\right)l_1\right) & -(1-\alpha) \\ \left(\frac{\beta_1}{\alpha_1-\beta_1}\right)\exp\left(\left(\alpha_1-\beta_1\right)l_1\right) & 1 & -\left(\frac{\beta_1}{\frac{\alpha_1}{1-\alpha}-\beta_1}\right)\exp\left(\left(\frac{\alpha_1}{1-\alpha}-\beta_1\right)l_1\right) & -1 \\ \frac{\beta_1}{\alpha_1-\beta_1} & 1 & 0 & 0 \\ 0 & 0 & \left(\frac{\frac{\alpha_1}{1-\alpha}}{\frac{\alpha_1}{1-\alpha}-\beta_1}\right)\exp\left(\left(\frac{\alpha_1}{1-\alpha}-\beta_1\right)l_2\right) & 1 \end{bmatrix}$$

In this chapter, in order to make sure that the matrix Λ in (5.11) is invertible, we make the following assumptions:

$$\alpha_1 \neq \beta_1 \text{ and } \alpha_1 \neq (1-\alpha)\,\beta_1$$

5.2.3 Linearized model

Let us consider the Hilbert state space $H := L^2(0,l_1)^2 \times L^2(l_1,l_2)^2 := L^2(0,l_1) \times L^2(0,l_1) \times L^2(l_1,l_2) \times L^2(l_1,l_2)$, where $X_1 \times X_2 \times X_3 \times X_4$ denotes the Hilbert space obtained as the cartesian product of the Hilbert spaces X_1, X_2, X_3 and X_4 equipped with the inner product defined by $\langle x,x\rangle_H = \langle x_1,x_1\rangle_{X_1} + \langle x_2,x_2\rangle_{X_2} + \langle x_3,x_3\rangle_{X_3} + \langle x_4,x_4\rangle_{X_4}$, where $[x_1,x_2,x_3,x_4]^T \in X_1 \times X_2 \times X_3 \times X_4$. $L^2(q_1,q_2)$ denotes the Hilbert space of Lebesgue square integrable functions $f : [q_1,q_2] \to R$ on (q_1,q_2), i.e., $\int_{q_1}^{q_2} |f(z)|^2 dz < \infty$, for $q_1 < q_2$. The inner product and the norm of $L^2(q_1,q_2)$ are defined by $\langle f,g\rangle_2 = \int_{q_1}^{q_2} f(z)g(z)dz$ and $\|f\|_2 = \sqrt{\langle f,f\rangle_2}$.

Let us define the following system state $R(t) \in H$:

$$R(t) := \begin{bmatrix} R_1^-(\cdot,t) \\ R_2^-(\cdot,t) \\ R_1^+(\cdot,t) \\ R_2^+(\cdot,t) \end{bmatrix} = \begin{bmatrix} T_1^-(\cdot,t) - T_{1e}^-(\cdot) \\ T_2^-(\cdot,t) - T_{2e}^-(\cdot) \\ T_1^+(\cdot,t) - T_{1e}^+(\cdot) \\ T_2^+(\cdot,t) - T_{2e}^+(\cdot) \end{bmatrix} \qquad (5.12)$$

and the new input $\Delta F_1(t) = F_1(t) - F_0$.

The linearization of the system (5.1), (5.2) around the equilibrium profiles (5.9), (5.10) leads to the following linear PDE system on the state space H:

$$\left.\begin{aligned}\frac{\partial R_1^-}{\partial t} &= m_1 \frac{\partial R_1^-}{\partial x} - m_3\left(R_1^- - R_2^-\right) + \frac{1}{\rho_1 s_1}\frac{dT_{1e}^-(x)}{dx}\Delta F_1(t)\\ \frac{\partial R_2^-}{\partial t} &= -m_2 \frac{\partial R_2^-}{\partial x} + m_4\left(R_1^- - R_2^-\right)\end{aligned}\right\} 0 < x < l_1 \tag{5.13}$$

$$\left.\begin{aligned}\frac{\partial R_1^+}{\partial t} &= (1-\alpha)\, m_1 \frac{\partial R_1^+}{\partial x} - m_3\left(R_1^+ - R_2^+\right) + \frac{1-\alpha}{\rho_1 s_1}\frac{dT_{1e}^+(x)}{dx}\Delta F_1(t)\\ \frac{\partial R_2^+}{\partial t} &= -m_2 \frac{\partial R_2^+}{\partial x} + m_4\left(R_1^+ - R_2^+\right)\end{aligned}\right\} l_1 < x < l_2 \tag{5.14}$$

with the boundary conditions

$$\begin{aligned}&R_1^-(l_1,t) = (1-\alpha)\, R_1^+(l_1,t)\\ &R_2^-(l_1,t) = R_2^+(l_1,t)\\ &R_2^-(0,t) = 0\\ &R_1^+(l_2,t) = 0\end{aligned} \tag{5.15}$$

where the physical parameters of the heat exchanger (5.13), (5.14) are defined by

$$m_1 = \frac{F_0}{\rho_1 s_1}, m_2 = \frac{F_2}{\rho_2 s_2}, m_3 = \frac{kl}{C_{p1}\rho_1 s_1}, m_4 = \frac{kl}{C_{p2}\rho_2 s_2}$$

Then, the equivalent state-space description of the linearized model (5.13)–(5.15) is given by the following linear time-invariant abstract differential equation on the Hilbert space H:

$$\begin{aligned}&\dot{z}(t) = Az(t) + Bu(t),\ z(0) = z_0 \in H\\ &y(t) = Cz(t)\end{aligned} \tag{5.16}$$

where the state of composite system $z(t)$, the input $u(t)$ and the output $y(t)$ are given by

$$z(t) = \begin{bmatrix} R_1^-(x,t)\\ R_2^-(x,t)\\ R_1^+(x,t)\\ R_2^+(x,t)\end{bmatrix},\ u(t) = \Delta F_1(t),\ \text{and}\ y(t) = R_2^+(l_2,t)$$

Here, the system operator A in the spatial interval $[0, l_1]$ and $[l_1, l_2]$ is defined on its domain as:

$$D(A) = \left\{ \begin{array}{l} h(\cdot) = [h_1(\cdot), h_2(\cdot), h_3(\cdot), h_4(\cdot)]^T \in H : \\ h \text{ is a.c, } \frac{dh(\cdot)}{dx} \in H, \\ h_1(l_1) = (1-\alpha) h_3(l_1), h_2(l_1) = h_4(l_1), h_2(0) = 0, h_3(l_2) = 0 \end{array} \right\}$$

(where a.c means that h is absolutely continuous) by

$$A = \begin{bmatrix} m_1 \frac{\partial}{\partial x} - m_3 & m_3 & 0 & 0 \\ m_4 & -m_2 \frac{\partial}{\partial x} - m_4 & 0 & 0 \\ 0 & 0 & (1-\alpha)\, m_1 \frac{\partial}{\partial x} - m_3 & m_3 \\ 0 & 0 & m_4 & -m_2 \frac{\partial}{\partial x} - m_4 \end{bmatrix} \tag{5.17}$$

The input and output operators are given by

$$\begin{aligned} B &= \begin{bmatrix} \frac{1}{\rho_1 s_1} \frac{dT_{1e}^-(x)}{dx} & 0 & \frac{1-\alpha}{\rho_1 s_1} \frac{dT_{1e}^+(x)}{dx} & 0 \end{bmatrix}^T \in L(U, H), \\ C &= \begin{bmatrix} 0 & 0 & 0 & C_\Lambda \end{bmatrix} \in L(H, Y) \end{aligned} \tag{5.18}$$

where for all $h(\cdot) \in D(C_\Lambda)$, $(C_\Lambda h)(x) = h(l_2)$. The input space U and the output space Y are real Hilbert spaces.

An explicit expression of the equilibrium profiles is presented. Based on this expression, the original nonlinear system with time varying coefficients is linearized and described by the linear PDEs with constant coefficients. It is easy to show that the system operator A in (5.17) is an infinitesimal generator of a C_0-semigroup T_A on H. Therefore, the initial value problem in the system (5.13)– (5.15) or (5.16) is well-posed and has a unique solution [31].

5.2.4 Transfer function representation of the linearized system

In this section, we compute the explicit expression of the plant transfer function: $G(s)$ based on the system governed by (5.13)–(5.15). We take the Laplace transform on both sides of

(5.13)–(5.15) with zero initial conditions and obtain:

$$\begin{bmatrix} \frac{\partial \hat{R}_1^-(x,s)}{\partial x} \\ \frac{\partial \hat{R}_2^-(x,s)}{\partial x} \end{bmatrix} = \begin{bmatrix} \alpha_1 + \alpha_2 s & -\alpha_1 \\ \beta_1 & -(\beta_1 + \beta_2 s) \end{bmatrix} \begin{bmatrix} \hat{R}_1^-(x,s) \\ \hat{R}_2^-(x,s) \end{bmatrix} + \begin{bmatrix} -\frac{1}{F_0}\frac{dT_{1e}^-(x)}{dx} \\ 0 \end{bmatrix} \Delta \hat{F}_1(s),\ 0 < x < l_1 \tag{5.19}$$

$$\begin{bmatrix} \frac{\partial \hat{R}_1^+(x,s)}{\partial x} \\ \frac{\partial \hat{R}_2^+(x,s)}{\partial x} \end{bmatrix} = \begin{bmatrix} \frac{\alpha_1 + \alpha_2 s}{1-\alpha} & -\frac{\alpha_1}{1-\alpha} \\ \beta_1 & -(\beta_1 + \beta_2 s) \end{bmatrix} \begin{bmatrix} \hat{R}_1^+(x,s) \\ \hat{R}_2^+(x,s) \end{bmatrix} + \begin{bmatrix} -\frac{1}{F_0}\frac{dT_{1e}^+(x)}{dx} \\ 0 \end{bmatrix} \Delta \hat{F}_1(s),\ l_1 < x < l_2 \tag{5.20}$$

where $\alpha_1 = \frac{kl}{F_0 C_{p1}}$, $\alpha_2 = \frac{\rho_1 s_1}{F_0}$, $\beta_1 = \frac{kl}{F_2 C_{p2}}$ and $\beta_2 = \frac{\rho_2 s_2}{F_2}$.

The boundary conditions are:

$$\begin{bmatrix} \hat{R}_1^-(l_1,s) \\ \hat{R}_2^-(l_1,s) \end{bmatrix} = \begin{bmatrix} 1-\alpha & 0 \\ 0 & 1 \end{bmatrix} \begin{bmatrix} \hat{R}_1^+(l_1,s) \\ \hat{R}_2^+(l_1,s) \end{bmatrix}, \quad \begin{bmatrix} \hat{R}_1^+(l_2,s) \\ \hat{R}_2^-(0,s) \end{bmatrix} = \begin{bmatrix} 0 \\ 0 \end{bmatrix} \tag{5.21}$$

For simplicity sake, we set

$$A_1(s) = \begin{bmatrix} \alpha_1 + \alpha_2 s & -\alpha_1 \\ \beta_1 & -(\beta_1 + \beta_2 s) \end{bmatrix},\ A_2(s) = \begin{bmatrix} \frac{\alpha_1 + \alpha_2 s}{1-\alpha} & -\frac{\alpha_1}{1-\alpha} \\ \beta_1 & -(\beta_1 + \beta_2 s) \end{bmatrix}$$

The solution of the differential equations (5.19)–(5.21) yields to:

$$\begin{aligned}\begin{bmatrix}\hat{R}_1^+(l_2,s)\\ \hat{R}_2^+(l_2,s)\end{bmatrix} &= \exp(A_2(s)(l_2-l_1))\begin{bmatrix}\frac{1}{1-\alpha} & 0\\ 0 & 1\end{bmatrix}\times\left\{\exp(A_1(s)l_1)\begin{bmatrix}\hat{R}_1^-(0,s)\\ \hat{R}_2^-(0,s)\end{bmatrix}\right.\\ &\left.+\textstyle\int_0^{l_1}\exp(A_1(s)(l_1-x))\begin{bmatrix}1\\ 0\end{bmatrix}\left(-\frac{1}{F_0}\frac{dT_{1e}^-(x)}{dx}\right)dx\Delta\hat{F}_1(s)\right\}\\ &+\textstyle\int_{l_1}^{l_2}\exp(A_2(s)(l_2-x))\begin{bmatrix}-\frac{1}{F_0}\frac{dT_1^+(x)}{dx}\\ 0\end{bmatrix}dx\Delta\hat{F}_1(s)\end{aligned} \tag{5.22}$$

From the previous section, the input and output are known to be $\Delta\hat{F}_1(s)$ and $\hat{R}_2^+(l_2,s)$, respectively. Naturally, based on the boundary conditions (5.21) the transfer function can be easily computed from the above solution (5.22) as follows:

$$G(s)=\frac{\hat{R}_2^+(l_2,s)}{\Delta\hat{F}_1(s)}=M(s)^{-1}(N_1(s)+N_2(s)) \tag{5.23}$$

where $M(s)$, $N_1(s)$ and $N_2(s)$ are given by

$$M(s)=\begin{bmatrix}0 & 1\end{bmatrix}\exp\left(-A_1(s)l_1\right)\begin{bmatrix}1-\alpha & 0\\ 0 & 1\end{bmatrix}\exp\left(-A_2(s)(l_2-l_1)\right)\begin{bmatrix}0\\ 1\end{bmatrix} \tag{5.24}$$

$$N_1(s)=\begin{bmatrix}0 & 1\end{bmatrix}\int_0^{l_1}\exp(-A_1(s)x)\begin{bmatrix}1\\ 0\end{bmatrix}\left(-\frac{1}{F_0}\frac{dT_{1e}^-(x)}{dx}\right)dx \tag{5.25}$$

$$\begin{aligned}N_2(s)=&\begin{bmatrix}0 & 1\end{bmatrix}\exp\left(-A_1(s)l_1\right)\begin{bmatrix}1-\alpha & 0\\ 0 & 1\end{bmatrix}\\ &\times\textstyle\int_{l_1}^{l_2}\exp\left(A_2(s)(l_1-x)\right)\begin{bmatrix}1\\ 0\end{bmatrix}\left(-\frac{1}{F_0}\frac{dT_1^+(x)}{dx}\right)dx\end{aligned} \tag{5.26}$$

The explicit expression of the transfer function is given calculated in the following:

It is straightforward to compute the following fundamental matrix equation:

$$\exp\left(-A_1(s)x\right) = \begin{bmatrix} A_{1,1}(s,x) & A_{1,2}(s,x) \\ A_{1,3}(s,x) & A_{1,4}(s,x) \end{bmatrix} \tag{5.27}$$

with

$$\begin{aligned}
A_{1,1}(s,x) &= \frac{a_{11} + a_{12}s}{2p_1(s)} \left(\exp(-\lambda_{11}(s)x) - \exp(-\lambda_{12}(s)x)\right) \\
&\quad + 0.5 \left(\exp(-\lambda_{11}(s)x) + \exp(-\lambda_{12}(s)x)\right) \\
A_{1,2}(s,x) &= \frac{\alpha_1}{p_1(s)} \left(\exp(-\lambda_{12}(s)x) - \exp(-\lambda_{11}(s)x)\right) \\
A_{1,3}(s,x) &= \frac{\beta_1}{p_1(s)} \left(\exp(-\lambda_{11}(s)x) - \exp(-\lambda_{12}(s)x)\right) \\
A_{1,4}(s,x) &= \frac{a_{11} + a_{12}s}{2p_1(s)} \left(\exp(-\lambda_{12}(s)x) - \exp(-\lambda_{11}(s)x)\right) \\
&\quad + 0.5 \left(\exp(-\lambda_{11}(s)x) + \exp(-\lambda_{12}(s)x)\right)
\end{aligned}$$

$$\exp\left(-A_2(s)x\right) = \begin{pmatrix} A_{2,1}(s,x) & A_{2,2}(s,x) \\ A_{2,3}(s,x) & A_{2,4}(s,x) \end{pmatrix} \tag{5.28}$$

with

$$\begin{aligned}
A_{2,1}(s,x) &= \frac{a_{21} + a_{22}s}{2p_2(s)} \left(\exp(-\lambda_{21}(s)x) - \exp(-\lambda_{22}(s)x)\right) \\
&\quad + 0.5 \left(\exp(-\lambda_{21}(s)x) + \exp(-\lambda_{22}(s)x)\right) \\
A_{2,2}(s,x) &= \frac{\alpha_1}{(1-\alpha)p_2(s)} \left(\exp(-\lambda_{22}(s)x) - \exp(-\lambda_{21}(s)x)\right) \\
A_{2,3}(s,x) &= \frac{\beta_1}{p_2(s)} \left(\exp(-\lambda_{21}(s)x) - \exp(-\lambda_{22}(s)x)\right) \\
A_{2,4}(s,x) &= \frac{a_{21} + a_{22}s}{2p_2(s)} \left(\exp(-\lambda_{22}(s)x) - \exp(-\lambda_{21}(s)x)\right) \\
&\quad + 0.5 \left(\exp(-\lambda_{21}(s)x) + \exp(-\lambda_{22}(s)x)\right)
\end{aligned}$$

where a_{11}, a_{12}, a_{21}, a_{22}, $p_1(s)$, $p_2(s)$, $\lambda_{11}(s)$, $\lambda_{12}(s)$, $\lambda_{21}(s)$, and $\lambda_{22}(s)$ are given by:

$$\begin{aligned}
a_{11} &= \alpha_1 + \beta_1, a_{12} = \alpha_2 + \beta_2 \\
a_{11} &= \frac{\alpha_1}{1-\alpha} + \beta_1, a_{11} = \frac{\alpha_2}{1-\alpha} + \beta_2 \\
p_1(s) &= \sqrt{(\alpha_1 - \beta_1)^2 + 2a_{11}a_{12}s + (a_{12}s)^2} \\
p_2(s) &= \sqrt{(\frac{\alpha_1}{1-\alpha} - \beta_1)^2 + 2a_{21}a_{22}s + (a_{22}s)^2} \\
\lambda_{11}(s) &= 0.5\left(\alpha_1 - \beta_1 + (\alpha_2 - \beta_2)s + p_1(s)\right) \\
\lambda_{12}(s) &= 0.5\left(\alpha_1 - \beta_1 + (\alpha_2 - \beta_2)s - p_1(s)\right) \\
\lambda_{21}(s) &= 0.5\left(\frac{\alpha_1}{1-\alpha} - \beta_1 + (\frac{\alpha_2}{1-\alpha} - \beta_2)s + p_2(s)\right) \\
\lambda_{22}(s) &= 0.5\left(\frac{\alpha_1}{1-\alpha} - \beta_1 + (\frac{\alpha_2}{1-\alpha} - \beta_2)s - p_2(s)\right)
\end{aligned}$$

By solving (5.24) and (5.28), one can obtain the expressions of $M(s)$, $N_1(s)$ and $N_2(s)$:

$$M(s) = \frac{W_1(s)}{4p_1(s)p_2(s)} \exp\left(-\lambda_{12}(s)l_1 - \lambda_{22}(s)(l_2 - l_1)\right) \tag{5.29}$$

$$N_1(s) = \frac{W_2(s)}{4p_1(s)p_2(s)} \exp\left(-\lambda_{12}(s)l_1 - \lambda_{22}(s)(l_2 - l_1)\right) \tag{5.30}$$

$$N_2(s) = \frac{W_3(s)}{4p_1(s)p_2(s)} \exp\left(-\lambda_{12}(s)l_1 - \lambda_{22}(s)(l_2 - l_1)\right) \tag{5.31}$$

where

$$\begin{aligned}
W_1(s) = {} & 4\alpha_1\beta_1\left(\exp\left(-p_1(s)l_1\right) - 1\right)\left(1 - \exp\left(-p_1(s)\left(l_2 - l_1\right)\right)\right) \\
& + \left(a_{11} + a_{12}s + p_1(s) + \left(p_1(s) - a_{11} - a_{12}s\right)\exp\left(-p_1(s)l_1\right)\right) \\
& \times \left(a_{21} + a_{22}s + p_2(s) + \left(p_2(s) - a_{21} - a_{22}s\right)\exp\left(-p_2(s)\left(l_2 - l_1\right)\right)\right)
\end{aligned}$$

$$W_2(s) = \frac{4\alpha_1\beta_1 C_0}{F_0}\left(\frac{\exp\left((\alpha_1-\beta_1)l_1\right)-\exp\left(\lambda_{12}(s)l_1\right)}{\alpha_1-\beta_1-\lambda_{12}(s)}\right.$$
$$\left.-\ \frac{\exp\left((\alpha_1-\beta_1-p_1(s))l_1\right)-\exp\left(\lambda_{12}(s)l_1\right)}{\alpha_1-\beta_1-\lambda_{11}(s)}\right)p_2(s)\exp\left(\lambda_{22}(s)\left(l_2-l_1\right)\right)$$

$$W_3(s) = -\frac{2\alpha_1\beta_1\tilde{C}_0\exp\left(\left(\frac{\alpha_1}{1-\alpha}-\beta_1\right)l_1\right)}{(1-\alpha)F_0}$$
$$\times\left((1-\alpha)\left(\exp\left(-p_1(s)l_1\right)-1\right)\left(W_{31}+W_{32}\right)+W_{33}\left(W_{34}-W_{35}\right)\right)$$

$$\begin{aligned}
W_{31} &= \left(a_{21}+a_{22}s+p_2(s)\right)\frac{\exp\left(\left(\frac{\alpha_1}{1-\alpha}-\beta_1-p_2(s)\right)(l_2-l_1)\right)-\exp(\lambda_{22}(s)(l_2-l_1))}{\frac{\alpha_1}{1-\alpha}-\beta_1-\lambda_{21}(s)}\\
W_{32} &= \left(p_2(s)-a_{21}+a_{22}s+\right)\frac{\exp\left(\left(\frac{\alpha_1}{1-\alpha}-\beta_1\right)(l_2-l_1)\right)-\exp(\lambda_{22}(s)(l_2-l_1))}{\frac{\alpha_1}{1-\alpha}-\beta_1-\lambda_{22}(s)}\\
W_{33} &= \left(a_{11}+a_{12}s+p_1(s)+\left(p_1(s)-a_{11}-a_{12}s\right)\exp\left(-p_1(s)l_1\right)\right)\\
W_{34} &= \frac{\exp\left(\left(\frac{\alpha_1}{1-\alpha}-\beta_1-p_2(s)\right)(l_2-l_1)\right)-\exp(\lambda_{22}(s)(l_2-l_1))}{\frac{\alpha_1}{1-\alpha}-\beta_1-\lambda_{21}(s)}\\
W_{35} &= \frac{\exp\left(\left(\frac{\alpha_1}{1-\alpha}-\beta_1\right)(l_2-l_1)\right)-\exp(\lambda_{22}(s)(l_2-l_1))}{\frac{\alpha_1}{1-\alpha}-\beta_1-\lambda_{22}(s)}
\end{aligned}$$

Now, one can obtain the explicit expression for the transfer function $G(s)$ through $W_1(s)$, $W_2(s)$ and $W_3(s)$, see (5.23) and (5.24)–(5.26):

$$G(s) = W_1^{-1}(s)\left(W_2(s)+W_3(s)\right) \tag{5.32}$$

A central objective is to synthesize a closed-loop state feedback regulation such that the controlled output $y(t)$ tracks a reference signal $y_r(t)$ generated by a known finite-dimensional signal process:

$$\begin{aligned}
\dot{w}(t) &= Sw(t), t \geq 0, w(0) \in \mathbb{C}^n && (5.33)\\
y_r(t) &= Qw(t), t \geq 0 && (5.34)
\end{aligned}$$

where Q is a matrix of appropriate dimensions. $S : D(S) \subset \mathbb{C}^n \to \mathbb{C}^n$ is a skew-Hermitian matrix whose eigenvalues are on the imaginary axis, i.e. iw_k where $i = \sqrt{-1}$. Then, we have

$$Sw = \sum_{k=1}^{n} iw_k \left\langle w, \phi_k \right\rangle \phi_k \tag{5.35}$$

where $(\phi_k)_{k\in N}$ are eigenvectors of S and form an orthonormal basis of $\mathbb{C}^n$. Then, $w(t)$ is given by

$$\begin{aligned} w(t) &= e^{St}w(0) = \sum_{k=1}^{n} e^{iw_k t} \langle w(0), \phi_k\rangle \phi_k \\ &= \sum_{k=1}^{n} (\cos(w_k t) + i\sin(w_k t)) \langle w(0), \phi_k\rangle \phi_k \end{aligned} \tag{5.36}$$

Remark 17. *In this chapter, the signal process (5.33) elaborated is the one that can generate arbitrary reference signals. More precisely, from (5.36), the components of $w(t)$ are the combination of $sin(w_k t)$ or $sin(w_k t + \varphi)$. Therefore, if we assign the desired values to w_k and n to be large enough, we can generate arbitrary reference signals $y_r(t)$ by selecting the adequate vector Q in (5.34).*

5.3 State Feedback Regulator Design

In this section, we proceed with the design of the state feedback regulator, based on the infinite-dimensional representation (5.16), (5.17), such that the following tracking error $e(t) = y(t) - y_r(t)$ attenuates exponentially to zero as $t \to +\infty$: i.e.,

$$\lim_{t\to\infty} e(t) = \lim_{t\to\infty} (y(t) - y_r(t)) = 0, \forall x(0) \in H, \forall w(0) \in \mathbb{C}^n \tag{5.37}$$

The system operator A defined by (5.17) is a non-spectral operator, i.e. the spectrum of A is empty, see [78]. This technical part is major obstacle in proving stability of the regulator design and the spectrum theory can not be utilized to extend traditional regulator design methods for spectral systems (e.g., parabolic PDE systems) to first order hyperbolic PDE systems. In order to proceed with the state feedback regulator problem, we first make the following assumptions:

Assumption 11. *The spectrum of the system (5.33), (5.34) is contained in the resolvent* *set of A: $\rho(A)$, i.e., $iw_k \in \rho(A)$ for $k \in N$.*

Assumption 12. *There exists the state feedback gain $K \in \mathcal{L}(H, U)$ such that $A + BK$ generates an exponentially stable C_0-semigroup $T_{AK}(t)$ on H, i.e, the pair (A, B) is stabilizable.*

Based on the above assumptions, the following proposition enables the design of the state feedback regulator so that the controlled output $y(t)$ tracks the reference signal $y_r(t)$.

Proposition 2. *Under Assumption 11, Assumption 12 and the assumption that C is $A-$admissible, (see Definition 1 in [70]) the state feedback regulator problem is solvable if there exist operators $\Pi \in \mathcal{L}(C^n, H)$ with $\Pi D(S) \subset D(A)$ and $\Gamma \in \mathcal{L}(C^n, U)$ such that the following constrained Sylvester equation holds:*

$$\Pi S = A\Pi + B\Gamma \tag{5.38}$$

$$C\Pi - Q = 0 \tag{5.39}$$

The state feedback law is given by:

$$u(t) = Kz(t) + (\Gamma - K\Pi)w(t) \tag{5.40}$$

where K stabilizes the pair (A, B).

Proof. Plug (5.40) into the system (5.16), the closed-loop system is in the following form:

$$\dot{z}(t) = (A + BK)z(t) + (B(\Gamma - K\Pi))\, w(t)$$

Then, the mild solution of the above equation yields to:

$$z(t) = T_{AK}(t)z(0) + \int_0^t T_{AK}(t - \tau)\, (B(\Gamma - K\Pi))\, w(\tau)d\tau$$

Because of (5.38), (5.39), the mild solution can be rewritten as:

$$\begin{aligned} z(t) &= T_{AK}(t)z(0) + \int_0^t T_{AK}(t-\tau)\left(\Pi S - (A+BK)\Pi\right) w(\tau) d\tau \\ &= T_{AK}(t)z(0) + \int_0^t T_{AK}(t-\tau)\left(\Pi \dot{w}(\tau) - (A+BK)\Pi w(\tau)\right) d\tau \\ &= T_{AK}(t)z(0) + \int_0^t \frac{d}{d\tau}\left(T_{AK}(t-\tau)\Pi w(\tau)\right) d\tau \\ &= T_{AK}(t)\left(z(0) - \Pi w(0)\right) + \Pi w(t) \end{aligned}$$

Then, the tracking error in (6.65) can be rewritten as:

$$\begin{aligned} e(t) &= Cz(t) - Qw(t) \\ &= CT_{AK}(t)\left(z(0) - \Pi w(0)\right) + \left(C\Pi - Q\right) w(t) \end{aligned}$$

$T_{AK}(t)$ is exponentially stable and C is $A-$admissible on H, thus (5.39) indicates that the tracking error decays to zero as $t \to +\infty$. In order to ensure that Sylvester equation (5.38), (5.39) has unique solution, A and S have no common eigenvalues, and this can be realized by letting the Assumption 11 hold (see [79]). □

5.3.1 Stability of the linearized system

In this section, the chapter provides sufficient conditions such that the system (5.13)–(5.15) is stable in the sense that the transfer function satisfies $G(s) \in H_\infty$ (belongs to the right half-plane, Hardy space, see [80]). In particular, it is proved that a classical countercurrent heat exchanger system is stable in [75].

Lemma 17. *The transfer function $G(s) \in H_\infty$ (right half-plane) if $W_1^{-1}(s)$ in (5.32) is analytical in $Re(s) \geq 0$.*

Proof. From (5.32), $W_1^{-1}(s)$ is analytic in $Re \geq 0$, which implies that $G(s)$ is analytic in $Re(s) \geq 0$. Now, we claim that $G(s)$ is bounded due to the following facts:

First, the exponential terms in $W_1(s)$, $W_2(s)$ and $W_3(s)$ have exponents whose real parts are negative.

Second, the polynomial parts in both $p_1(s)p_2(s)/W_1(s)$ and $(W_1(s)+W_2(s))$ are with the identical order of the numerator and that of the denominator. Therefore, $p_1(s)p_2(s)/W_1(s)$ and $(W_1(s)+W_2(s))$ are bounded in $Re(s) \geq 0$.

According to the definition of $p_1(s)$ and $p_2(s)$, $G(s)$ can be rewritten as:

$$G(s) = \frac{p_1(s)p_2(s)}{W_1(s)} \left(W_2(s) + W_3(s)\right) \frac{1}{p_1(s)p_2(s)} \tag{5.41}$$

From (5.41), $G(s)$ is clearly bounded in $Re(s) \geq 0$ and therefore by definition, $G(s) \in H_\infty$ (right-half plane). □

Proposition 3. *Assume that $\alpha_1 \neq \beta_1$ and $\alpha_1/(1-\alpha) \neq \beta_1$, then $W_1^{-1}(s)$ is analytical in $Re(s) \geq 0$ if*

$$w_1 w_2 < 1 \tag{5.42}$$

where

$$w_1 = \frac{4\alpha_1\beta_1}{\left(\alpha_1 + \beta_1 + |\alpha_1 - \beta_1|\right)\left(\frac{\alpha_1}{1-\alpha} + \beta_1 + \left|\frac{\alpha_1}{1-\alpha} - \beta_1\right|\right)} \tag{5.43}$$

$$w_2 = \frac{\left(1 + \exp(-|\alpha_1 - \beta_1|\, l_1)\right)\left(1 + \exp\left(-\left|\frac{\alpha_1}{1-\alpha} - \beta_1\right|(l_2 - l_1)\right)\right)}{\left(1 - \frac{4\alpha_1\beta_1 \exp(-|\alpha_1-\beta_1| l_1)}{(\alpha_1+\beta_1+|\alpha_1-\beta_1|)^2}\right)\left(1 - \frac{\frac{4\alpha_1\beta_1}{1-\alpha}\exp\left(-\left|\frac{\alpha_1}{1-\alpha}-\beta_1\right|(l_2-l_1)\right)}{\left(\frac{\alpha_1}{1-\alpha}+\beta_1+\left|\frac{\alpha_1}{1-\alpha}-\beta_1\right|\right)^2}\right)} \tag{5.44}$$

Proof. In (5.32), $W_1(s)$ can be written as:

$$W_1(s) = \hat{Q}_1(s)\hat{Q}_2(s) - \hat{P}_1(s)\hat{P}_2(s)$$

where

$$\hat{Q}_1(s) = a_{11} + a_{12}s + p_1(s) + (p_1(s) - a_{11} - a_{12}s)\exp(-p_1(s)l_1)$$

$$\hat{Q}_2(s) = a_{21} + a_{22}s + p_2(s) + (p_2(s) - a_{21} - a_{22}s)\exp(-p_2(s)(l_2 - l_1))$$

$$\hat{P}_1(s) = 2\beta_1\left(1 - \exp(-p_1(s)l_1)\right)$$

$$\hat{P}_2(s) = 2\alpha_1\left(1 - \exp(-p_2(s)(l_2 - l_1))\right)$$

From $\hat{Q}_2(s)$, we can write:

$$\frac{1}{\hat{Q}_2(s)} = \frac{1}{a_{21} + a_{22}s + p_2(s)} \times \frac{1}{1 + \frac{(p_2(s) - a_{21} - a_{22}s)}{a_{21} + a_{22}s + p_2(s)} \exp(-p_2(s)\,(l_2 - l_1))}$$

It is easy to see that:

$$\left| \frac{(p_2(s) - a_{21} - a_{22}s)}{a_{21} + a_{22}s + p_2(s)} \exp(-p_2(s)\,(l_2 - l_1)) \right| < 1$$

which implies that $1/\hat{Q}_2(s) \in H_\infty$. In the same way, we can prove that $1/\hat{Q}_1(s)\hat{Q}_2(s) \in H_\infty$.

In particular,

$$\frac{1}{W_1(s)} = \frac{1}{\hat{Q}_1(s)\hat{Q}_2(s)} \times \frac{1}{1 - \frac{\hat{P}_1(s)\hat{P}_2(s)}{\hat{Q}_1(s)\hat{Q}_2(s)}}$$

where

$$\frac{\hat{P}_1(s)\hat{P}_2(s)}{\hat{Q}_1(s)\hat{Q}_2(s)} = \frac{4\alpha_1\beta_1}{(a_{11}+a_{12}s+p_1(s))(a_{21}+a_{22}s+p_2(s))}$$
$$\times \frac{(1-\exp(-p_1(s)l_1))(1-\exp(-p_2(s)(l_2-l_1)))}{\left(1+\frac{4\alpha_1\beta_1}{(a_{11}+a_{12}s+p_1(s))^2}\exp(-p_1(s)l_1)\right)\left(1+\frac{4\alpha_1\beta_1/(1-\alpha)}{(a_{21}+a_{22}s+p_2(s))^2}\exp(-p_2(s)(l_2-l_1))\right)}$$

Then, the condition (5.42) means $\left|\frac{\hat{P}_1(s)\hat{P}_2(s)}{\hat{Q}_1(s)\hat{Q}_2(s)}\right| < 1$, i.e., $1/W_1(s)$ is analytic in $Re(s) \geq 0$. □

5.3.2 The stabilization feedback gain

From the previous section, sufficient conditions have been given such that $G(s) \in H_\infty$, in the sense that the system generator A defined by (5.17) generates an exponentially stable C_0-semigroup e^{At} on the state space H, i.e., $\left\|e^{At}\right\| \leq M_0 e^{-\varepsilon t}$ where $M_0 > 0$ and $\varepsilon > 0$. In addition, it is reasonable that $-\varepsilon \in \rho(A)$, since ε can be chosen such that $-\varepsilon > w_0$, where w_0 is the growth bound of A. Therefore, once the system generator A is exponentially stable, Assumption 11 and Assumption 12 hold naturally (see [80]). In this section, the following theorem provides a sufficient condition that proposes an alternative way to select a simple novel stabilization feedback gain ('low gain') such that $A + BK$ is an infinitesimal generator of an exponentially stable C_0-semigroup $T_{AK}(t)$ on H.

Lemma 18. *Under the fact that A is the generator of an exponentially stable C_0-semigroup on the state space H and with assumption that the operator C is $A-$admissible. There exists the stabilization feedback gain K of the form:*

$$K = kC \tag{5.45}$$

such that the perturbed operator $A + BK$ is an infinitesimal generator of an exponentially stable C_0-semigroup on H for each $k \in [-k_*, k_*]$ where $k_* > 0$.

Proof. The proof is similar to the proof part of Thm 4.3.7 in [62]. □

Remark 18. *During the proof of Lemma 18, we just need to make sure that the inequality $\left\|(I - kBCR(\lambda; A))^{-1}\right\|_{\mathcal{L}(H,H)} < +\infty$ holds, since $\sup\limits_{\mathrm{Re}(\lambda)\geq -\varepsilon} \|R(\lambda; A)\|_{\mathcal{L}(H,H)} \leq M$. Then, we actually can conclude that for any $k \neq \pm\frac{1}{\|B\|_H K_1}$ and $|k| < +\infty$, $\left\|(I - kBCR(\lambda; A))^{-1}\right\|_{\mathcal{L}(H,H)} < +\infty$. In this chapter, we chose an alternative way to limit the selection of k in a small range $[-k_*, k_*]$ with $k_* < \frac{1}{\|B\|_H K_1}$, i.e, 'low gain'. In other words, $k \in [-k_*, k_*]$ is a sufficient condition ensuring $\left\|(I - kBCR(\lambda; A))^{-1}\right\|_{\mathcal{L}(H,H)} < +\infty$. In practice, alternatively k can also be selected outside of the range $[-k_*, k_*]$ as long as $(I - kBCR(\lambda; A)) \neq 0$ and* $\sup\left\{\|R(\lambda; A + BK)\|_{\mathcal{L}(H,H)}; \mathrm{Re}(\lambda) \geq -\frac{\varepsilon}{2}\right\} < +\infty$.

Remark 19. *According to the form of the feedback stabilization gain (5.45), the control law $u(t)$ in (5.40) has the form:*

$$u(t) = ky(t) + (\Gamma - kC\Pi)w(t)$$

In this case, if the pair (Q, S) is observable, a finite-dimensional observer can be designed to estimate the exosystem state $w(t)$ through the reference $y_r(t)$. Assume that the controlled output $y(t)$ and the reference signal $y_r(t)$ are measurable, actually an output feedback regulator can be synthesized to realize the tracking control.

5.4 Numerical Simulations

From the previous section, the dynamical evolution of the linearized system is given as the variation dynamics around the equilibrium profiles. In this section, we first present the temperature equilibrium profiles and then the evolution of the linearized system with a set of physical parameters. Subsequently, the results developed for the state feedback regulator design are applied.

First, the values of the parameters appearing in the system (5.13), (5.14) are given in Table 5.2. According to the values in Table 5.2 and the equations (5.9)-(5.11), the equilibrium

Table 5.2: The values of model parameters.

α_1	β_1	α_2	β_2	l_1	l_2	α	T_{01}	T_{02}	T_{03}	F_0
0.02	0.01	0.1	0.05	100	200	0.65	80	15	20	30

temperature profiles are presented in Figure 5.4. Utilizing the values of parameters in Table 5.2, we can calculate $w_1 = 0.175$ and $w_2 = 1.6939$ which obviously satisfy the inequality in (5.42), i.e., $w_1 w_2 = 0.2964 < 1$. Therefore, the operator A is an infinitesimal generator of an exponentially stable semigroup e^{At} on H. Moreover, we can see that the linearized system is stable in Figure 5.5 and Figure 5.6, where we set initial conditions as:

$$\begin{aligned}
R_1^-(x,0) &= 10\cos\left(\tfrac{\pi x}{2l_2}\right), & R_2^-(x,0) &= 5\sin\left(\tfrac{\pi x}{l_1}\right), 0 < x < l_1 \\
R_1^+(x,0) &= (1-\alpha)10\cos\left(\tfrac{\pi x}{2l_2}\right), & R_2^+(x,0) &= 5\sin\left(\tfrac{\pi x}{l_1}\right), l_1 < x < l_2
\end{aligned}$$

The primary objective of this chapter is to construct a state feedback regulator that will properly shape the amplitude and phase of the output. Thus, we now proceed with the design of the operators K, Π and Γ in the state feedback law (5.40). In particular, K is a stabilizing feedback operator and in addition K together with Π and Γ adjusts the amplitude and the phase of the output.

First, according to Theorem 18, we choose the stabilization feedback gain as: $K = kC$. Therefore, we need first to verify the A-admissibility of the operator C. Since, we can

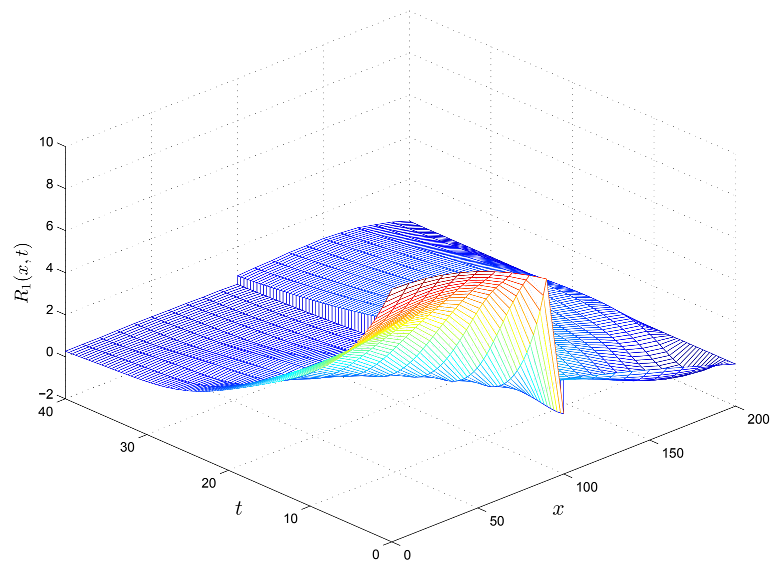

Figure 5.5: Evolution of the state of linearized system: $R_1(x,t)$ with zero input, i.e., $u(t) = 0$.

calculate:

$$\begin{aligned}
\left\| Ce^{At}z(x) \right\|_Y &= \left\| \begin{bmatrix} 0 & 0 & 0 & C_\Lambda \end{bmatrix} \begin{bmatrix} e^{A_1 t} & 0 \\ 0 & e^{A_2 t} \end{bmatrix} \begin{bmatrix} R_1^-(x,t) \\ R_2^-(x,t) \\ R_1^+(x,t) \\ R_2^+(x,t) \end{bmatrix} \right\|_Y \\
&= \left\| \begin{bmatrix} 0 & C_\Lambda \end{bmatrix} e^{A_2 t} \begin{bmatrix} R_1^+(x,t) \\ R_2^+(x,t) \end{bmatrix} \right\|_Y \\
&= \left\| \begin{bmatrix} 0 & 1 \end{bmatrix} e^{A_2 t} \begin{bmatrix} R_1^+(l_2,t) \\ R_2^+(l_2,t) \end{bmatrix} \right\|_Y
\end{aligned} \tag{5.46}$$

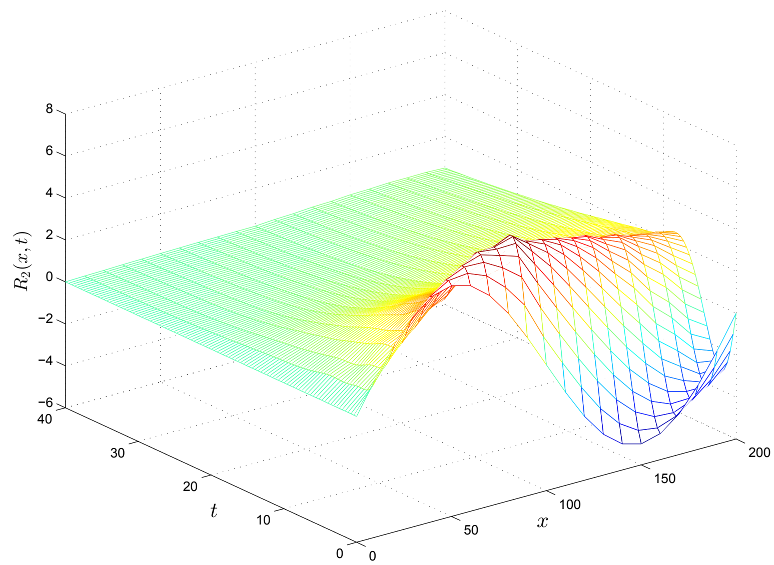

Figure 5.6: Evolution of the state of linearized system: $R_2(x,t)$ with zero input, i.e., $u(t) = 0$.

then, we can rewrite (5.46) as:

$$\left\| Ce^{At}z(x) \right\|_Y = \left\| \begin{bmatrix} 0 & 0 & 0 & 1 \end{bmatrix} e^{At} \begin{bmatrix} 0 \\ 0 \\ R_1^+(l_2,t) \\ R_2^+(l_2,t) \end{bmatrix} \right\|_Y$$

$$\leq \begin{bmatrix} 0 & 0 & 0 & 1 \end{bmatrix} \left\| e^{At} z(l_2) \right\|_H$$
$$\leq \begin{bmatrix} 0 & 0 & 0 & 1 \end{bmatrix} M_0 e^{-\varepsilon t} \| z(x) \|_H$$

Thus, C is $A-$admissible. The performance of a 'low gain' controller is investigated in Figure 5.7. Without loss of generality, the temperature evolution $R_1^+(\cdot,t)$ at point $x = 10$ is chosen in Figure 5.7. Based on the performance of the controller in Figure 5.7, the range of k can be set as $k \in [-1, 1]$ and we choose $k = -0.7$ in this example.

Then, we design the exosystem (signal process) of the form (5.33), (5.34) to generate the

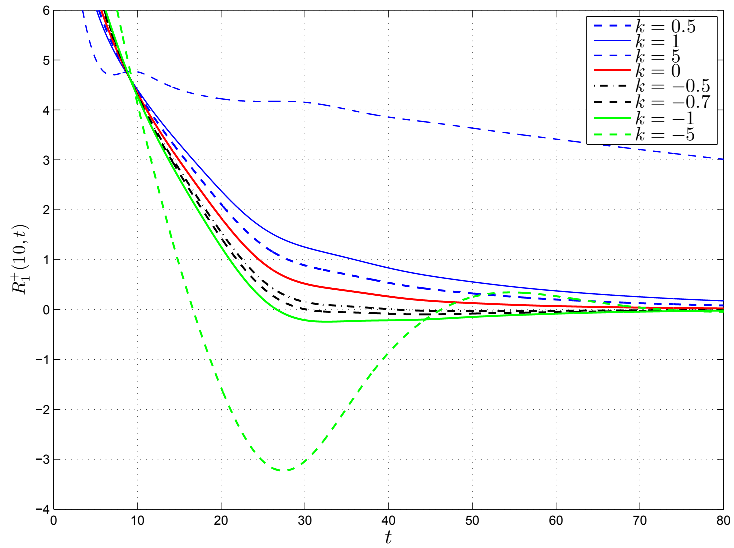

Figure 5.7: The performance of a 'low gain' controller according to different values of k, based on the temperature evolution $R_1^+(10,t)$.

reference signal $y_r(t)$, where the matrices S, Q and the initial value w_0 are chosen as:

$$S = \begin{bmatrix} 0 & 0 & 0 \\ 0 & 0 & 2 \\ 0 & -2 & 0 \end{bmatrix}, \; Q = \begin{bmatrix} 1 & 1 & 0 \end{bmatrix}$$
$$w_0 = \begin{bmatrix} -33 & 0 & 10 \end{bmatrix}^T$$

such that this process gives

$$w(t) = \begin{bmatrix} w_1(t) \\ w_2(t) \\ w_3(t) \end{bmatrix} = \begin{bmatrix} -33 \\ 10\sin(2t) \\ 10\cos(2t) \end{bmatrix}$$

and then, $y_r(t) = -33 + 10sin(2t)$.

Remark 20. *Here, we design the reference signal as: $y_r(t) = -33 + 10sin(2t)$. One can note that in the original nonlinear system, steady output $T_{2e}^+(l_2) \approx 33$. We design the state feedback regulator such that the output $R_2^+(l_2,t)$ of the linearized system tracks $y_r(t)$. From the* *previous section, we know that the output of the original system* $T_2^+(l_2,t) = R_2^+(l_2,t) + T_2^+(l_2)$ *which implies under the control of the state feedback regulator, that* $T_2^+(l_2,t)$ *tracks the signal* $y_r' = 10sin(2t)$.

We now turn to the calculation of Π and Γ such that the constrained Sylvester equation (5.38), (5.39) holds. From Proposition 1, since $\Pi \in \mathcal{L}(C^3, H)$ and $\Gamma \in \mathcal{L}(C^3, U)$, we set Π and Γ as:

$$(\Pi w)(x) = \begin{bmatrix} \Pi_{11}^-(x) & \Pi_{12}^-(x) & \Pi_{13}^-(x) \\ \Pi_{21}^-(x) & \Pi_{22}^-(x) & \Pi_{23}^-(x) \\ \Pi_{11}^+(x) & \Pi_{12}^+(x) & \Pi_{13}^+(x) \\ \Pi_{21}^+(x) & \Pi_{22}^+(x) & \Pi_{23}^+(x) \end{bmatrix} \begin{bmatrix} w_1(t) \\ w_2(t) \\ w_3(t) \end{bmatrix} \tag{5.47}$$

where $\Pi_{ji}^-(x)$ are defined in $0 < x < l_1$ and $\Pi_{ji}^+(x)$ are defined in $l_1 < x < l_2$, where $j = 1,2$ and $i = 1,2,3$.

$$\Gamma = \begin{bmatrix} \gamma_1 & \gamma_2 & \gamma_3 \end{bmatrix} \in \mathcal{L}(C^3, U) \tag{5.48}$$

Now, one can rewrite the equation (5.47) as:

$$\Pi(x) = \begin{bmatrix} \Pi_1(x) & \Pi_2(x) & \Pi_3(x) \end{bmatrix}$$

According to (5.38), (5.39), one obtains:

$$A\Pi_1(x) = -B\gamma_1 \tag{5.49}$$

$$A\Pi_2(x) + 2\Pi_3(x) = -B\gamma_2 \tag{5.50}$$

$$A\Pi_3(x) - 2\Pi_2(x) = -B\gamma_3 \tag{5.51}$$

$$C\Pi_1(x) = 1,\ C\Pi_2(x) = 1,\ C\Pi_3(x) = 0 \tag{5.52}$$

From (5.49) and (5.52), one obtains:

$$\begin{aligned} & C\Pi_1(x) = -C(0-A)^{-1}B\gamma_1 = G(0)\gamma_1 = 1 \\ & \Rightarrow \gamma_1 = \tfrac{1}{G(0)} = 6.239 \end{aligned} \tag{5.53}$$

Multiplying (5.51) by $i = \sqrt{-1}$ and adding the results to (5.50), one has:

$$i\,(i2 - A)\,\Pi_3(x) + (i2 - A)\,\Pi_2(x) = B\,(\gamma_2 + i\gamma_3) \tag{5.54}$$

Recall that $i2 \in \rho(A)$, one can write the above equation as:

$$C\Pi_2(x) + iC\Pi_3(x) = C(i2 - A)^{-1}B\,(\gamma_2 + i\gamma_3) = G(i2)\,(\gamma_2 + i\gamma_3) \tag{5.55}$$

One can define the notation:

$$\mu_1 = \mathrm{Re}\,(G(i2))\,,\ \mu_2 = \mathrm{Im}\,(G(i2))$$

where Re and Im are the real part and imaginary part.

Now, one can write (5.55) in terms of μ_1 and μ_2:

$$C\Pi_2(x) + iC\Pi_3(x) = \gamma_2\mu_1 - \gamma_3\mu_2 + i\,(\gamma_2\mu_2 + \gamma_3\mu_1)$$

From (5.52), one obtains:

$$\gamma_2\mu_1 - \gamma_3\mu_2 = C\Pi_2(x) = 1 \tag{5.56}$$

$$\gamma_2\mu_2 + \gamma_3\mu_1 = C\Pi_3(x) = 0 \tag{5.57}$$

(5.56), (5.57) provide the explicit expression of γ_2 and γ_3, namely:

$$\begin{aligned} \gamma_2 &= \tfrac{\mu_1}{\mu_1^2+\mu_2^2} = \tfrac{\mathrm{Re}(G(i2))}{|G(i2)|^2} = -5.9872, \\ \gamma_3 &= -\tfrac{\mu_2}{\mu_1^2+\mu_2^2} = -\tfrac{\mathrm{Im}(G(i2))}{|G(i2)|^2} = 7.3687 \end{aligned}$$

Now, we obtain all the components of Γ and we note that the transfer function $G(s)$ is essential.

Given γ_1, γ_2 and γ_3, one can solve (5.49)–(5.51) to obtain Π:

$$\begin{bmatrix} A_1 & 0 \\ 0 & A_2 \end{bmatrix} \begin{bmatrix} \Pi_{11}^-(x) \\ \Pi_{21}^-(x) \\ \Pi_{11}^+(x) \\ \Pi_{21}^+(x) \end{bmatrix} = - \begin{bmatrix} \frac{1}{\rho_1 s_1} \frac{dT_1^-(x)}{dx} \\ 0 \\ \frac{1-\alpha}{\rho_1 s_1} \frac{dT_1^+(x)}{dx} \\ 0 \end{bmatrix} \gamma_1 \tag{5.58}$$

$$\begin{bmatrix} A_1 & 0 \\ 0 & A_2 \end{bmatrix} \begin{bmatrix} \Pi_{12}^-(x) \\ \Pi_{22}^-(x) \\ \Pi_{12}^+(x) \\ \Pi_{22}^+(x) \end{bmatrix} + 2 \begin{bmatrix} \Pi_{13}^-(x) \\ \Pi_{23}^-(x) \\ \Pi_{13}^+(x) \\ \Pi_{23}^+(x) \end{bmatrix} = - \begin{bmatrix} \frac{1}{\rho_1 s_1} \frac{dT_1^-(x)}{dx} \\ 0 \\ \frac{1-\alpha}{\rho_1 s_1} \frac{dT_1^+(x)}{dx} \\ 0 \end{bmatrix} \gamma_2 \tag{5.59}$$

$$\begin{bmatrix} A_1 & 0 \\ 0 & A_2 \end{bmatrix} \begin{bmatrix} \Pi_{13}^-(x) \\ \Pi_{23}^-(x) \\ \Pi_{13}^+(x) \\ \Pi_{23}^+(x) \end{bmatrix} - \begin{bmatrix} \Pi_{12}^-(x) \\ \Pi_{22}^-(x) \\ \Pi_{12}^+(x) \\ \Pi_{22}^+(x) \end{bmatrix} = - \begin{bmatrix} \frac{1}{\rho_1 s_1} \frac{dT_1^-(x)}{dx} \\ 0 \\ \frac{1-\alpha}{\rho_1 s_1} \frac{dT_1^+(x)}{dx} \\ 0 \end{bmatrix} \gamma_3 \tag{5.60}$$

It should be noted that according to the definition of $D(A)$, the following boundary conditions are supposed to be satisfied:

$$\Pi_{1i}^-(l_1) = (1-\alpha)\,\Pi_{1i}^+(l_1), \Pi_{2i}^-(l_1) = \Pi_{2i}^+(l_1), \Pi_{1i}^+(l_2) = 0, \Pi_{2i}^-(0) = 0, i = 1, 2, 3 \tag{5.61}$$

The equations (5.58)–(5.61) can be solved off-line numerically e.g., finite difference.

Then, we now substitute the operators K, Π and Γ into (5.40) and apply the feedback control law to the linearized system:

$$\begin{aligned}
u(t) &= Kz(t) + (\Gamma - K\Pi)w(t) \\
&= kC \begin{bmatrix} R_1^-(x,t) \\ R_2^-(x,t) \\ R_1^+(x,t) \\ R_2^+(x,t) \end{bmatrix} + \left(\Gamma - kC \begin{bmatrix} \Pi_{11}^-(x) & \Pi_{12}^-(x) & \Pi_{13}^-(x) \\ \Pi_{21}^-(x) & \Pi_{22}^-(x) & \Pi_{23}^-(x) \\ \Pi_{11}^+(x) & \Pi_{12}^+(x) & \Pi_{13}^+(x) \\ \Pi_{21}^+(x) & \Pi_{22}^+(x) & \Pi_{23}^+(x) \end{bmatrix} \right) w(t) \\
&= kR_2^+(l_2,t) + \begin{bmatrix} \gamma_1 - \Pi_{21}^+(l_2) & \gamma_2 - \Pi_{22}^+(l_2) & \gamma_3 - \Pi_{23}^+(l_2) \end{bmatrix} \begin{bmatrix} w_1(t) \\ w_2(t) \\ w_3(t) \end{bmatrix}
\end{aligned}$$

with $C = \begin{bmatrix} 0 & 0 & 0 & C_\Lambda \end{bmatrix}$. The results are shown in Figure 5.8, Figure 5.9 and Figure 5.10. In Figure 5.8, under the control the proposed state feedback regulator, the output of linearized system (5.13)–(5.15): $R_2^+(l_2,t)$ tracks the reference signal $y_r(t) = -33 + 10sin(2t)$ very well. Moreover, Figure 5.8 also shows that the non-minimum phase phenomenon appears in the linearized system.

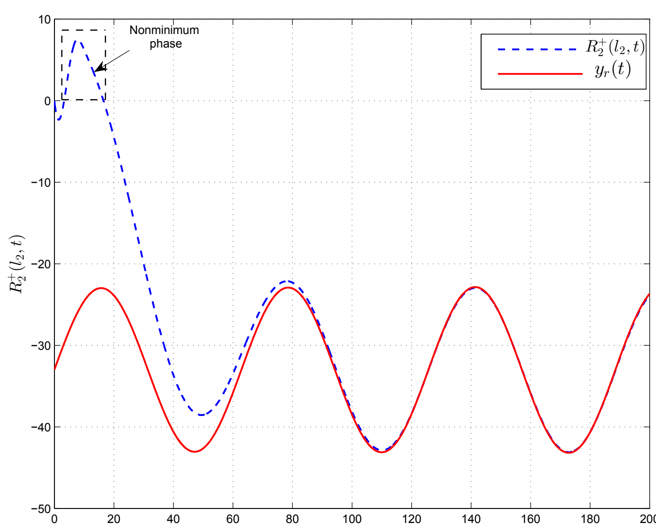

Figure 5.8: Evolution of the linearized system output: $R_2^+(l_2,t)$ tracks the reference signal $y_r(t)$ under the control of the state feedback regulator shown in (5.40).

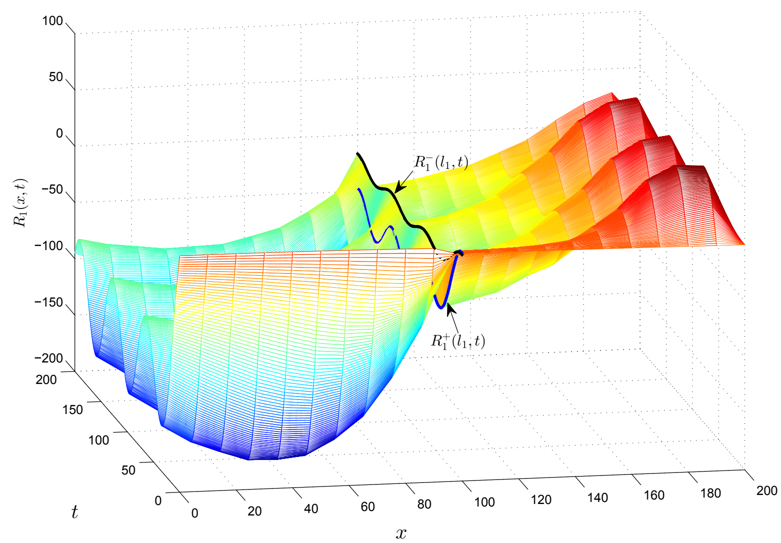

Figure 5.9: Evolution of the state of the linearized system: $R_1(x,t)$ under the control of the proposed regulator in (5.40).

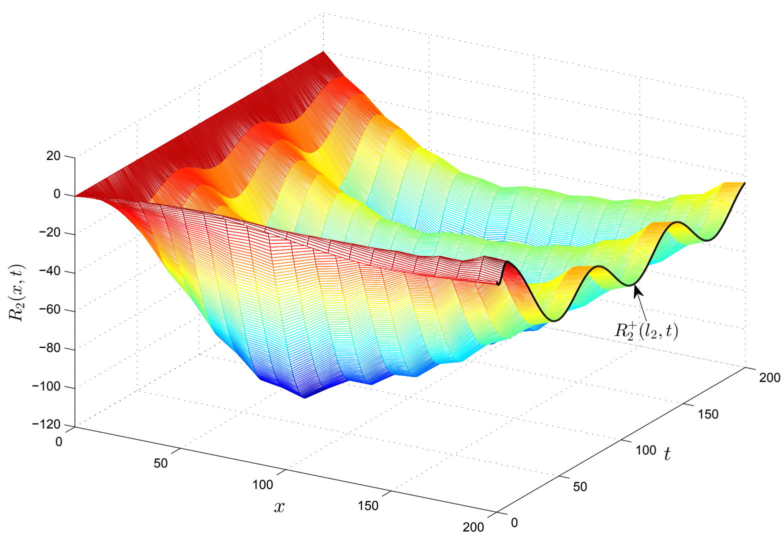

Figure 5.10: Evolution of the state of the linearized system: $R_2(x,t)$ under the control of the proposed regulator (5.40).

As for the states evolution of the original nonlinear system (5.1), (5.2), through the transformation (5.12) and the input $F_1(t) = F_0 + u(t) = F_0 + Kz(t) + (\Gamma - K\Pi)w(t)$, we can figure out that:

$$\begin{bmatrix} T_1^-(x,t) \\ T_2^-(x,t) \\ T_1^+(x,t) \\ T_2^+(x,t) \end{bmatrix} = \begin{bmatrix} R_1^-(x,t) + T_{1e}^-(x) \\ R_2^-(x,t) + T_{2e}^-(x) \\ R_1^+(x,t) + T_{1e}^+(x) \\ R_2^+(x,t) + T_{1e}^+(x) \end{bmatrix}$$

and the output $T_2^+(l_2, t)$ will track the reference signal $y_r'(t) = 10sin(2t)$.

5.5 Conclusions

This chapter considers the state feedback regulator design problem (in particular a tracking problem) for the network of countercurrent heat exchangers governed by two sets of hyperbolic PDEs. Since the controlled system is nonlinear with respect to the control input, equilibrium profiles of the states are utilized to deal with the linearization of a nonlinear system. Then, the explicit expression of transfer function is calculated and is utilized to analyze the dynamic of the resulting linearized system. Moreover, the sufficient conditions are given such that the system generator A generates an exponentially stable C_0-semigroup on state space H. With the precondition that the operator C is $A-$admissible, we proposed a 'low-gain' stabilization feedback controller, i.e., $K = kC$ so that $A + BK$ generates an exponentially stable C_0-semigroup on H. Consequently, in this chapter the state feedback regulator solves the output regulation problem for the countercurrent heat exchanger system based on the linearized model. In the simulation part, the proposed controller is applied in a numerical example. Detailed calculation procedures for all the parameters of the state feedback controller are provided. The results show the capability of the proposed controller to ensure satisfactory tracking of the reference signal.

Chapter 6

Optimal tracking control for the coupled plug flow reactor system with temperature output feedback

6.1 Introduction

Boundary control of distributed parameter systems is the most attractive area of design and control application realizations due to its appealing nature that already build industrial infrastructure and/or facilities may be additionally operationally improved by addition of the actuation power at the domains boundary (see [81], [82] and therein).

In the control literature, the optimal control problem belongs to the class of important control problems. In [27], variational approach was utilized to developed optimal control law for finite-dimensional systems and the similar variational method was extended to solve the constrained optimal state estimation problems for parabolic PDE systems in Chapter 2. Moreover, in [14], an algebraic operator Riccati equation was solved for LQ optimal control problem for infinite-dimensional systems and this approach was later applied to a class of distributed control hyperbolic PDEs, see [37]. Although the LQ optimal control law was extended to address the boundary control problem for parabolic PDE-ODE systems in [81], the considered system has to be pre-proccessed by applying the transformation in [14] such that the boundary control problem can be transformed into distributed control problem. However, applying the approach in [81] and [37] may result in a spatial distributed input which can not be applied at the boundary point. In [83], the variational approach was extended to deal with stabilization problem for scalar boundary controlled diffusion reaction process and this approach was utilized in a very restrictive way for 2×2 hyperbolic systems in [84]. Therefore, the boundary optimal control problem for coupled hyperbolic PDE systems is still an interesting topic to be addressed. In this chapter, we will construct an optimal boundary controller without the pre-processing the considered boundary controlled systems.

The output regulation problem or servo-problem is one classical and essential control problem. The problem is formulated as regulator design for the fixed plant such that the controlled output tracks a desired reference signal (and/or reject disturbance) generated by an exosystem. In order to generalize the well-developed theory of finite-dimensional systems to infinite-dimensional systems, significant efforts have been made: the geometric methods developed in [45] in finite-dimensional systems were extended to address output regulation problems for spectral infinite-dimensional systems (see [57] and [31]).

The contribution in this work is that we develop a boundary optimal controller to address tracking problems of linear coupled hyperbolic PDE systems. The weak variation approach and full state feedback internal model control (IMC) theory are combined together to realize the construction of optimal boundary controller. In particular, the reference signal to be tracked is generated by an exosystem which is well known in IMC theory and we consider the generation of ramp and even polynomial signals which are non-trivial in nature and in a literature usually only sinusoidal and step-like signal are considered, see [57] and [53].

In this work, a finite-time optimal tracking controller is designed for linear boundary-controlled coupled hyperbolic PDE systems via weak variations. This work is organized as follows: The considered plug flow reactor is introduced in Section 2. Then, the optimal control and output regulation problems are stated in Section 3. Numerical example is presented in Section 4 to verify the performance of the proposed optimal regulator. The last section includes conclusions.

6.2 System description

6.2.1 Nonlinear PDE model

We consider a nonisothermal plug flow reactor shown in Figure 6.1, with the following chemical reaction happening:

$$A \to qB$$

with the positive reaction stoichiometric coefficient, i.e. $q > 0$. Generally, based on mass and energy balance principles, the dynamics of tubular reactors are demonstrated by nonlinear coupled PDEs. Suppose that the above reaction kinetics are given by first-order kinetics w.r.t the reactant concentration c_A (mol/L) and the temperature $T(K)$, the dynamics of the reaction process can be described by the following first-order hyperbolic PDEs with T_J and c_B (mol/L) denoting the jacket temperature and the product concentration, respectively, where T_{out} is the outlet temperature $T(l,\tau)$:

$$\partial_\tau T = -v\partial_\zeta T + \frac{\Delta H}{\rho C_p} k_0 c_A \exp\left(-\frac{E}{RT}\right) - \frac{4h}{\rho C_p d}(T - k_1 T_{out} - T_J) \tag{6.1}$$

$$\partial_\tau c_A = -v\partial_\zeta c_A - k_0 c_A \exp\left(-\frac{E}{RT}\right) \tag{6.2}$$

$$\partial_\tau c_B = -v\partial_\zeta c_B + q k_0 c_A \exp\left(-\frac{E}{RT}\right) \tag{6.3}$$

with the boundary and initial conditions given, for $(\tau, \zeta) \in \mathbb{R}^+ \times [0, l]$, by

$$\begin{aligned} &T(0,\tau) = T_{in}(\tau), c_A(0,\tau) = c_{A,in}, c_B(0,\tau) = 0, \\ &T(\zeta,0) = T_0(\zeta), c_A(\zeta,0) = c_{A,0}(\zeta), c_B(\zeta,0) = 0. \end{aligned} \tag{6.4}$$

Here and in the following chapter, ∂_t and ∂_ζ denote the partial derivatives w.r.t temporal variable t and spatial variable ζ, respectively. In equations (6.1)–(6.4), v, ΔH, ρ, C_p, k_0, E, R, h, d, T_{in} and $c_{A,in}$ represent the superficial fluid velocity, the heat of reaction, the density, the specific heat, the kinetic constant, the activation energy, the ideal gas constant, the wall heat transfer coefficient, the reactor diameter, the inlet temperature, and the inlet reactant concentration, respectively. The values of these parameters are given in Table 6.1. In particular, the inlet temperature will be used as control variable of this process. Additionally, τ, ζ and l are the temporal and spatial variables, and the reactor length, respectively. In this system, the output temperature T_{out} is used as a feedback since this setup can help to save energy for the real industry so that it can reduce the energy consumption for the producing of the jacket temperature.

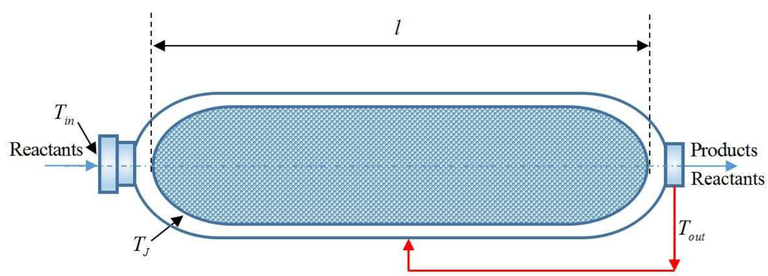

Figure 6.1: The sketchy of the plug flow reactor with the temperature output feedback and this configuration is motivated by [4].

Remark 21. *In practice, it is expected that* $0 \leq T(\zeta,\tau) \leq T_{\max}$ *and* $0 \leq c_A(\zeta,\tau) \leq c_{A,in}$, $\forall \tau \geq 0$ *and* $\forall \zeta \in [0,l]$. *Here the temperature upper bound* $T_{\max}$ *could possibly be* $+\infty$. *It turns out that the case* $T_{\max} < +\infty$ *is the most interesting one for the stability analysis of the open-loop model.*

6.2.2 Temperature and Concentration Equilibrium Profiles

In this chapter, we are concerned with equilibrium profiles of the system (6.1)–(6.4) with the form:

$$[T_e(\cdot), c_{Ae}(\cdot), c_{Be}(\cdot)]^T \tag{6.5}$$

Table 6.1: Process parameters used in the simulation.

process parameters	notations	numerical values
superficial fluid velocity	v	$0.25\ m/s$
length of the reactor	l	1 m
activation energy	E	$11250\ cal/mol$
kinetic constant	k_0	$10^6\ s^{-1}$
inlet reactant concentration	$c_{A,in}$	$0.02\ mol/L$
heat transfer coefficient	$\frac{4h}{\rho C_p d}$	$0.2\ s^{-1}$
ideal gas constant	R	$1.986\ cal/(mol.K)$
equilibrium temperature	T_e	$340\ K$
	$\hat{\delta}$	0.25

Given fixed jacket temperature T_J in (6.1), solving the equations (6.1)–(6.4) with zero temperature and concentrations changes, i.e. $\partial_\tau T = 0$, $\partial_\tau c_A = 0$ and $\partial_\tau c_B = 0$, yields equilibrium profiles for temperature $T_e(\zeta)$ and concentrations $c_{Ae}(\zeta)$, $c_{Be}(\zeta)$. In Figure 6.2 and Figure 6.3, equilibrium profiles for $T_e(\zeta)$ and $c_{Ae}(\zeta)$ are plotted under different jacket temperatures: $T_J = 200^oC$ and $T_J = 300^oC$.

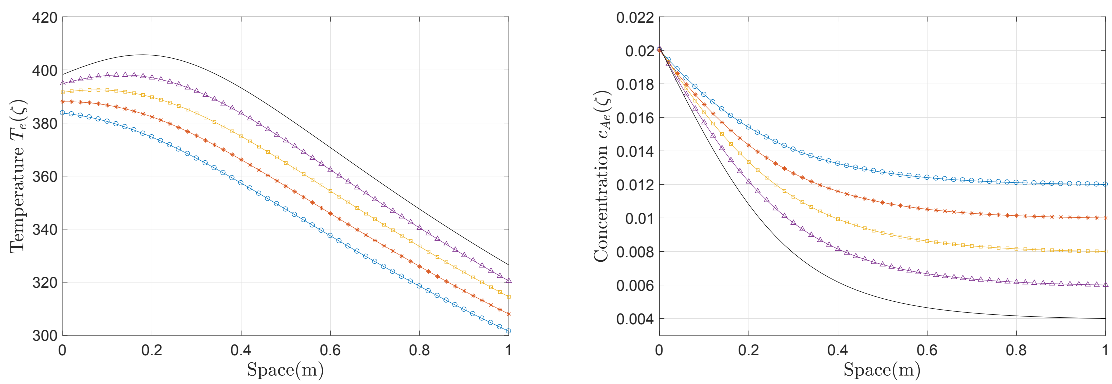

(a) (b)

Figure 6.2: Given $T_J = 200^oC$: (a) Temperature equilibrium profile; (b) Concentration profile. In the concentration profiles, we always keep boundary conditions as $c_{Ae}(0) = c_{A,in} = 0.02$mol/L.

Obviously, It is easy to see that both steady state temperature $T_e(\zeta)$ and concentration $c_{Ae}(\zeta)$ are spatially varying while the jacket temperature T_J is constant. Actually, alternative

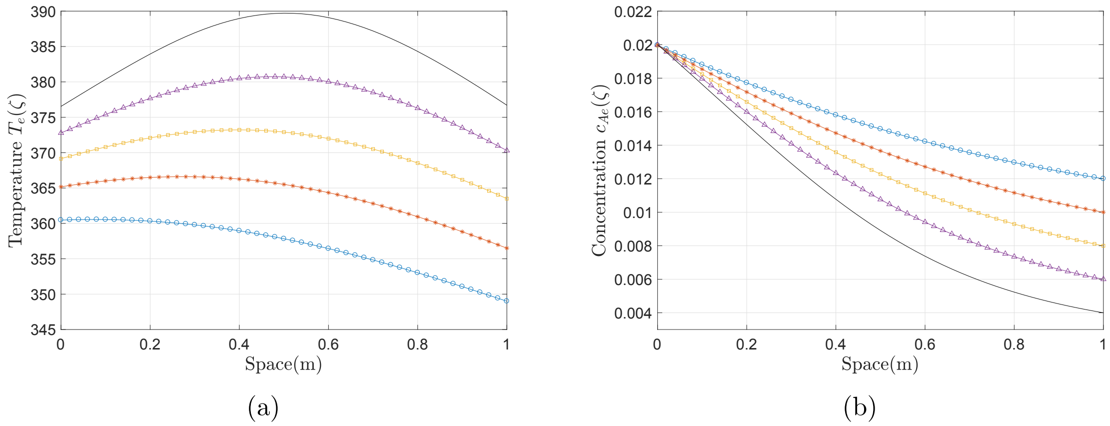

Figure 6.3: Given $T_J = 300^oC$: (a) Temperature equilibrium profile; (b) Concentration profile. In the concentration profiles, we always keep boundary conditions as $c_{Ae}(0) = c_{A,in} = 0.02$mol/L.

can be chosen such that the temperature equilibrium profile to be constant, i.e.

$$T_e(\zeta) = T_e > 0,\ \zeta \in [0, l]. \tag{6.6}$$

Then, equilibrium profiles must satisfy the boundary conditions in (6.4). According to the continuity of the function T_e, we have $T_e(\zeta) = T_{ine}$ for all $\zeta \in [0, l]$, in view of (6.5), where T_{ine} is a constant equilibrium value of $T_{in}(\tau)$ in (6.4). In other word, the constant inlet temperature determines that of the constant temperature equilibrium profile.

Due to the constant temperature equilibrium profile, it is easy to compute the reactant and product concentration equilibrium profiles:

$$c_{Ae}(\zeta) = c_{Ain} \exp(\beta_e \zeta), \zeta \in [0, l] \tag{6.7}$$

$$c_{Be}(\zeta) = q c_{Ain} \left(1 - \exp(\beta_e \zeta)\right),\ \zeta \in [0, l]. \tag{6.8}$$

where β_e is the negative constant given by $\beta_e = -(k_0/v \exp(-E/RT_e)) < 0$. Therefore, the corresponding jacket temperature equilibrium profile is as follows:

$$T_{Je}(\zeta) = (1 - k_1)T_e - \frac{vd\Delta H}{4h}\beta_e c_{Ain}\exp(\beta_e\zeta) \tag{6.9}$$

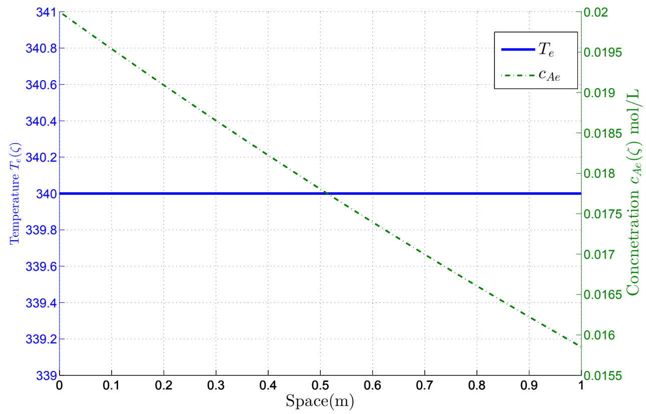

Figure 6.4: Temperature and reactant concentration equilibrium profiles.

6.2.3 Linearized PDE model

In the system (6.1)–(6.4), the product concentration c_B can be immediately calculated once the reactant concentration c_A and the temperature T are known. Hence, we only consider the first two state components, namely the reactor temperature T and the reactant concentration c_A. In following, we transform the system into dimensionless model by defining the state variables: θ_1 and θ_2 given by:

$$\theta_1 = \frac{T - T_e}{T_e}, \theta_2 = \frac{c_{A,in} - c_A}{c_{A,in}} \tag{6.10}$$

Dimensionless temporal and spatial variables are given by $t := \tau v/l$ and $z := \zeta/l$. Moreover, the jacket temperature is assumed to be kept at the equilibrium profile given by (6.9), i.e., $T_J = T_{Je}(\zeta)$. Then, the resulting system has the form with $\theta_{in} = (T_{in} - T_e)/T_e$ and

$\theta_{Je} = (T_{Je} - T_e)/T_e$, given by:

$$\begin{aligned} \partial_t \theta_1 = & -\partial_z \theta_1 - \beta\theta_1 + \hat{\alpha}\hat{\delta}(1-\theta_2)\exp\left(\tfrac{\mu\theta_1}{\theta_1+1}\right) \\ & +\beta k_1(1+\theta_1(1,t)) + \beta\theta_{Je} \end{aligned} \tag{6.11}$$

$$\partial_t \theta_2 = -\partial_z \theta_2 + \hat{\alpha}(1-\theta_2)\exp\left(\frac{\mu\theta_1}{\theta_1+1}\right) \tag{6.12}$$

with boundary conditions given as follows:

$$\theta_1(0,t) = \theta_{in}, \theta_2(0,t) = 0. \tag{6.13}$$

and initial conditions:

$$\theta_1(z,0) = \frac{T_0(zl) - T_e}{T_e}, \theta_2(z,0) = \frac{c_{A,in} - c_{A,0}(zl)}{c_{A,in}} \tag{6.14}$$

In the above equations, the parameters are given by, in terms of the original parameters:

$$\begin{aligned} \mu &= \tfrac{E}{RT_e}, \hat{\alpha} = \tfrac{k_0 l}{v}\exp(-\mu) \\ \beta &= \tfrac{4hl}{\rho C_p d v}, \hat{\delta} = \tfrac{\Delta H}{\rho C_p}\tfrac{c_{A,in}}{T_e}. \end{aligned}$$

Therefore, from (6.6)–(6.8) and (6.10), dimensionless equilibrium profiles are given by:

$$\theta_{1e} = 0, \theta_{2e} = \frac{c_{A,in} - c_{Ae}}{c_{A,in}}, \theta_{ine} = 0 \tag{6.15}$$

Then, let us consider the following transformation:

$$\widehat{x}_1 = \theta_1 - \theta_{1e}, \widehat{x}_2 = \theta_2 - \theta_{2e}, \widehat{u}_{in} = \theta_{in} - \theta_{ine} \tag{6.16}$$

The linearization of the system (6.12)–(6.16) around the equilibrium yields the following linear coupled hyperbolic PDE systems:

$$\partial_t \widehat{x}_1 = -\partial_z \widehat{x}_1 + \gamma_1(z)\widehat{x}_1 + \delta_1(z)\widehat{x}_2 + \beta k_1 \widehat{x}_1(1,t), \tag{6.17}$$

$$\partial_t \widehat{x}_2 = -\partial_z \widehat{x}_2 + \gamma_2(z)\widehat{x}_1 + \delta_2(z)\widehat{x}_2, \tag{6.18}$$

$$\widehat{x}_1(0,t) = \widehat{u}_{in}(t),\ \widehat{x}_2(0,t) = 0. \tag{6.19}$$

$$\widehat{x}_1(z,0) = \frac{T_0(zl) - T_e}{T_e}, \widehat{x}_2(z,0) = \frac{c_{Ae}(zl) - c_{A,0}(zl)}{c_{A,in}} \tag{6.20}$$

where the parameter functions are given by:

$$\begin{aligned}
\gamma_1(z) &= -\beta + \tfrac{\hat{\alpha}\hat{\delta}\mu\exp(\mu_e)}{(1+\theta_{1e})^2}\left(1-\theta_{2e}\right), \delta_1(z) = -\hat{\alpha}\hat{\delta}\exp\left(\mu_e\right), \\
\gamma_2(z) &= \tfrac{\hat{\alpha}\mu\exp(\mu_e)}{(1+\theta_{1e})^2}\left(1-\theta_{2e}\right), \delta_2(z) = -\hat{\alpha}\exp\left(\mu_e\right).
\end{aligned}$$

and the function μ_e is given by $\mu_e = \frac{\mu\theta_{1e}}{1+\theta_{1e}}$. Since $\theta_{1e} = 0$, $\mu_e = 0$. Consequently, one has:

$$\begin{aligned}
\gamma_1(z) &= -\beta + \hat{\alpha}\hat{\delta}\mu\left(1-\theta_{2e}\right), \delta_1 = -\hat{\alpha}\hat{\delta}, \\
\gamma_2(z) &= \hat{\alpha}\mu\left(1-\theta_{2e}\right), \delta_2 = -\hat{\alpha}.
\end{aligned}$$

Let us apply the following the notations and the new coordinates:

$$\begin{aligned}
&\varphi_1(z) = \exp\left(-\textstyle\int_0^z \gamma_1(s)ds\right), \\
&\varphi_2(z) = \exp\left(-\textstyle\int_0^z \delta_2(s)ds\right) = \exp(\hat{\alpha}z), \\
&\varphi(z) = \tfrac{\varphi_1(z)}{\varphi_2(z)}, \beta_1(z) = \beta\tfrac{\varphi_1(z)}{\varphi_1(1)}k_1 \\
&x_1(z,t) = \varphi_1(z)\widehat{x}_1(z,t), x_2(z,t) = \varphi_2(z)\widehat{x}_2(z,t) \\
&\alpha_1(z) = \varphi^{-1}(z)\gamma_2(z), \alpha_2(z) = \varphi(z)\delta_1
\end{aligned}$$

Then, the system (6.17)–(6.19) is equivalent to the following system:

$$\partial_t x_1(z,t) = -\partial_z x_1(z,t) + \alpha_2(z)x_2(z,t) + \beta_1(z)x_1(1,t) \tag{6.21}$$

$$\partial_t x_2(z,t) = -\partial_z x_2(z,t) + \alpha_1(z)x_1(z,t) \tag{6.22}$$

$$x_1(0,t) = U(t), x_2(0,t) = 0 \tag{6.23}$$

$$x_1(z,0) = \varphi_1(z)\frac{T_0(zl) - T_e}{T_e}, x_2(z,0) = \varphi_2(z)\frac{c_{Ae}(zl) - c_{A,0}(zl)}{c_{A,in}} \tag{6.24}$$

where the input is given by $U(t) := \varphi_1(0)\widehat{u}(t)$. In particular, we assume the output to be controlled is defined by

$$y(t) = \mathcal{C}\begin{bmatrix} x_1(t) \\ x_2(t) \end{bmatrix} \tag{6.25}$$

In this chapter, boundary, pointwise, as well as distributed outputs $y(t)$ are taken into account, which can be formulated by the formal output operator:

$$\mathcal{C}h = \sum_{j=1}^{m} f_j^T h(z_j) + \int_0^1 c^T(z)h(z)dz \tag{6.26}$$

for $h \in \mathbb{C}^2$ with $f_j \in \mathbb{R}^2$, $z_j \in [0,1]$, $j = 1,2,...,m$, and $c^T(z) = [c_i(z)] \in \mathbb{R}^2$ with $c_i(z) \in L_2(0,1)$, $i = 1,2$. When considering the case of a pointwise (including boundary) output, i.e., $z_j \in [0,1)$ and $c = 0$ in (6.26), we assume that the resulting output $y(t)$ in (6.25) is independent from the BC (6.23).

For the linearized system (6.21)–(6.24), with parameters given in Table 6.1, system parameters $\alpha_1(z)$, $\alpha_2(z)$ and $\beta_1(z)$ are shown in Figure 6.5.

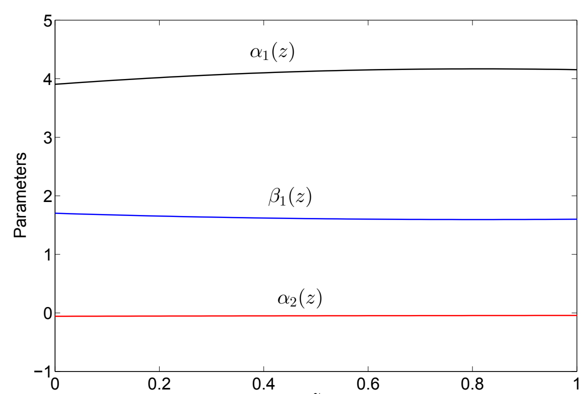

Figure 6.5: The evolution of the state $x_1(z,t)$ of the open-loop system (6.21)–(6.24).

When the parameter k_1 is chosen as $k_1 = 2$, with the set of parameters given in Table 6.1 the linearized system (6.21)–(6.24) is unstable as shown in Figure 6.6 and Figure 6.7. Furthermore, the stability analysis of the model (6.21)–(6.24) is given in the following: Let us define the operator A:

$$[Ah](z) = \begin{bmatrix} -\partial_z & \alpha_2(z) \\ \alpha_1(z) & -\partial_z \end{bmatrix} \begin{bmatrix} h_1(z) \\ h_2(z) \end{bmatrix} + \begin{bmatrix} \beta_1(z) \\ 0 \end{bmatrix} h_1(1)$$

with the domain $D(A) = \{h \in L^2(0,1)^2 : \partial_z h \in L^2(0,1)^2, h(0) = 0\}$, where $h(z) = \begin{bmatrix} h_1(z) \\ h_2(z) \end{bmatrix}$, $\alpha_1(z) > 0$, $\alpha_2(z) < 0$ and $\beta_1(z) > 0$.

Now, by assuming $\lambda \in \mathbb{C}$ to be eigenvalues of A: one has

$$Ah(z) = \lambda h(z), h(z) \neq 0$$

By expanding the above equation, one gets:

$$\frac{\partial}{\partial z}\begin{bmatrix} h_1(z) \\ h_2(z) \end{bmatrix} = \begin{bmatrix} -\lambda & \alpha_2(z) \\ \alpha_1(z) & -\lambda \end{bmatrix} \begin{bmatrix} h_1(z) \\ h_2(z) \end{bmatrix} + \begin{bmatrix} \beta_1(z) \\ 0 \end{bmatrix} h_1(1), \begin{bmatrix} h_1(0) \\ h_2(0) \end{bmatrix} = 0$$

Solving the above equation yields the solution:

$$\begin{bmatrix} h_1(z) \\ h_2(z) \end{bmatrix} = \int_0^z \left(\exp\left(\int_s^z \begin{bmatrix} -\lambda & \alpha_2(\eta) \\ \alpha_1(\eta) & -\lambda \end{bmatrix} d\eta \right) \right) \beta_1(s) ds \begin{bmatrix} 1 \\ 0 \end{bmatrix} h_1(1)$$

Premultiplying the above equation by $\begin{bmatrix} 1 & 0 \end{bmatrix}$ and evaluating $z = 1$ yields

$$h_1(1) = \begin{bmatrix} 1 & 0 \end{bmatrix} \int_0^1 \left(\exp\left(\int_s^1 \begin{bmatrix} -\lambda & \alpha_2(\eta) \\ \alpha_1(\eta) & -\lambda \end{bmatrix} d\eta \right) \right) \beta_1(s) ds \begin{bmatrix} 1 \\ 0 \end{bmatrix} h_1(1)$$

Namely, one has

$$1 = \begin{bmatrix} 1 & 0 \end{bmatrix} \int_0^1 \left(\exp\left(\int_s^1 \begin{bmatrix} -\lambda & \alpha_2(\eta) \\ \alpha_1(\eta) & -\lambda \end{bmatrix} d\eta \right) \right) \beta_1(s) ds \begin{bmatrix} 1 \\ 0 \end{bmatrix}$$
$$= \begin{bmatrix} 1 & 0 \end{bmatrix} \int_0^1 \left(\begin{bmatrix} ex_1(s) & ex_2(s) \\ ex_3(s) & ex_4(s) \end{bmatrix} \exp\left(\int_s^1 \begin{bmatrix} -\lambda & 0 \\ 0 & -\lambda \end{bmatrix} \right) d\eta \right) \beta_1(s) ds \begin{bmatrix} 1 \\ 0 \end{bmatrix}$$

where $\begin{bmatrix} ex_1(s) & ex_2(s) \\ ex_3(s) & ex_4(s) \end{bmatrix} = \exp\left(\int_s^1 \begin{bmatrix} 0 & \alpha_2(\eta) \\ \alpha_1(\eta) & 0 \end{bmatrix} d\eta \right)$ and $\exp\left(\int_s^1 \begin{bmatrix} -\lambda & 0 \\ 0 & -\lambda \end{bmatrix} d\eta \right) =$ $\begin{bmatrix} \exp(-\lambda(1-s)) & 0 \\ 0 & \exp(-\lambda(1-s)) \end{bmatrix}$. If we define the transformation matrix:

$$T(s) = \begin{bmatrix} 1 & \sqrt{\frac{-\hat{\alpha}_2(s)}{\hat{\alpha}_1(s)}} i \\ \sqrt{\frac{\hat{\alpha}_1(s)}{-\hat{\alpha}_2(s)}} i & 1 \end{bmatrix}, T^{-1}(s) = \frac{1}{2} \begin{bmatrix} 1 & -\sqrt{\frac{-\hat{\alpha}_2(s)}{\hat{\alpha}_1(s)}} i \\ -\sqrt{\frac{\hat{\alpha}_1(s)}{-\hat{\alpha}_2(s)}} i & 1 \end{bmatrix}$$

with $\hat{\alpha}_1(s) = \int_s^1 \alpha_1(\eta) d\eta$ and $\hat{\alpha}_2(s) = \int_s^1 \alpha_2(\eta) d\eta$, then we have:

$$T(s) \left(\int_s^1 \begin{bmatrix} 0 & \alpha_2(\eta) \\ \alpha_1(\eta) & 0 \end{bmatrix} d\eta \right) T^{-1}(s) = \begin{bmatrix} \left(i\sqrt{-\hat{\alpha}_1(s)\hat{\alpha}_2(s)} \right) & 0 \\ 0 & -\left(i\sqrt{-\hat{\alpha}_1(s)\hat{\alpha}_2(s)} \right) \end{bmatrix}$$

Therefore, we get

$$\exp\left(\int_s^1 \begin{bmatrix} 0 & \alpha_2(\eta) \\ \alpha_1(\eta) & 0 \end{bmatrix} d\eta \right) = T^{-1}(s)$$
$$\times \begin{bmatrix} \exp\left(i\sqrt{-\hat{\alpha}_1(s)\hat{\alpha}_2(s)} \right) & 0 \\ 0 & -\exp\left(i\sqrt{-\hat{\alpha}_1(s)\hat{\alpha}_2(s)} \right) \end{bmatrix} T(s)$$
$$= \begin{bmatrix} ex_1(s) & ex_2(s) \\ ex_3(s) & ex_4(s) \end{bmatrix}$$

where the elements $ex_1(s)$, $ex_2(s)$,$ex_2(s)$ and $ex_2(s)$ are given by:

$$\begin{aligned}
ex_1(s) &= \tfrac{1}{2}\left(\exp\left(i\sqrt{-\hat{\alpha}_1(s)\hat{\alpha}_2(s)}\right) + \exp\left(-i\sqrt{-\hat{\alpha}_1(s)\hat{\alpha}_2(s)}\right)\right) \\
&= \cos\left(\sqrt{-\hat{\alpha}_1(s)\hat{\alpha}_2(s)}\right) \\
ex_2(s) &= \tfrac{1}{2}i\sqrt{\tfrac{-\hat{\alpha}_2(s)}{\hat{\alpha}_1(s)}}\left(\exp\left(i\sqrt{-\hat{\alpha}_1(s)\hat{\alpha}_2(s)}\right) - \exp\left(-i\sqrt{-\hat{\alpha}_1(s)\hat{\alpha}_2(s)}\right)\right) \\
&= -\sqrt{\tfrac{-\hat{\alpha}_2(s)}{\hat{\alpha}_1(s)}}\sin\left(\sqrt{-\hat{\alpha}_1(s)\hat{\alpha}_2(s)}\right) \\
ex_3(s) &= -\tfrac{1}{2}i\sqrt{\tfrac{\hat{\alpha}_1(s)}{-\hat{\alpha}_2(s)}}\left(\exp\left(i\sqrt{-\hat{\alpha}_1(s)\hat{\alpha}_2(s)}\right) - \exp\left(-i\sqrt{-\hat{\alpha}_1(s)\hat{\alpha}_2(s)}\right)\right) \\
&= \sqrt{\tfrac{\hat{\alpha}_1(s)}{-\hat{\alpha}_2(s)}}\sin\left(\sqrt{-\hat{\alpha}_1(s)\hat{\alpha}_2(s)}\right) \\
ex_4(s) &= \tfrac{1}{2}\left(\exp\left(i\sqrt{-\hat{\alpha}_1(s)\hat{\alpha}_2(s)}\right) + \exp\left(-i\sqrt{-\hat{\alpha}_1(s)\hat{\alpha}_2(s)}\right)\right) \\
&= \cos\left(\sqrt{-\hat{\alpha}_1(s)\hat{\alpha}_2(s)}\right)
\end{aligned}.$$

Finally, we obtain:

$$\begin{aligned}
1 &= \begin{bmatrix} 1 & 0 \end{bmatrix} \int_0^1 \left(\begin{bmatrix} ex_1(s) & ex_2(s) \\ ex_3(s) & ex_4(s) \end{bmatrix} \exp\left(\int_s^1 \begin{bmatrix} -\lambda & 0 \\ 0 & -\lambda \end{bmatrix}\right) d\eta\right) \beta_1(s) ds \begin{bmatrix} 1 \\ 0 \end{bmatrix} \\
&= \int_0^1 ex_1(s)\beta_1(s)\exp\left(\lambda(s-1)\right) ds
\end{aligned}$$

From the above equation, it is easy to conclude that for the case $ex_1(s)\beta_1(s) > 1$, the real part of eigenvalue λ has to be always positive, which indicates that the model (6.21)–(6.24) is unstable.

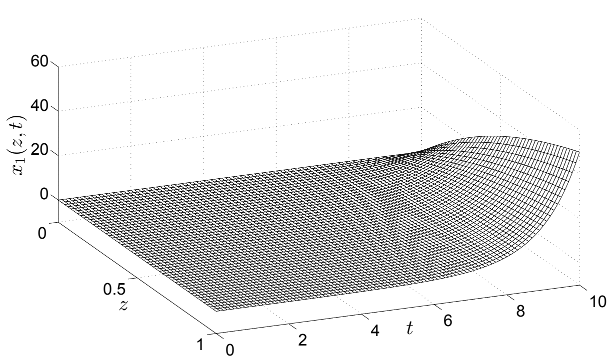

Figure 6.6: The evolution of the state $x_1(z,t)$ of the open-loop system (6.21)–(6.24).

In this chapter, the objective is to design boundary controllers such that the following conditions are satisfied:

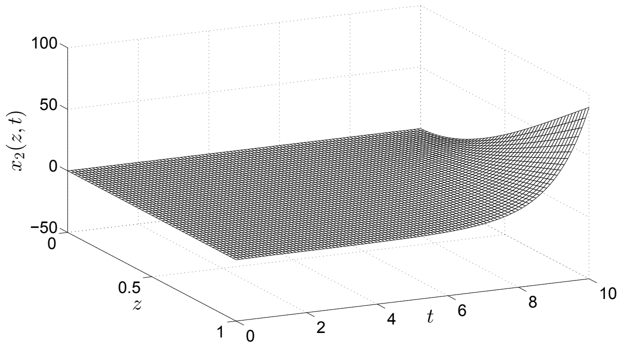

Figure 6.7: The evolution of the state $x_2(z,t)$ of the open-loop system (6.21)–(6.24).

(i). the entire closed-loop system is stable;

(ii). the tracking error $e_y(t) = y(t) - y_r(t)$ decays to zero as $t \to +\infty$, for any initial conditions, i.e.,

$$\lim_{t\to+\infty} e_y(t) = 0 \tag{6.27}$$

where $y_r(t)$ is the desired reference signal.

6.3 Optimal state feedback tracking controller

6.3.1 Optimal stabilization controller

In this section, we derive necessary conditions for the open-loop (linear quadratic) LQ optimality problem by applying weak variational approach. Consequently, the differential algebraic Riccati equations are developed for the finite-time state-feedback controller design.

6.3.1.1 Open-loop Controller

We are interested in the finite-time open-loop LQ optimal control problem for the system (6.21)–(6.23). Let us condition the LQ optimal control problem on a finite-time horizon $t \in [0, T]$

$$
\begin{aligned}
J = &\tfrac{1}{2}\textstyle\int_0^T [\langle x_1(z,t), q_1(x_1(z,t))\rangle]dt \\
&+\tfrac{1}{2}\textstyle\int_0^T [\langle x_2(z,t), q_2(x_2(z,t))\rangle + RU^2(t)]dt \\
&+\tfrac{1}{2}\langle x_1(z,T), P_{f_1}(x_1(z,T))\rangle \\
&+\tfrac{1}{2}\langle x_2(z,T), P_{f_2}(x_2(z,T))\rangle
\end{aligned}
\tag{6.28}
$$

Here, the symbols $q_1 \geq 0$, $q_2 \geq 0$, $R \geq 0$, $P_{f_1} \geq 0$ and $P_{f_2} \geq 0$ are weighting kernels for states, input and terminal states of the closed-loop system. In particular, the positivity of R is used to guarantee the boundedness of control signals. The following theorem provides necessary conditions for open-loop optimal control problem of (6.21)–(6.23) in finite-time horizon.

Theorem 16. *Consider the linear coupled hyperbolic PDEs given by (6.21)–(6.23) defined on the finite-time horizon $t \in [0,T]$ and the cost function (6.28). If we define the nominal states, control and co-states that minimize the cost function as: $x_1^*(z,t)$, $x_2^*(z,t)$, $U^*(t)$, $\lambda_1(z,t)$ and $\lambda_2(t)$, then the necessary conditions for optimality are as follows:*

$$\partial_t x_1^*(z,t) = -\partial_z x_1^*(z,t) + \alpha_2(z)x_2^*(z,t) + \beta_1(z)x_1^*(1,t) \tag{6.29}$$

$$\partial_t x_2^*(z,t) = -\partial_t x_2^*(z,t) + \alpha_1(z)x_1^*(z,t) \tag{6.30}$$

$$-\partial_t \lambda_1 = q_1(x_1^*) + \partial_z \lambda_1 + \alpha_1(z)\lambda_2(z,t) \tag{6.31}$$

$$-\partial_t \lambda_2 = q_2(x_2^*) + \partial_z \lambda_2 + \alpha_2(z)\lambda_1(z,t) \tag{6.32}$$

with boundary conditions:

$$x_1^*(0,t) = U^*(t),\ x_2^*(0,t) = 0 \tag{6.33}$$

$$\lambda_1(1,t) = \int_0^1 \lambda_1(z,t)\beta_1(z)dz,\ \lambda_2(1,t) = 0 \tag{6.34}$$

and initial/terminal conditions:

$$x_1^*(z,0) = x_{10}(z),\ x_2^*(z,0) = x_{20}(z) \tag{6.35}$$

$$\lambda_1(z,T) = P_{f_1}\left(x_1^*(z,T)\right), \ \lambda_2(z,T) = P_{f_2}\left(x_2^*(z,T)\right) \tag{6.36}$$

where the optimal control input is:

$$U^* = -\frac{1}{R}\lambda_1(0,t) \tag{6.37}$$

Proof. We introduce the perturbation from the optimal solution:

$$\begin{aligned}
x_1(z,t) &= x_1^*(z,t) + \varepsilon\delta x_1(z,t) \\
x_2(z,t) &= x_2^*(z,t) + \varepsilon\delta x_2(z,t) \\
U(t) &= U^*(t) + \varepsilon\delta U(t)
\end{aligned}$$

Plugging the above equations into the cost function:

$$\begin{aligned}
&J\left(x_1^* + \varepsilon\delta x_1, x_2^* + \varepsilon\delta x_2, U^* + \varepsilon\delta U\right) \\
&= \tfrac{1}{2}\int_0^T \left[\langle x_1^* + \varepsilon\delta x_1, q_1\left(x_1^* + \varepsilon\delta x_1\right)\rangle\right]dt \\
&+\tfrac{1}{2}\int_0^T \left[\langle x_2^* + \varepsilon\delta x_2, q_2\left(x_2^* + \varepsilon\delta x_2\right)\rangle + R(U^* + \varepsilon\delta U)^2\right]dt \\
&+\tfrac{1}{2}\left\langle x_1^*(z,T) + \varepsilon\delta x_1(z,T), P_{f_1}\left(x_1^*(z,T) + \varepsilon\delta x_1(z,T)\right)\right\rangle \\
&+\tfrac{1}{2}\left\langle x_2^*(z,T) + \varepsilon\delta x_2(z,T), P_{f_2}\left(x_2^*(z,T) + \varepsilon\delta x_2(z,T)\right)\right\rangle
\end{aligned}$$

Then, we define a functional:

$$\begin{aligned}
&g(\varepsilon) = \tfrac{1}{2}\int_0^T \left[\langle x_1^* + \varepsilon\delta x_1, q_1 (x_1^* + \varepsilon\delta x_1)\rangle\right]dt \\
&+\tfrac{1}{2}\int_0^T \left[\langle x_2^* + \varepsilon\delta x_2, q_2 (x_2^* + \varepsilon\delta x_2)\rangle + R(U^* + \varepsilon\delta U)^2\right]dt \\
&+\tfrac{1}{2}\langle x_1^*(z,T) + \varepsilon\delta x_1(z,T), P_{f_1}(x_1^*(z,T) + \varepsilon\delta x_1(z,T))\rangle \\
&+\tfrac{1}{2}\langle x_2^*(z,T) + \varepsilon\delta x_2(z,T), P_{f_2}(x_2^*(z,T) + \varepsilon\delta x_2(z,T))\rangle \\
&+\int_0^T \left[\langle \lambda_1(z,t), -\partial_z x_1^* - \varepsilon\partial_z\delta x_1 + \alpha_2(z)x_2^* + \alpha_2(z)\varepsilon\delta x_2\rangle\right]dt \\
&+\int_0^T \left[\langle \lambda_1(z,t), \beta_1(z)x_1^*(1,t) + \beta_1(z)\varepsilon\delta x_1(1,t)\rangle\right]dt \\
&+\int_0^T \left[\langle \lambda_1(z,t), -\partial_t (x_1^* + \varepsilon\delta x_1)\rangle\right]dt \\
&+\int_0^T \left[\langle \lambda_2(z,t), -\partial_z x_2^* - \varepsilon\partial_z\delta x_2 + \alpha_1(z)x_1^* + \alpha_1(z)\varepsilon\delta x_1\rangle\right]dt \\
&+\int_0^T \left[\langle \lambda_2(z,t), -\partial_t (x_2^* + \varepsilon\delta x_2)\rangle\right]dt
\end{aligned}$$

where last four terms accounts for the system dynamics constraint (6.21)–(6.22) in a Lagrangian form. As a consequence, the necessary conditions for optimality is $dg(\varepsilon)/d\varepsilon|_{\varepsilon=0} = 0$. Differentiating $g(\varepsilon)$ yields:

$$\begin{aligned}
&\tfrac{d}{d\varepsilon}g(\varepsilon) = \int_0^T \left[\langle \delta x_1, q_1 (x_1^* + \varepsilon\delta x_1)\rangle\right]dt \\
&+\int_0^T \left[\langle \delta x_2, q_2 (x_2^* + \varepsilon\delta x_2)\rangle + R(U^* + \varepsilon\delta U)\delta U\right]dt \\
&+\langle \delta x_1(z,T), P_{f_1}(x_1^*(z,T) + \varepsilon\delta x_1(z,T))\rangle \\
&+\langle \delta x_2(z,T), P_{f_2}(x_2^*(z,T) + \varepsilon\delta x_2(z,T))\rangle \\
&+\int_0^T \left[\left\langle \lambda_1(z,t), -\partial_z\delta x_1 + \alpha_2(z)\delta x_2 - \tfrac{\partial}{\partial t}(\delta x_1)\right\rangle\right]dt \\
&+\int_0^T \left[\left\langle \lambda_2(z,t), -\partial_z\delta x_2 + \alpha_1(z)\delta x_1 - \tfrac{\partial}{\partial t}(\delta x_2)\right\rangle\right]dt \\
&+\int_0^T \left[\langle \lambda_1(z,t), \beta_1(z)\delta x_1(1,t)\rangle\right]dt
\end{aligned} \tag{6.38}$$

By applying integration by parts, some terms in above equation can be simplified:

$$\begin{aligned}
&\langle \lambda_1(z,t), -\partial_z\delta x_1\rangle \\
&= -\lambda_1(1,t)\delta x_1(1,t) + \lambda_1(0,t)\delta U(t) + \langle \partial_z\lambda_1, \delta x_1\rangle
\end{aligned}$$

$$\langle \lambda_2(z,t), -\partial_z \delta x_2 \rangle$$
$$= -\lambda_2(1,t)\delta x_2(1,t) + \langle \partial_z \lambda_2, \delta x_2 \rangle$$

Moreover, we can also compute:

$$\int_0^T [\langle \lambda_1(z,t), \partial_t (\delta x_1) \rangle] dt$$
$$= \langle \lambda_1(z,T), \delta x_1(z,T) \rangle - \int_0^T [\langle \partial_t \lambda_1, \delta x_1 \rangle] dt$$

$$\int_0^T [\langle \lambda_2(z,t), \partial_t (\delta x_2) \rangle] dt$$
$$= \langle \lambda_2(z,T), \delta x_2(z,T) \rangle - \int_0^T [\langle \partial_t \lambda_2, \delta x_2 \rangle] dt$$

Substituting these equations into (6.38) and evaluating it at $\varepsilon = 0$ leads to:

$$\begin{aligned}
&\tfrac{d}{d\varepsilon} g(\varepsilon)\Big|_{\varepsilon=0} = \\
&\int_0^T [\langle \delta x_1, q_1(x_1^*) + \partial_t \lambda_1 + \partial_z \lambda_1 + \alpha_1(z)\lambda_2(z,t) \rangle] dt \\
&+ \int_0^T [\langle \delta x_2, q_2(x_2^*) + \partial_t \lambda_2 + \partial_z \lambda_2 + \alpha_2(z)\lambda_1(z,t) \rangle] dt \\
&+ \int_0^T [R(U^*) + \lambda_1(0,t)] \delta U dt \\
&+ \langle \delta x_1(z,T), P_{f_1}(x_1^*(z,T)) - \lambda_1(z,T) \rangle \\
&+ \langle \delta x_2(z,T), P_{f_2}(x_2^*(z,T)) - \lambda_2(z,T) \rangle \\
&+ \int_0^T [\langle \lambda_1(z,t), \beta_1(z) \rangle - \lambda_1(1,t)] \, \delta x_1(1,t) dt \\
&+ \int_0^T [-\lambda_2(1,t)\delta x_2(1,t)] dt
\end{aligned}$$

Therefore, the following necessary optimality conditions are obtained:

$$\begin{aligned}
&-\partial_t \lambda_1 = q_1(x_1^*) + \partial_z \lambda_1 + \alpha_1(z)\lambda_2(z,t) \\
&-\partial_t \lambda_2 = q_2(x_2^*) + \partial_z \lambda_2 + \alpha_2(z)\lambda_1(z,t) \\
&\lambda_1(1,t) = \int_0^1 \lambda_1(z,t)\beta_1(z) dz, \lambda_2(1,t) = 0 \\
&\lambda_1(z,T) = P_{f_1}(x_1^*(z,T)), \lambda_2(z,T) = P_{f_2}(x_2^*(z,T)) \\
&U^* = -\tfrac{1}{R}\lambda_1(0,t)
\end{aligned}$$

This completes the proof. $\square$

6.3.1.2 State-feedback Controller

Now, we are considering the state-feedback controller design problem. First, we define the following linear transformation that relates the co-states λ_1 and λ_2 to the states x_1 and x_2:

$$\begin{aligned}\lambda_1(z,t) &= \int_0^1 P_{11}(z,y,t)x_1^*(y,t)dy \\ &\quad+ \int_0^1 P_{12}(z,y,t)x_2^*(y,t)dy \\ \lambda_2(z,t) &= \int_0^1 P_{21}(z,y,t)x_1^*(y,t)dy \\ &\quad+ \int_0^1 P_{22}(z,y,t)x_2^*(y,t)dy\end{aligned} \tag{6.39}$$

Moreover, the terms in previous section are denoted by:

$$\begin{aligned}q_1\left(x_1^*(z,t)\right) &= \int_0^1 q_1(z,y)x_1^*(y,t)dy \\ q_2\left(x_2^*(z,t)\right) &= \int_0^1 q_2(z,y)x_2^*(y,t)dy \\ P_{f_1}\left(x_1^*(z,t)\right) &= \int_0^1 P_{f_1}(z,y)x_1^*(y,t)dy \\ P_{f_2}\left(x_2^*(z,t)\right) &= \int_0^1 P_{f_2}(z,y)x_2^*(y,t)dy\end{aligned}$$

Then, we have the following result for the boundary controlled linear coupled hyperbolic PDE systems.

Theorem 17. *The optimal boundary control in state-feedback form is given by:*

$$\begin{aligned}U^*(t) = &-\tfrac{1}{R}\int_0^1 P_{11}(0,y,t)x_1^*(y,t)dy \\ &-\tfrac{1}{R}\int_0^1 P_{12}(0,y,t)x_2^*(y,t)dy\end{aligned} \tag{6.40}$$

where the time varying transformation kernel $P_1(z,y,t)$ is the solution of the following differential algebraic Riccati equations:

$$\begin{aligned}&-\partial_t P_{11}(z,y,t) = \partial_y P_{11}(z,y,t) + \partial_z P_{11}(z,y,t) \\ &+\alpha_1(y)P_{12}(z,y,t) + \alpha_1(z)P_{21}(z,y,t) + q_1(z,y) \\ &-\tfrac{1}{R}P_{11}(z,0,t)P_{11}(0,y,t)\end{aligned} \tag{6.41}$$

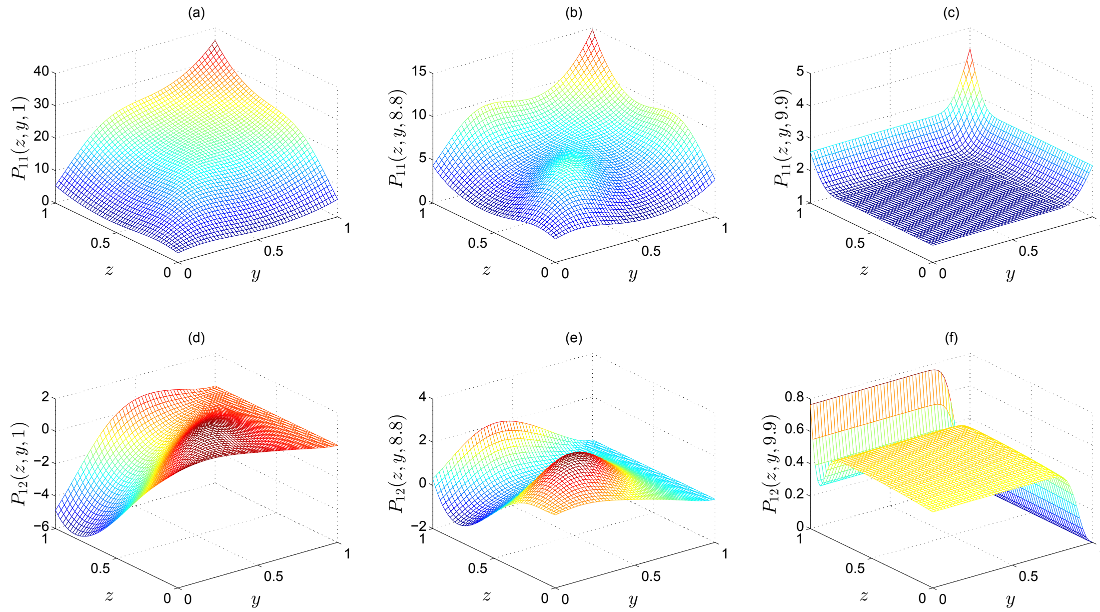

Figure 6.8: The evolutions of the $P_{11}(z,y,t)$ and $P_{12}(z,y,t)$.

$$\begin{aligned}&-\partial_t P_{12}(z,y,t) = \partial_y P_{12}(z,y,t) + \partial_z P_{12}(z,y,t)\\&+\alpha_2(y)P_{11}(z,y,t) + \alpha_1(z)P_{22}(z,y,t)\\&-\tfrac{1}{R}P_{11}(z,0,t)P_{12}(0,y,t)\end{aligned} \tag{6.42}$$

$$\begin{aligned}&-\partial_t P_{21}(z,y,t) = \partial_y P_{21}(z,y,t) + \partial_z P_{21}(z,y,t)\\&+\alpha_1(y)P_{22}(z,y,t) + \alpha_2(z)P_{11}(z,y,t)\\&-\tfrac{1}{R}P_{21}(z,0,t)P_{11}(0,y,t)\end{aligned} \tag{6.43}$$

$$\begin{aligned}&-\partial_t P_{22}(z,y,t) = \partial_y P_{22}(z,y,t) + \partial_z P_{22}(z,y,t)\\&+\alpha_2(y)P_{21}(z,y,t) + \alpha_2(z)P_{12}(z,y,t) + q_2(z,y)\\&-\tfrac{1}{R}P_{21}(z,0,t)P_{12}(0,y,t)\end{aligned} \tag{6.44}$$

with boundary conditions:

$$\begin{aligned}&P_{11}(z,1,t) = \textstyle\int_0^1 P_{11}(z,y,t)\beta_1(y)dy,\\&P_{11}(1,y,t) = \textstyle\int_0^1 P_{11}(z,y,t)\beta_1(z)dz,\\&P_{12}(1,y,t) = \textstyle\int_0^1 P_{12}(z,y,t)\beta_1(z)dz,\\&P_{12}(z,1,t) = 0\end{aligned} \tag{6.45}$$

$$
\begin{aligned}
&P_{21}(z,1,t) = \int_0^1 P_{21}(z,y,t)\beta_1(y)dy \\
&P_{21}(1,y,t) = 0, \\
&P_{22}(z,1,t) = 0, P_{22}(1,y,t) = 0
\end{aligned}
\tag{6.46}
$$

and terminal conditions:

$$
P_{11}(z,y,T) = P_{f1}(z,y),\ P_{12}(z,y,T) = 0 \tag{6.47}
$$

$$
P_{21}(z,y,T) = 0,\ P_{22}(z,y,T) = P_{f2}(z,y) \tag{6.48}
$$

Proof. To proof this theorem, one just needs to evaluate λ_1 and λ_2 in (6.31), (6.32), (6.34) and (6.36) using the linear transformation (6.39). (6.42) and three boundary conditions for $P_{11}(1,y,t)$, $P_{21}(1,y,t)$ and $P_{22}(1,y,t)$ are directly resulted from the boundary conditions in (6.34) and other three boundary conditions for $P_{11}(z,1,t)$, $P_{21}(z,1,t)$ and $P_{22}(z,1,t)$ arise from integration by parts. □

It is noted that for the infinite-time horizon, the optimal boundary stabilization controller is given by the following form:

$$
\begin{aligned}
\bar{U}^*(t) = &-\tfrac{1}{R}\int_0^1 \bar{P}_{11}(0,y)x_1^*(y,t)dy \\
&-\tfrac{1}{R}\int_0^1 \bar{P}_{12}(0,y)x_2^*(y,t)dy
\end{aligned}
\tag{6.49}
$$

where $\bar{P}_{11}(z,y)$ is the steady-state solution of the differential algebraic Riccati equations (6.41)–(6.44) with boundary conditions given in (6.45)–(6.46).

Now, we apply the optimal stabilization control law (6.37) or (6.40) and the results are shown in Figure 6.9 and Figure 6.10. Moreover, the evolutions of corresponding $P_{11}(z,y,t)$ and $P_{12}(z,y,t)$ at some sampled time instants are shown in Figure 6.8.

Compared with states shown in Figure 6.6 and Figure 6.7, the closed-loop system is stabilized by applying the optimal control law (6.40) in Figure 6.9 and Figure 6.10.

Now, we set the initial conditions for the original nonlinear plant (6.1)–(6.4) as $T_0(\zeta) = Te$

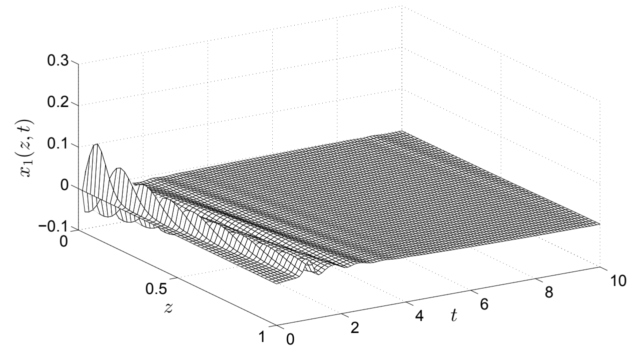

Figure 6.9: The evolution of the state $x_1(z,t)$ of closed-loop system (6.21)–(6.24) with the optimal control law (6.40).

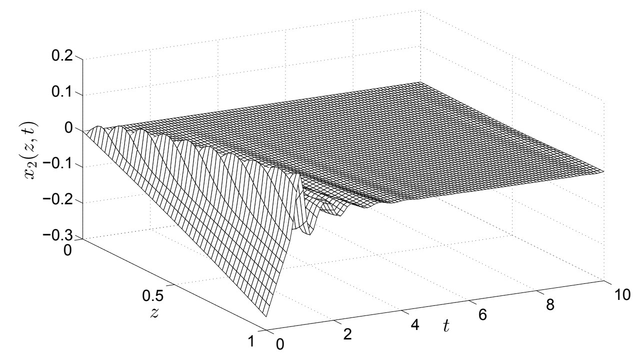

Figure 6.10: The evolution of the state $x_2(z,t)$ of closed-loop system (6.21)–(6.24) with the optimal control law (6.40).

and $c_{A0}(\zeta) = c_{A,in}$. Then, applying the resulting control law (6.40) back to the original plant (6.1)–(6.4) yields the profiles shown in Figure 6.11 and Figure 6.12.

6.3.2 Tracking controller design

By applying the above technique, the stability of the linearized closed-loop system is ensured. In this section, the objective is to design a feedforward regulator such that (6.27) can be realized for the stable closed-loop system. In this work, we assume that the reference signal $y_r(t)$ is generated by a known finite-dimensional exosystem:

$$\dot{v}(t) = Sv(t), v(0) \in \mathbb{C}^n \tag{6.50}$$

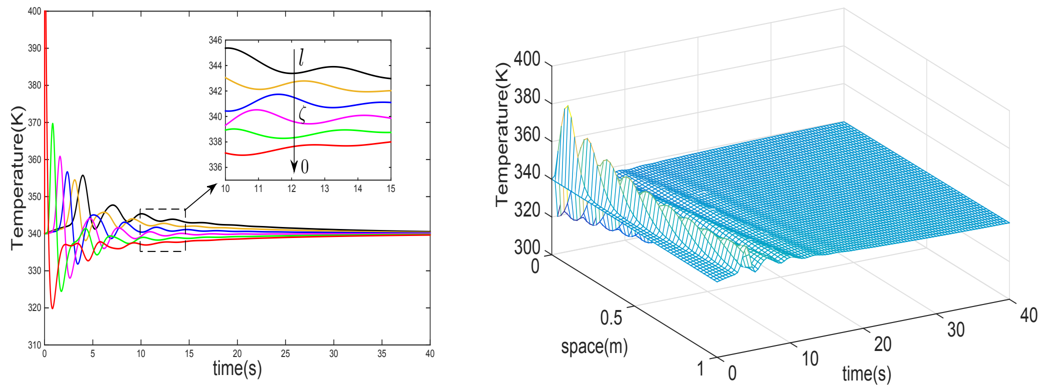

Figure 6.11: The evolution of the state $x_2(z,t)$ of closed-loop system (6.21)–(6.24) with the optimal control law (6.40).

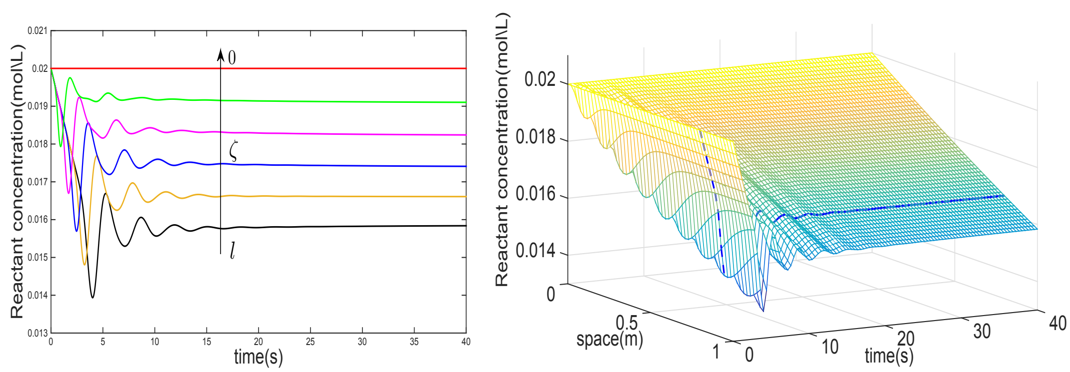

Figure 6.12: The evolution of the state $x_2(z,t)$ of closed-loop system (6.21)–(6.24) with the optimal control law (6.40).

$$y_r(t) = q_r^T v(t), t \geq 0 \tag{6.51}$$

with q_r matrix of appropriate dimensions which is assumed to be known for the regulator design.

Assumption 13. *$S : D(S) \subset \mathbb{C}^n \to \mathbb{C}^n$ is a skew-Hermitian matrix having all its eigenvalues on imaginary axis: $S = bdiag(S_n, S_m)$. In particular, the matrix S_n is a n_n-dimensional nilpotent block, i.e. $\sigma(S_n) = \{0\}$ and the matrix S_m is a diagonalizable matrix with dimensions n_m. Note that $n_n + n_m = n$. This allows the modeling of steplike, ramp, polynomial-type and sinusoidal exogenous signals.*

In order to solve the boundary controlled output tracking problem, the finite-time optimal state feedback controller with a feedforward of the signal model states is considered:

$$
\begin{aligned}
x_1(0,t) &= U_v^*(t) \\
&= -\tfrac{1}{R}\int_0^1 P_{11}(0,y,t)x_1(y,t)dy \\
&\quad -\tfrac{1}{R}\int_0^1 P_{12}(0,y,t)x_2(y,t)dy + m_v^T(t)v(t)
\end{aligned}
\tag{6.52}
$$

The feedback gain $P_{11}(0,y,t)$ and $P_{12}(0,y,t)$ are solutions of Riccati equations in Theorem 17 and the feedforward gain $m_v(t)^T$ has to be determined. Consequently, the corresponding infinite-time optimal tracking control law $\bar{U}_v^*(t)$ is given by:

$$
\begin{aligned}
x_1(0,t) &= \bar{U}_v^*(t) \\
&= -\tfrac{1}{R}\int_0^1 \bar{P}_{11}(0,y)x_1(y,t)dy \\
&\quad -\tfrac{1}{R}\int_0^1 \bar{P}_{12}(0,y)x_2(y,t)dy + \bar{m}_v^T v(t)
\end{aligned}
\tag{6.53}
$$

We have the following result which provides a choice of $m_v^T(t)$ and $\bar{m}_v^T$.

Theorem 18. *The feedforward gain for the signal model states has the following form:*

$$
\begin{aligned}
m_v^T(t) &= \tfrac{1}{R}\int_0^1 P_{11}(0,y,t)m_1^T(y)dy \\
&\quad +\tfrac{1}{R}\int_0^1 P_{12}(0,y,t)m_2^T(y)dy + m_1^T(0)
\end{aligned}
\tag{6.54}
$$

such that the output regulation (6.27) can be achieved, where the spatial varying vectors $m_1^T(z)$ and $m_2^T(z)$ are the solutions of the following regulator equations:

$$
d_z m_1^T(z) = -m_1^T(z)S + \alpha_2(z)m_2^T(z) + \beta_1(z)m_1^T(1) \tag{6.55}
$$

$$
d_z m_2^T(z) = -m_2^T(z)S + \alpha_1(z)m_1^T(z) \tag{6.56}
$$

with boundary conditions:

$$m_2^T(0) = 0, \mathcal{C}\begin{bmatrix} m_1^T \\ m_2^T \end{bmatrix} - q_r^T = 0 \tag{6.57}$$

Proof. In order to determine the feedforward gain m_v^T, we introduce for (6.21)–(6.23) and (6.50) error states:

$$\begin{bmatrix} e_1(z,t) \\ e_2(z,t) \end{bmatrix} = \begin{bmatrix} x_1(z,t) \\ x_2(z,t) \end{bmatrix} - \begin{bmatrix} m_1^T(z) \\ m_2^T(z) \end{bmatrix} v(t) \tag{6.58}$$

where $m_1^T(z)$ and m_2^T have to be found. By applying (6.21)-(6.22), (6.50) and (6.58), one obtains:

$$\partial_t e_1(z,t) = -\partial_z e_1(z,t) + \alpha_2(z)e_2(z,t) + \beta_1(z)e_1(1,t) \tag{6.59}$$

$$\partial_t e_2(z,t) = -\partial_z e_2(z,t) + \alpha_1(z)e_1(z,t) \tag{6.60}$$

if $m_1^T(z)$ and $m_2^T(z)$ satisfy the following conditions:

$$d_z m_1^T(z) = -m_1^T(z)S + \alpha_2(z)m_2^T(z) + \beta_1(z)m_1^T(1) \tag{6.61}$$

$$d_z m_2^T(z) = -m_2^T(z)S + \alpha_1(z)m_1^T(z) \tag{6.62}$$

The boundary conditions (6.23) and (6.52) give:

$$\begin{aligned} e_1(0,t) &= -\tfrac{1}{R}\int_0^1 P_{11}(0,y,t)e_1(y,t)dy \\ &\quad -\tfrac{1}{R}\int_0^1 P_{12}(0,y,t)e_2(y,t)dy \\ e_2(0,t) &= 0 \end{aligned} \tag{6.63}$$

if $m_1^T(0)$ and $m_2^T(0)$ satisfy the following conditions:

$$
\begin{aligned}
m_1^T(0) &= m_v^T(t) - \tfrac{1}{R}\int_0^1 P_{11}(0,y,t)m_1^T(y)dy \\
&\qquad -\tfrac{1}{R}\int_0^1 P_{12}(0,y,t)m_2^T(y)dy \\
m_2^T(0) &= 0
\end{aligned}
\tag{6.64}
$$

Finally, the tracking error $e(t)$ in (6.27) becomes:

$$
e(t) = \mathcal{C}\begin{bmatrix} e_1(t) \\ e_2(t) \end{bmatrix} \tag{6.65}
$$

if the following condition holds:

$$
\mathcal{C}\begin{bmatrix} m_1^T \\ m_2^T \end{bmatrix} - q_r^T = 0
$$

According to the illustration in previous sections, the error system (6.59)–(6.60) with (6.63) is stable optimally and therefore the tracking error $e(t)$ in (6.65) decays to zero optimally, which proves the output regulation (6.27) is achieved. Moreover, summarizing equations with respect to $m_1^T(z)$ and $m_2^T(z)$ yields the conclusion of the theorem. This concludes the proof. □

As a result, the corresponding feedforward gain in infinite-time horizon is given by:

$$
\begin{aligned}
\bar{m}_v^T &= \tfrac{1}{R}\int_0^1 \bar{P}_{11}(0,y)m_1^T(y)dy \\
&\quad +\tfrac{1}{R}\int_0^1 \bar{P}_{12}(0,y)m_2^T(y)dy + m_1^T(0)
\end{aligned}
\tag{6.66}
$$

The existence of the solutions $m_1^T(z)$ and $m_2^T(z)$ is essential to the feasibility of the feedforward controller. Therefore, the following lemma studies the solvability of the regulator equations (6.55)–(6.57).

Lemma 19. *(Regulator Equations) The transfer function of (6.21)–(6.25) from $U(t)$ to $y(t)$*

is $G(s) = \mathcal{C}\left(\Delta_1(s,z)\begin{bmatrix}1\\0\end{bmatrix} + \Delta_2(s,z)\begin{bmatrix}1\\0\end{bmatrix}\Delta_m(s,1)\right)$ *with* $\Delta_1(s,z) = \exp\left(\int_0^z A_\alpha(s,\xi)d\xi\right)$, $\Delta_2(s,z) = \int_0^z \left(\exp\left(\int_\xi^z A_\alpha(s,\eta)d\eta\right)\beta_1(\xi)\right)d\xi,\ A_\alpha(s,z) = \begin{bmatrix}-s & \alpha_2(z)\\ \alpha_1(z) & -s\end{bmatrix}$ *and*

$$\Delta_m(s,1) = \frac{\begin{bmatrix}1 & 0\end{bmatrix}\Delta_1(s,1)\begin{bmatrix}1\\0\end{bmatrix}}{\left(1 - \begin{bmatrix}1 & 0\end{bmatrix}\Delta_2(s,1)\begin{bmatrix}1\\0\end{bmatrix}\right)}.$$

Then, we can find a unique solution $m_1^T(z)$ *and* $m_2^T(z)$ *if the condition* $G(\lambda) \neq 0, \forall \lambda \in \sigma(S)$ *holds.*

Proof. From Assumption 13, we assume the $\{\psi_k\}$ with $k = 1, \cdots, n_n$ are eigenvectors of S_n with zero eigenvalues and $\{\phi_k\}$ with $k = 1, \cdots, n_m$ are eigenvectors of S_m. Moreover, λ_k with $k = 1, \cdots, n_m$ are assumed to be eigenvalues of S_m. As a consequence, equations (6.61)–(6.62) can be decoupled into:

$$\begin{aligned} d_z m_{n1}^T(z) &= -m_{n1}^T(z)S_n + \alpha_2(z)m_{n2}^T(z) + \beta_1(z)m_{n1}^T(1) \\ d_z m_{n2}^T(z) &= -m_{n2}^T(z)S_n + \alpha_1(z)m_{n1}^T(z) \end{aligned} \tag{6.67}$$

$$\begin{aligned} d_z m_{m1}^T(z) &= -m_{m1}^T(z)S_m + \alpha_2(z)m_{m2}^T(z) + \beta_1(z)m_{m1}^T(1) \\ d_z m_{m2}^T(z) &= -m_{m2}^T(z)S_m + \alpha_1(z)m_{m1}^T(z) \end{aligned} \tag{6.68}$$

with $m_1^T(z) = \left[m_{n1}^T(z), m_{m1}^T(z)\right]$ and $m_2^T(z) = \left[m_{n2}^T(z), m_{m2}^T(z)\right]$. First, we focus on the solving of (6.67): postmultiplying (6.67) by $\{\phi_k\}$ with $k = 1, \cdots, n_n$ yields (since $S_n\phi_k = 0$):

$$\begin{aligned} &\left(d_z m_{n1}^T(z) - \alpha_2(z)m_{n2}^T(z) - \beta_1(z)m_{m1}^T(1)\right)\phi_k = 0 \\ &\left(d_z m_{n2}^T(z) - \alpha_1(z)m_{n1}^T(z)\right)\phi_k = 0 \end{aligned} \tag{6.69}$$

Since (6.69) holds for all $\{\phi_k\}$ with $k = 1, \cdots, n_n$, we can easily obtain:

$$d_z \begin{bmatrix} m_{n1}^T(z) \\ m_{n2}^T(z) \end{bmatrix} = \begin{bmatrix} 0 & \alpha_2(z) \\ \alpha_1(z) & 0 \end{bmatrix} \begin{bmatrix} m_{n1}^T(z) \\ m_{n2}^T(z) \end{bmatrix} + \begin{bmatrix} \beta_1(z) \\ 0 \end{bmatrix} m_{n1}^T(1)$$

From boundary conditions (6.64), we have $m_2^T(0) = 0$ and thus $m_{n2}^T(0) = 0$. Therefore, the general solution is given by:

$$\begin{bmatrix} m_{n1}^T(z) \\ m_{n2}^T(z) \end{bmatrix} = \Delta_1(0,z) \begin{bmatrix} 1 \\ 0 \end{bmatrix} m_{n1}^T(0) + \Delta_2(0,z) \begin{bmatrix} 1 \\ 0 \end{bmatrix} m_{n1}^T(1)$$

with $\Delta_1(0,z) = \exp\left(\int_0^z A_\alpha(0,s)ds\right)$, $\Delta_2(0,z) = \int_0^z \left(\exp\left(\int_s^z A_\alpha(0,\eta)d\eta\right)\beta_1(s)\right) ds$ and $A_\alpha(0,z) = \begin{bmatrix} 0 & \alpha_2(z) \\ \alpha_1(z) & 0 \end{bmatrix}$. Here '0' in Δ_1, Δ_2 and A_α denotes zero eigenvalue of S_n. Immediately, one has:

$$m_{n1}^T(1) = \frac{\begin{bmatrix} 1 & 0 \end{bmatrix} \Delta_1(0,1) \begin{bmatrix} 1 \\ 0 \end{bmatrix}}{\left(1 - \begin{bmatrix} 1 & 0 \end{bmatrix} \Delta_2(0,1) \begin{bmatrix} 1 \\ 0 \end{bmatrix}\right)} m_{n1}^T(0) = \Delta_m(0,1) m_{n1}^T(0)$$

Obviously, $\begin{bmatrix} 1 & 0 \end{bmatrix} \Delta_1(0,1) \begin{bmatrix} 1 \\ 0 \end{bmatrix}$ and $\begin{bmatrix} 1 & 0 \end{bmatrix} \Delta_2(0,1) \begin{bmatrix} 1 \\ 0 \end{bmatrix}$ are scalars, since $\Delta_2(0,1)$ and $\Delta_2(0,1)$ are 2×2 matrices. If we assume the vector $q_r^T = \left[q_{nr}^T, q_{mr}^T\right]$ with $q_{nr}^T \in C^{1 \times n_n}$ and $q_{mr}^T \in C^{1 \times n_m}$, then applying the output operator $\mathcal{C}$ leads to

$$\left(\mathcal{C}\left(\Delta_1(0,z)\right) \begin{bmatrix} 1 \\ 0 \end{bmatrix} + \mathcal{C}\left(\Delta_2(0,z)\right) \begin{bmatrix} 1 \\ 0 \end{bmatrix} \Delta_m(0,1) \right) m_{n1}^T(0) = q_{nr}^T$$

Therefore, in order to compute $m_{n1}^T(0)$ uniquely, the sufficient and necessary condition is that

$$\mathcal{C}\left((\Delta_1(0,z))\begin{bmatrix}1\\0\end{bmatrix}+(\Delta_2(0,z))\begin{bmatrix}1\\0\end{bmatrix}\Delta_m(0,1)\right)\neq 0 \tag{6.70}$$

holds.

Now, we turn to solve the equations (6.68). As defined in previous section, the matrix S_m is diagonalizable, there exists a similarity transformation $V^{-1}SV = diag\,(\lambda_1,\cdots\lambda_{n_m})$. With $V=[\phi_1,\cdots\phi_{n_m}]$. Postmultiplying (6.68) by V leads to a set of decoupled ODEs:

$$\begin{aligned}
&d_z m^*_{m1k}(z) = -\lambda_k m^*_{m1k}(z) + \alpha_2(z) m^*_{m2k}(z) + \beta_1(z) m^*_{m1k}(1)\\
&d_z m^*_{m2k}(z) = -\lambda_k m^*_{m2k}(z) + \alpha_1(z) m^*_{m1k}(z)\\
&m^*_{m2k}(0) = 0, \mathcal{C}\begin{bmatrix}m^*_{m1k}\\m^*_{m2k}\end{bmatrix} = q^*_{mrk}
\end{aligned}$$

with $m^*_{m1k}(z) = m^T_{m1}(z)\phi_k$, $m^*_{m2k}(z) = m^T_{m2}(z)\phi_k$ and $q^*_{mrk} = q^T_{mr}\phi_k$ for $k=1,\cdots,n_m$. Repeating the similar calculation for $m^T_{n1}(z)$ and $m^T_{n2}(z)$, one has:

$$\begin{bmatrix}m^*_{m1k}(z)\\m^*_{m2k}(z)\end{bmatrix} = \left(\Delta_1(\lambda_k,z)\begin{bmatrix}1\\0\end{bmatrix}+\Delta_2(\lambda_k,z)\begin{bmatrix}1\\0\end{bmatrix}\Delta_m(\lambda_k,1)\right)m^*_{m1k}(0)$$

Then, by applying the operator $\mathcal{C}$ to the above equation, we have:

$$\mathcal{C}\left(\Delta_1(\lambda_k,z)\begin{bmatrix}1\\0\end{bmatrix}+\Delta_2(\lambda_k,z)\begin{bmatrix}1\\0\end{bmatrix}\Delta_m(\lambda_k,1)\right)m^*_{m1k}(0) = q^*_{mrk}$$

with $\Delta_1(\lambda_k,z) = \exp\left(\int_0^z A_\alpha(\lambda_k,s)ds\right)$, $\Delta_2(\lambda_k,z) = \int_0^z\left(\exp\left(\int_s^z A_\alpha(\lambda_k,\eta)d\eta\right)\beta_1(s)\right)ds$, $A_\alpha(\lambda_k,z) =$

$$\begin{bmatrix} -\lambda_k & \alpha_2(z) \\ \alpha_1(z) & -\lambda_k \end{bmatrix}$$ and

$$\Delta_m(\lambda_k, 1) = \frac{\begin{bmatrix} 1 & 0 \end{bmatrix} \Delta_1(\lambda_k, 1) \begin{bmatrix} 1 \\ 0 \end{bmatrix}}{\left(1 - \begin{bmatrix} 1 & 0 \end{bmatrix} \Delta_2(\lambda_k, 1) \begin{bmatrix} 1 \\ 0 \end{bmatrix}\right)}$$

.

It is only possible to compute $m^*_{m1k}(0)$ when the condition:

$$\mathcal{C}\left(\Delta_1(\lambda_k, z) \begin{bmatrix} 1 \\ 0 \end{bmatrix} + \Delta_2(\lambda_k, z) \begin{bmatrix} 1 \\ 0 \end{bmatrix} \Delta_m(\lambda_k, 1)\right) \neq 0 \tag{6.71}$$

for any $\lambda_k \in \sigma(S_m)$ holds. Taking the Laplace transformation of the system (6.21)–(6.23) leads to:

$$\begin{aligned} \partial_z \begin{bmatrix} \hat{x}_1(z,s) \\ \hat{x}_2(z,s) \end{bmatrix} &= \begin{bmatrix} -s & \alpha_2(z) \\ \alpha_1(z) & -s \end{bmatrix} \begin{bmatrix} \hat{x}_1(z,s) \\ \hat{x}_2(z,s) \end{bmatrix} + \begin{bmatrix} \beta_1(z) \\ 0 \end{bmatrix} \hat{x}_1(1,s) \\ \begin{bmatrix} \hat{x}_1(0,s) \\ \hat{x}_2(0,s) \end{bmatrix} &= \begin{bmatrix} \hat{U}(s) \\ 0 \end{bmatrix} \\ \hat{Y}(s) &= \mathcal{C} \begin{bmatrix} \hat{x}_1(s) \\ \hat{x}_2(s) \end{bmatrix} \end{aligned}$$

Therefore, the transfer function from $U(t)$ to $y(t)$ is:

$$G(s) = \mathcal{C}\left(\Delta_1(s, z) \begin{bmatrix} 1 \\ 0 \end{bmatrix} + \Delta_2(s, z) \begin{bmatrix} 1 \\ 0 \end{bmatrix} \Delta_m(s, 1)\right)$$

Here functions $\Delta_1(s,z)$, $\Delta_2(s,z)$ and $\Delta_m(s,1)$ can be obtained via replacement of 'λ_k' by 's' in above functions $\Delta_1(\lambda_k,z)$, $\Delta_2(\lambda_k,z)$ and $\Delta_m(\lambda_k,1)$.

Combining (6.70) and (6.71), the solvability condition is $G(\lambda) \neq 0$ for $\lambda \in \sigma(S)$. Once $m_{n1}^T(0)$ and $m_{m1k}^*(0)$ with $k = 1, \cdots, n_m$ are obtained, $m_{m1}^T(0)$ can be computed through $m_{m1}^T(0) = \left[m_{m11}^*(0), m_{m12}^*(0), \cdots, m_{m1n_m}^*(0)\right] V^{-1}$. Furthermore, $m_1^T(0) = \left[m_{n1}^T(0), m_{m1}^T(0)\right]$ can be obtained. Consequently, $m_1^T(z)$ and $m_2^T(z)$ are calculated. This completes the proof.

$\square$

6.4 Numerical simulations

In previous section, the proposed optimal control law given in Theorem 16 and Theorem 17 has been employed to realize the stabilization of the considered linearized system (6.21)–(6.24) and thus the original nonlinear plant (6.1)–(6.4) around its equilibrium profile.

In this section, we are interested in the realization of the tracking control of the linearized system through the proposed boundary tracking controller given in (6.52). Without loss of generality, we are considering the control of $x_2(0.8,t)$, i.e., the reactant concentration at the point $\zeta = 0.8m$. Obviously, the output to be controlled is included in the formulation (6.26), i.e., $\mathcal{C}\begin{bmatrix} x_1 \\ x_2 \end{bmatrix} = [0,1] \times \begin{bmatrix} x_1(\cdot,t) \\ x_2(0.8,t) \end{bmatrix}$. We assume that the reference signal $y_r(t)$ for the system (6.21)–(6.25) to track is the combination of ramp and step-like signal given by:

$$y_r(t) = \begin{cases} 0.05t, \ 0 \leq t \leq 4 \\ 0.25, \ 4 \leq t \leq 25 \\ 0.15, \ 25 \leq t \leq 50 \end{cases}$$

Therefore, it can be modelled by (6.50)–(6.51) with $q_r^T = \begin{cases} \begin{bmatrix} 0 & 0.05 \end{bmatrix}, 0 \leq t \leq 4 \\ \begin{bmatrix} 0.25 & 0 \end{bmatrix}, 4 \leq t \leq 25 \\ \begin{bmatrix} 0.15 & 0 \end{bmatrix}, 25 \leq t \leq 50 \end{cases}$,

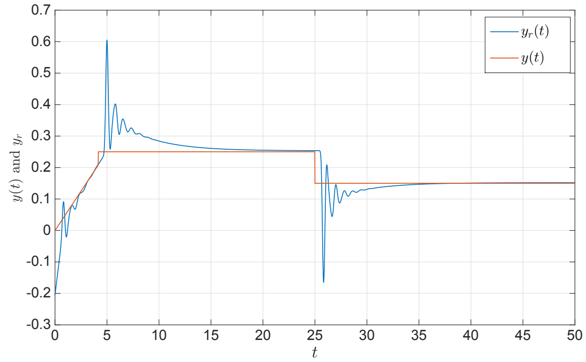

Figure 6.13: The evolution of the controlled output $y(t)$ and the reference signal $y_r(t)$.

$S = \begin{bmatrix} 0 & 0 \\ 1 & 0 \end{bmatrix}$ and initial condition $v(0) = \begin{bmatrix} 1 & 0 \end{bmatrix}^T$. Obviously, the matrix S is a nilpotent matrix with eigenvalues $\{0, 0\}$ and thus $\phi_1 = \begin{bmatrix} 0 \\ 1 \end{bmatrix}, \phi_2 = \begin{bmatrix} 0 \\ -1 \end{bmatrix}$. Therefore, in order to achieve the stabilization of the model (6.21)–(6.24) in $t \in [0\ 50]$, we choose the terminal time $T = 60$ in (6.47)–(6.48) such that the corresponding Riccati equation can be solved.

From the proof of Lemma 19, the transfer function is essential to the feasibility of the proposed tracking controller and the existence of feedforward gain $m_v^T(t)$ in (6.52). In this example, only $G(0)$ is needed since the matrix S just has zero eigenvalues. Based on the formulation of the transfer function in Lemma 19 and the setup of the controlled output $y(t)$, one can compute $G(0)$ in this example:

$$G(0) = \begin{bmatrix} 0 & 1 \end{bmatrix} \left(\Delta_1(0, 0.8) \begin{bmatrix} 1 \\ 0 \end{bmatrix} + \Delta_2(0, 0.8) \begin{bmatrix} 1 \\ 0 \end{bmatrix} \Delta_m(0, 1) \right) = -0.2966$$

Consequently, based on the formulation in the proof of Lemma 19, one has:

$$m_1^T(0) = \begin{cases} \begin{bmatrix} 0 & -0.1686 \end{bmatrix}, 0 \leq t \leq 4 \\ \begin{bmatrix} -0.8428 & 0 \end{bmatrix}, 4 \leq t \leq 25 \\ \begin{bmatrix} -0.5057 & 0 \end{bmatrix}, 25 \leq t \leq 50 \end{cases}$$

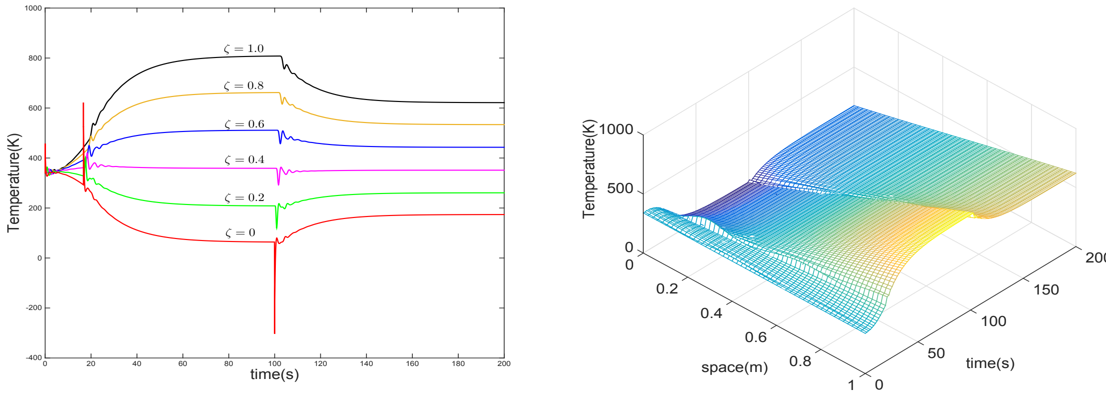

Figure 6.14: The evolution and distribution of the temperature $T(\zeta, \tau)$ of closed-loop system (6.1)–(6.4) with the proposed optimal boundary control law. The red line with $\zeta = 0$ denotes the evolution of $T(0, \tau)$, i.e. $T_{in}(\tau)$.

and thus $m_1^T(z)$ and $m_2^T(z)$ are calculated immediately. From the formulation (6.54), the time varying feedforward gain $m_v^T(t)$ can be obtained. As a result, (6.52) realizes the optimal tracking, as shown in Figure 6.13. To drive $y(t)$ to track the reference signal $y_r(t)$, it directly means that the reactant concentration at the point $\zeta = 0.8$ tracks the following reference signal (black dashed line in left subfigure in Figure 6.15):

$$c_A(0.8, \tau) = \begin{cases} 0.0166 - 0.000206\tau, \; 0 \leq \tau \leq 16 \\ 0.0125, \; 16 \leq \tau \leq 100 \\ 0.0141, \; 100 \leq \tau \leq 200 \end{cases}$$

The corresponding optimal tracking input $T(0, \tau)$ is shown in Figure 6.14 (red line with $\zeta = 0$).

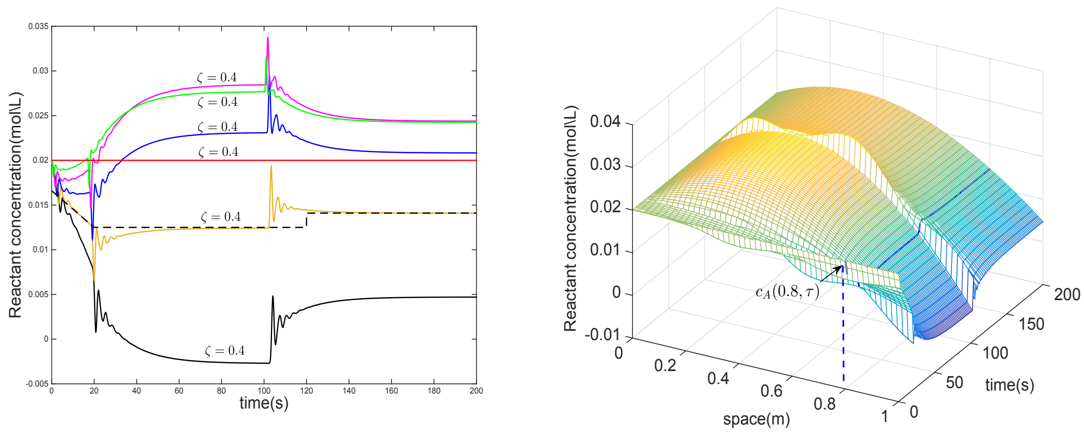

Figure 6.15: The evolution and distribution of the temperature $c_A(\zeta, \tau)$ of closed-loop system (6.1)–(6.4) with the proposed optimal boundary control law. The line with $\zeta = 0.8$ denotes the evolution of the output concentration $c_A(0.8, \tau)$ and the black dashed line is the reference signal.

6.5 Conclusion

This chapter presented an optimal LQ output regulator to address the tracking control problem for the boundary controlled linear hyperbolic partial differential equation (PDE) systems. In the considered hyperbolic systems, a boundary output feedback was taken into account and the resulting systems are unstable. This can be seen in Figure 6.6 and Figure 6.7. The proposed optimal boundary control law solved the stabilization problem via weak variational approach. Consequently, a feedforward boundary regulator equipped with the optimal stabilization boundary control law realized the optimal tracking control. The proposed approach was directly applied a plug flow reactor with temperature output feedback and the simulation results indicated that the performance of the given optimal boundary regulator was well.

Chapter 7

Receding horizon optimal operation and control of a solar-thermal district heating system

7.1 Introduction

In this chapter, the operation strategies and control policies solar-thermal heating (STDH) systems are considered. More specifically, the STDH system is composed of solar-collector system, energy storage system, gas boiler system and district heating system. Moreover, the mathematical models for different subsystems are provided. Based on the given models, optimal operation strategies and optimal control policies are investigated. In particular, the desired temperature tracking problems and the maximization problems of the collected and stored energy are considered and studied. Receding horizon optimal control approaches are applied and therein both single objective and multi-objective optimization problems are formulated. More precisely, the single objective optimization problems are solved using SQP method and the multi-objective optimization problems are solved by genetic algorithm. Moreover, for the control of the district heating system, the internal model based servo-control method and the receding horizon optimal control method are combined to realize the desired district temperature tracking.

7.2 System description

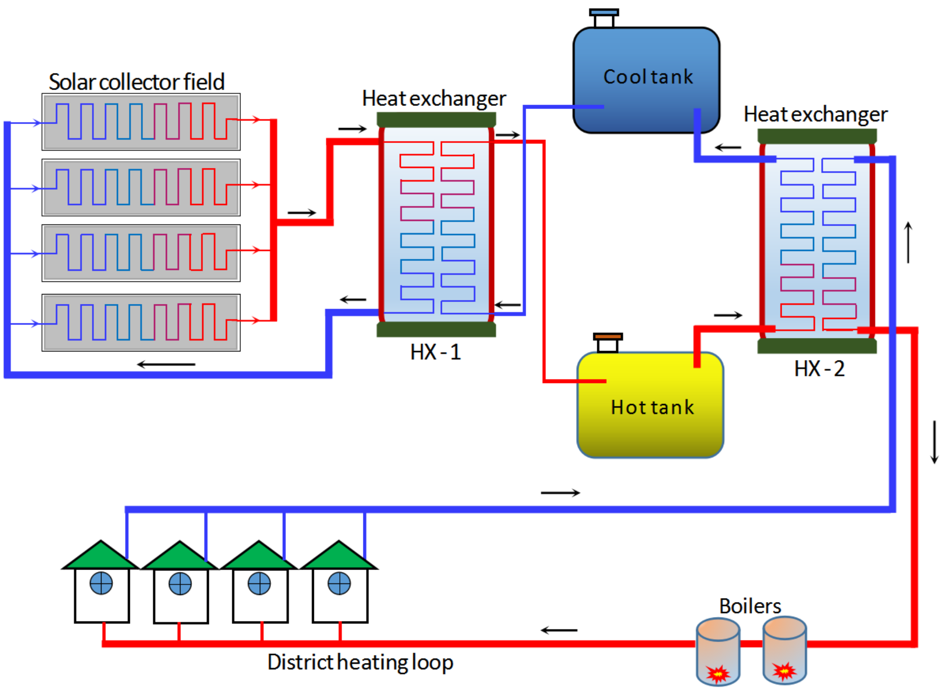

Figure 7.1: Plant scheme of the solar thermal district heating system.

7.2.1 Model of distributed solar collector field

A solar collector absorber surface absorbs heat from the solar irradiance and transfers the heat to the oil flowing through a pipe usually welded to the absorber surface and placed inside the collector. Therefore, coupled differential equations are employed to describe the dynamics of the solar collector field [85]. In general, to derive the mathematic model for the solar collector field, the following assumptions are usually made:

a1. The fluid in the solar collector is assumed to be incompressible and having constant specific heat capacity and density.

a2. Along the pipe in the solar collector, the pressure in the fluid is assumed to be constant.

a3. The environmental temperature around the pipe wall changes over time but not over space.

Consequently, the dynamics of the distributed solar collector field are modelled by the following system of coupled partial differential equations (PDE) according to the energy balance:

$$\begin{aligned} \rho_m C_m A_m \tfrac{\partial T_{sol,m}}{\partial t}(t,\zeta) &= \mu_0 GI(t) - D_m \pi h_l (T_{sol,m}(t,\zeta) - T_a(t)) \\ &\quad - D_f \pi h_t (T_{sol,m}(t,\zeta) - T_{sol,f}(t,\zeta)) \end{aligned} \tag{7.1}$$

$$\begin{aligned} \rho_f C_f A_f \tfrac{\partial T_{sol,f}}{\partial t}(t,\zeta) &= -\rho_f C_f v_{sol,f}(t) \tfrac{\partial T_{sol,f}}{\partial \zeta}(t,\zeta) \\ &\quad + D_f \pi h_t (T_{sol,m}(t,\zeta) - T_{sol,f}(t,\zeta)) \end{aligned} \tag{7.2}$$

with the boundary condition:

$$T_{sol,f}(t,0) = T_{sol,fin}(t) \tag{7.3}$$

where the subindex m indicates the metal and f means the fluid. All the parameters and variable in (7.1)–(7.3) are given in Table 7.1.

In addition, a simplified dynamical model neglecting heat losses and metal temperature was used by several researchers [86][38], given by

$$\rho_f C_f \frac{\partial T_{sol,f}}{\partial t}(t,\zeta) = -\rho_f C_f v_{sol}(t) \frac{\partial T_{sol,f}}{\partial \zeta}(t,\zeta) + \mu_0 GI(t) \tag{7.4}$$

with the boundary condtion

$$T_{sol,f}(t,0) = T_{sol,fin}(t) \tag{7.5}$$

where $T_{sol,f}(t,\zeta)$ is the oil temperature at position ζ along the tube, and $T_{sol,fin}(t)$ is the inlet oil temperature. In this work, to fully express the dynamics of the solar collector system, the mathematic model (7.1)–(7.3) is mainly considered.

Table 7.1: Solar plant model variables and parameters in (7.1)–(7.3).

Symbol	Value and units	Description
t	s	Time $t \in [0, +\infty)$
ζ	m	Space $\zeta \in [0, L]$
L_{sol}	18m	Solar collector field length
ρ_m	1100kg m^{-3}	Metal density
ρ_f	756kg m^{-3}	Oil density
C_m	$440JK^{-1}kg^{-1}$	Metal specific heat capacity
C_f	$1100JK^{-1}kg^{-1}$	Oil specific heat capacity
A_m	$0.0038m^2$	Metal cross-sectional area
A_f	$0.0013m^2$	Oil cross-sectional area
$T_{sol,m}$	^oC	Metal temperature
$T_{sol,f}$	^oC	Oil temperature
$T_a(t)$	^oC	Ambient temperature
$I(t)$	W/m^2	Direct solar radiation
η_0	0.67	Collector optical efficiency
G	$0.9143m$	Collector aperture
h_l	$20.773Wm^{-1}K^{-1}$	Global coefficient of thermal losses
h_t	$1283.2Wm^{-1}K^{-1}$	Coefficient of metal-oil transmission
D_f	$0.04m$	Inner diameter of the pipe line
D_m	$0.07m$	External diameter of the pipe line
$T_{sol,fin}$	^oC	Collector inlet temperature
$T_{sol,fout}$	^oC	Collector outlet temperature
$v_{sol,f}(t)$	m^3s^{-1}	Oil pump volumetric flow rate

For the considered solar-thermal collector system, one important objective is to maintain the outlet temperature in a desired reference set-point. The outlet temperature is given by:

$$T_{sol,fout}(t) = T_{sol,f}(t, L_{sol}) \tag{7.6}$$

Inspired by [87], the overall heat collected by the fluid in the solar collector within a certain time range $[t, t + t_f]$ is defined by the following relation:

$$\begin{aligned} H_{sol}(t, t_f) = &\int_t^{t+t_f} C_f \left(T_{sol,fout}(\tau) - T_{sol,fin}(\tau)\right) \rho_f v_{sol,f}(\tau) d\tau \\ &+ \int_0^{L_{sol}} \rho_f A_f C_f \left(T_{sol,f}(t_f, \zeta) - T_{sol,f}(0, \zeta)\right) d\zeta \end{aligned} \tag{7.7}$$

The effects of the inlet temperature T_{fin} of the fluid entering the solar collector system and the fluid volumetric flow rate $v_{sol,f}$, on the gained heat were studied in a range domain of 1-25 ^oC of the inlet temperature and using a volumetric flow rate between 1 and 20 m^3h^{-1}.

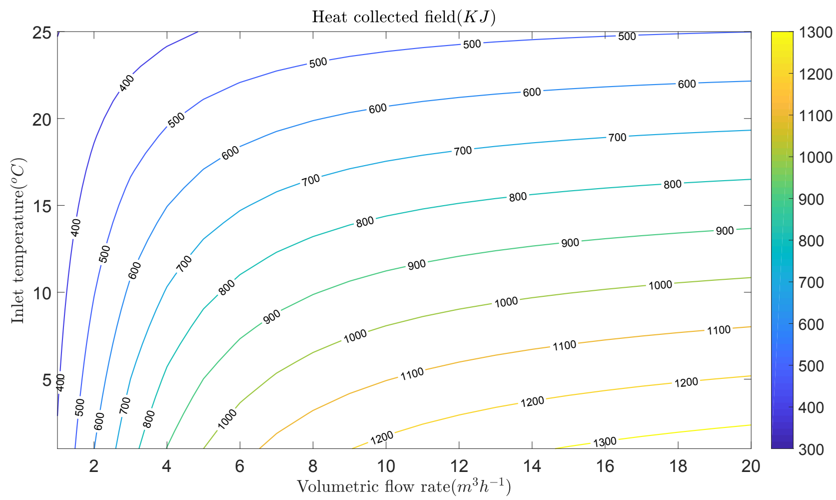

Figure 7.2: Effect of inlet temperature(^oC) and the volumetric flow rate(m^3h^{-1}) on the heat collected $H_{sol}(KJ)$ by the solar collector field.

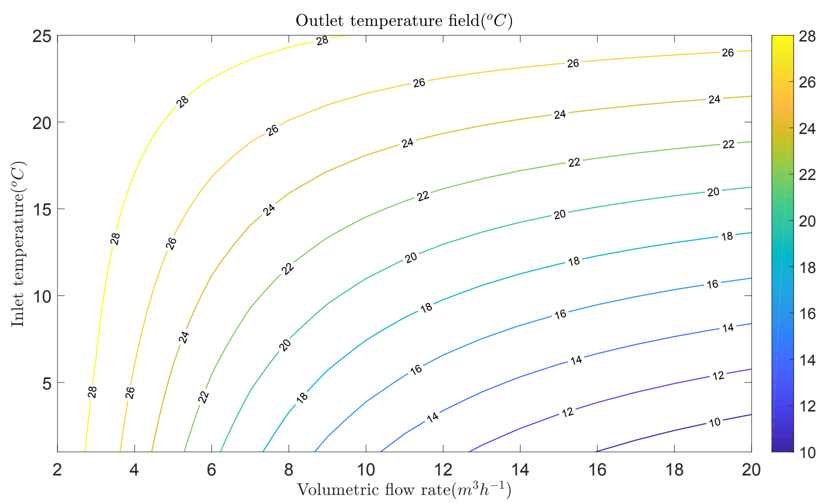

Figure 7.3: Effect of inlet temperature(^oC) and the volumetric flow rate(m^3h^{-1}) on the average outlet temperature(^oC) of the solar collector field.

From Figure 7.2, it is possible to denote that the hear collected by the solar collector field increases in proportion to the fluid volumetric flow rate, while it decreases in proportion to the inlet temperature. In contrast, From Figure 7.3, the outlet temperature decreases while the fluid flow rate increases, and given a fixed fluid flow rate, the high inlet temperature yields the high average outlet temperature. By analyzing Figure 7.2 and Figure 7.3, it can be affirmed that it is possible to maximum the collected energy and manipulating the outlet temperature by adjusting the inlet temperature and the fluid flow rate. However, in practice, it is more realistic to change the fluid flow rate $v_{sol,f}(t)$. Therefore, in the following of this chapter, we will focus on obtaining a sequence of optimal fluid flow rate such that the outlet temperature can tracking some desired set-point and the collected energy is maximized.

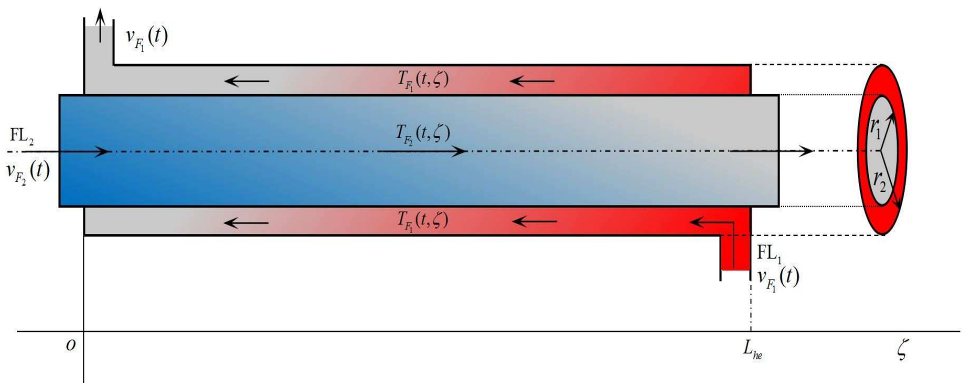

Figure 7.4: Scheme of the heat exchanger.

7.2.2 Model of heat exchanger system

In this solar-thermal district heating system, the typical counter-current heat exchangers shown in Figure 7.4, are utilized to transfer the gained heat between the solar collector field and the storage tanks and between the tanks and the heating loop systems. In Figure 7.1, the following set of hyperbolic partial differential equations are employed to present the dynamics of fluid temperature in the internal and external pipes respectively:

$$
\begin{aligned}
\rho_f C_f A_{F_1} \frac{\partial T_{F_1}}{\partial t}(t,\zeta) &= \rho_f C_f v_{F_1}(t) \frac{\partial T_{F_1}}{\partial \zeta}(t,\zeta) \\
&\qquad - k\varphi \left(T_{F_1}(t,\zeta) - T_{F_2}(t,\zeta) \right) \\
\rho_w C_w A_{F_2} \frac{\partial T_{F_2}}{\partial t}(t,\zeta) &= -\rho_w C_w v_{F_2}(t) \frac{\partial T_{F_2}}{\partial \zeta}(t,\zeta) \\
&\qquad + k\varphi \left(T_{F_1}(t,\zeta) - T_{F_2}(t,\zeta) \right)
\end{aligned}
\tag{7.8}
$$

From Figure 7.1, the fluid in the solar collector field collects the heat from the solar irradiance and transfers the gained heat to the storage hot tank through the heat exchanger: HX-1. In Figure 7.4, the hot fluid from the solar collector-FL$_1$ entering into the external pipe at the right side: $\zeta = L_{he}$ heats the cool water entering the internal pipe at the left side: $\zeta = 0$. Consequently, we have the following boundary conditions:

$$\begin{aligned} T_{F_1}(t, L_{he}) &= T_{sol,fout}(t) \\ T_{F_2}(t, 0) &= T_{F_2 in} \end{aligned} \tag{7.9}$$

One of important objectives for the considered heat exchanger is to maintain the water temperature at the outlet of the internal pipe in some desired reference values. The outlet water temperature exiting the heat exchanger is given by:

$$T_{F_2 out}(t) = T_{F_2}(t, L_{he}) \tag{7.10}$$

Moreover, the system parameter descriptions are given in Table 7.2. Since the heat exchanger HX-1 is connected to the solar collector, the hot fluid flow rate $v_{F_1}(t)$ is equal to $v_{sol,f}(t)$.

Another important objective is to maximize the stored energy. Since the inlet oil and water temperature can not be changed arbitrarily, only the fluid flow rates can be manipulated such that the outlet water temperature can be controlled to the desired value, and the stored energy can be maximized as well.

From Figure 7.5, it is straightforward to see that The water temperature at the outlet $\zeta = L_{he}$ of the heat exchanger decreases in proportional to the cool water flow rate $v_{F_2}(t)$, while it is slightly influenced by the hot oil flow rate $v_{F1}(t)$ at low flow rates $v_{F_1}(t)$. The gained heat by the storage tanks through the heat exchanger shows a hyperbolic functionality with two flow rates. In particular, at low flow rate v_{F_2} and/or v_{F_1}, the flow rate v_{F_1} and/or v_{F_2} does not significantly affect the gained heat through the heat exchanger. While at higher flow rate v_{F_1} and/or v_{F_2}, a significant increase can be seen. By analyzing Figure 7.5, it can be

Table 7.2: Heat exchanger variables and parameters in (7.8)–(7.10).

Symbol	Value and units	Description
L_{he}	$12m$	Heat exchanger length
r_1	$0.02m$	Radius of the inner pipe
r_2	$0.04m$	Radius of the external pipe
$A_{F_1} = \pi(r_2^2 - r_1^2)$	$0.0038m^2$	Area of hot oil
$A_{F_2} = \pi r_1^2$	$0.0013m^2$	Area of cool water
ρ_f	756kg m^{-3}	Oil density
ρ_w	1000kg m^{-3}	Water density
C_f	$1100JK^{-1}kg^{-1}$	Oil specific heat capacity
C_w	$4184JK^{-1}kg^{-1}$	Water specific heat capacity
k	$2000Wm^{-2}K^{-1}$	Heat exchanger coefficient
$\varphi = 2\pi r_1$	$0.1257m$	Contact circumference of heat exchanger
T_{F_1}	^oC	Oil temperature
T_{F_2}	^oC	Water temperature
T_{F_2in}	15^oC	Inlet water temperature
T_{F_2out}	^oC	Outlet water temperature
v_{F_1}	m^3s^{-1}	Oil pump volumetric flow rate
v_{F_2}	m^3s^{-1}	Water pump volumetric flow rate

confirmed that it is possible to maximize the stored energy through the heat exchanger and control the water outlet temperature at the outlet of the heat exchanger by manipulating flow rate v_{F_1} and v_{F_2}.

7.2.3 Model of district heating loop system

The district heating loop system consists of the natural gas boiler and district heating model. The gas boiler system has several limitations in time to construct the mathematic model related the available measurements. The only measurements are fluid flow and its inlet and outlet temperatures as well as the gas boiler on/off signal. In general, it is not easy to obtain the information about the internal structure of the gas boiler and any direct measure of the gas flow and temperatures. Therefore, when modeling the gas boiler, these limitations have to be taken into account. The following model is employed to describe the transient

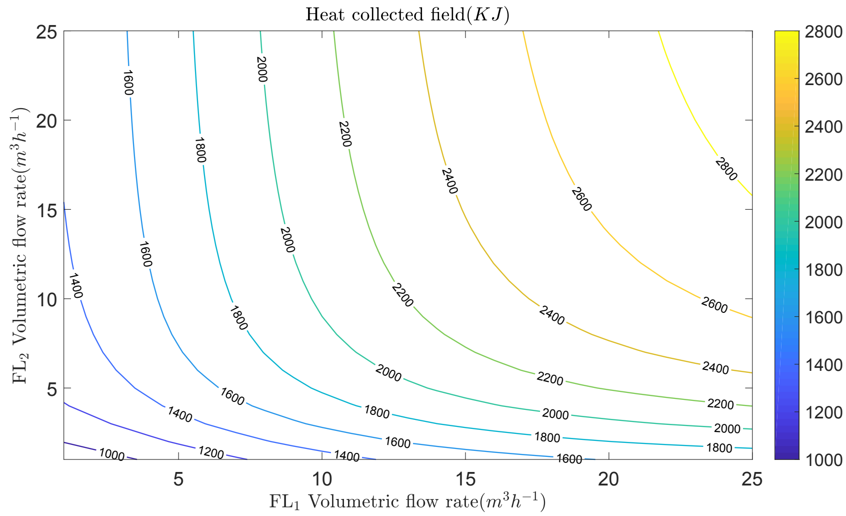

Figure 7.5: Effect of the hot oil volumetric flow rate(m^3h^{-1}) and the cool water volumetric flow rate (m^3h^{-1}) on the stored heat into the storage tanks through the heat exchanger.

dynamics of temperature in the gas boiler system:

$$\begin{aligned} \rho_w C_w V_{bol}\tfrac{dT_{bol}}{dt}(t) &= \rho_w C_w v_{bol}(t)(T_{bol,in}(t) - T_{bol}(t)) \\ &\quad + H_R(t)h_{fg}(Reg(t)T_{gas}(t) - T_{bol}(t)) \end{aligned} \tag{7.11}$$

$$\rho_w C_w A_{dis}\tfrac{\partial T_{dis}}{\partial t}(t,\zeta) = -\rho_w C_w v_{dis}\tfrac{\partial T_{dis}}{\partial \zeta}(t,\zeta), \zeta \in [0, L_{dis}] \tag{7.12}$$

The boundary condition for the district heating loop system is as follows:

$$T_{dis}(t,0) = T_{bol}(t) \tag{7.13}$$

where V_{bol} is the gas boiler fluid volume. T_{bol}, $T_{bol,in}$ and T_{dis} are the gas boiler outlet, inlet temperatures and district fluid heating temperature, respectively. $v_{bol}(t)$ is the flow rate entering the boiler system. Moreover, T_{gas} is the gas combustion temperature. h_{fg} is the approximated heat transfer coefficient between the fluid and the gas combustion. $Reg(t)$ is the gas boiler regulator defining the gas boiler power between 0% and 100%. $H_R(t)$ is the gas boiler on/off signal: 1 denotes turning on and 0 denotes turning off. The description of variables and parameters in the district heating system are provided in Table 7.3.

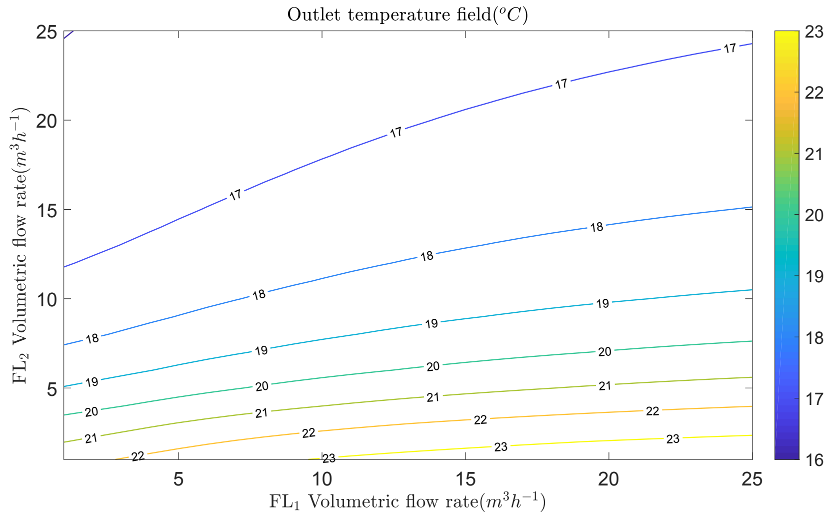

Figure 7.6: Effect of the hot oil volumetric flow rate(m^3h^{-1}) and the cool water volumetric flow rate (m^3h^{-1}) on the average outlet temperature(^oC) of the heat exchanger.

Table 7.3: District heating system variables and parameters in (7.11)–(7.13).

Symbol	Value and units	Description
L_{dis}	$40m$	District heating loop length
A_{dis}	$0.004m^2$	Heating system area
v_{dis}	$0.02m^3s^{-1}$	Flow rate of water in heating system
v_{bol}	m^3s^{-1}	Flow rate of water in boiler
V_{bol}	$0.07m^3$	Flow volume in boiler
H_R	$-$	Gas heater on/off signal
h_{fg}	$2623W/^oC$	Heat transfer coefficient
Reg	$-$	Gas heater regulator
T_{gas}	133^oC	Gas combustion temperature
$T_{bol,in}$	$18\ ^oC$	Temperature of flow entering boiler
T_{bol}	^oC	Temperature of flow in boiler
T_{dis}	^oC	Temperature of flow in district system
C_w	$4184JK^{-1}kg^{-1}$	Water specific heat capacity
ρ_w	1000kg m^{-3}	Water density

For the district heating loop system, the objective is to control the district system outlet temperature $T_{dis,out}(t) = T_{dis}(t, L_{dis})$ to track the desired value. For the case that the stored energy is enough to support district heating demand, then the gas boiler is exclude, i.e., $H_R(t) = 0$. While the tank stored energy can not satisfy the heating demand, then the gas boiler has to join into the heating system, i.e., $H_R(t) = 1$.

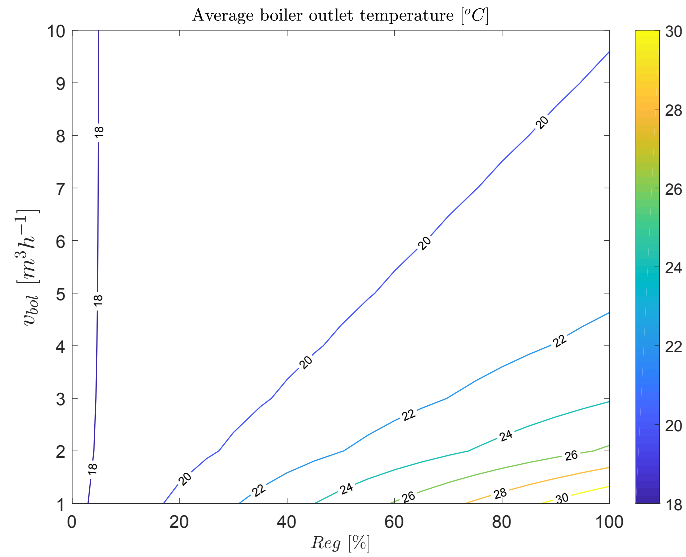

Figure 7.7: Effect of the boiler volumetric flow rate $v_{bol}(m^3h^{-1})$ and the value of gas boiler regulator Reg on the average outlet temperature(^oC) of the boiler.

7.3 Optimal operation and control of SDHS

7.3.1 Optimal operation strategy for the solar collector

We are concerned with the optimal temperature tracking control problem and the collected energy maximization problem within the time interval $[t, t+t_f]$. More precisely, the subsection is focused on obtaining a sequence of optimal fluid flow rate $v_{sol,f}(t)$ in $[t, t+t_f]$ such that the above objectives can be achieved. It is easy to observe that the considered solar collector system (7.1)–(7.2), heat exchangers (7.8) and gas boiler system (7.11) are nonlinear given that fluid flow rates $v_{sol,f}(t)$, $v_{F2}(t)$ and $v_{bol}(t)$ are manipulated variables. For the control of nonlinear systems, there has been a rapidly growing interest in utilizing receding horizon/moving horizon control schemes, which is based on solving a finite horizon optimal control problem over an interval $[t, t+t_f]$ and then applying a part of the computed control sequence from $[t, t+t_s]$ where $t_s < t_f$. Successive application of this control scheme will yield a feedback control law since the control action depends on the current state. However, due to that the optimization problem is solved over finite horizon, the stability is not ensured. Usually, in practical application, this problem can be addressed by enlarging the prediction

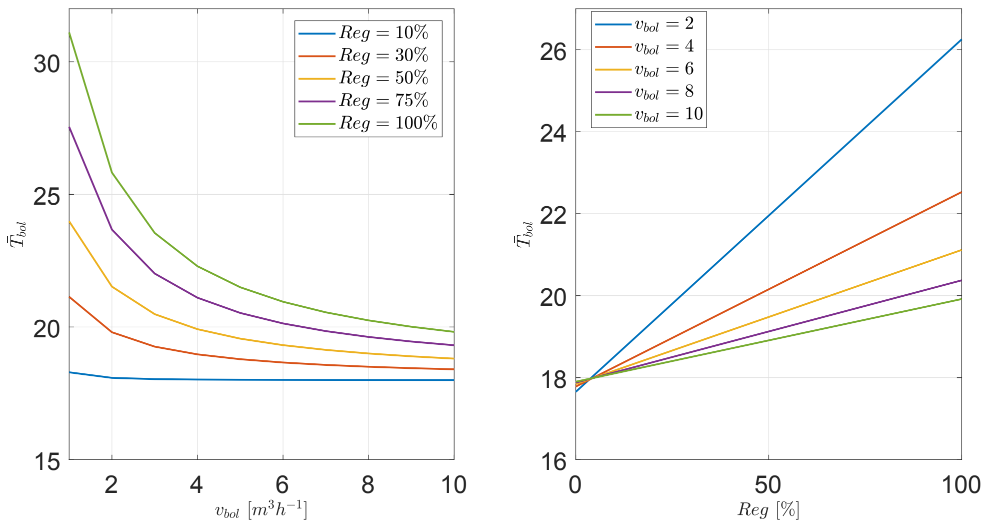

Figure 7.8: Effect of the boiler volumetric flow rate $v_{bol}(m^3h^{-1})$ and the value of gas boiler regulator Reg on the average outlet temperature(^oC) of the boiler.

horizon but this brings additional computational mission. Actually, for the stabilization problem in order to guarantee the closed-loop stability of the receding horizon scheme, different methods have been developed: a terminal stat equality constraint $x(t + t_f) = 0$ was introduced by Keerthi and Gilbert [88] to the finite-horizon optimization problem. Additionally, Chen and Allgöwer [89] proposed an approach using a quadratic endpoint penalty of the form $ax(t + t_f)^T Qx(t + t_f)$ for some $a > 0$ and some positive definite matrix Q. In this work, since the goal is to achieve desired temperature trajectory tracking, the modified quadratic terminal penalty $(T_{sol,fout}(t + t_f) - T_{des}(t + t_f))^2$ is added in the cost function as well. In particular, in the following section, the performances are compared for cases that the cost function is equipped with and without the quadratic terminal penalty.

7.3.1.1 Optimal temperature tracking control of the solar collector

The objective of the optimal control here is to find the input sequence (fluid flow rate v_{sol}(t)) that minimize a cost function, based on a desired temperature trajectory over a prediction horizon $[0, t_f]$. First, the simplest cost function is considered including the errors between the predict model outputs $T_{sol,fout}(t) = T_{sol,f}(t, L_{sol})$ and the reference trajectory $T^{sol}_{des}(t)$. In addition, it includes the change in the input $v_{sol,f}$ as well over a control horizon $[0, t_s]$. This results in the following optimization problem:

$$\begin{aligned} &\min_{v_{sol,f}} J(t, T_{sol,f}, t_f, T_{des}^{sol}) \\ &\text{s.t.} \qquad (7.1) - (7.3), (7.6) \\ &\qquad\qquad v_{\min}^{sol} \leq v_{sol,f} \leq v_{\max}^{sol} \end{aligned} \tag{7.14}$$

where the cost function is given by

$$\begin{aligned} J = & s_1 \int_t^{t+t_f} \left(T_{sol,fout}(\tau) - T_{des}^{sol}(\tau)\right)^2 d\tau \\ & + s_2 \int_t^{t+t_s} \left(\frac{dv_{sol}(\tau)}{d\tau}\right)^2 d\tau \\ & + s_1 \left(T_{sol,fout}(t+t_f) - T_{des}^{sol}(t+t_f)\right)^2 \end{aligned}$$

Note that in above cost function, the parameter s_1 denotes the weighting to the tracking reference error in the prediction and the parameter s_2 stands for the control increment in the control horizon. Moreover, the lower bound $v_{\min}^{sol}$ for the flow rate $v_{sol,f}(t)$ is given to ensure good operation conditions of the solar collector plant and the upper bound $v_{\max}^{sol}$ is due to the physical limitations of the fluid pump [90].

7.3.1.2 Solar collector outlet temperature tracking and maximization of gained heat

The practical chemical and mechanical optimal control problems often includes multiple and conflicting objectives. This usually causes a set of Pareto optimal solutions [91]. The popular exploited approaches to obtain this set are (a) the weighted sum of the individual objectives or (b) genetic algorithm [92]. In the former one, the cost function is consisting of different weighted single-objectives and the optimal control problems are solved using deterministic optimization routines. While in the latter one, a number of candidate solutions is updated based on repeated cost computations. In general, a multi-objective optimal control problem can be given by:

$$\min_{\boldsymbol{u}(t)} \{J_1, \cdots, J_n\} \tag{7.15}$$

$$\begin{aligned} &\text{subject to:} \\ &\tfrac{d\boldsymbol{x}(t)}{dt} = \boldsymbol{f}\left(\boldsymbol{x}(t), \boldsymbol{u}(t), \boldsymbol{\theta}, t\right), t \in [0, t_f], \end{aligned} \tag{7.16}$$

$$\boldsymbol{b}(\boldsymbol{x}(0), \boldsymbol{x}(t_f), \boldsymbol{\theta}) = \boldsymbol{0}, \tag{7.17}$$

$$\boldsymbol{c}_p(\boldsymbol{x}(t), \boldsymbol{u}(t), \boldsymbol{\theta}, t) \leq \boldsymbol{0}, \tag{7.18}$$

$$\boldsymbol{c}_t(\boldsymbol{x}(t_f), \boldsymbol{u}(t_f), \boldsymbol{\theta}, t_f) \leq \boldsymbol{0}, \tag{7.19}$$

where $\boldsymbol{x}$ and $\boldsymbol{u}$ are the state variables and the control variables, respectively. $\boldsymbol{\theta}$ denote the parameters and $\boldsymbol{f}$ represent the dynamic system equations on the time interval $t \in [0, t_f]$ equipped with initial and terminal conditions given by $\boldsymbol{b}$. The vectors $\boldsymbol{c}_p$ and $\boldsymbol{c}_t$ are path and terminal inequality constraints on the states and inputs. The admissible set $\mathcal{S}$ is defined to be a set of feasible inputs $\boldsymbol{u}(t)$ such that the dynamic equation as well as the path, boundary and terminal constraints in (7.16)–(7.19) are satisfied. A solution $\boldsymbol{u}_1(t) \in \mathcal{S}$ is Pareto optimization if and only if there exists no other solution $\boldsymbol{u}_2(t) \in \mathcal{S}$ such that $J_i(\boldsymbol{u}_2(t)) \leq J_i(\boldsymbol{u}_1(t))$ for all $i \in \{1, \cdots, n\}$ and $J_j(\boldsymbol{u}_2(t)) \leq J_j(\boldsymbol{u}_1(t))$ for at least one $j \in \{1, \cdots, n\}$.

In this chapter, two conflicting objectives optimal control problem will be studied: the optimal outlet temperature tracking control and the maximization of gained solar heat. To realize these two objectives simultaneously, two types of optimization problems are considered: single objective and multi-objective optimization problems in this section.

- Case 1: Single-objective

To simultaneously realize the temperature tracking control and the maximization of gained heat, we formulate a cost function including tracking cost function J given in (7.14) and the economic cost function H_{sol} - gained heat within time interval $[t, t + t_f]$ with different weightings w_1 and w_2. This results in the following single-objective minimization problem:

$$\begin{aligned}
&\min_{v_{sol,f}(t)} J_S\left(t, T_{sol,f}, t_f, T_{des}^{sol}\right) \\
&\text{s.t.} \qquad (7.1)-(7.3),(7.6) \\
&\qquad v_{\min}^{sol} \leq v_{sol,f} \leq v_{\max}^{sol}
\end{aligned} \tag{7.20}$$

where the cost function J_S is defined by

$$J_S\left(t, T_{sol,f}, t_f, T_{des}^{sol}\right) = w_1 J(t, T_{sol,f}, t_f, T_{des}^{sol}) - w_2 H_{sol}(t, t_f)$$

with positive weightings $w_1 \geq 0$ and $w_2 \geq 0$. It is straightforward to see that $w_1 = 0$ means that the target is only to maximize the collected heat while $w_2 = 0$ directly implies that the temperature trajectory tracking is the primary goal. However, if one wants to realize these two targets simultaneously, it is required to find a trade-off between them by adjusting the values of weighting w_1 and w_2. In practice, actually it is not easy to the 'best' decision, i.e., the values of w_1 and w_2. Therefore, in following an alternative way is proposed, namely multi-objective optimization.

- Case 2: Multi-objective

Provided the formulations for the tracking control cost function $J(t, T_{sol,f}, t_f, T_{des}^{sol})$ defined in (7.14) and the gained solar heat given in (7.7), a multi-objective optimization problem can be written as follows:

$$\begin{aligned}
&\min_{v_{sol,f}(t)} \left\{J(t, T_{sol,f}, t_f, T_{des}^{sol}), -H_{sol}(t, t_f)\right\} \\
&\text{s.t.} \qquad (7.1)-(7.3),(7.6) \\
&\qquad v_{\min}^{sol} \leq v_{sol,f} \leq v_{\max}^{sol}
\end{aligned} \tag{7.21}$$

Apparently, the minimization of the tracking cost function J and the maximization of economical function H_{sol} will conflict against each other. In this chapter, genetic algorithm will be employed to provide a set of trade-off optimal solutions, popularly known as Pareto-optimal solutions.

7.3.2 Optimal operation strategy for the energy storage system

In the process delivering the gained solar heat from the solar collector plant to the storage tank, the countercurrent heat exchanger HX-1 plays an important role, see Figure 7.1. As the analysis in Section 7.2, by manipulating flow rates of fluid FL_1 and FL_2 (see Figure 7.4), one is able to change the temperature of the fluid FL_2 at the outlet as well the stored heat into the storage hot tank. In this subsection, both the solar collector plant and the heat exchanger HX-1 are considered simultaneously (see Figure 7.9) and optimal operation strategies will be studied to achieve the fluid FL_2 outlet temperature tracking control and the maximization of the stored heat into the hot tank. Similarly, two different optimization problems will be formulated as the illustration in Section 7.3.1.2

- Case 1: Single-objective

$$\begin{aligned} &\min_{v_{F_1}(t),v_{F_2}(t)} J_H\left(t, T_{F_2}, t_f, T_{des}^{F_2}\right) \\ &\text{s.t.} \qquad (7.1)-(7.3) \\ &\qquad\qquad (7.8)-(7.10) \end{aligned} \tag{7.22}$$

where the cost function is defined as:

$$J_H\left(t, T_{F_2}, t_f, T_{des}^{F_2}\right) = w_1 J_{F_2}\left(t, T_{F_2}, t_f, T_{des}^{F_2}\right) - w_2 H_{stor}(t, t_f)$$

with J_{F_2} and H_{stor} given by, respectively

$$\begin{aligned} J_{F_2}\left(t, T_{F_2}, t_f, T_{des}^{F_2}\right) = &\, s_1 \int_t^{t+t_f} \left(T_{F_2 out}(\tau) - T_{des}^{F_2}(\tau)\right)^2 d\tau \\ &+ s_2 \int_t^{t+t_f} \left(\frac{dv_{F_1}(\tau)}{d\tau}\right)^2 d\tau \\ &+ s_1 \left(T_{F_2 out}(t+t_f) - T_{des}^{F_2}(t+t_f)\right)^2 \end{aligned} \tag{7.23}$$

$$H_{stor}(t,t_f) = \int_t^{t+t_f} C_w\left(T_{F_2out}(\tau) - T_{F_2in}(\tau)\right)\rho_w v_{F_2}(\tau)d\tau$$
$$+ \int_0^{L_{he}} \rho_w A_{F_2} C_w\left(T_{F_2}(t_f,\zeta) - T_{F_2}(0,\zeta)\right)d\zeta \tag{7.24}$$

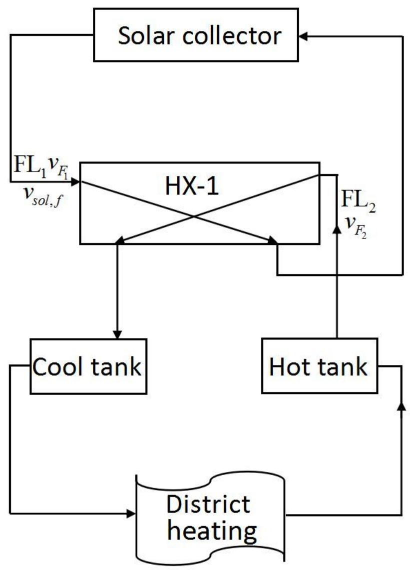

Figure 7.9: Schematic diagram of the heat exchanger HX-1 coupled with the solar collector plant.

- Case 2: Multi-objective

$$\begin{aligned} \min_{v_{F_1}(t), v_{F_2}(t)} \quad & \left\{ J_{F_2}\left(t, T_{F_2}, t_f, T_{des}^{F_2}\right), H_{stor}\left(t, t_f\right) \right\} \\ \text{s.t.} \quad & (7.1) - (7.3) \\ & (7.8) - (7.10) \end{aligned} \tag{7.25}$$

with J_{F_2} and H_{stor} defined in (7.23) and (7.24), respectively.

7.3.3 Servo-control of the boiler-heating system

In this section, we will consider the case that the stored energy is not enough to support the heating requirements. Therefore, the boiler system has to joint to supply the energy. Observe the boiler-heating system (7.11)-(7.13), it is easy to find that the boiler system (7.11) and the heating system (7.12) are coupled only through the boundary condition in

(7.13). Moreover, for the boiler system (7.11), the manipulated inputs are the gas boiler regulator $Reg(t)$ that ranges from %0 to %100 and the flow rate $v_{bol}(t)$, and for the district heating system (7.13), the input is the gas boiler outlet temperature $T_{bol}(t)$. Then, based on the characteristics of the considered boiler-heating system (7.11)-(7.13), we propose the following algorithm:

A1. Applying Internal Model Principle based servo-control approach to the district heating system (7.12) generates a sequence of desired input $T^*_{bol}(t)$ which can be regarded as the set-point for the boiler outlet temperature $T_{bol}(t)$ such that the required district temperature $T^*_{dis}(t)$ can be achieved, i.e., $\lim_{t\to\infty}(T_{dis}(t, L_{dis}) - T^*_{dis}(t)) = 0$.

A2. Using receding horizon optimal control drives the boiler system (7.11) such that the boiler outlet temperature $T_{bol}(t)$ tracks the desired temperature $T^*_{bol}(t)$.

7.3.3.1 Servo-control of the heating system

Suppose that the district requirements i.e., $T^*_{dis}(t)$ are known, then we can formulate these signals through the following signal process:

$$\dot{w}(t) = Sw(t) \tag{7.26}$$

$$T^*_{dis}(t) = Fw(t) \tag{7.27}$$

where the matrix S is a skew-Hermitian matrix and has all its eigenvalues on imaginary axis. Namely, the spectrum of S can be given by $\sigma(S) = 0 \cup \{iw_k\}, k = 1, 2\cdots, n-1$ or $\sigma(S) = \{iw_k\}, k = 1, 2\cdots, n$. In fact, this configuration allows the modelling of steplike and sinusoidal exogenous signals.

In this section, given available $T^*_{dis}(t)$, our target is to design the following controller:

$$\begin{aligned} \dot{\hat{w}}(t) &= S\hat{w}(t) + K(T^*_{dis}(t) - F\hat{w}(t)) \\ T^*_{bol}(t) &= m_w^T\hat{w}(t) \end{aligned} \tag{7.28}$$

such that the outlet district heating temperature $T_{dis}(t, L_{dis})$ can track the required temperature $T^*_{dis}(t)$.

Theorem 19. *Suppose that the pair (F, S) is observable and the spatial-varying vector satisfies the following differential equation:*

$$\begin{aligned} &\tfrac{v_{dis}}{A_{dis}}\tfrac{dm^T}{d\zeta}(\zeta) + m^T(\zeta)S = 0 \\ &m^T(L_{dis}) = F \end{aligned} \tag{7.29}$$

If the feedforward gain m^T_w given by $m^T_w = m^T(\zeta = 0)$ and there exists K such that $S + KF$ is Hurwitz, then applying the control law in (7.28) can drive the outlet district heating temperature $T_{dis}(t, L_{dis})$ to track the required temperature $T^*_{dis}(t)$.

Proof. First, we can define a tracking error variable:

$$\tilde{e}(t, \zeta) = T_{dis}(t, \zeta) - m^T(\zeta)\hat{w}(t) \tag{7.30}$$

Consequently, we will have:

$$\begin{aligned} \tfrac{\partial \tilde{e}}{\partial t}(t, \zeta) &= \tfrac{\partial T_{dis}}{\partial t}(t, \zeta) - m^T(\zeta)\tfrac{d\hat{w}}{dt}(t) \\ \tfrac{\partial \tilde{e}}{\partial \zeta}(t, \zeta) &= \tfrac{\partial T_{dis}}{\partial \zeta}(t, \zeta) - \tfrac{dm^T}{d\zeta}(\zeta)\hat{w}(t) \end{aligned}$$

Substituting the above equations into (7.12) leads to the following expression:

$$\frac{\partial \tilde{e}}{\partial t}(t, \zeta) = -\frac{v_{dis}}{A_{dis}}\frac{\partial \tilde{e}}{\partial \zeta}(t, \zeta) - \frac{v_{dis}}{A_{dis}}\frac{dm^T}{d\zeta}(\zeta)\hat{w}(t) - m^T(\zeta)\frac{d\hat{w}}{dt}(t) \tag{7.31}$$

According to (7.27), (7.28) and (7.31),

$$\frac{\partial \tilde{e}}{\partial t}(t, \zeta) = -\frac{v_{dis}}{A_{dis}}\frac{\partial \tilde{e}}{\partial \zeta}(t, \zeta) - \left(\frac{v_{dis}}{A_{dis}}\frac{dm^T}{d\zeta}(\zeta) + m^T(\zeta)S\right)\hat{w}(t) + m^T(\zeta)KF\Delta w(t) \tag{7.32}$$

with $\Delta w(t) = \hat{w}(t) - w(t)$. The boundary condition for (7.31) is given by:

$$\begin{aligned} \tilde{e}(t,0) &= T_{dis}(t,0) - m^T(0)\hat{w}(t) \\ &= m_w^T \hat{w}(t) - m^T(0)\hat{w}(t) \end{aligned} \tag{7.33}$$

Moreover, the tracking error $e(t) = T_{dis}(t, L_{dis}) - T^*_{dis}(t)$ can be expressed as follows:

$$\begin{aligned} e(t) &= T_{dis}(t, L_{dis}) - Fw(t) \\ &= \tilde{e}(t, L_{dis}) + \left(m^T(L_{dis}) - F\right)\hat{w}(t) + F\Delta w(t) \end{aligned} \tag{7.34}$$

Subtracting (7.26) from (7.28) gives the dynamical system for $\Delta w(t)$:

$$\frac{d\Delta w}{dt}(t) = (S + KF)\,\Delta w(t)$$

Since the matrix $S + KF$ is Hurwitz, $\Delta w(t)$ decays to zero exponentially. In this case, the equations (7.32), (7.33) and (7.34) reduce to the following form:

$$\begin{aligned} \tfrac{\partial \tilde{e}}{\partial t}(t,\zeta) &= -\tfrac{v_{dis}}{A_{dis}}\tfrac{\partial \tilde{e}}{\partial \zeta}(t,\zeta) \\ \tilde{e}(t,0) &= 0 \\ e(t) &= \tilde{e}(t, L_{dis}) \end{aligned} \tag{7.35}$$

if the conditions in theorem are satisfied, i.e.,

$$\begin{aligned} &\tfrac{v_{dis}}{A_{dis}}\tfrac{dm^T}{d\zeta}(\zeta) + m^T(\zeta)S = 0 \\ &m^T(L_{dis}) = F \\ &m_w^T = m^T(\zeta = 0) \end{aligned}$$

It is easy to see that the system (7.35) is exponentially stable and therefore the tracking error $e(t) = T_{dis}(t, L_{dis}) - T^*_{dis}(t)$ will decay to zero exponentially. In other words, the outlet heating temperature will meet the requirement. $\square$

7.3.3.2 Optimal tracking control of the boiler system

Based on the algorithm **A1-A2**, through the servo-control applied to the district heating system (7.12), the desired temperature from the boiler system $T^*_{bol}(t)$ is obtained. In this section, the receding horizon optimal control is employed to address the tracking problem of the boiler system (7.11) such that the boiler outlet temperature $T_{bol}(t)$ tracks the obtained set-point temperature $T^*_{bol}(t)$. As a result, the following optimization problem is formulated:

$$\begin{aligned} \min_{v_{bol}, Reg} \ & J_{bol} = \int_t^{t+t_f} \left(T_{bol}(\tau) - T^*_{bol}(\tau)\right)^2 d\tau \\ \text{s.t.} \quad & (7.11) \\ & 0 \leq Reg \leq 1 \\ & 0 \leq v_{bol} \leq 1 \end{aligned} \tag{7.36}$$

Solving the above optimization problem provides a sequence of optimal inputs: v_{bol} and Reg. Additionally, in order to smooth the operations on the flow rate v_{bol} and the regulator Reg, the cost function can be improved as:

$$\begin{aligned} J_{bol} = & \int_t^{t+t_f} \left(T_{bol}(\tau) - T^*_{bol}(\tau)\right)^2 d\tau \\ & + \int_t^{t+t_s} \left(\tfrac{dv_{bol}}{d\tau}(\tau)\right)^2 d\tau + \int_t^{t+t_s} \left(\tfrac{dReg}{d\tau}(\tau)\right)^2 d\tau \end{aligned}$$

7.4 Boundary state observer design for the solar collector system

From the previous section, full temperature states of the solar collector $T_{sol,m}(t,\zeta)$ and $T_{sol,f}(t,\zeta)$ are used to serve the receding horizon controller design. Nevertheless, in practice it is impossible to apply a distributed sensing to measure the full state information. The available measurements are those of the solar irradiance $I(t)$ using a pyrheliometer [93], of the environment temperature $T_a(t)$ and of the output temperature $T_{sol,f}(t, L_{sol})$. To overcome this restriction, we develop a boundary state observer with the available measurements and prove the convergence of the observer.

We propose the state observer with the following form:

$$\begin{aligned}\rho_m C_m A_m \tfrac{\partial \hat{T}_{sol,m}}{\partial t}(t,\zeta) &= \mu_0 G I(t) - D_m \pi h_l (\hat{T}_{sol,m}(t,\zeta) - T_a(t)) \\ &\quad - D_f \pi h_t (\hat{T}_{sol,m}(t,\zeta) - \hat{T}_{sol,f}(t,\zeta))\end{aligned} \tag{7.37}$$

$$\begin{aligned}\rho_f C_f A_f \tfrac{\partial \hat{T}_{sol,f}}{\partial t}(t,\zeta) &= -\rho_f C_f v_{sol,f}(t) \tfrac{\partial \hat{T}_{sol,f}}{\partial \zeta}(t,\zeta) \\ &\quad + D_f \pi h_t (\hat{T}_{sol,m}(t,\zeta) - \hat{T}_{sol,f}(t,\zeta))\end{aligned} \tag{7.38}$$

with the initial and boundary conditions:

$$\hat{T}_{sol,f}(0,\zeta) = T_{sol,f0}(\zeta) \tag{7.39}$$

$$\hat{T}_{sol,f}(t,0) = T_{sol,fin}(t) - \kappa \Delta T_{sol,f}(t, L_{sol}) \tag{7.40}$$

where $\Delta T_{sol,f}(t,\zeta) = \hat{T}_{sol,f}(t,\zeta) - T_{sol,f}(t,\zeta)$ is the observer error and $\Delta T_{sol,f}(t, L_{sol})$ is the correction term (output error). This state observer is a Luenberger-like observer but the correction term $\Delta T_{sol,f}(t, L_{sol})$ is just injected in the boundary condition $\hat{T}_{sol,f}(t,0)$ rather than being injected in the state equation.

Based on the plant (7.1)-(7.3) and the observer (7.37)-(7.40), the observer error system can be directly given by:

$$\begin{aligned}\rho_m C_m A_m \tfrac{\partial \Delta T_{sol,m}}{\partial t}(t,\zeta) &= -(D_m \pi h_l + D_f \pi h_t) \Delta T_{sol,m}(t,\zeta) \\ &\quad + D_f \pi h_t \Delta T_{sol,f}(t,\zeta)\end{aligned} \tag{7.41}$$

$$\begin{aligned}\rho_f C_f A_f \tfrac{\partial \Delta T_{sol,f}}{\partial t}(t,\zeta) &= -\rho_f C_f v_{sol,f}(t) \tfrac{\partial \Delta T_{sol,f}}{\partial \zeta}(t,\zeta) \\ &\quad + D_f \pi h_t (\Delta T_{sol,m}(t,\zeta) - \Delta T_{sol,f}(t,\zeta))\end{aligned} \tag{7.42}$$

with the boundary condition:

$$\Delta T_{sol,f}(t,0) = -\kappa \Delta T_{sol,f}(t, L_{sol}) \tag{7.43}$$

Theorem 20. *If $\kappa^2 \leq e^{-\mu}$ where μ is a tuning positive parameter, the proposed boundary state observer in (7.37)-(7.40) exponentially converges, i.e., the observer error system (7.41)-(7.43) is exponentially stable.*

Proof. Define the following Lyapunov candidate function that was proposed in [33] to study the exponential stability of hyperbolic systems of conservation laws:

$$V(t) = \int_0^{L_{sol}} \left(qe^{-\mu\zeta}(\Delta T_{sol,m}(t,\zeta))^2 + pe^{-\mu\zeta}(\Delta T_{sol,f}(t,\zeta))^2\right)d\zeta \tag{7.44}$$

The derivative of $V(t)$ with respect to time t can be written as:

$$\begin{aligned}\dot{V}(t) &= \textstyle\int_0^{L_{sol}} \left(2qe^{-\mu\zeta}\Delta T_{sol,m}(t,\zeta)\frac{\partial \Delta T_{sol,m}}{\partial t}(t,\zeta) + 2pe^{-\mu\zeta}\Delta T_{sol,f}(t,\zeta)\frac{\partial \Delta T_{sol,f}}{\partial t}(t,\zeta)\right)d\zeta \\ &= -\textstyle\int_0^{L_{sol}} \left(2q\left(\alpha_1+\alpha_2\right)e^{-\mu\zeta}\left(\Delta T_{sol,m}(t,\zeta)\right)^2\right)d\zeta \\ &\quad + \left(2q\alpha_2 + 2p\alpha_3\frac{v_{sol,f}(t)}{A_f}\right)\textstyle\int_0^{L_{sol}} \left(e^{-\mu\zeta}\Delta T_{sol,m}(t,\zeta)\Delta T_{sol,f}(t,\zeta)\right)d\zeta \\ &\quad - \textstyle\int_0^{L_{sol}} \left(2p\frac{v_{sol,f}(t)}{A_f}e^{-\mu\zeta}\Delta T_{sol,f}(t,\zeta)\frac{\partial \Delta T_{sol,f}}{\partial \zeta}(t,\zeta)\right)d\zeta \\ &\quad -2\alpha_3\frac{v_{sol,f}(t)}{A_f}\textstyle\int_0^{L_{sol}} \left(pe^{-\mu\zeta}(\Delta T_{sol,f}(t,\zeta))^2\right)d\zeta\end{aligned} \tag{7.45}$$

where the parameters α_1, α_2 and α_3 are given by:

$$\alpha_1 = \frac{D_m\pi h_l}{\rho_m C_m A_m}, \alpha_2 = \frac{D_f\pi h_t}{\rho_m C_m A_m}, \alpha_3 = \frac{D_f\pi h_t}{\rho_f C_f A_f}$$

Obviously, α_1, α_2 and α_3 are positive numbers.

Applying integration by parts, it is straightforward to compute:

$$\begin{aligned}\dot{V}(t) &= -\textstyle\int_0^{L_{sol}} \left(2q\left(\alpha_1+\alpha_2\right)e^{-\mu\zeta}(\Delta T_{sol,m}(t,\zeta))^2\right)d\zeta \\ &\quad + \left(2q\alpha_2 + 2p\alpha_3\frac{v_{sol,f}(t)}{A_f}\right)\textstyle\int_0^{L_{sol}} \left(e^{-\mu\zeta}\Delta T_{sol,m}(t,\zeta)\Delta T_{sol,f}(t,\zeta)\right)d\zeta \\ &\quad -p\frac{v_{sol,f}(t)}{A_f}\left((\Delta T_{sol,f}(t,L_{sol}))^2e^{-\mu} - (\Delta T_{sol,f}(t,0))^2\right) \\ &\quad - \left(2\alpha_3\frac{v_{sol,f}(t)}{A_f} + \frac{v_{sol,f}(t)}{A_f}\mu\right)\textstyle\int_0^{L_{sol}} \left(pe^{-\mu\zeta}(\Delta T_{sol,f}(t,\zeta))^2\right)d\zeta\end{aligned} \tag{7.46}$$

Using the boundary condition in (7.43) leads to:

$$
\begin{aligned}
\dot{V}(t) = &-\int_0^{L_{sol}} \left(2q\left(\alpha_1+\alpha_2\right)e^{-\mu\zeta}(\Delta T_{sol,m}(t,\zeta))^2\right)d\zeta \\
&+\left(2q\alpha_2+2p\alpha_3\tfrac{v_{sol,f}(t)}{A_f}\right)\int_0^{L_{sol}}\left(e^{-\mu\zeta}\Delta T_{sol,m}(t,\zeta)\Delta T_{sol,f}(t,\zeta)\right)d\zeta \\
&-\left(2\alpha_3\tfrac{v_{sol,f}(t)}{A_f}+\tfrac{v_{sol,f}(t)}{A_f}\mu\right)\int_0^{L_{sol}}\left(pe^{-\mu\zeta}(\Delta T_{sol,f}(t,\zeta))^2\right)d\zeta \\
&-p\tfrac{v_{sol,f}(t)}{A_f}\left(e^{-\mu}-\kappa^2\right)\left(\Delta T_{sol,f}(t,L_{sol})\right)^2
\end{aligned}
\tag{7.47}
$$

Observe (7.47), we can conclude that as long as the condition $\kappa^2 \le e^{-\mu}$ is satisfied, then it is possible to chose a large positive number μ to ensure $\dot{V}(t) < -\alpha V(t)$ with $\alpha > 0$. In other words, the observer error system (7.41)-(7.43) is exponentially stable. □

7.5 Results and discussion

7.5.1 Observer design for the solar collector system

With the parameters given in Table 7.1, we first design the boundary observer the system (7.1)-(7.3) with the measured outlet temperature $T_{sol,f}(t, L_{sol})$. According to Theorem 20, in order to guarantee the exponential convergence of the designed observer (7.37)-(7.40), here the injection gain κ is chosen as $\kappa = 0.5$. In Figure 7.10, without lose of generality, the temperatures at the points $\zeta = 0.3L_{sol}$ and $\zeta = L_{sol}$ are shown. Moreover, the evolutions of observer error on time scale and space scale are also presented. The estimated temperatures converge to the real temperature very fast and correspondingly, the observer errors decay to zero exponentially.

7.5.2 Optimal operation for the solar collector system

7.5.2.1 Optimal outlet temperature tracking control

In this subsection, we formulated the optimization problem in (7.14) to present and address the optimal outlet temperature tracking problem. In particular, since the prediction horizon

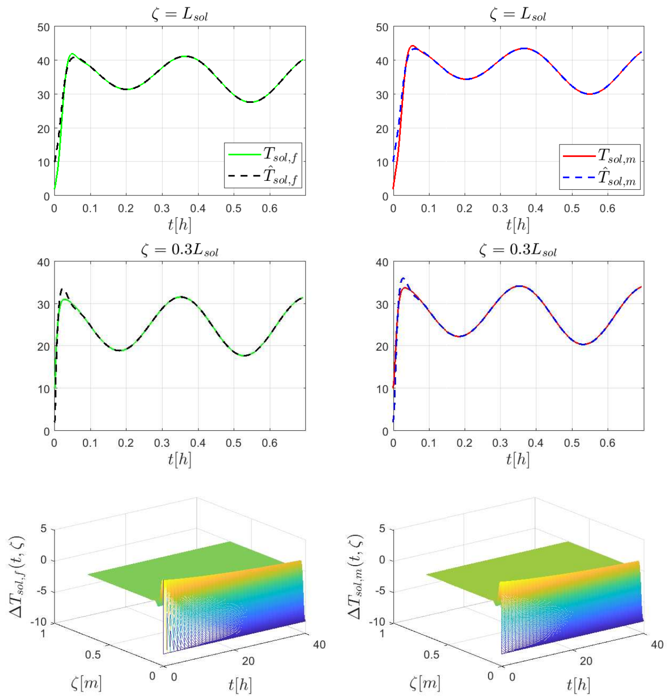

Figure 7.10: The solar collector temperatures $T_{sol,f}$ and $T_{sol,m}$, the estimated temperatures $\hat{T}_{sol,f}$ and $\hat{T}_{sol,m}$ and observer errors $\Delta T_{sol,f}$ and $\Delta T_{sol,m}$.

is always chosen as a finite-time horizon, the following different cases are discussed in this section:

Case 1. The cost function is formulated with terminal penalty:

$$\begin{aligned} J = s_1 \int_t^{t+t_f} &\left(T_{sol,fout}(\tau) - T_{des}^{sol}(\tau)\right)^2 d\tau \\ &+ s_2 \int_t^{t+t_s} \left(\frac{dv_{sol}(\tau)}{d\tau}\right)^2 d\tau \\ &+ s_1 \left(T_{sol,fout}(t+t_f) - T_{des}^{sol}(t+t_f)\right)^2 \end{aligned}$$

Case 2. The cost function is formulated without terminal penalty:

$$\begin{aligned} J = s_1 \int_t^{t+t_f} &\left(T_{sol,fout}(\tau) - T_{des}^{sol}(\tau)\right)^2 d\tau \\ &+ s_2 \int_t^{t+t_s} \left(\frac{dv_{sol}(\tau)}{d\tau}\right)^2 d\tau \end{aligned}$$

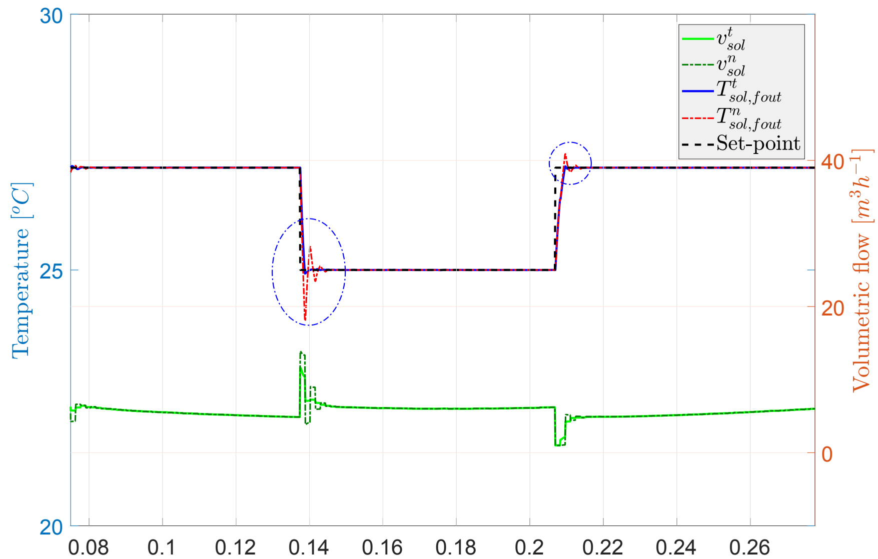

Figure 7.11: The outlet temperature of the solar collector field under the receding horizon control with terminal penalty and without terminal penalty, respectively.

In Figure 7.11, it is very clear to see that there are larger vibrations (red dash line) by applying the optimal control without terminal penalty, when the reference trajectory switches from one set-point to another set-point. Nevertheless, applying the optimal control involving the optimization cost function in **Case 1** has a better performance.

7.5.2.2 Optimal temperature tracking control and maximization of collected heat

Based on the formulations in (7.20) and (7.21), the receding horizon optimal control algorithms with single objective and multi-objective are applied. In particular, the single objective optimal control algorithms with different values of weights: $w_1 = 10$, $w_2 = 1$ and $w_1 = 10$, $w_2 = 50$ are applied and compared. The results are shown in Figure 7.13. For the case $w_1 = 10$ and $w_2 = 1$, the control has a better tracking performance while the collected energy is relatively low, which can be seen in Figure 7.14 (the blue bar), whereas in the case $w_1 = 10$ and $w_2 = 50$, the control algorithm has a very poor tracking performance but the solar collector collects higher energy (the grey bar). In other aspect, the genetic algorithm

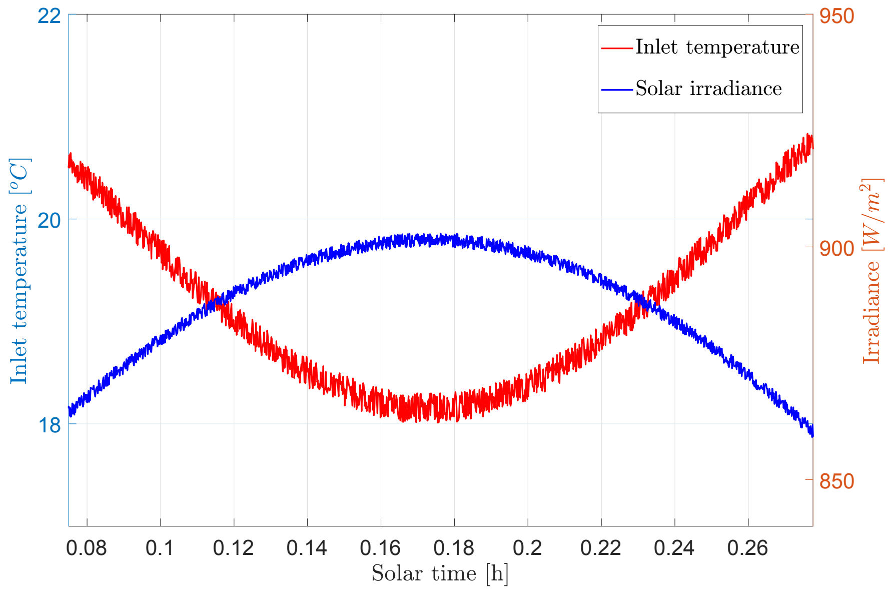

Figure 7.12: The outlet temperature of the solar collector field and the solar irradiance.

(GA) is used to solve the multi-objective optimization problem given in (7.21), see [92]. In Figure 7.13 and Figure 7.14, solving the multi-objective optimization problem leads to a better tracking performance as well as a relatively high collected energy (the yellow bar).

7.5.3 Optimal operation of the energy storage system

The flow rates control of heat exchanger HX-1 in Figure 7.1 is crucial to the maximization of stored energy into the storage system as well as the outlet temperature of the heat exchanger. Since the outlet temperature tracking control and the maximization of the stored energy are conflict objective, the single objective and multi-objective optimization problems formulated in Section 7.3.2 are studied and solved to find a trade-off to achieve the maximization of the stored energy as well as the tracking control of the outlet temperature. Particularly, when considering the single-objective optimization, two different cases are studied, i.e. $w_1 = 100$, $w_2 = 2$ and $w_1 = 100$, $w_2 = 2000$. Consequently, in the former case, manipulating the resulting flow rates v_{F_1} and v_{F_2} yields a better tracking control performance but low stored energy in the storage system. Nevertheless, the latter case gives a high stored energy but poor tracking control performance. Finally, the multi-objective optimization problem is

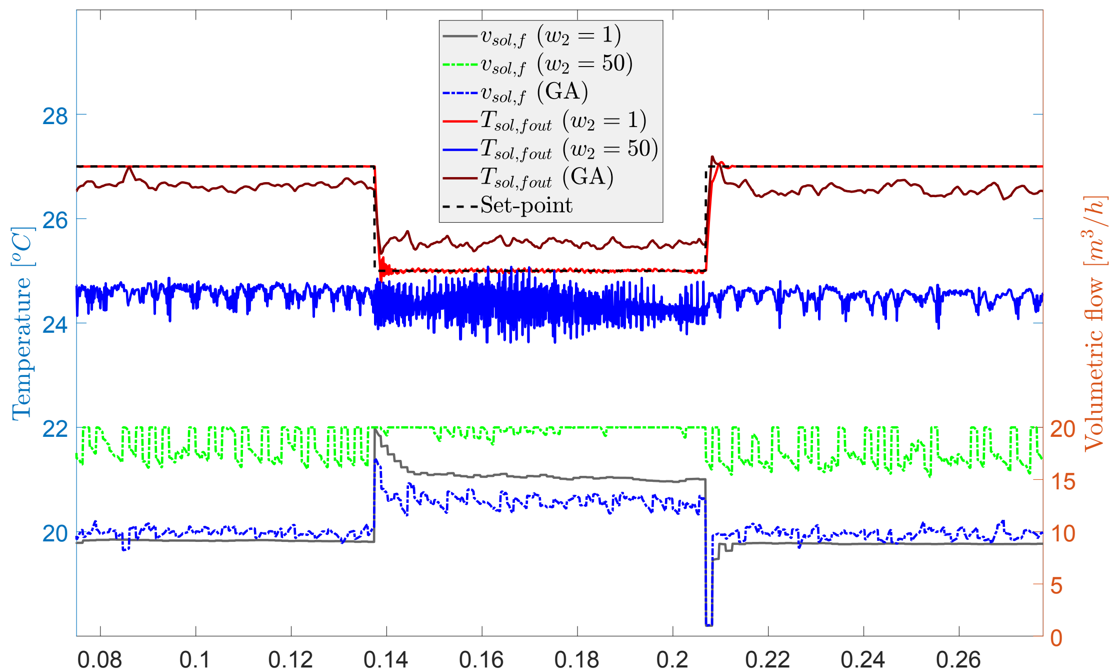

Figure 7.13: The outlet temperature of the solar collector filed under the receding horizon control without terminal penalty.

solved using GA. Figure 7.15 and Figure 7.17 shows that multi-objective optimal control provides a better tracking performance and relatively maximized stored energy.

7.5.4 Servo-control of the boiler-heating system

For the simplicity, we assume that the required district temperature is a periodic signal given by: $T^*_{dis}(t) = 22 + sin(0.02t)$. In fact, this signal can be modelled by the exogenous signal process (7.26)-(7.27) with $S = \begin{bmatrix} 0 & 0 & 0 \\ 0 & 0 & 0.02 \\ 0 & -0.02 & 0 \end{bmatrix}$, $F = \begin{bmatrix} 22 & 1 & 0 \end{bmatrix}$ and $w(0) = \begin{bmatrix} 1 \\ 0 \\ 1 \end{bmatrix}$.

As a consequence, solving (7.26) gives $w(t) = \begin{bmatrix} 1 \\ \sin(0.02t) \\ \cos(0.02t) \end{bmatrix}$. It is straightforward to obtain the feedforward gain $m_w^T = \begin{bmatrix} 22 & 0.9872 & 0.1593 \end{bmatrix}$. Moreover, it is easy to see

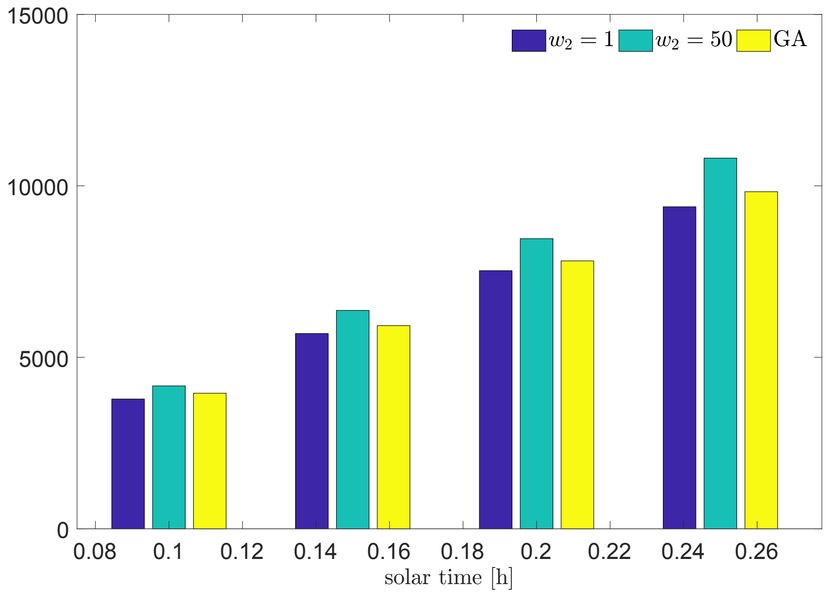

Figure 7.14: The collected energy under different control sequences obtained by solving different optimization problems.

that the matrix $S + KF$ is Hurwitz with $K = \begin{bmatrix} 1 \\ 1 \\ 1 \end{bmatrix}$. By applying the control law in (7.28), the desired boiler temperature $T^*_{bol}(t)$ is obtained such that the district outlet temperature $T_{dis,out}(t)$ tracks the desired temperature T^*_{dis} and satisfies the demand of customers. Given the resulting desired boiler temperature T^*_{bol}, the receding horizon optimal control is applied to achieve the periodical trajectory tracking control. In particular, two control cases are discussed. In one case, the gas boiler regulator is fixed as $Reg = 100\%$ and the optimal control is applied to generate a sequence of optimal input-boiler water flow rate v_{bol} such that the boiler outlet temperature $T_{bol}(t)$ tracks the expected temperature $T^*_{bol}(t)$. The performance of the controller and the corresponding water flow rate are shown in Figure 7.20. Moreover, the second case considers a constant water flow rate $v_{bol} = 1\ m^3h^{-1}$ and the receding horizon optimal control provides a sequence of optimal value of the gas boiler regulator $Reg(t)$, see Figure 7.21.

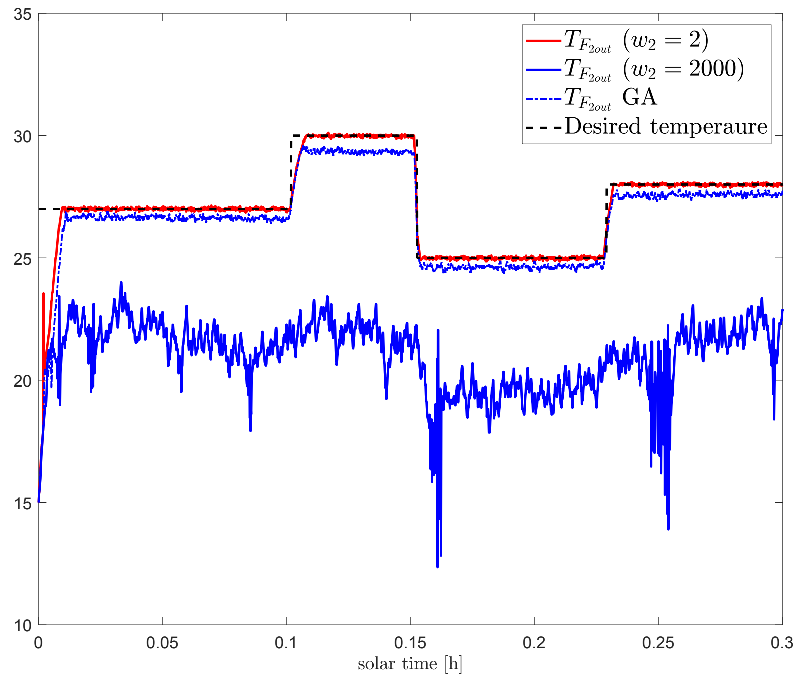

Figure 7.15: The outlet temperature of the heat exchanger under the receding horizon control with single objective and multi-objective, respectively.

7.6 Conclusion

This chapter addressed the optimal operation and control problems for a solar-thermal system, more specifically, a solar-thermal district heating system composed of a solar collector system, heat exchangers, gas boiler, and the district heating system. In particular, single objective and multi-objective optimization problems are considered in the framework of the receding horizon optimal control to address the problems on the outlet temperature tracking and the maximization of the collected/stored energy through the solar collector and heat exchanger systems. Furthermore, the multi-objective optimization problems were solved using genetic algorithm and the corresponding receding horizon optimal control can provide satisfactory results.

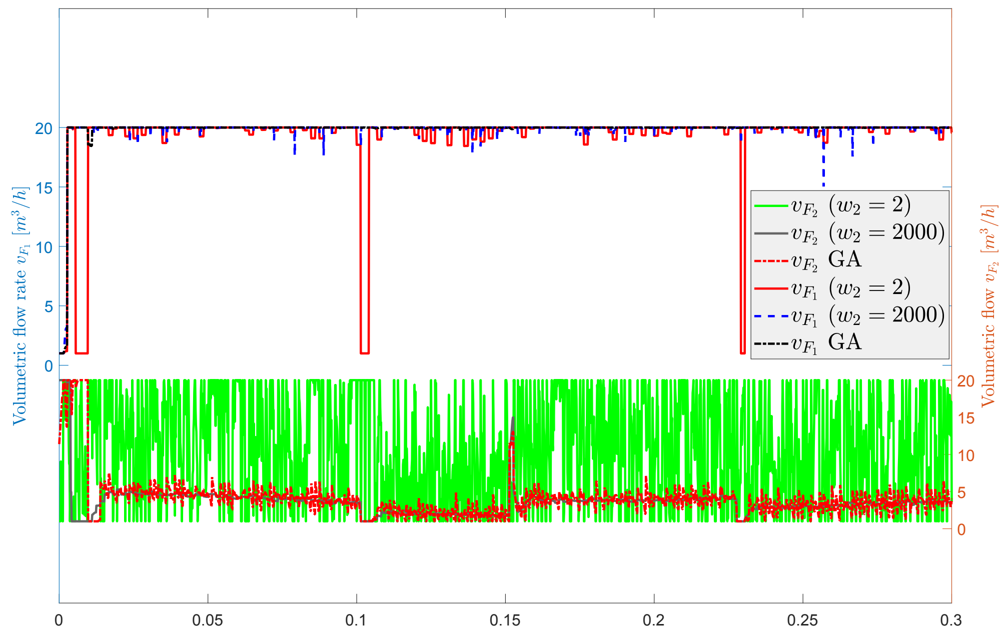

Figure 7.16: The manipulated flow rates $v_{F_1}(t)$ and $v_{F_2}(t)$ entering the heat exchanger generated by solving single-objective and multi-objective optimization problems.

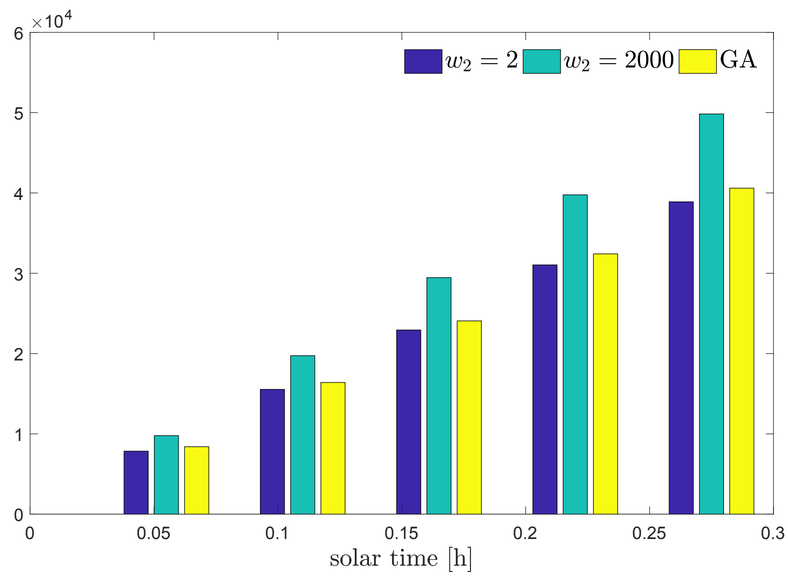

Figure 7.17: The outlet temperature of the solar collector filed under the receding horizon control without terminal penalty.

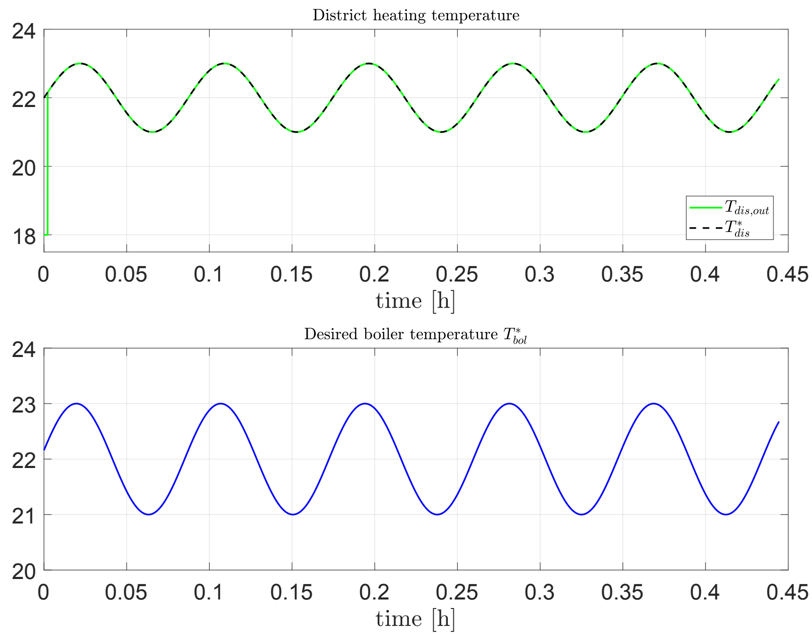

Figure 7.18: The district outlet temperature under the servo-control law in (7.28).

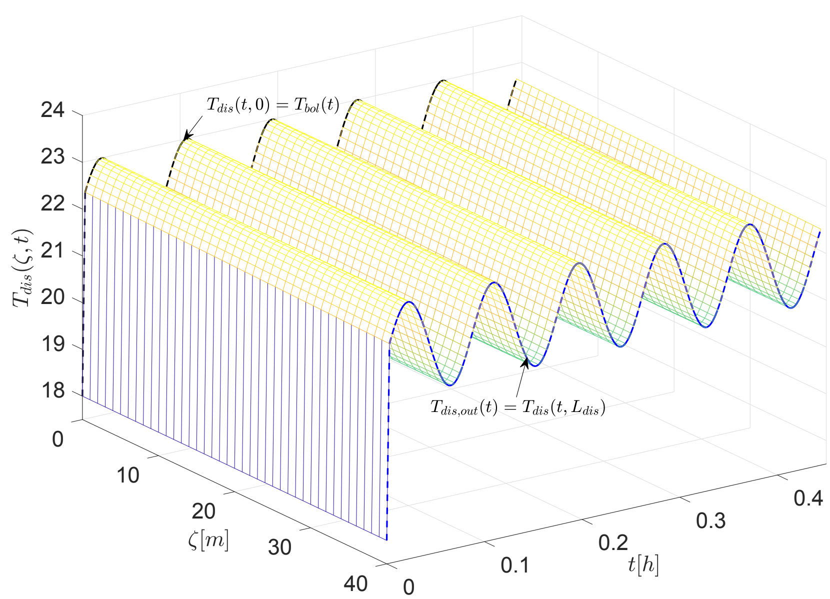

Figure 7.19: The entire temperature distribution along the length of pipeline and evolution along the time domain.

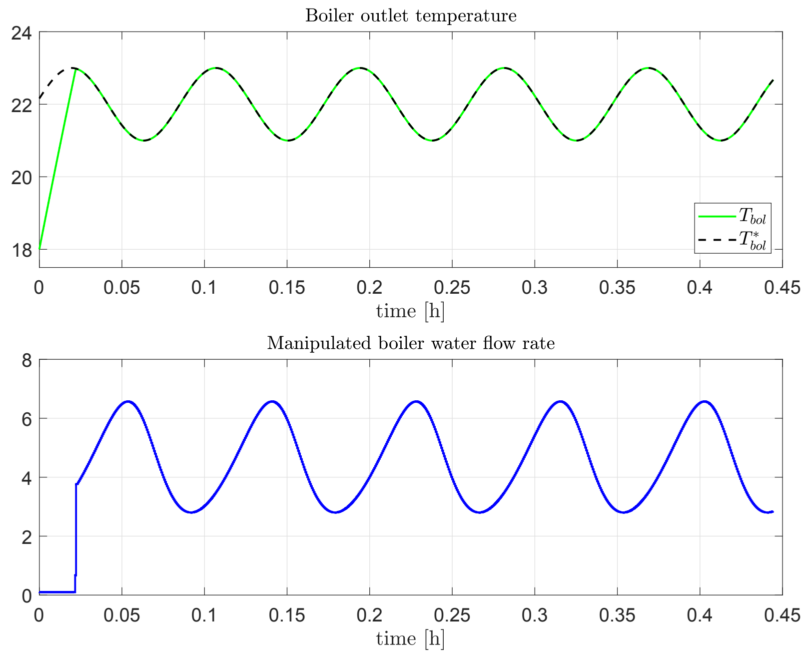

Figure 7.20: The evolution of the boiler outlet temperature $T_{bol}(t)$ under optimal control input $v_{bol}(t)$ with $Reg = 100\%$.

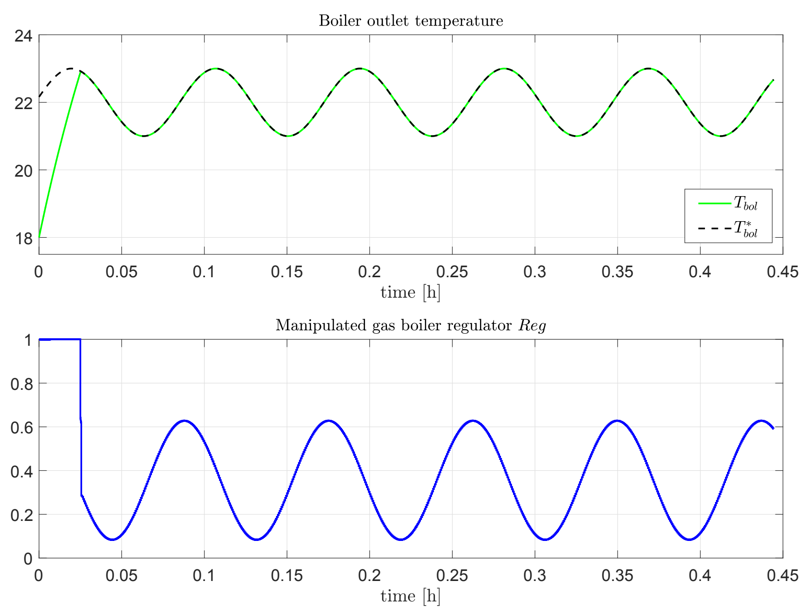

Figure 7.21: The evolution of the boiler outlet temperature $T_{bol}(t)$ under optimal control input $Reg(t)$ with constant flow rate $v_{bol} = 1\ m^3h^{-1}$.

Chapter 8

Conclusions and Future work

Partial differential equations (PDE) have been widely used to model large class of systems and processes in chemical, mechanical, manufacturing, biomedical and pharmaceutical engineering. The state estimation and control of PDE systems have received significant attention in recent years. In control theory, output regulation problem (also called regulator problem) is an important control problem in automatic control theory. Roughly stated, the output regulation problem is a tracking and disturbance rejection problem. The reference trajectory and disturbances are usually generated by an exosystem that is neutrally stable. There usually exist two versions of the regulator problem: state feedback and error feedback regulator problem. All the information of the state of the plant and the exosystem is provided to the state feedback regulator and only the tracking error is available to the error feedback regulator. In this thesis, another case was considered such that the novel output feedback regulators were proposed for the first order hyperbolic PDE systems and more general PDE systems to account for the situation in which the system is not observable through the controlled output but the observable measurement is available.

8.1 Conclusions

In Chapter 2, this thesis addressed optimal constrained state estimation problem for finite and infinite-dimensional chemical process systems. More precisely, using the prior information as inequality constraint with respect to the systems state, the augmented Hamiltonian was obtained and improved state estimation equations were developed. Finally, the results were demonstrated through illustrative examples of chemical process systems.

In Chapter 3, different forms of hyperbolic PDE systems were involved. In particular, distributed and boundary control problems were considered in Section 3.2, 3.3 and Section 3.4, respectively. Moreover, classical exosystems and extended exosystems were presented and proposed in this thesis. In order to solve the output regulation problems, different forms of Sylvester equations were obtained. Correspondingly, sufficient conditions were investigated and provided to guarantee the solvability of Sylvester equations and thus the feasibility of the regulators.

To complement the works in Chapter 3, Chapter 4 developed novel output feedback and error feedback regulators for general distributed parameter systems. In the output feedback regulator design, the measurements available for the regulator do not belong to the set of controlled outputs and are able to ensure the observability of the considered systems. The proposed output feedback regulator with the injection of the measurement $y_m(t)$ and reference $y_r(t)$ can realize both the plant and the exosystem states estimation, disturbance rejection and reference signal tracking, simultaneously. Moreover, new design approach provides an alternative choice for seeking the output injection gain in a traditional error feedback regulator design. The regulator parameters are easily configured to solve the output regulation problems, and to ensure the stability of the closed-loop systems. The results are demonstrated via computer simulation in two types of representative systems: the parabolic partial differential equation (PDE) system and the first order hyperbolic PDE system.

In the aspect of applications, Chapter 5 considered the state feedback regulator problem for a network of countercurrent heat exchangers. The system is described by two sets of hyperbolic partial differential equations (PDEs) and the model is nonlinear with respect to the control input. To deal with the nonlinearity, the equilibrium temperature profile was calculated and utilized in the linearization of the original nonlinear system. Then, based on infinite-dimensional representation, the state feedback regulator problem (in particular the tracking problem) was considered, where the target is to design a controller that, while guaranteeing the stability of the closed-loop system, drives the controlled output to track a reference signal generated by an exosystem with its spectrum on the imaginary axis. Given the explicit expression of the transfer function, sufficient conditions were provided such that the resulting linearized system is causal and stable. Given that the controlled system is stable, a simple and novel method was introduced to provide the stabilization feedback gain K, such that the controlled system tracks the reference signal.

In Chapter 6, for a plug flow reactor with actuation applied only at the inlet of the reactor, the optimal linear quadratic (LQ) boundary output regulator was designed. In the procedure of the regulator design, the weak variational approach was applied. In particular, the time-varying state feedback gain was determined by solving Riccati-type PDEs and this thesis introduced the linear quadratic regulator design to the class of boundary controlled hyperbolic PDE systems. Along the line of LQ design, an optimal boundary tracking regulator was proposed and designed such that the output of the considered reaction process tracks the desired reference signal generated by an exosystem. A simulation example was included to show performance of the proposed approach.

Chapter 7 investigated optimal operation strategy and optimal control for a solar-thermal district heating system. More precisely, optimal operation strategies on the fluid flow rate inside the solar collector tube were studied such that the outlet temperature can be maintained in a desired reference value and moreover the heat (energy) gained by the solar collector is maximized within a certain time period. In particular, this target was formulated as a single-objective optimization problem and a multi-objective optimization problem, respectively. For the energy storage system, the heat exchanger plays an important role in the heat transfer process and the maximization of the energy stored. Therefore, two freedoms-fluid flow rates in the heat exchanger were included and the control policy were explored to realize the multiple objectives. In the district heating loop system, a gas heater system collaborate with the solar thermal system to meet the heating demand. For this coupled system, a receding horizon optimal controller and a state-space based servo-controller were developed to address the desired district temperature tracking problem.

8.2 Future work

This thesis developed optimal state estimation approach for spectral PDE systems to account for the problems with equality and inequality constraints on the state and output. Nevertheless, there remains open questions regarding the optimal control and the optimal state estimation for non-spectral PDE system such as the first-order hyperbolic PDE systems. In particular, through the investigation of variational approaches, the constrained optimal control and state estimation problems will be interesting and possibly solved.

More important part of this thesis is the development of novel servo-controllers for various distributed parameter systems and the proposed approaches addresses full state, tracking error and output feedback output regulation problems. However, all developed methods are based on the continuous plants and exosystems. From the practical perspective, it will more interesting to consider the output regulation in the framework of discrete systems. Moreover, the servo-control problems for time-varying and parameter varying distributed parameter systems with time-delay will be interesting and challenging.

In practice, it is common to meet the case that multiple objectives and/or conflict objectives may happen at the same time for a real process. This can be seen in Chapter 7. How to find the trade-off among there objectives is interesting and challenging. Moreover, the investigations on solving multi-objective optimization problems with PDE constraints are more attractive works in future.

Bibliography

[1] Kenneth R Muske and James B Rawlings. Model predictive control with linear models. *AIChE Journal*, 39(2):262–287, 1993.

[2] Stevan Dubljevic, Nael H El-Farra, Prashant Mhaskar, and Panagiotis D Christofides. Predictive control of parabolic PDEs with state and control constraints. *International Journal of Robust and Nonlinear Control*, 16(16):749–772, 2006.

[3] Willis Harmon Ray. *Advanced process control*. McGraw-Hill, New York, 1981.

[4] Hideki Sano. Exponential stability of a mono-tubular heat exchanger equation with output feedback. *Syst. Control Lett.*, 50(5):363–369, 2003.

[5] Dan Simon and Tien Li Chia. Kalman filtering with state equality constraints. *IEEE Transactions on Aerospace and Electronic Systems*, 38(1):128–136, 2002.

[6] Kenneth R Muske, James B Rawlings, and Jay H Lee. Receding horizon recursive state estimation. In *American Control Conference, 1993*, pages 900–904. IEEE, 1993.

[7] Christopher V Rao, James B Rawlings, and Jay H Lee. Constrained linear state estimationa moving horizon approach. *Automatica*, 37(10):1619–1628, 2001.

[8] Dan Simon. Kalman filtering with state constraints: a survey of linear and nonlinear algorithms. *IET Control Theory & Applications*, 4(8):1303–1318, 2010.

[9] Chun Yang and Erik Blasch. Kalman filtering with nonlinear state constraints. *IEEE Transactions on Aerospace and Electronic Systems*, 45(1):70–84, 2009.

[10] Christopher V Rao, James B Rawlings, and David Q Mayne. Constrained state estimation for nonlinear discrete-time systems: Stability and moving horizon approximations. *IEEE Transactions on Automatic Control*, 48(2):246–258, 2003.

[11] Pramod Vachhani, Raghunathan Rengaswamy, Vikrant Gangwal, and Shankar Narasimhan. Recursive estimation in constrained nonlinear dynamical systems. *AIChE Journal*, 51(3):946–959, 2005.

[12] Panagiotis D Christofides and Prodromos Daoutidis. Finite-dimensional control of parabolic PDE systems using approximate inertial manifolds. In *Decision and Control, 1997., Proceedings of the 36th IEEE Conference on*, volume 2, pages 1068–1073. IEEE, 1997.

[13] Joseph J Winkin, Denis Dochain, and Philippe Ligarius. Dynamical analysis of distributed parameter tubular reactors. *Automatica*, 36(3):349–361, 2000.

[14] Ruth F Curtain and Hans Zwart. *An introduction to infinite-dimensional linear systems theory*, volume 21. Springer, New York, 1995.

[15] Stevan Dubljevic, Panagiotis D Christofides, and Ioannis G Kevrekidis. Distributed nonlinear control of diffusion–reaction processes. *International journal of robust and nonlinear control*, 14(2):133–156, 2004.

[16] L Mohammadi, I Aksikas, S Dubljevic, and JF Forbes. LQ-boundary control of a diffusion-convection-reaction system. *International Journal of Control*, 85(2):171–181, 2012.

[17] T Yu, John H Seinfeld, and W Harmon Ray. Filtering in nonlinear time delay systems. *IEEE Transactions on Automatic Control*, 19(4):324–333, 1974.

[18] Victor M Zavala and Lorenz T Biegler. Optimization-based strategies for the operation of low-density polyethylene tubular reactors: Moving horizon estimation. *Computers & Chemical Engineering*, 33(1):379–390, 2009.

[19] M. B. Ajinkya, W. H. Ray, T. K. Yu, and J. H. Seinfeld. The application of an approximate non-linear filter to systems governed by coupled ordinary and partial differential equations. *International Journal of Systems Science*, 6(4):313–332, 1975.

[20] MA Soliman and W Harmon Ray. Nonlinear state estimation of packed-bed tubular reactors. *AIChE Journal*, 25(4):718–720, 1979.

[21] P Stavroulakis and PE Sarachik. Design of optimal controllers for distributed systems using finite dimensional state observers. In *Decision and Control including the 12th Symposium on Adaptive Processes, 1973 IEEE Conference on*, pages 105–109. IEEE, 1973.

[22] Stevan Dubljevic, Prashant Mhaskar, Nael H El-Farra, and Panagiotis D Christofides. Predictive control of transport-reaction processes. *Computers & Chemical engineering*, 29(11):2335–2345, 2005.

[23] DJ Cooper, WF Ramirez, and DE Clough. Comparison of linear distributed-parameter filters to lumped approximants. *AIChE journal*, 32(2):186–194, 1986.

[24] Ruth F Curtain, Hartmut Logemann, Stuart Townley, and Hans Zwart. *Well-posedness, stabilizability and admissibility for Pritchard Salamon systems*. Inst. für Dynamische Systeme, 1992.

[25] Bert Van Keulen. H∞-control for distributed parameter systems: A state-space approach: A state space approach. 1993.

[26] Dan Simon. *Optimal state estimation: Kalman, H infinity, and nonlinear approaches*. John Wiley & Sons, 2006.

[27] Arthur Earl Bryson. *Applied optimal control: optimization, estimation and control*. CRC Press, 1975.

[28] RF Curtain and AJ Pritchard. Infinite dimensional linear systems theory. *Lecture notes in control and information sciences*, 8, 1978.

[29] George Weiss. Transfer functions of regular linear systems. I. Characterizations of regularity. *Transactions of the American Mathematical Society*, 342(2):827–854, 1994.

[30] Toshihiro Kobayashi and Shigeru Hitotsuya. Observers and parameter determination for distributed parameter systems. *International Journal of Control*, 33(1):31–50, 1981.

[31] Vivek Natarajan, David S Gilliam, and George Weiss. The state feedback regulator problem for regular linear systems. *IEEE Transactions on Automatic Control*, 59(10):2708–2723, 2014.

[32] Ilyasse Aksikas, Joseph J Winkin, and Denis Dochain. Optimal LQ-feedback regulation of a nonisothermal plug flow reactor model by spectral factorization. *IEEE Transactions on Automatic Control*, 52(7):1179–1193, 2007.

[33] J-M Coron, Brigitte d'Andrea Novel, and Georges Bastin. A strict Lyapunov function for boundary control of hyperbolic systems of conservation laws. *IEEE Transactions on Automatic Control*, 52(1):2–11, 2007.

[34] Georges Bastin and Jean-Michel Coron. On boundary feedback stabilization of non-uniform linear 2× 2 hyperbolic systems over a bounded interval. *Systems & Control Letters*, 60(11):900–906, 2011.

[35] Saurabh Amin, Falk M Hante, and Alexandre M Bayen. On stability of switched linear hyperbolic conservation laws with reflecting boundaries. In *Hybrid Systems: Computation and Control*, pages 602–605. Springer Berlin Heidelberg, New York, 2008.

[36] Jonathan de Halleux, Christophe Prieur, J-M Coron, Brigitte d'Andréa Novel, and Georges Bastin. Boundary feedback control in networks of open channels. *Automatica*, 39(8):1365–1376, 2003.

[37] Ilyasse Aksikas, Adrian Fuxman, J Fraser Forbes, and Joseph J Winkin. LQ control design of a class of hyperbolic PDE systems: Application to fixed-bed reactor. *Automatica*, 45(6):1542–1548, 2009.

[38] Tor A Johansen and Camilla Storaa. Energy-based control of a distributed solar collector field. *Automatica*, 38(7):1191–1199, 2002.

[39] BaoZhu Guo and XiYin Liang. Differentiability of the c_0-semigroup and failure of riesz basis for a mono-tubular heat exchanger equation with output feedback: a case study. *Semigroup Forum*, 69(3):462–471, 2004.

[40] Hideki Sano. Output tracking control of a parallel-flow heat exchange process. *Systems & Control Letters*, 60(11):917–921, 2011.

[41] Fu Zheng, Cheng-li Zhang, and Bao-zhu Guo. Exponential stability of the mono-tubular heat exchanger equation with time delay in boundary observation. *arXiv preprint arXiv:1503.01866*, 2015.

[42] Valerie Dos Santos Martins, Yongxin Wu, and Mickael Rodrigues. Design of a proportional integral control using operator theory for infinite dimensional hyperbolic systems. *IEEE Transactions on Control Systems Technology,*, 22(5):2024–2030, 2014.

[43] Dieter Armbruster, Daniel E Marthaler, Christian Ringhofer, Karl Kempf, and Tae-Chang Jo. A continuum model for a re-entrant factory. *Operations research*, 54(5):933–950, 2006.

[44] Michael La Marca, Dieter Armbruster, Michael Herty, and Christian Ringhofer. Control of continuum models of production systems. *Automatic Control, IEEE Transactions on*, 55(11):2511–2526, 2010.

[45] Bruce A Francis. The linear multivariable regulator problem. *SIAM Journal on Control and Optimization*, 15(3):486–505, 1977.

[46] WM Wonham. Tracking and regulation in linear multivariable systems. *SIAM Journal on Control*, 11(3):424–437, 1973.

[47] Edward J Davison. The robust control of a servomechanism problem for linear time-invariant multivariable systems. *IEEE Transactions on Automatic Control*, 21(1):25–34, 1976.

[48] Bruce A Francis and W Murray Wonham. The internal model principle of control theory. *Automatica*, 12(5):457–465, 1976.

[49] Lassi Paunonen and Seppo Pohjolainen. Internal model theory for distributed parameter systems. *SIAM Journal on Control and Optimization*, 48(7):4753–4775, 2010.

[50] Mark R Opmeer and Olof J Staffans. Optimal control on the doubly infinite continuous time axis and coprime factorizations. *SIAM Journal on Control and Optimization*, 52(3):1958–2007, 2014.

[51] Johannes Maria Schumacher. A direct approach to compensator design for distributed parameter systems. *SIAM journal on control and optimization*, 21(6):823–836, 1983.

[52] Joachim Deutscher. Output regulation for linear distributed-parameter systems using finite-dimensional dual observers. *Automatica*, 47:2468–2473, 2011.

[53] Joachim Deutscher. A backstepping approach to the output regulation of boundary controlled parabolic pdes. *Automatica*, 57:56–64, 2015.

[54] Miroslav Krstic and Andrey Smyshlyaev. Backstepping boundary control for first-order hyperbolic PDEs and application to systems with actuator and sensor delays. *Systems & Control Letters*, 57(9):750–758, 2008.

[55] Ilyasse Aksikas, Joseph J Winkin, and Denis Dochain. Stability analysis of an infinite-dimensional linearized plug flow reactor model. In *IEEE Conference on Decision and Control*, 2004.

[56] Tosio Kato. *Perturbation theory for linear operators*, volume 132. Springer, 1995.

[57] CI Byrnes, István G Laukó, David S Gilliam, and Victor I Shubov. Output regulation for linear distributed parameter systems. *IEEE Transactions on Automatic Control*, 45(12):2236–2252, 2000.

[58] Timo Hämäläinen and Seppo Pohjolainen. Robust regulation of distributed parameter systems with infinite-dimensional exosystems. *SIAM Journal on Control and Optimization*, 48(8):4846–4873, 2010.

[59] Ch I Byrnes, DS Gillam, and VI Shubov. Geometric theory of output regulation for linear distributed parameter systems. *Research directions in distributed parameter systems*, pages 139–165, 2003.

[60] Ruth Curtain and Kirsten Morris. Transfer functions of distributed parameter systems: A tutorial. *Automatica*, 45(5):1101–1116, 2009.

[61] Thomas Kailath. *Linear systems*, volume 156. Prentice-Hall Englewood Cliffs, NJ, 1980.

[62] Marius Tucsnak and George Weiss. *Observation and control for operator semigroups*. Springer, 2009.

[63] Xiaodong Xu, Biao Huang, and Stevan Dubljevic. State feedback output regulation for a class of hyperbolic PDE systems. In *Control Conference (ECC), 2015 European*, pages 521–526. IEEE, 2015.

[64] Federico Bribiesca-Argomedo and Miroslav Krstic. Backstepping-forwarding control and observation for hyperbolic pdes with fredholm integrals. *IEEE Trans. Autom. Control*, 60(8):2145–2160, 2015.

[65] Jean-Michel Coron, Long Hu, and Guillaume Olive. Stabilization and controllability of first-order integro-differential hyperbolic equations. *Journal of Functional Analysis*, 271(12):3554–3587, 2016.

[66] Ole Morten Aamo. Disturbance rejection in 2×2 linear hyperbolic systems. *IEEE Transactions on Automatic Control*, 58(5):1095–1106, 2013.

[67] L Paunonen and S Pohjolainen. Robust controller design for infinite-dimensional exosystems. *International Journal of Robust and Nonlinear Control*, 24(5):825–858, 2014.

[68] Jérémy R Dehaye and Joseph J Winkin. LQ-optimal boundary control of infinite-dimensional systems with Yosida-type approximate boundary observation. *Automatica*, 67:94–106, 2016.

[69] Lassi Paunonen. Controller design for robust output regulation of regular linear systems. *IEEE Transactions on Automatic Control*, 61(10):2974–2986, 2016.

[70] Chengzhong Xu and Hamadi Jerbi. A robust PI-controller for infinite-dimensional systems. *International Journal of Control*, 61(1):33–45, 1995.

[71] Marius Tucsnak and George Weiss. Well-posed systems-The LTI case and beyond. *Automatica*, 50:1757–1779, 2014.

[72] Richard Rebarber and George Weiss. Internal model based tracking and disturbance rejection for stable well-posed systems. *Automatica*, 39(9):1555–1569, 2003.

[73] Joachim Deutscher. Backstepping design of robust output feedback regulators for boundary controlled parabolic PDEs. *IEEE Trans. Autom. Control*, PP(99):1, 2015.

[74] Lassi Paunonen. Designing controllers with reduced order internal models. *IEEE Transactions on Automatic Control,*, 60(3):775–780, 2015.

[75] John C Friedly. *Dynamic Behavior of Processes*. Prentice-Hall Englewood Cliffs, New Jersey, 1972.

[76] Ahmed Maidi, Moussa Diaf, and Jean-Pierre Corriou. Boundary geometric control of a counter-current heat exchanger. *Journal of Process Control*, 19(2):297–313, 2009.

[77] Jean-Michel Coron, Brigitte D'Andréa-Novel, and Georges Bastin. A strict Lyapunov function for boundary control of hyperbolic systems of conservation laws. *IEEE Transactions on Automatic Control,*, 52(1):2–11, 2007.

[78] Ilyasse Aksikas, Adrian Fuxman, J Fraser Forbes, and Joseph J Winkin. LQ control design of a class of hyperbolic PDE systems: Application to fixed-bed reactor. *Automatica*, 45(6):1542–1548, 2009.

[79] CI Bymes, István G Laukó, David S Gilliam, and Victor Shubov. Output regulation for linear distributed parameter systems. *IEEE Transactions on Automatic Control,*, 45(12):2236–2252, 2000.

[80] Ruth F Curtain and Hans Zwart. *An Introduction to Infinite Dimensional Linear Systems Theory*, volume 21. Springer Science & Business Media, New York, 2012.

[81] Amir Alizadeh Moghadam, Ilyasse Aksikas, Stevan Dubljevic, and J Fraser Forbes. Boundary optimal (LQ) control of coupled hyperbolic PDEs and ODEs. *Automatica*, 49(2):526–533, 2013.

[82] Mojtaba Izadi, Javad Abdollahi, and Stevan S Dubljevic. Pde backstepping control of one-dimensional heat equation with time-varying domain. *Automatica*, 54:41–48, 2015.

[83] Scott J Moura and Hosam K Fathy. Optimal boundary control of reaction–diffusion partial differential equations via weak variations. *Journal of Dynamic Systems, Measurement, and Control*, 135(3):034501, 2013.

[84] Agus Hasan, Lars Imsland, Ivan Ivanov, Snezhana Kostova, and Boryana Bogdanova. Optimal boundary control of 2× 2 linear hyperbolic pdes. In *Control and Automation (MED), 2016 24th Mediterranean Conference on*, pages 164–169. IEEE, 2016.

[85] Maria Stefania Carmeli, Francesco Castelli-Dezza, Marco Mauri, Gabriele Marchegiani, and Daniele Rosati. Control strategies and configurations of hybrid distributed generation systems. *Renewable Energy*, 41:294–305, 2012.

[86] Rui N Silva, João Miranda Lemos, and Luís M Rato. Variable sampling adaptive control of a distributed collector solar field. *IEEE Transactions on Control Systems Technology*, 11(5):765–772, 2003.

[87] S Farahat, F Sarhaddi, and H Ajam. Exergetic optimization of flat plate solar collectors. *Renewable Energy*, 34(4):1169–1174, 2009.

[88] S Keerthi and Elmer G Gilbert. Optimal infinite-horizon feedback laws for a general class of constrained discrete-time systems: Stability and moving-horizon approximations. *Journal of optimization theory and applications*, 57(2):265–293, 1988.

[89] Hong Chen and Frank Allgöwer. A quasi-infinite horizon nonlinear model predictive control scheme with guaranteed stability. *Automatica*, 34(10):1205–1217, 1998.

[90] EF Camacho, FR Rubio, M Berenguel, and L Valenzuela. A survey on control schemes for distributed solar collector fields. part i: Modeling and basic control approaches. *Solar Energy*, 81(10):1240–1251, 2007.

[91] Kaisa Miettinen. *Nonlinear multiobjective optimization*, volume 12. Springer Science & Business Media, 2012.

[92] Abdullah Konak, David W Coit, and Alice E Smith. Multi-objective optimization using genetic algorithms: A tutorial. *Reliability Engineering* & *System Safety*, 91(9):992–1007, 2006.

[93] Cristina M Cirre, Manuel Berenguel, Loreto Valenzuela, and Ryszard Klempous. Reference governor optimization and control of a distributed solar collector field. *European Journal of Operational Research*, 193(3):709–717, 2009.